INSTITUTO OSWALDO CRUZ
Doutorado em Biologia Celular e Molecular

FIOCRUZ

Estudo do papel do sistema de fatores de crescimento semelhantes à Insulina (IGFs) na fisiopatogenia da hanseníase

Luciana Silva Rodrigues

Rio de Janeiro
2010

Ministério da Saúde
FIOCRUZ
Fundação Oswaldo Cruz

INSTITUTO OSWALDO CRUZ
Pós-Graduação em Biologia Celular e Molecular

Autora: Luciana Silva Rodrigues

Estudo do papel do sistema de fatores de crescimento semelhantes à Insulina (IGFs) na fisiopatogenia da hanseníase

Tese apresentada ao Instituto Oswaldo Cruz do Rio de Janeiro, como parte dos requisitos para obtenção do título de Doutor em Ciências na área de Biologia Celular e Molecular.

Oritentadora: Dra. Maria Cristina Vidal Pessolani
Co-orientadora: Dra. Euzenir Nunes Sarno

Rio de Janeiro
2010

Catalogação na fonte

Biblioteca de Manguinhos – CICT – FIOCRUZ

Rodrigues, Luciana Silva

Estudo do papel do sistema de fatores de crescimento semelhantes à Insulina (IGFs) na fisiopatogenia da hanseníase. / Luciana Silva Rodrigues.
Rio de Janeiro; 2010.

xvi, 154p.;il.

Tese (Doutorado) – Instituto Oswaldo Cruz, Rio de Janeiro. Biologia Celular e Molecular, 2010.

1. Hanseníase; 2. IGF-I; 3. células de Schwann; 4. episódios reacionais

I. Título II. Rodrigues, L.S.

Ministério da Saúde
FIOCRUZ
Fundação Oswaldo Cruz

INSTITUTO OSWALDO CRUZ
Pós-Graduação em Biologia Celular e Molecular

Autora: Luciana Silva Rodrigues

Estudo do papel do sistema de fatores de crescimento semelhantes à Insulina (IGFs) na fisiopatogenia da hanseníase

Oritentadora: Dra. Maria Cristina Vidal Pessolani
Co-orientadora: Dra. Euzenir Nunes Sarno

Aprovada em: 20/07/2010.

EXAMINADORES:

Dr. Sérgio Antunes – Instituto Oswaldo Cruz – Presidente
Dra. Hiro Goto – Instituto de Medicina Tropical de São Paulo (USP) – Titular
Dra. Carmem Cabanelas Pazos Moura – Universidade Federal do Rio de Janeiro – Titular
Dra. Ximena Illarramendi – Instituto Oswaldo Cruz – Suplente/Revisor
Dra. Clarissa M. Maya Monteiro – Instituto Oswaldo Cruz - Suplente

Rio de Janeiro, 20 de Julho de 2010.

"Tenho em mim todos os sonhos do mundo".

Fernando Pessoa

Agradecimentos

A Deus, por renovar em mim, a cada dia, a vontade de seguir em frente e acreditar que era possível. Agradeço por cada obstáculo pessoal e profissional vencido durante esta jornada e a todas as pessoas que Ele colocou em meu caminho e que me auxiliaram em vários momentos;

Aos meus pais, pelo exemplo de força e coragem e, sobretudo por estarem sempre ao meu lado;

Ao meu marido Marcello pelo seu amor, apoio incondicional e dedicação à nossa família; e, à nossa linda menina Giovanna, pela alegria que traz às nossas vidas;

À minha querida e eterna Mestra, Dra. Maria Cristina Vidal Pessolani, por sua competência e carinho, com os quais me conduziu até aqui. Devo a ela esta conquista e espero que nosso convívio, durante estes longos anos, tenha demonstrado toda a minha admiração, gratidão e respeito;

À Dra. Euzenir Nunes Sarno, minha querida co-orientadora, igualmente essencial para o desenvolvimento deste trabalho. Agradeço muito por seu apoio durante todo este processo. Suas palavras de apoio e incentivo constantes me impulsionaram sempre a tentar fazer o melhor para honrar sua confiança;

À querida Elisa da Silva Maeda, por sua dedicação e grande contribuição neste trabalho;

À Dra. Mariana Hacker, por sua paciência e compreensão durante as incansáveis análises estatísticas;

À Dra. Ximena Illarramendi, pela atenção que dedicou a este trabalho não somente como revisora, mas, sobretudo na verificação do banco de dados dos pacientes selecionados;

À Dra. Maria Renata Sales Nogueira Costa, do Instituto Lauro Souza Lima – Bauru (SP), que mais do que colaboradora do trabalho se tornou, sobretudo uma grande amiga;

Ao Dr. Geraldo Pereira pelas discussões científicas sempre interessantes e pela revisão do trabalho;

Ao Dr. Victor Túlio Ribeiro Rezende pela amizade e contribuição direta neste trabalho durante sua passagem pelo nosso laboratório;

À Dra. Ilda Akemi e Neura Silveira, do Laboratório Central do Instituto Nacional do Câncer (INCA), por permitirem e auxiliarem nossas primeiras dosagens de IGF;

À Dra. Mônica Freira, do Laboratório Sérgio Franco, pelo carinho com que me recebeu e por ter facilitado ao máximo e com grande boa vontade a dosagem de IGF em nossas amostras;

À Eliane, Rose e Daniel, do Laboratório de Hanseníase, que tão gentilmente contribuíram na localização, separação e conferência dos soros de pacientes utilizados neste trabalho;

À Dra. Katherine Antunes de Mattos pelo incentivo no desenvolvimento dos projetos e oportunidade de colaboração em seus trabalhos;

Ao Dr. Flávio Alves Lara pelo apoio em todas as horas e incansável luta pela obtenção de nervos para purificação de células de Schwann primárias;

Às minhas queridas amigas e companheiras: Marjorie Mendonça, Michelle Lopes e Tatiana Pereira da Silva pela amizade sincera, carinho e atenção em todos os momentos;

Aos queridos amigos do Laboratório de Microbiologia Celular: Ágatha Barreto (querida ex-aluna de iniciação científica), Leonardo Ribeiro, Júlio Jablonski, Carlos Robertha Lemes, Lívia Lobato, Carlos Adriano, André Dias, Fernanda, Viviane Gonçalves, Natasha Linhares, Juliana, Débora, Rafael. Obrigada pelo carinho de todos vocês e pela agradável convivência;

A todos os amigos do Pavilhão de Hanseníase, em especial ao Harrison Magdinier (pelas palavras certas nos momentos certos), Cynthia Chester, Luana, Flávia, Roberta Olmo, Daniele Fonseca, Thaís Porto, Verônica Schmitz, Sr. Salles, Cristiane e José Augusto;

Ao CNPq, pelo apoio financeiro e à equipe da Pós-Graduação em Biologia Celular e Molecular do Instituto Oswaldo Cruz pelo apoio e atenção;

Certamente, muitos são os amigos e tenho claro, muito a agradecer. Meus sinceros agradecimentos e carinho a todos que contribuíram direta ou indiretamente e que não foram citados aqui.

Lista de Figuras

Lista de Símbolos e Abreviaturas

ALS	Subunidade ácido-lábil
BB	*borderline borderline*
BCG	bacilo de Calmette-Guérin
BL	*borderline* lepromatoso
BT	*borderline* tuberculóide
CD	grupo de diferenciação
CS	célula de Schwann
DG	distroglicana
DNA	ácido desoxirribonucléico
ENH	eritema nodoso hansênico
ELISA	ensaio imunoenzimático
GH	hormônio do crescimento
HLA	antígeno leucocitário humano
Hlp	proteína semelhante à histona
I	indeterminado
IFN-γ	interferon gama
IGF-1R	receptor de IGF tipo 1
IGFBP-	proteína ligadora de IGF
IGFs	fatores de crescimento semelhantes à insulina
IgG	imunoglobulina G
IgM	imunoglobulina M
IL-	interleucina
kDa	quiloDalton
kg	quilograma
LAM	lipoarabinomanana
LBP	proteína ligadora de laminina
LL	lepromatoso lepromatoso
LT	linfotoxina
MAPK	proteínas quinases ativadas por mitógenos
MB	multibacilar
MBP	proteína básica da mielina

MCP-1	proteína-1 quimiotática de monócitos
mg	miligrama
mL	mililitro
NF-1	neurofibromatose tipo 1
ng	nanograma
NT3	neurotrofina-3
OMS	organização mundial de saúde
P0	proteína zero
PACRG	gene co-regulador da parkina
PARK2	gene da parkina
pb	pares de base
PB	paucibacilar
PBMC	células mononucleares de sangue periférico
PDGF-BB	fator de crescimento derivado de plaquetas-BB
PDIM	dimicocerosato ftiocerol
PGL-I	glicolipídeo fenólico I
PI3-K	fosfatidilinositol 3-quinase
PIMs	monosídeos fosfatidilinositol
PL	fosfolipídeos
PQT	poliquimioterapia
PS	fosfatidilserina
RANTES	Fator regulador expresso e secretado por células T normais
RNA-m	ácido ribonucléico mensageiro
RR	reação reversa
Th	células T auxiliares
TMM	monomicolato trealose
TNF-α	fator de necrose tumoral-alfa
TT	tuberculóide tuberculóide
μg	micrograma

Sumário

Resumo

A lesão neural é uma das principais consequências da hanseníase e responsável pela instalação de deformidades e incapacidades físicas, além de contribuir para o estigma da doença. O dano ao nervo é exacerbado com o desenvolvimento de episódios reacionais (Tipo I e Tipo II) e está correlacionado à resposta imunológica desenvolvida pelo indivíduo, contra o *Mycobacterium leprae* – agente etiológico da hanseníase que apresenta especial tropismo por macrófagos e células de Schwann (CS) nos nervos periféricos. Os fatores de crescimento semelhante à Insulina (IGFs) são hormônios peptídicos implicados no metabolismo, indução de proliferação, inibição de apoptose e diferenciação de diferentes tipos celulares. Evidências da literatura apontam também propriedades imunomoduladoras e anti-inflamatórias do IGF-I. O objetivo do presente estudo visa a investigação da participação do sistema IGF na infecção pelo *M. leprae*. Inicialmente, verificamos o efeito anti-apoptótico da bactéria sobre CS humanas primárias e da linhagem ST88-14 cultivadas em condições livres de soro pela inibição da ativação de caspase-3. Demonstramos, ainda, através de ensaios de imunocitoquímica, que o bacilo é capaz de induzir a proliferação da CS, tal efeito provavelmente mediado pela indução de IGF-I, confirmado pela técnica de RT-PCR quantitativo e pela detecção da proteína em sobrenadantes de cultura através de ensaio imunoenzimático. Na segunda etapa do trabalho, avaliamos a participação do IGF-I circulante na evolução natural da hanseníase. Utilizando ELISA quimioluminescente, quantificamos os níveis de IGF-I, da principal proteína ligadora de IGF (IGFBP-3) e TNF-α no soro de indivíduos sadios e pacientes que desenvolveram ou não quadros reacionais ao longo do tratamento. No caso dos pacientes reacionais, a dosagem de IGF-I, IGFBP-3 e TNF-α foi realizada em duas etapas: i) no momento do diagnóstico e ii) durante o aparecimento da reação, antes do tratamento específico. Inicialmente, numa comparação entre pacientes que não desenvolveram reação, verificamos que 81% e 72% dos pacientes lepromatosos (LL) apresentaram níveis de IGF-I e IGFBP-3, respectivamente, abaixo do normal por idade, diferentemente dos pacientes com outras formas clínicas. Dentre os pacientes reacionais, 93% e 86% do grupo BL também apresentou níveis de IGF-I e IGFBP-3, respectivamente, abaixo do normal por idade, diferentemente do grupo BL não-reacional, que apresentou níveis de IGFs similares aos indivíduos sadios. Durante o desenvolvimento dos episódios reacionais, houve uma queda dos níveis de IGF-I, IGFBP-3 e da relação IGF/TNF-α no grupo LL com reação tipo II. Já no grupo de pacientes BL, observamos um aumento dos níveis de IGF-I e IGFBP-3, como uma tentativa de alcançar os níveis normais. Nossos dados sugerem a

participação destes fatores de crescimento endócrinos na íntima relação entre bacilo e a CS, como uma estratégia de obtenção e manutenção de um nicho favorável de multiplicação e, ainda, os revelam como potenciais candidatos a biomarcadores dos episódios reacionais na hanseníase.

Abstract

Neural injury is a major consequence of leprosy and responsible for the disabilities installation, beyond to contribute to the stigma of the disease. The nerve damage is exacerbated by the development or leprosy reactions (Type I and Type II) and is correlated to the immune response against *Mycobacterium leprae* – etiologic agent of leprosy that has especial tropism for macrophages and Schwann cells (SC) in peripheral nerves. Insulin-like growth factors (IGFs) are peptide hormones involved in metabolism, proliferation induction, apoptosis inhibition and cell differentiation. Evidence from the literature also indicate immunomodulatory and anti-inflammatory properties of IGF-I. The aim of this study is to investigate the involvement of IGF system in the *M. leprae* infection. Initially, we verified the anti-apoptotic effect of the bacteria on human primary CS and ST88-14 lineage growing in serum-free conditions by inhibiting caspase-3 activation. It was also demonstrated by immunocytochemistry, that the bacillus is able to induce the SC proliferation, this effect is probably mediated by induction of IGF-I, as verified by quantitative RT-PCR and confirmed by protein detection supernatants using immunoenzimatic assay (ELISA). On the second phase we evaluate the participation of circulating IGFs in the natural course of leprosy. Through chemioluminescent ELISA, we quantified the IGF-I, the main IGF binding protein (IGFBP-3) and TNF-α serum levels in healthy individuals and patients who developed or not reactional states during the treatment. In the case of reactional patients, the IGF-I, IGFBP-3 and TNF-α was performed in two steps: i) at the diagnosis of leprosy and ii) during reactional episode, prior to specific treatment. Initially, a comparison of nonreactional patients, we found that 81% and 72% of lepromatous leprosy (LL) showed IGF-I and IGFBP-3 levels, respectively, below normal for age, unlike patients with other clinical forms. Among the reactional patients, 93% and 86% of BL group also showed IGF-I and IGFBP-3 levels, respectively, below normal for age, unlike the nonreactional BL group, wich showed similar levels of IGFs to healthy individuals. During the development of reactional episodes, there was a decrease in the levels of IGF-I, IGFBP-3 and the IGF/TNF-α ratio in the LL group with type II reaction. In the BL group undergoing type II reaction, the IGF-I and IGFBP-e levels increased, as an attempt to reach normal levels. Our data suggest the involvement of these growth factors in the relationship between bacilli and CS as a strategy for obtaining and maintaining a favorable niche for multiplication, and also reveal the IGFs as potencial candidates for biomarkers of reactional episodes in leprosy.

CAPÍTULO 1: Introdução

1. Hanseníase

1.1 Considerações gerais

A Hanseníase é uma doença infecciosa e de caráter crônico causada pelo *Mycobacterium leprae*, um patógeno intracelular obrigatório que infecta preferencialmente macrófagos e células de Schwann (Kaplan e Cohn, 1986). Suas principais manifestações incluem lesões de pele, mucosas e nervos periféricos que variam ao longo de um amplo espectro de formas clínicas. A hanseníase é uma das doenças mais antigas da história da humanidade. Relatos bíblicos oriundos do Antigo Testamento mostram que a hanseníase era tratada como "castigo divino" e "impureza de espírito" por ser uma doença contagiosa e levar a incapacidade e deformidades físicas. Em 1970, o Brasil extinguiu oficialmente a palavra lepra e a substituiu por hanseníase em homenagem ao médico norueguês Gerhard Armauer Hansen (1841-1912), que em 1873 descobriu o agente etiológico da infecção.

A hanseníase pode afetar indivíduos em todas as idades e de ambos os sexos. Trata-se de uma infecção sem a participação de vetores ou hospedeiros intermediários e que tem o homem como seu principal reservatório. Seu modo de transmissão ainda não foi bem definido, entretanto acredita-se que, devido à fisiologia do bacilo, que apresenta baixa virulência e alta infectividade, a transmissão ocorreria, preferencialmente, entre indivíduos residentes no mesmo domicílio através das secreções das vias respiratórias (nariz e boca) dos pacientes multibacilares. Outros fatores como o tempo de exposição, a carga bacilar (Douglas e col., 2004) e as condições sócio-econômicas das populações expostas (Düppre e col., 2008) podem determinar quais indivíduos poderão desenvolver a doença. Além disso, cada vez mais tem sido mostrado que fatores genéticos do hospedeiro têm influência na susceptibilidade à doença. O estudo de Mira e colaboradores (2004) identificou polimorfismos numa região do cromossomo 6q25-q26 que abrange dois genes, PARK2 e PACRG, associados a uma maior susceptibilidade à doença. Outros estudos demonstram o envolvimento de alelos e haplótipos do complexo HLA, mais especificamente HLA-DR2 e DR-3 (Shaw e col., 2001; Mira, 2006) e, ainda polimorfismos na região promotora para os genes TNF e linfotoxina-alfa (LTA) (Santos e col., 2002; Alcais e col., 2007), como importantes fatores de risco genético para susceptibilidade às formas clínicas da hanseníase. Adicionalmente, estudos de associação

baseados em populações mostraram o efeito protetor de haplótipos específicos do gene interleucina-10 (IL-10), tanto à hanseníase *per se* quanto à forma multibacilar (Moraes e col., 2004; Moraes e col., 2006).

O diagnóstico da hanseníase é principalmente clínico e epidemiológico – baseado nos sinais e sintomas (anestesia, nervos espessados e lesões cutâneas), no exame da pele, dos nervos periféricos e no histórico epidemiológico. É acrescido, ainda, de exames laboratoriais para a pesquisa do bacilo em esfregaço de linfa (baciloscopia) e do exame histopatológico.

A hanseníase é uma doença curável e com tratamento gratuito. O primeiro antibiótico efetivo contra o *M. leprae* foi a dapsona, porém devido às expressivas notificações de cepas resistentes, em 1982 a Organização Mundial de Saúde (OMS) implantou o tratamento com a multidrogaterapia (MDT) ou poliquimioterapia (PQT) que consiste na administração de um conjunto de drogas: dapsona (100 mg por dia), clofazimina (300 mg uma vez por mês e 50 mg por dia) e rifampicina (600 mg uma vez por mês). Este esquema foi introduzido no Brasil em 1991.

Embora a PQT tenha contribuído significativamente para a diminuição da prevalência da hanseníase (WHO, 1998), a erradicação da doença parece algo distante. Ainda hoje a hanseníase é considerada um grave problema de saúde pública e está fortemente relacionada com os baixos níveis de desenvolvimento social e econômico. Índia, Brasil, Indonésia, Congo, Nepal, Nigéria, Etiópia e Tanzânia seguem no "ranking" dos países com o maior número de novos casos detectados em 2008. A prevalência global no início de 2009 foi de cerca de 213.000 casos registrados e o número de casos novos registrados em 2008 foi 249.007 (WHO, 2009; Figura 1). Em 2007, a taxa de detecção no Brasil foi de 21,2/100.000 habitantes, considerada muito alta. As regiões Norte, Centro-Oeste e Nordeste são consideradas hiperendêmicas por deterem a maior concentração de casos, apresentando taxas de detecção alarmantes que chegam a 50 casos por 100.000 habitantes. Estima-se que a cada ano seja registrada uma média de 400.000 casos em todo o mundo, dos quais, aproximadamente 40.000 são provenientes do Brasil e, destes, cerca de 3.000 casos foram diagnosticados com deformidades físicas instaladas (Ministério da Saúde, 2008).

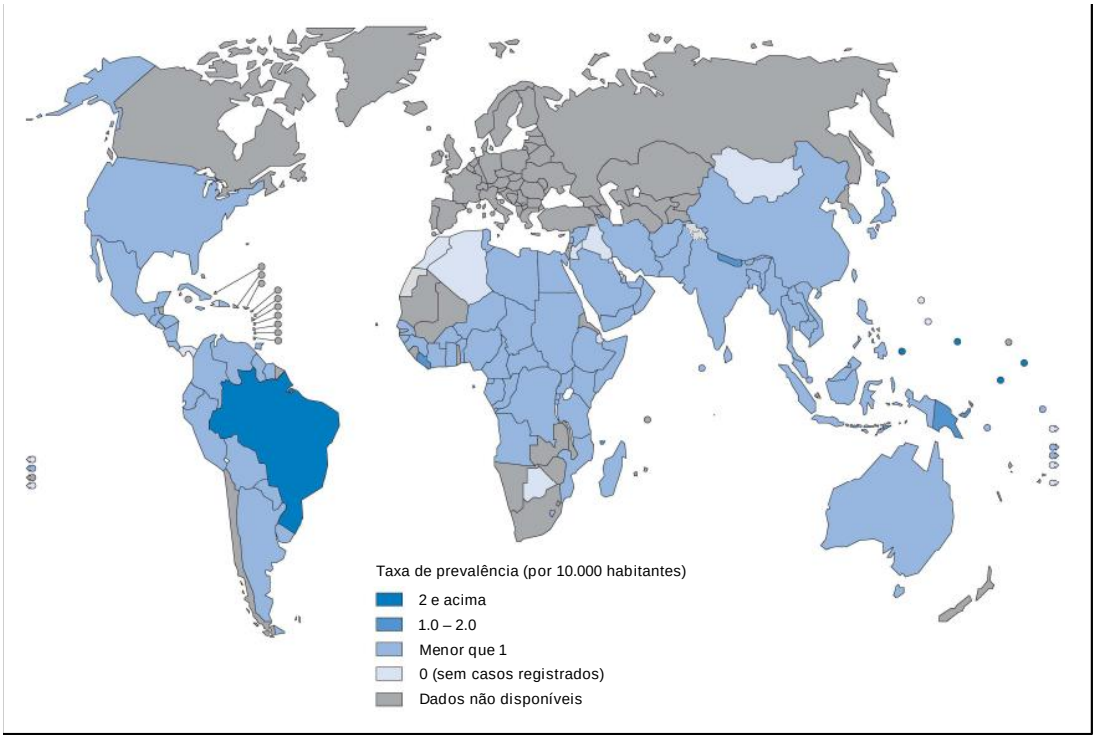

Figura 1: Distribuição global da hanseníase. Mapa mostrando a prevalência da doença no início de 2009. (WHO, 2010)

1.2 O Agente Etiológico

O *Mycobacterium leprae* foi identificado por Gerhard Henrik Armauer Hansen em 1874 como o primeiro agente causador de uma doença infecciosa (Hansen, 1874), entretanto até os dias atuais ainda não é possível cultivá-lo *in vitro* – fato que dificulta seriamente o estudo de sua biologia e dos mecanismos pelo qual se utiliza para invadir os nervos periféricos. Trata-se de um patógeno intracelular obrigatório e apresenta tropismo por fagócitos mononucleares e células de Schwann dos nervos periféricos (Bloom, 1986; Kaplan e Cohn, 1986).

O gênero *Mycobacterium* inclui mais de 70 espécies, sendo sua maioria saprófitas que habitam o solo e a água e, inócuos ao homem e outros animais. Este gênero pertence à ordem dos Actinomycetales e família Mycobacteriaceae. Além dos *M. leprae*, outros patógenos importantes deste gênero podem ser citados, como o *Mycobacterium tuberculosis* – causador da tuberculose humana, o *Mycobacterium avium* e o *Mycobacterium intracellulare*, espécies oportunistas para o homem.

O *M. leprae* é uma bactéria gram-positiva, em forma de bastonete e que apresenta crescimento lento, fazendo uma divisão binária a cada 12-14 dias (WHO 1987). É considerado um bacilo álcool-ácido resistente, ou seja, uma vez corado pela fucsina não se descora pela lavagem com álcool e ácido (Método de Ziehl-Neelsen). Compartilha com outras micobactérias características como a abundância de lipídeos na forma de ácidos micólicos (ácidos graxos saturados de elevado peso molecular) e lipoarabinomanana (LAM) em seu envelope celular, conforme pode ser observado na figura 2. Além disso, mais externamente, apresenta glicolipídeos, com destaque para o PGL-I presente exclusivamente no *M. leprae* e responsável pela especificidade imunológica ao bacilo. O PGL-I foi descrito inicialmente em 1981 por Shirley Hunter e Patrick Brennan e desde então desperta interesse no que diz respeito à sua utilização como diagnóstico precoce da infecção (Hunter e Brennan, 1981; Lefford e col., 1991), bem como seu papel relevante na interação patógeno-célula hospedeira (Schlesinger e Horwitz, 1991). Foi demonstrado que a estimulação com *M. leprae* podem induzir a produção de TNF-α *in vitro*, indicando que componentes do bacilo podem modular a resposta imune específica do hospedeiro (Sampaio e col., 1992; Sampaio e col., 2000).

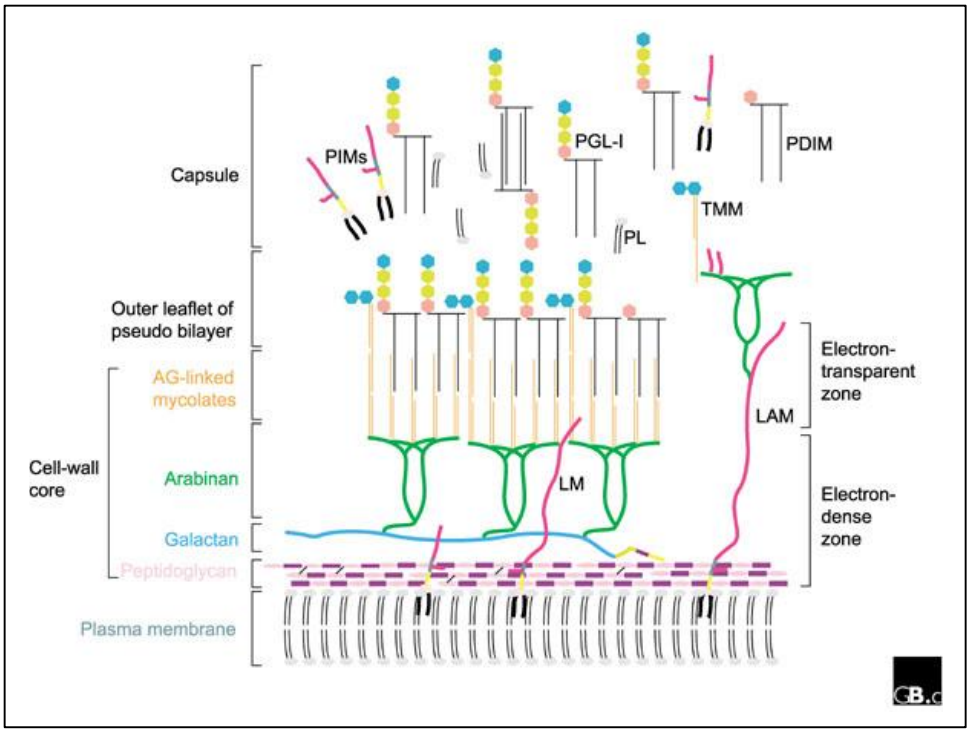

Figura 2: Modelo esquemático da parede celular do *M. leprae* (Vissa e Brennan, 2001). A membrana plasmática é envolvida por uma parede celular composta por peptidoglicana ligada covalentemente a araginogalactana. Ácidos micólicos estão ligados aos resíduos terminais de arabinose. A camada mais externa apresenta: monomicolato trealose (TMM), glicolipídeo fenólico 1 (PGL-1), monosídeos fosfatidilinositol (PIMs), dimicocerosato ftiocerol (PDIM) e fosfolipídeos (PL).

Em 1960, Charles Shepard demonstrou que a inoculação de 10^3 a 10^4 bacilos (provenientes de biópsias humanas) em coxim plantar de camundongos Balb/c promovia uma multiplicação limitada do *M. leprae* durante 9 a 12 meses (Shepard, 1960). O mesmo autor demonstrou também que, camundongos timectomizados apresentavam uma infecção generalizada quando inoculados com *M. leprae*, entretanto, após o limite de multiplicação ter sido alcançado, as bactérias começavam a perder sua viabilidade (Shepard, 1962; Shepard e Chang, 1962). Em 1971, verificou-se que o tatu de nove bandas (*Dasypus novencinctus*) permite o crescimento do bacilo de forma disseminada durante 18 a 24 meses, sendo considerado um hospedeiro naturalmente suscetível. Os animais apresentam uma forma disseminada da doença, com comprometimento da pele, medula óssea, linfonodos, fígado, baço, pulmões e olhos (Kirchheimer e Storrs, 1971). Consegue-se mais de 10^9 bacilos por grama de tecido e desde então, esta tem sido a origem da massa bacteriana utilizada para os estudos bioquímicos, imunológicos e de biologia molecular. Além do tatu de nove bandas, somente macacos mangabei e chimpanzés foram encontrados naturalmente infectados com o *M. leprae* (revisto por Pessolani e col., 2003).

Mais recentemente, outra fonte de *M.leprae* vem sendo também utilizada para estudos, esta derivada de camundongos congenitamente (*nude*) ou experimentalmente atímicos. Estes animais são extremamente susceptíveis à infecção pelo *M. leprae* – o qual requer um alto grau de imunodeficiência em hospedeiros experimentais. Cerca de 2×10^7 bacilos inoculados no coxim plantar de camundongos *nude* permitem a obtenção de aproximadamente 0,5 a 1×10^{10} bacilos num período de, aproximadamente, 6 meses após a inoculação. Após purificação, os bacilos podem ser utilizados vivos por até uma semana ou letalmente irradiados (Truman e Krahenbuhl, 2001).

A conclusão do sequenciamento do genoma do *M. leprae* em 2001 (Cole e col., 2001) é considerada um marco importante para o conhecimento da biologia desta micobactéria. Apenas 49,5% do genoma do *M. leprae* contêm genes que codificam para proteínas, 27% pseudogenes (somando um total de 1.116 pseudogenes ou genes degenerados, assim donominados por apresentarem perda de regiões necessárias à sua transcrição e/ou tradução) e 23,7% não foram codificados, provavelmente por causa de mutações. Quando comparamos seu genoma ao do *M. tuberculosis* verificamos uma perda maciça de genes pelo *M. leprae*, o que poderia explicar o seu longo tempo de geração e sua incapacidade de se multiplicar *in vitro*. Análises do genoma têm revelado defeitos na regulação de vias catabólicas e sistemas de transporte, justificando assim, o fato do *M. leprae* ser um patógeno intracelular obrigatório (revisto por Vissa e Brennan, 2002).

1.3 Classificação

A hanseníase se manifesta segundo um amplo espectro de formas clínicas resultante do grau de resposta imune celular desenvolvida por cada indivíduo contra o *M. leprae*. A classificação atualmente adotada de Ridley e Jopling (1966) combina critérios clínicos, bacteriológicos e, principalmente, imunológicos e histopatológicos. Segundo esta classificação, em um extremo do espectro encontra-se os pacientes lepromatosos (LL), que apresentam alta carga bacilar – devido à ineficiente resposta celular contra a bactéria – e múltiplas lesões. No outro extremo do espectro, estão os pacientes tuberculóides (TT) que apresentam uma forte resposta celular ao *M. leprae*. Em geral, eles apresentam uma única lesão, com poucos bacilos. Entre estes dois extremos estão as formas intermediárias, denominadas *borderline*: *borderline* lepromatoso (BL), *borderline borderline* (BB) e *borderline* tuberculóide (BT), onde a resposta imune celular é maior ou menor acordo com a proximidade ao pólo tuberculóide ou lepromatoso, respectivamente (Figura 3).

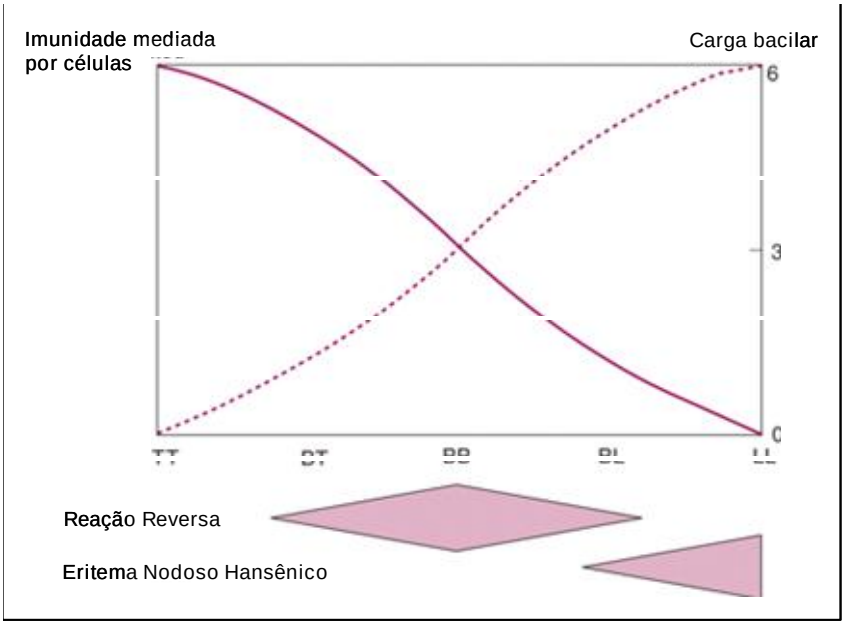

Figura 3: Formas clínicas da hanseníase de acordo com a classificação de Ridley e Jopling (1966). Modelo esquemático adaptado de Walker e Lockwood (2006).

A grande maioria dos indivíduos expostos ao *M. leprae* não desenvolve a doença. De um modo geral, os indivíduos que se infectam inicialmente apresentam a forma Indeterminada (I) da doença – considerada o início das manifestações clínicas. As lesões apresentadas pelos

pacientes são máculas hipopigmentadas com alterações de sensibilidade que podem evoluir para a cura espontânea ou para qualquer uma das formas clínicas do espectro, quando não tratadas.

Para facilitar os esquemas terapêuticos, a OMS estabeleceu uma classificação operacional dos pacientes em dois grupos: paucibacilares (PB) e multibacilares (MB). Dentro deste esquema, os pacientes paucibacilares compreendem as formas TT, BT e I, devido ao limitado número de bacilos encontrados nas lesões. Já as formas BB, BL e LL constituem os pacientes multibacilares, que apresentam uma elevada carga bacilar (WHO, 1987). Visando uma identificação mais rápida dos pacientes, o Ministério da Saúde fez, ainda, uma adaptação nesta classificação incluindo a baciloscopia, o número e a distribuição das lesões cutâneas e o número de troncos nervosos afetados. A duração da PQT é de seis meses para os pacientes PB e de 12 a 24 meses para os MB (Britton e Lockwood, 2004).

1.4 Resposta imunológica na hanseníase

É sabido que a apresentação clínica da hanseníase está fortemente correlacionada ao padrão imunológico desenvolvido por cada indivíduo frente ao *M. leprae*. De um lado, os pacientes tuberculóides mostram uma resposta imune celular parcialmente eficiente que é responsável pelo controle da disseminação da infecção. Do outro lado, os pacientes lepromatosos são incapazes de produzir interferon-gama (IFN-γ) e, consequentemente, apresentam resposta imune celular baixa ou ausente, o que possibilita a lenta replicação e a disseminação do bacilo (Nogueira e col., 1983; Godal, 1984).

Em 1991, Yamamura e colaboradores utilizaram o paradigma Th1/Th2 para explicar os diferentes perfis de resposta imune entre pacientes tuberculóides e lepromatosos. Neste estudo, através da análise de expressão gênica de citocinas a partir de RNA mensageiro (RNAm) extraído de lesões de pacientes, verificaram que a expressão de IL-2, linfotoxina (LT) e IFN-γ estava aumentada nas lesões tuberculóides. Por outro lado, a expressão dos genes para IL-4, IL-5 e IL-10 foi mais evidente na pele dos pacientes com a forma lepromatosa. De forma similar, análises de expressão gênica e secreção de citocinas em células mononucleares de sangue periférico (PBMC) mostram que pacientes lepromatosos exibiram um padrão Th2, enquanto que os tuberculóides Th1 (Misra e col., 1995). Além disso, o IFN-γ, considerado a molécula-chave na resposta protetora não só em pacientes como em contatos domiciliares (Sampaio e col., 1991; Lima e col., 2000), pode ser observado nas formas brandas e intermediárias da doença. Ensaios clínicos utilizando inoculações de IFN-γ

em pacientes multibacilares confirmam o efeito imunoestimulador desta citocina, bem como o aumento da atividade microbicida de macrófagos nas lesões inoculadas (Sampaio e col., 1992).

Os pacientes tuberculóides possuem uma intensa resposta e apresentam uma ou poucas lesões e, estas se caracterizam pela formação de granulomas epitelióides bem definidos e infiltrado de linfócitos CD4+ produtores de IFN-γ (Yamamura e col., 1991). Devido à intensa e efetiva resposta celular, habitualmente não se observam bacilos nos exames bacteriológicos. As lesões têm aspecto descamativo no qual o crescimento de pêlos é deficiente (ou ausente) e, frequentemente são anestésicas devido à destruição das terminações nervosas na derme (revisto por Walker e Lockwood, 2006). A forte imunidade celular é confirmada pelo intenso infiltrado inflamatório, predominantemente composto por células T e expressão de citocinas em resposta a antígenos do *M. leprae*, avaliados *in vitro* e através do teste cutâneo de reatividade (reação de Mitsuda).

Já nos pacientes lepromatosos, a proliferação maciça do *M. leprae* resulta em múltiplas lesões cutâneas, que podem se apresentar como máculas, placas, pápulas, nódulos ou infiltração difusa. As lesões cutâneas apresentam atrofia epidérmica e na derme observam-se granulomas não organizados com raros linfócitos, predominantemente CD8+. No infiltrado inflamatório destacam-se macrófagos de aspecto vacuolizado (devido ao acúmulo de lipídeos) que estão altamente infectados com *M. leprae* e podem ser observados em vários níveis da pele (revisto por Walker e Lockwood, 2006). Altos títulos de anticorpos contra o glicolipídeo fenólico I (PGL-I) e outras proteínas específicas do *M. leprae* podem ser detectados na urina e no sangue destes pacientes (Roche e col., 1990; Triccas e col., 1996; Cho e col., 2001).

Os grupos *borderline* (BT, BB e BL) são considerados formas instáveis da doença e, a distinção entre os subgrupos de maior resistência (BT) para os de menor resistência (BL) baseia-se na indiferenciação progressiva dos macrófagos, diminuição do número de linfócitos e no aumento do número de bacilos nos granulomas e ramos nervosos. As lesões dos pacientes BT podem mostrar raros bacilos e granuloma formado por células epitelióides focalizadas por zona periférica de linfócitos com presença de células gigantes de Langerhans, algumas vezes numerosas. Nos casos BB o número de bacilos é maior apresentam células epitelióides espalhadas de forma difusa por todo o granuloma e não focalizadas por zonas de linfócitos (revisto por Goulart e col., 2002). A forma BL apresenta granuloma composto de macrófagos indiferenciados que contém gande número de bacilos. Entretanto, diferentemente da forma LL, o granuloma dos casos BL apresentam áreas de instensa infiltração linfocitária (Ridley, 1990).

1.5 Os episódios reacionais

Ao longo da evolução da doença aproximadamente metade dos pacientes desenvolve pelo menos um dos chamados episódios reacionais (Nery e col., 1998; Gillis, 2000), que constituem episódios agudos de resposta inflamatória e imunológica súbita que podem ocorrer antes, durante ou após o tratamento poliquimioterápico. Estes quadros reacionais são classificados como reação tipo I ou reversa (RR) e reação tipo II, cuja manifestação clínica mais frequente é o eritema nodoso hansênico (ENH) (Ridley, 1969). Mais atualmente é aceita uma terceira forma clínica de reação hansênica, denominada neurite isolada – caracterizada dor espontânea ou à compressão de tronco nervoso, acompanhada ou não de espessamento e sem associação com o quadro cutâneo observado na reação tipo I ou tipo II (revisto por Nery e col., 2006). Os episódios reacionais podem levar a piora do quadro clínico dos pacientes, aumentando o dano neural e contribuindo para a instalação de incapacidades e deformidades físicas. Por inúmeras vezes as manifestações clínicas oriundas dos quadros reacionais levam o paciente a procurar ajuda médica e, só então, a doença é diagnosticada.

Nery e colaboradores (1998) verificaram que 57% dos pacientes multibacilares, incluídos no estudo, evoluíram para algum dos quadros reacionais durante o tratamento poliquimioterápico. Também foi observado que 91% dos pacientes LL apresentaram eritema nodoso, enquanto 93% dos pacientes BB e 57% dos pacientes BL apresentaram reação reversa.

1.5.1 Reação Tipo I

A reação tipo I ou reversa é mais comum em pacientes com as formas *borderline* (Van Brakel e col., 1994; Nery e col., 1998) e estima-se que cerca de um terço destes pacientes pode apresentar este tipo de episódio reacional, principalmente nos primeiros seis meses de PQT (Lienhardt e col., 1994). A RR caracteriza-se pela inflamação aguda das lesões de pele pré-existentes, tornando-as eritematosas e edematosas. As máculas tornam-se placas e podem evoluir com descamação (Figura 4). Podem surgir novas lesões assemelhando-se às demais. Também pode ser observado edema de mãos, pés e face. Geralmente, estas manifestações são localizadas, com neurites isoladas ou acompanhadas de lesões cutâneas, independentemente da forma clínica do paciente. Dados histopatológicos das lesões de pele de pacientes com RR revelam a expansão do granuloma com um aumento do número de células epitelióides, células gigantes multinucleadas e linfócitos, além da redução do número de bacilos. A duração deste

quadro reacional pode variar de semanas a meses (revisto por Foss, 2003; Nery e col., 2006). De modo geral, não são observadas alterações hematológicas e bioquímicas em exames laboratoriais durante a RR.

Figura 4: Aspecto de lesão cutânea em paciente com reação tipo I (Walker e Lockwood, 2006).

A perda da função sensitivo-motora é uma das mais frequentes e graves consequências da RR, devido ao espessamento neural. O acometimento dos nervos ulnar e tibial posterior leva à instalação súbita de mão "em garra" e pé "caído" e deve receber rápida e precoce intervenção para evitar que se tornem alterações permanentes (Van Brakel e Khawas, 1994; Croft e col., 1999).

O processo que leva ao surgimento da RR tem sido associado a uma súbita reativação da resposta imune mediada por células contra antígenos do *M. leprae*, o que constitui um exemplo típico da reação de hipersensibilidade tardia ou reação tipo IV (Job, 1994). Embora a causa e os mecanismos desta reativação da resposta imune não sejam totalmente compreendidos, alguns estudos têm demonstrado que durante a RR ocorre um aumento da proliferação de linfócitos específicos contra o *M. leprae* (Godal e col., 1973; Barnetson e col., 1976). A expressão de citocinas pró-inflamatórias como IFN-γ, IL-2 e TNF-α encontra-se aumentada em lesões de pele (Yamamura e col., 1992; Khanolkar-Young e col., 1995; Little e

col., 2001), contribuindo para a formação do granuloma, aumento da atividade microbicida dos macrófagos e inflamação (Verhagen e col., 1997).

Durante a RR pode ser observado um aumento na expressão de citocinas pró-inflamatórias tanto a nível local, em lesões de pele (Verhagen e col., 1997; Moraes e col., 1999; Little e col., 2001; Atkinson e col., 2004), quanto sistêmico, em soro ou plasma (Tung e col., 1987; Moraes e col., 1999; Faber e col., 2004; Lyer e col., 2007; Stefani e col., 2009) ou, ainda, a produção *in vitro* por células mononucleares circulantes (Anderson e col., 2005). O padrão de citocinas encontrado por muitos autores indica que a RR representa um aumento espontâneo da resposta Th1. Entretanto, em conjunto, estes estudos parecem não distinguir claramente os eventos imunológicos pertinentes ao episódio reacional daqueles oriundos da inflamação, *per se* (revisto por Scollard e col., 2006). Além disso, é discutido que a análise isolada de níveis circulantes de citocinas durante a RR pode não refletir a resposta imune nas lesões, o ponto-chave dos eventos que ocorrem neste tipo de reação (Anderson e col., 2005).

Análises a partir de biópsias de pele de pacientes durante a RR demonstram o aumento da expressão de RNA mensageiro (RNA-m) para IFN-γ, TNF-α, IL-2, IL-8 e IL-12 (Yamamura e col., 1992; Moraes e col., 1999; Teles e col., 2002). A expressão de RNA-m das quimiciocinas IL-8, proteína-1 quimiotática de monócitos (MCP-1) e o fator regulado por ativação, expresso e secretado por células T normais (RANTES) também se encontra aumentada nas lesões cutâneas durante a RR (Kirkaldy e col., 2003).

Como fatores de risco para o desenvolvimento da reação reversa estão incluídos a manifestação da forma *borderline* (Lockwood e col., 1993; Van Brakel e col., 1994), detecção do DNA de *M. leprae* em lesões de pele em pacientes com uma única lesão (Souza e col., 2007), a idade (Ranque e col., 2007; Souza e col., 2007), vacinação com BCG (Montestruc, 1960; Convit e col., 1986), o grau de incapacidade apresentado pelo paciente (Schreuder, 1998) e a gravidez (Lockwood e Sinha, 1999). A presença de anticorpos anti-PGL-I concomitante com a positividade do teste de Mitsuda também foi sugerida como fator de risco e marcador da RR (Roche e col., 1997). O risco de RR é mais elevado durante o primeiro ano do tratamento com PQT nos pacientes multibacilares (Becx-Bleumink e col., 1992; Van Brakel e col., 1994) e, para os pacientes paucibacilares, os primeiros seis meses subsequentes ao término da PQT constituem, ainda, um período de risco para o desenvolvimento de RR (Becx-Bleumink e col., 1992).

O tratamento da RR deve ser realizado imediatamente com a introdução de anti-inflamatórios, especialmente, os costicosteróides, que tem como principal objetivo reduzir a reação inflamatória, especialmente a neural (revisto por Scollard e col., 2006). Prednisona (1 a 2 mg/kg/dia) deve ser introduzida e conforme avaliação médica com evidências de melhora

ou regressão clínica, a dose deve ser reduzida em intervalos e quantidades fixas (em geral, 5-10 mg/semana) até a retirada completa do medicamento.

1.5.2 Reação Tipo II

A reação tipo II ocorre com maior freqüência entre pacientes multibacilares (BL e LL), principalmente na forma lepromatosa polar (Nery e col., 1998; Pocaterra e col., 2006). Estes episódios acontecem, principalmente, durante o segundo e o terceiro ano após o início da PQT (Kumar e col., 2004) e, devido sua gravidade, constitui-se como uma das principais prioridades no manejo de pacientes com hanseníase para prevenção de incapacidades (revisto por Guerra e col., 2004).

São consideradas três variantes clínicas: (i) eritema nodoso hansênico; (ii) eritema multiforme ou polimórfico e (iii) fenômeno de Lucio (revisto por Cuevas e col., 2007). O eritema nodoso hansênico (ENH) é a forma mais comum da reação tipo II e a hipótese inicialmente aceita e mais escrita para a dinâmica do aparecimento deste quadro é a de que durante o tratamento ocorra a destruição maciça do bacilo com liberação de frações antigênicas do *M. leprae* e, subsequente indução da formação de anticorpos específicos. Este processo resultaria na reação por imuno complexo circulante (Tipo III), na classificação de Coombs e Gell (1963), com depósito de complexo antígeno-anticorpo nos espaços teciduais, vasos sanguíneos e linfáticos (Wemambu e col., 1969; Waters e col., 1972). Essas alterações imunológicas culminam com o aparecimento abrupto de nódulos e/ou placas infiltradas, avermelhadas e dolorosas (Figura 5), com posterior ulceração e formação de necrose – caracterizando o ENH necrotizante. O surgimento das lesões obedece a uma distribuição simétrica, bilateral e difusa que atinge a face, tronco e membros. Níveis sanguíneos elevados de IL-1β e TNF-α são observados (Sarno e col., 1991), relacionando-se ao comprometimento sistêmico observado no ENH, onde o paciente apresenta febre alta, perda de peso, falta de apetite, mal-estar geral com dores musculares e ósseas, edema nas extremidades do corpo e presença de nervos doloridos e espessados. As lesões pré-existentes tendem a se manter inalteradas.

Exames laboratoriais podem mostram leucocitose com neutrofilia e aumento de plaquetas e de proteínas da reação inflamatória aguda, como a proteína C reativa. Também são observados aumento das imunoglobulinas IgG e IgM, e das frações C2 e C3 do complemento. A histopatologia das lesões cutâneas evidencia infiltrado inflamatório

neutrofílico, perivascular, compatível com vasculite e numerosos bacilos fragmentados e granulosos (revisto por Foss, 2003).

Figura 5: Aspecto das lesões cutâneas durante eritema nodoso hansênico. Imagem gentilmente cedida pelo Dr. Jason Antônio Barreto do Instituto Lauro Souza Lima (ILSL), Bauru – SP.

O curso natural do ENH pode levar de uma a duas semanas, entretanto podem persistir durante anos como formas crônicas e recorrentes, tendo manifestações clínicas intermitentes ou contínuas (Trao e col., 1994), dependendo da resposta inflamatória do paciente. A avaliação clínica deve ser voltada para a investigação das alterações de pele, nervos, olhos, articulações, rins, testículos, vias aéreas superiores, entre outras. A intensidade dos quadros clínicos pode variar entre discretos, que apresentam poucas lesões sem comprometimento do estado geral do paciente, a casos graves com formação de lesões vesículo-bolhosas e que podem ulcerar e evoluir para necrose, acompanhadas de febre alta, mal-estar, cefaléia, náuseas e vômitos (revisto por Foss, 2003; Guerra e col., 2004).

A patogênese do ENH tem sido sugerida como resultante do efeito direto de citocinas inflamatórias sobre componentes dos vasos sanguíneos, levando à ativação de células endoteliais e leucócitos na derme (Sampaio, 1994). Níveis elevados de citocinas pró-inflamatórias são observados sistemicamente, em soro ou plasma (Sarno e col., 1991; Lyer e col., 2007; Stefani e col., 2009). Outros estudos, a partir de biópsias de lesões cutâneas, mostram um aumento nos níveis de RNA-m para as citocinas IFN-γ, TNF-α e IL-12 (Yamamura e col., 1992; Sreenivasan e col., 1998; Moraes e col., 1999), indicando a ativação de uma resposta celular a nível local, embora Yamamura e colaboradores (1992) tenham

evidenciado um concomitante e persistente aumento de RNA-m para citocinas com perfil de resposta Th2, como IL-4, IL-5 e IL-10.

A manifestação da forma polar lepromatosa configura um importante fator de risco para o desenvolvimento do ENH, assim como o índice baciloscópico elevado (4) (Pocaterra e col., 2006; Manandhar e col., 1999). São descritos, ainda, outros fatores, como gênero (Browne, 1963), idade adulta (Sehgal e col., 1988; Chopra e col., 1990; Manandhar e col., 1999), gravidez e lactação (Lockwood e Sinha, 1998). Outras infecções, estresse físico e imunização também são considerados fatores de risco, mas ainda sem comprovações. Pacientes multibacilares submetidos a inoculações mensais com IFN-γ durante seis meses apresentaram uma frequência de ENL maior do que aqueles que só recebiam a PQT (Sampaio e col., 1991, 1992).

Para o tratamento do ENH preconiza-se repouso e terapêutica anti-inflamatória, além da prevenção de novos episódios. A talidomida, nas doses de 100-300 mg/dia, é a droga de primeira escolha, recomendada pelo Ministério da Saúde, para o manejo do ENH agudo e recorrente. Porém, o medicamento é expressamente proibido para mulheres em idade fértil, devido ao seu efeito teratogênico, bem como em casos de associação do ENH com neurite. Nestes casos é indicado o uso de corticosteróide. A pentoxifilina tem sido administrada isoladamente ou em associação com a prednisona, e tem apresentado resultados satisfatórios (Ministério da Saúde, 1994; Lockwood, 1996; Naafs e col., 1996; Nery e col., 2000).

Existe um imenso interesse voltado para a determinação de marcadores clínicos ou laboratoriais que identifiquem pacientes com risco aumentado para o desenvolvimento dos episódios reacionais. Sobretudo como um auxílio na prevenção da instalação das incapacidades e deformidades físicas.

1.6 Neurites e dano neural na hanseníase

A lesão neural na hanseníase está correlacionada à capacidade do *M. leprae* invadir os nervos periféricos, alojando-se preferencialmente no interior de células de Schwann. O comprometimento neural está presente em todas as formas clínicas, sobretudo durante os episódios reacionais. A neuropatia é resultante do processo inflamatório decorrente da resposta imune, desenvolvida pelo indivíduo, contra antígenos do *M. leprae*; e sem dúvida, consiste o fator determinante para o aparecimento de deformidades que podem levar às incapacidades permanentes nos pacientes. Caracteriza-se pela presença de dor espontânea ou à palpação, num tronco nervoso, acompanhada ou não de comprometimento da função; ou

ainda o comprometimento isolado, com ausência de dor, conhecido por neurite silenciosa (Duncan e Pearson, 1982). Estudos mostram que existe uma correlação entre a ocorrência de neurites e o desenvolvimento de incapacidades físicas durante e, mesmo após o tratamento poliquimioterápico (Pimentel e col., 2004). Além disso, a alteração das funções sensitivas, motoras e autonômicas – provocadas pela neurite – predispõe ao dano secundário decorrente de trauma, pressão anormal e infecções (Van Brakel e Kawas, 1994; revisto por Nery e col., 2006).

Histopatologicamente, as lesões de pele de pacientes com a forma polar tuberculóide apresentam perda da integridade estrutural dos nervos afetando as fibras sensoriais e motoras levando à perda da sensibilidade. Em pacientes com a forma polar lepromatosa existe um menor envolvimento dos nervos da pele, entretanto ocorre um comprometimento mais profundo que leva principalmente à perda da função motora e, consequentemente, à paralisia. Uma grande quantidade de bacilos é encontrada no endoneuro – no interior de células de Schwann e macrófagos, e em menor grau no perineuro (revisto por Vissa e Brennan, 2002). Durante os episódios reacionais, os nervos mais afetados são o ulnar, o fibular e o tibial posterior.

Embora os mecanismos patogênicos do dano ao nervo ainda não tenham sido completamente elucidados, sabe-se que alguns fatores estão possivelmente envolvidos, tais como as alterações bioquímicas nas células de Schwann decorrentes da presença *per se* do *M. leprae*, e a resposta imune local desencadeada pela liberação de mediadores inflamatórios no nervo. Dados da OMS (1998) indicam que cerca de vinte e cinco por cento dos pacientes com hanseníase sofrem algum grau de incapacidade durante a evolução da doença e, metade destes permanece com deformidades incapacitantes ao longo da vida. Estes dados ressaltam a importância de se estudar e melhor compreender os mecanismos que desencadeiam a lesão neural na hanseníase, bem como o desenvolvimento de ferramentas terapêuticas visando um auxílio ao tratamento.

1.7 A célula de Schwann

As células de Schwann (CS) foram identificadas por Theodor Schwann (1810-1882) e constituem as células gliais do sistema nervoso periférico, onde desempenham um importante papel na homeostasia tecidual. São comparáveis aos oligodendrócitos do sistema nervoso central por compartilharem a capacidade de produção da membrana que envolve as porções alongadas do neurônio, chamada de bainha de mielina.

As CS têm origem na crista neural e, por ação das neuregulinas secretadas pelos neurônios, passam pelos estágios de CS precursora e CS imatura até chegar à CS diferenciada apresentando o fenótipo mielinizante ou não-mielinizante nos nervos maduros (Figura 6). Além das suas diferenças morfológicas, estes dois fenótipos têm expressão gênica diferenciada e, particularmente as CS mielinizantes expressam principalmente RNAm de várias proteínas da mielina, entre elas, a proteína zero (P0), a proteína básica da mielina (MBP) e periaxina. Krox-20 e POU são importantes fatores de transcrição envolvidos no processo de mielinização (revisto por Jessen e Mirsky, 1999; 2005). A formação de bainha de mielina pela CS é dependente da presença dos axônios e da lâmina basal que circunda a fibra nervosa (Bunge, 1993). Esta lâmina basal é composta principalmente por laminina-2, colágeno IV, heparan sulfato, entre outros componentes da matriz extracelular que são produzidos principalmente pela CS (revisto por Chernousov e Carey, 2000).

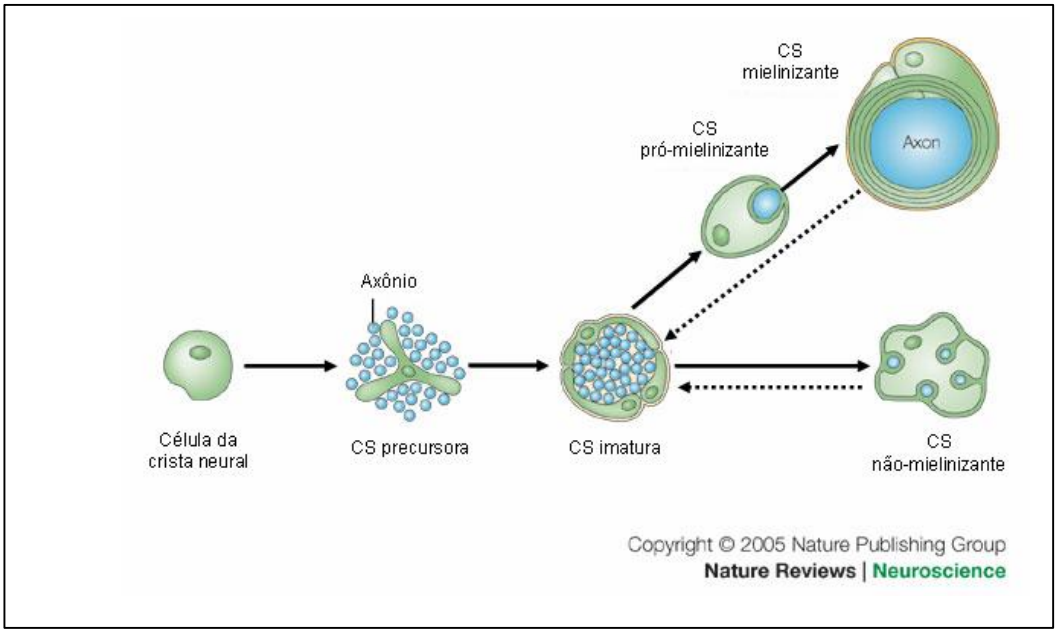

Figura 6: Principais estágios do desenvolvimento das células de Schwann. Modelo adaptado de Jessen e Mirsky (2005). Setas pontilhadas indicam que CS maduras de ambos os fenótipos podem retornar à fase imatura.

Um aspecto importante na biologia destas células e que permite sua atuação nos processos de regeneração do nervo é a sua capacidade de sobreviver mesmo na ausência do axônio. Durante o desenvolvimento dos nervos, a sinalização do axônio é essencial para a sobrevivência, proliferação e diferenciação da CS. Entretanto, CS maduras mielinizantes ou não-mielinizantes, através de um processo denominado desdiferenciação, revertem a um fenótipo imaturo, quando os axônios com os quais elas fazem contato sofrem degeneração por transecção do nervo (revisto por Mirsky e Jessen, 1999; 2005). Meier e colaboradores (1999) mostraram que enquanto CS precursoras são dependentes de fatores neuronais para a manutenção de sua sobrevivência, as CS maduras são capazes de secretar fatores de crescimento que através da sua ação autócrina e parácrina promovem sua sobrevivência. Importantes componentes destes sinais de sobrevivência são os fatores de crescimento semelhantes à Insulina (IGFs), neurotrofina-3 (NT3), endotelina e o fator de crescimento derivado de plaquetas (PDGF-BB). Este processo é crucial para a regeneração dos nervos periféricos, no qual as CS contribuem fornecendo substrato e fatores tróficos que irão permitir o apoio e o crescimento dos axônios lesionados.

Os modelos *in vitro* de cultura de CS e CS-neurônio tem oferecido importantes contribuições no entendimento não só da neurobiologia desta célula, bem como na sua interação com o nervo periférico e, eventualmente com agentes patogênicos. Entretanto a dificuldade do isolamento e purificação de CS de nervos periféricos de mamíferos adultos impõe a utilização de linhagens celulares. A linhagem de CS humanas ST88-14 foi isolada de um tumor maligno de um paciente com neurofibromatose tipo 1 (NF-1; neurofibromatose de Von Recklinghausen tipo 1) (Fletcher e col., 1991) – uma doença neurológica congênita, hereditária e autossômica dominante, caracterizada principalmente por múltiplas manchas hiperpigmentadas e neurofibromas. Estes neurofibromas são tumores benignos e que podem surgir em qualquer parte do corpo, inclusive em cavidades, sendo os de localização dérmica os mais comuns (revisto por Espig e col., 2008). As CS ST88-14 são de fácil cultivo, apresentam um bom crescimento em baixas concentrações de soro e formam múltiplas camadas. (Yan e col., 1995). Assim como as CS primárias, as células desta linhagem são positivas para os marcadores S-100, P0 e MBP (Morrissey e col., 1991; Rutkowiski e col., 1992; Ryan e col., 1994). Estudos de interação com o *M. leprae* demonstraram que a linhagem ST88-14 apresenta uma boa taxa de associação após apenas duas horas de incubação com a bactéria (Alves e col., 2004) e o mecanismo de adesão bacteriana a estas células se assemelha ao descrito em culturas primárias (Marques e col., 2000; 2001), validando, assim a utilização desta linhagem celular em modelos de estudo da interação de CS

em, pelo menos, momentos iniciais da infecção e assim como estudos da própria fisiologia da célula.

1.8 A interação do *M. leprae* com a célula de Schwann

Embora o caráter crônico da hanseníase, aliado à falta de um modelo experimental que mimetize os estágios iniciais da infecção sejam fatores limitantes, um número substancial de estudos utilizando culturas de CS ou co-culturas de CS-neurônio têm conseguido avanços importantes no que diz respeito à interação do bacilo de Hansen com sua célula hospedeira.

O tropismo do *M. leprae* pelos nervos periféricos é explicado pela aderência específica do bacilo ao domínio globular (domínio G) da cadeia $\alpha 2$ da laminina-2 – a isoforma mais abundante de laminina presente na lâmina basal e que envolve a CS (Rambukkana e col., 1997). Esta ligação parece ocorrer através de duas adesinas principais presentes na superfície do *M. leprae*: o glicolipídio fenólico-I (Ng e col., 2000) e a proteína LBP/Hlp (Shimoji e col., 1999; Marques e col., 2000). Complementando estes estudos, o complexo distroglicana (DG) foi identificado como um dos possíveis receptores de laminina-2 presentes na membrana da CS e envolvido na adesão bacteriana (Rambukkana e col.,1998).

Uma vez no interior da célula hospedeira, os efeitos do *M. leprae* sobre a fisiologia da CS ainda são pouco conhecidos. Em nosso laboratório, Alves e colaboradores (2004), verificaram que a internalizarão do *M. leprae* na CS ST88-14 é dependente de vias de sinalização celular envolvidas no processo de fagocitose. No mesmo trabalho, verificou-se a localização de bacilos viáveis em vesículas não acidificadas na CS ST88-14 e macrófagos da linhagem RAW, contrastando com a localização preferencial dos bacilos letalmente irradiados em lisossomos. Estes resultados indicam que o patógeno é capaz de modular ativamente a via endocítica na CS, inibindo a fusão fagolisossomal e favorecendo sua sobrevivência.

Estudos mais recentes mostram que CS infetadas com *M. leprae* apresentam alterações tanto na morfologia quanto na expressão de moléculas de adesão celular (Hagge *et al*., 2002). Um outro dado que indica uma modulação do metabolismo da CS pelo *M. leprae* é a observação recente em nosso laboratório mostrando uma modulação negativa da expressão do gene PHEX (gene regulador de fosfato com homologia a endopeptidases no cromossomo X) da célula hospedeira. Este gene está envolvido na regulação do metabolismo de fosfato e seu bloqueio pelo *M. leprae* pode estar associado à hipocalcemia observada nos pacientes com hanseníase (Silva e col., 2010).

Dados da literatura sugerem uma relação harmoniosa entre o *M. leprae* e a CS. Análises histopatológicas, obtidas a partir de biópsias de nervo de pacientes com a forma lepromatosa, mostram CS altamente infectadas e com aparente ausência de toxicidade ou morte celular (Antia e Shetty, 1997). Por isso, é amplamente aceito que uma vez dentro da CS o bacilo se multiplique lentamente durante anos. Mukherjee e Antia (1985) obtiveram significativa multiplicação do *M. leprae* sem evidências de toxicidade celular em culturas de gânglios de raiz dorsal (DRG) de camundongos neonatos. Rambukkana e colaboradores (2002) demonstraram que o *M. leprae* promove desmielinização contato-dependente na ausência de células do sistema imune sem causar morte das CS. Ao contrário, diante deste efeito direto do *M. leprae*, as CS proliferam em decorrência da ativação da via de sinalização Erk 1/2, e mantêm a infecção por um longo período (Tapinos e Rambukkana, 2005). Em virtude da desmielinização, as CS entrariam no processo e desdiferenciação, garantindo um aumento do número de CS amielínicas, que constituem as células hospedeiras preferenciais do bacilo. O fato das CS mielinizantes serem extremamente resistentes à invasão pelo *M. leprae* reforçam a hipótese de que o processo de desmielinização por esta micobactéria constitui uma interessante estratégia de sobrevivência. Os dados mencionados sugerem que pelo menos no início da infecção, quando o infiltrado inflamatório ainda é escasso no nervo, pode existir uma relação harmoniosa entre o *M. leprae* e a célula hospedeira, permitindo assim a manutenção de um nicho favorável para sua sobrevivência e proliferação.

A interação do *M. leprae* com a CS durante a fase inicial da infecção constitui uma etapa crucial para o estabelecimento e disseminação da doença. Desse modo, a compreensão das estratégias utilizadas pelo *M. leprae* para a colonização bem sucedida do nervo periférico pode ser utilizada no desenvolvimento de novas ferramentas para o controle desta doença.

2. Apoptose e infecções

Apoptose é um mecanismo muito bem regulado de morte celular geneticamente programada e tem um papel crucial na homeostasia dos tecidos, além de participar da patogênese de certo número de doenças. Na hanseníase, pouco se sabe sobre a interação do *M. leprae* com a CS, no que diz respeito à modulação das vias apoptóticas na célula hospedeira. Na literatura, são encontrados vários trabalhos mostrando que a modulação da apoptose da célula hospedeira representa uma importante estratégia de sobrevivência de patógenos intracelulares. A seguir, uma breve descrição das características deste tipo de morte celular e as vias de sinalização envolvidas neste processo.

Em 1972, Kerr e seus colaboradores, sugeriram o termo grego "*apoptosis*", que significa "o ato de cair" – usado em referência às folhas das árvores que caem no outono – para designar "perdas necessárias", indicando que este tipo de morte celular tem papel importante para a manutenção e desenvolvimento dos seres vivos. A apoptose é caracterizada por alterações morfológicas e bioquímicas marcantes e coordenadas: inicialmente ocorre a ativação de caspases que leva a alteração no potencial da membrana mitocondrial acompanhada do aumento intracelular de Ca^{++} e do pH. Consequentemente, a perda da permeabilidade da membrana externa da mitocôndria permite a liberação de proteínas para o citoplasma, incluindo citocromo c e outros fatores pró-apoptóticos. Paralelamente, é observada a retração da célula que leva à perda da aderência com a matriz extracelular e células vizinhas. A ativação de endonucleases específicas leva à clivagem da cromatina em fragmentos de aproximadamente 200pb e finalmente, o processo culmina com a desintegração da célula em corpos apoptóticos (revisto por Vermes e col., 2000). A perda da assimetria lipídica, observada pela translocação de resíduos de fosfatidilserina (PS) para a camada externa na membrana plasmática sinaliza para a opsonização dos corpos apoptóticos, sem que um processo inflamatório seja iniciado (revisto por Holdenrieder e Stieber, 2004; Grivicich e col., 2007).

As caspases são, reconhecidamente, moléculas-chave na cascata que leva a apoptose. Estas proteínas pertencem à família das cisteínas proteases (possuem uma cisteína no sítio ativo) que têm a capacidade de reconhecer e clivar substratos que possuam resíduos de aspartato (Nicholson e Thornberry, 1997). As caspases são sintetizadas como precursores inativos denominados zimogênios (Hengartner, 2000) e, após um sinal de morte celular, são ativadas por clivagem proteolítica e, finalmente levam à condensação e fragmentação nuclear e externalização de PS de membrana para reconhecimento da célula apoptótica pelos macrófagos (revisto por Grivicich e col., 2007). A morte celular por apoptose, mediada pela

ativação de caspases, tem sido extensivamente estudada e, atualmente três vias sinalizadoras de apoptose são aceitas de acordo com a caspase iniciadora ativada. São elas: a via dos receptores de morte ou extrínseca, utilizando a caspase-8; a via mitocondrial ou intrínseca, na qual a liberação de proteínas do interior da mitocôndria leva à ativação de caspase-9 (Figura 7) e a via de estresse do retículo endoplasmático (que utiliza a via mitocondrial), atribuída à ativação de caspase-12 (revisto por Guimarães e Linden, 2004).

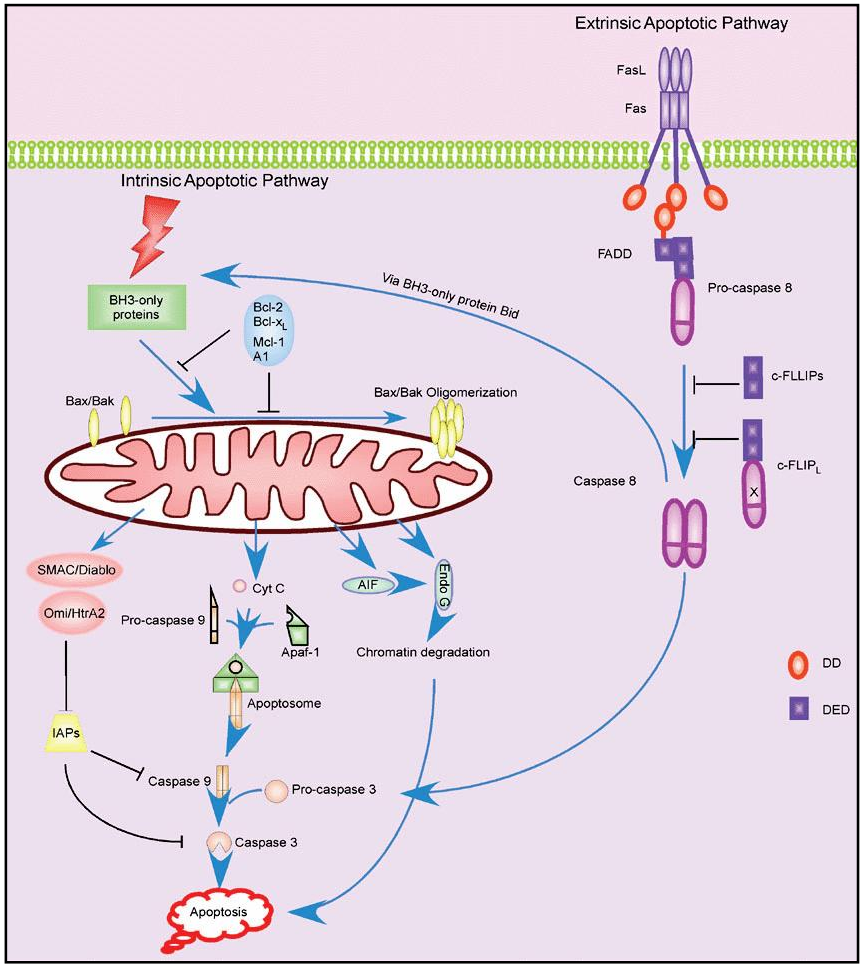

Figura 7: Vias sinalizadoras de apoptose. A via intrínseca ou mitocondrial é ativada por estresse intracelular, ausência de fatores de crescimento e controlada por membros da família Bcl-2. Já a via extrínseca é ativada pela ligação de "sinais de morte" aos receptores cognatos na superfície celular (Zhang e col., 2005).

A via intrínseca é ativada por estresse intracelular, danos ao DNA ou ausência de fatores de crescimento. Nesta via, os estímulos que levam à morte celular convergem para a mitocôndria – principal mediador deste tipo de morte. Ocorre a indução de permeabilização da membrana externa da mitocôndria seguida pela liberação de citocromo c, Smac/Diablo, AIF ("apoptosis inducing factor") e endonuclease G. O citocromo c é normalmente

encontrado na face interna da membrana mitocondrial e está associado com cardiolipinas, exclusivamente encontradas na mitocôndria. Os membros da família Bcl-2, como Bcl-2 e Bcl-XL inibem a apoptose por prevenirem a liberação de citocromo c e são consideradas proteínas anti-apoptóticos (revisto por Hengartner, 2000). Evidências sugerem que a dissociação de citocromo c das cardiolipinas é uma etapa crítica para a liberação de citocromo c para o citosol e a indução de apoptose (Orrenius, 2004). Após sua liberação, o citocromo c forma um complexo denominado apoptossomo, contendo Apaf-1 ("apoptosis protease-activing factor-1"), o iniciador pró-caspase-9 e o citocromo c. Este complexo leva à clivagem de pró-caspase-9 e inicia a cascata de caspases efetoras como pró-caspases–3, –6 e –7. A liberação de Smac/Diablo contribui para a inibição de IAPs ("apoptotics proteins"), impedindo a ativação de caspases pelo bloqueio da clivagem destas pró-enzimas. A translocação do AIF para o núcleo inicia a condensação da cromatina e, finalmente, à fragmentação do DNA (revisto por Martinvalet e col., 2005).

A via extrínseca é desencadeada pela ligação de ligantes específicos aos receptores de morte pertencentes à superfamília de genes do TNF, são eles: Fas (CD95 ou Apo-1), TNF-R1, DR3 (Apo-3), DR4 e DR5 (Apo-2) e que estão localizados na superfície celular. Os ligantes que ativam estes receptores são moléculas estruturalmente relacionadas, também pertencentes à superfamília do TNF, tais como: FasL (ligante de Fas), TNF-α, linfotoxina-α, Apo3L, Apo2L ou TRAIL (Ashkenazi e Dixit, 1998). Estes ligantes específicos induzem a trimerização do receptor e ocorre a associação de proteínas intracelulares aos domínios de morte. No caso dos receptores Fas/Apo1/CD95, a pró-caspase 8 se associa ao complexo formado e é ativada por autoclivagem. Logo após, caspases efetoras são ativadas levando a célula à apoptose (Wallach e col., 1999) (Figura 7).

Além da ausência de fatores de crescimento e dos receptores de morte, agentes patogênicos também podem induzir o processo de morte celular por apoptose, bem como inibi-lo para seu próprio benefício (revisto por Knodler e Finlay, 2001) durante o processo infeccioso, conforme será discutido a seguir.

2.1 Modulação da apoptose em processos infecciosos

Crescentes evidências têm demonstrado que a apoptose tem um importante papel na patogênese de uma variedade de infecções. As estratégias utilizadas por patógenos para invadir, proliferar e, eventualmente, escapar da célula hospedeira têm sido descritas ao longo dos anos. Patógenos intracelulares facultativos parecem induzir a apoptose da célula hospedeira (Mills e col., 1993; Muller e col., 1996; Kwaik, 1998) numa tentativa de escape frente à extinção de nutrientes. Enquanto isso, patógenos intracelulares obrigatórios ativamente inibem as vias sinalizadoras de apoptose da célula hospedeira como garantia do estabelecimento de um nicho favorável à sua replicação e sobrevivência. Na literatura encontramos diversos exemplos de bactérias intracelulares obrigatórias, incluindo *Rickettsia rickettsii* (Clifton e col., 1998), *Chlamydia trachomatis* (Fan e col., 1998), *Chlamydia psittaci* (Coutinho-Silva e col., 2001) e *Chlamydia pneumoniae* (Rajalingam e col., 2001) que ativamente bloqueiam a apoptose em suas células hospedeiras.

Sabe-se que a virulência das micobactérias está intimamente relacionada à sua capacidade de interferir na maquinaria da célula hospedeira e sobreviver dentro do fagossomo, como uma alternativa para garantir sua disseminação. Vários trabalhos descrevem a capacidade de *M. tuberculosis* (Malik e col., 2003; Maiti e col., 2001) e moléculas relacionadas como LAM (Vergne e col., 2003) e fosfatidilinositol (Fratti e col., 2003), em prevenir a maturação do fagossomo e, ainda, prevenir a apoptose da célula hospedeira (Velmurugan e col., 2007).

Em 2003, Hernandez e colaboradores demonstraram a indução de apoptose em macrófagos humanos infectados com *M. leprae*. Ainda neste trabalho, os autores demonstraram a expressão de RNA mensageiro para os genes Bax e Bak, que estão diretamente envolvidos na regulação da apoptose. Em contraste, o *M. leprae* parece inibir a apoptose de células da linhagem THP-1, diferentemente da infecção com BCG, através da regulação negativa de genes pró-apoptóticos como Bad e Bak e induzindo membros anti-apoptóticos da família Bcl-2, como Mcl-1 (Hasan e col., 2006). A infecção com *M. leprae* viável purificado de camundongos *nude* não foi capaz de induzir apoptose de macrófagos (Lahiri e col., 2010). Na interação do *M. leprae* com CS, Silva e colaboradores (2008) verificaram que o bacilo induz baixos níveis de apoptose em CS da linhagem ST88-14. Entretanto a lipoproteína 16 kDa do *M. leprae* ou alta infecção foram capazes de induzir apoptose em CS (Oliveira e col., 2003; 2005).

3. O sistema de fatores de crescimento semelhantes à Insulina

Os fatores de crescimento semelhante à insulina (IGFs) constituem um complexo sistema de hormônios peptídicos (IGF-I e IGF-II), receptores de membrana (IGF-1R e IGF-2R) e proteínas ligantes (IGFBPs 1-6) que regulam positiva ou negativamente a ligação dos IGFs aos seus receptores. Os IGFs são polipeptídios, com massa molecular de aproximadamente 7,5 kDa, que possuem propriedades pleiotrópicas que incluem ações biológicas como crescimento, proliferação, prevenção de apoptose, diferenciação celular, migração, além de efeitos no metabolismo, tais como síntese de proteínas (revisto por Denley e col., 2005). Tais ações, comuns a IGF-I e IGF-II, são mediadas, principalmente, pelo receptor tipo 1 (IGF-1R) – uma glicoproteína composta de duas subunidades extracelulares (α) e duas transmembranares (β), cujo domínio intracelular é uma tirosina quinase que apresenta cerca de 80% de similaridade estrutural com o receptor de insulina. O domínio intracelular de IGF-1R fosforila muitos substratos celulares desencadeando a ativação, principalmente, de duas vias de transdução de sinal: MAPK (proteínas quinases ativadas por mitógenos) e PI3-K (fosfatidilinositol 3-quinase), especialmente implicadas na indução de proliferação celular e inibição de apoptose. O estudo das ações mediadas principalmente por IGF-I vem ganhando destaque devido seu papel neuroprotetor *in vivo* em neuropatias onde a produção excessiva de citocinas pró-inflamatórias é observada (Venters e col., 2000; revisto por O´Connor e col., 2008).

A maioria do IGF-I circulante tem origem no fígado sob regulação do hormônio do crescimento (GH). Este, por sua vez, é produzido pela glândula pituitária (ou hipófise) sob regulação de fatores hipotalâmicos (revisto por Clemmons, 2007). Na circulação, IGF-I atua como um fator endócrino no controle do crescimento e metabolismo através do chamado eixo somatotrófico (GH-IGF-I), mas pode também ser produzido por diferentes tecidos agindo de maneira autócrina e parácrina com um fator de crescimento (Russo e col., 2005).

Em indivíduos sadios, IGF-I circula em concentrações relativamente altas, variando de 150 a 400ng/mL de acordo com a idade (Clemmons, 2007). Durante a puberdade apresentam os maiores picos de sua produção e declinam com o avanço da idade (Rudman e col., 1990; Jones e Clemmons, 1995), como resultado da secreção reduzida de GH (Rosen e Conover, 1997). Cerca de 90% do IGF-I circulante encontra-se ligado a IGFBP-3 – a principal proteína ligadora de IGF-I (Jones e Clemmons, 1995) – formando um complexo ternário com a subunidade ácido-lábil (ALS), servindo como o principal reservatório de IGF-I no plasma (Baxter, 2000). Este complexo altera a meia-vida do IGF-I livre de menos de 15 minutos para

16 horas. Todos os três componentes deste complexo trimérico são sintetizados pelo fígado sob regulação do GH.

Diferentes fatores podem determinar a concentração e biodisponibilidade do IGF-I circulante, agindo basicamente através de duas formas: (a) diretamente, como o GH, a insulina, o "status" nutricional e transtornos alimentares (anorexia/bulimia), condições patológicas (por exemplo, sepse), hormônios tireoidianos e afinidade de ligação da ALS pelo complexo IGF-I-IGFBP-3; (b) indiretamente, podemos citar a idade, prática de exercícios físicos, hormônios sexuais ou provenientes da glândula adrenal e citocinas inflamatórias (revisto por Rosen e Pollak, 1999; Clifford e Pollak, 1999; O`Connor e col., 2008). Fatores genéticos podem também estar relacionados com a variação dos níveis de IGF-I, conforme sugerido por trabalhos de Rosen e colaboradores (1997; 1998) que investigaram polimorfismos em pequenas regiões do gene IGF-I.

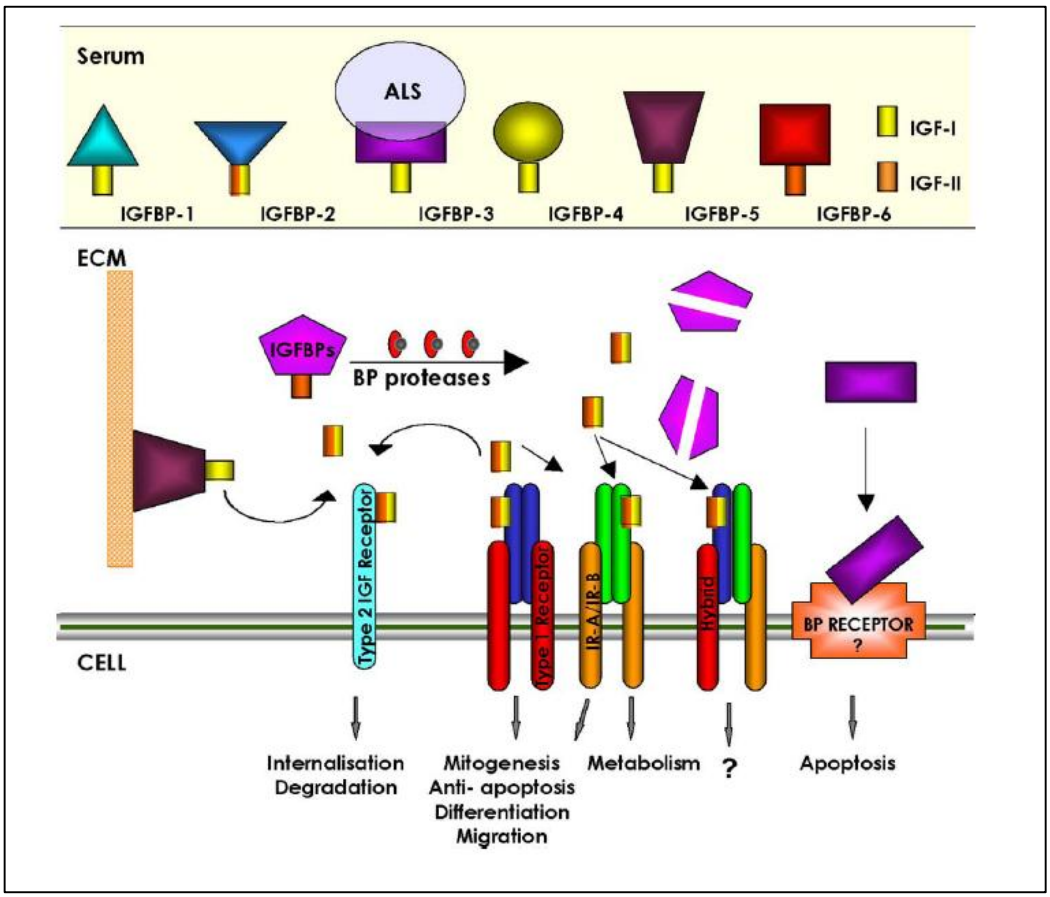

Figura 8: Esquema do sistema de fatores de crescimento semelhante à Insulina. O sistema IGF é constituído pelos receptores (IGF-1R, duas isoformas híbridas do receptor tipo 1 e IGF-2R), os polipeptídios IGF-I e IGF-II e seis proteínas ligadoras, IGFBP-1 a -6. Os IGFs circulam predominantemente em complexos formados por IGF-IGFBP-subunidade ácido-lábil (ALS), o que prolonga a meia-vida dos IGFs. IGF-2R modula a biodisponibilidade de IGF-II (Denley e col., 2005).

3.1 IGF-I e ações como fator de crescimento

Embora a origem primária da produção de IGF-I seja a célula hepática, este hormônio polipeptídico pode ser produzido por muitos tipos celulares e exercer, além das funções endócrinas, efeitos autócrinos e parácrinos como fatores de crescimento para os tecidos. Uma das primeiras ações biológicas de IGF-I descritas foi o efeito na proliferação celular (Svoboda e col., 1980). Além desta, outras funções igualmente importantes são também atribuídas a este fator de crescimento, como inibição de apoptose e indução de diferenciação. É importante ressaltar que todas estas ações são mediadas pelo receptor IGF-1R, que após ligação com IGF-I, ativa vias de sinalização envolvidas na regulação na proliferação, inibição de apoptose e diferenciação.

Em processos de regeneração do nervo, IGF-I pode ser secretado por CS, monócitos/macrófagos, células musculares e endoteliais. Além disso, podem afetar a ativação de CS no auxílio ao alongamento do axônio (revisto por Rabinovsky, 2004) e induzir produção de mielina (Cheng e col., 1999).

A ação anti-apoptótica de IGF-I sobre as CS foi inicialmente descrita por Delaney e colaboradores (1999). Os autores utilizaram como modelo células de Schwann isoladas de nervo ciático de ratos e verificaram que IGF-I promoveu a sobrevivência de CS cultivadas em meio sem soro por até três dias. Neste estudo, também evidenciaram que o hormônio IGF-I utiliza a via de sinalização PI3-K para prevenir a ativação de caspase-3, que ocorre rapidamente após a retirada de soro. Muitos processos celulares são regulados por esta via, como metabolismo e transporte de glicose, síntese de proteínas, mitose e diferenciação (Marte e col., 1997), além de estar especialmente relacionada à inibição de apoptose (revisto por Butler e col., 1998; e por Kooijman, 2006). Ainda em 1999, Syroid e colaboradores utilizaram o mesmo modelo descrito por Delaney e colaboradores (1999) para mostrar a participação de IGF-I na regulação da sobrevivência de CS mediada por seu receptor específico IGF-IR. Um componente integral da via PI3-K é a proteína quinase B (PKB), também chamada de Akt (serina/treonina quinase), pode ser estimulada pelo IGF-1R. Estudos mostram que a prevenção de apoptose mediada por IGF-I é diminuída em células expressando um dominante negativo de Akt (Dudek e col., 1997; Kulik e Weber, 1997). Adicionalmente, estudos *in vitro* demonstram que o tratamento de oligodendrócitos com IGF-I previne a apoptose induzida por TNF-α (Ye e D´Ercole, 1999). Outras evidências reforçam o papel anti-apoptótico e neuroprotetor de IGF-I frente ao TNF-α (Wang e col., 2003). Estas evidências indicam o IGF-I como um potencial candidato em estratégias terapêuticas em desordens neurológicas.

No contexto de infecções, relatos recentes indicam que IGF-I favorece a infecção por *Leishmania amazonensis*, um patógeno intracelular obrigatório que infecta macrófagos. Estudos *in vitro* demonstraram um aumento do tamanho de lesões de pele de camundongos infectados com formas promastigostas de *Leishmania* pré-tratadas com IGF-I, além de um aumento na proliferação deste parasita (Goto e col., 1998; Gomes e col., 2000). Estudos posteriores provenientes do mesmo grupo demonstraram que IGF-I atua diretamente como um fator de crescimento para *Leishmania amazonensis*, além de bloquear a ativação de macrófagos e modular a resposta inflamatória local (Gomes e col., 2001; Vendrame e col., 2007).

3.2 Interação entre o eixo GH-IGF-IGFBP e o sistema imune

As interações entre o sistema neuro-endócrino e o sistema imune desempenham um papel crítico na manutenção da homeostasia do organismo durante os mais variados processos inflamatórios. Neste contexto, um crescente entendimento do controle da inflamação pelo sistema neuro-endócrino vem proporcionando avanços importantes no entendimento sobre a fisiopatogenia de uma gama de doenças imuno-inflamatórias. No sistema nervoso central (SNC) têm sido mostradas propriedades antagônicas do IGF-I em relação ao TNF-α (Ye & D´Ercole, 1999; Wang e col., 2003), indicando que um balanço entre os sistemas endócrino e imunológico é essencial para a manutenção da homeostasia tecidual.

Um dos principais mecanismos de regulação recíproca entre estes sistemas se dá através da ativação do eixo hipotálamo-pituitária-adrenal (HPA) por citocinas pró-inflamatórias, com a consequente secreção de glicocorticóides pela glândula adrenal que, por sua vez, inibem a resposta imune e inflamatória garantindo o retorno do organismo à homeostasia (revisto por Borghetti e col., 2009). A inflamação igualmente regula a atividade do eixo somatotrófico (GH-IGF-IGFBP). Estes hormônios não só alteram o metabolismo celular, mas também interagem com as citocinas e glicocorticóides modulando a resposta imune e inflamatória. Particularmente em infecções persistentes ou inflamações sistêmicas ocorre uma inibição do eixo GH-IGF-IGFBP com a consequente diminuição dos níveis de IGF-I. Este perfil diferenciado leva à imunossupressão e contribui para o desenvolvimento de distúrbios endócrino-metabólicos em diversas patologias (revisto por Mesotten e Van den Bergue, 2006; Borghetti e col., 2009), conforme descrito a seguir.

3.3 IGF-I circulante em situações patológicas

Vários trabalhos têm associado alterações dos níveis circulantes de IGF-I com muitas doenças crônicas e outros estados patológicos. Níveis elevados de IGF-I são observados na acromegalia e diferentes tipos de câncer, sendo inclusive para este último um indicador de risco quando associados a outros fatores (Chan e col., 1998). Já os níveis reduzidos de IGF-I podem ser explicados por numerosas condições, tais como deficiência de GH, má nutrição, sepse (Karinch e col., 2001) e caquexia (devido ao importante papel de IGF-I na manutenção da massa músculo-esquelética) provocada por diversos distúrbios como câncer ou doenças infecciosas como a tuberculose e a síndrome da imunodeficiência adquirida (AIDS) (Spinola-Castro e col., 2008).

Ao longo das últimas décadas, inúmeros trabalhos vêm apontando que a interação entre o sistema IGF e citocinas pró-inflamatórias é crítica e, muitas vezes determinante, na evolução de diferentes patologias. Foram observados níveis plasmáticos elevados de TNF-α, IL-1β, IL-6 e IL-8 em pacientes com doença obstrutiva pulmonar crônica, enquanto os níveis de IGF-I encontravam-se diminuídos durante a fase a aguda da doença (Kythreotis e col., 2009). Em pacientes com Alzheimer, os níveis séricos de TNF-α são elevados e negativamente correlacionados com IGF-I (Alvarez e col., 2007). Também foi mostrado que em pacientes com HIV, o grau de neurodegeneração em consequência da elevada produção de TNF-α foi correlacionado à redução dos níveis séricos de IGF-I (Jain e col., 1998; Laue e col., 1990).

Os níveis circulantes de IGF-I também se encontram alterados em diversas doenças causadas por bactérias e parasitos. Bariceviæe colaboradores (2004) mostraram que pacientes infectados com *Helicobacter pylori* apresentam níveis circulantes de IGF-I reduzidos em associação com elevados níveis de cortisol – um indicador da expressão de citocinas pró-inflamátórias. Nos quadros de sepse, os níveis de IGF-I também se encontram diminuídos (Karinch e col., 2001; Ashare e col., 2008).

As ações pleiotrópicas de IGF-I e as evidências de sua interação com processos inflamatórios e infecciosos nos levaram a investigar a possível participação do sistema IGF na fisiopatogenia da hanseníase, não só na relação direta do *M. leprae* com a célula hospedeira, como também durante a evolução natural da doença. A compreensão das estratégias utilizadas pela bactéria para a colonização bem sucedida do nervo periférico pode ser utilizada no desenvolvimento de novas ferramentas no controle da doença.

CAPÍTULO 2: Objetivos

Objetivo Geral:

Avaliar a participação dos fatores de crescimento semelhantes à Insulina (IGFs) na fisiopatogenia da hanseníase.

Objetivos Específicos:

- Analisar a ativação de caspase-3 em culturas de células de Schwann (CS) estimuladas com *M. leprae* e mantidas em meio sem soro;

- Comparar a capacidade de proliferação de CS humanas estimuladas ou não com *M. leprae* e cultivadas em meio sem soro;

- Investigar a capacidade do *M. leprae* modular a expressão de RNA mensageiro para IGF-I e IGF-II em células de Schwann humanas;

- Quantificar os níveis de IGF-I em sobrenadantes de culturas de células de Schwann humanas estimuladas ou não com *M. leprae*;

- Determinar os níveis séricos de IGF-I, IGFBP-3 e TNF-α em indivíduos sadios, pacientes com hanseníase antes e durante os episódios reacionais e, ainda, comparar estes níveis com aqueles observados em pacientes que não sofreram reação;

- Avaliar se os níveis de IGF-I e IGFBP-3 observados nos pacientes encontram-se dentro da faixa de normalidade definida por sexo e idade.

CAPÍTULO 3: Resultados

Mycobacterium leprae induces insulin-like growth factor and promotes survival of Schwann cells upon serum withdrawal

Luciana Silva Rodrigues[1], Elisa da Silva Maeda[1], Maria Elizabete da Costa Moreira[2], Antônio Jorge Tempone[1], Lívia Silva Lobato[1], Victor Túlio Ribeiro Resende[1], Lucinéia Alves[1], Shaila Rossle[3], Ulysses Gazos Lopes[3] and Maria Cristina Vidal Pessolani[1].

[1]Laboratório de Microbiologia Celular, Instituto Oswaldo Cruz, Rio de Janeiro, RJ – Brasil; [2]Laboratório de Medicina Experimental, Instituto Nacional do Câncer, Rio de Janeiro, RJ – Brasil; [3]Laboratório de Parasitologia Molecular, Instituto de Biofísica Carlos Chagas Filho, Universidade Federal do Rio de Janeiro (UFRJ), Rio de Janeiro, RJ – Brasil.

Cellular Microbiology. 2010. 12 (1): 42-54

Mycobacterium leprae induz o fator de crescimento semelhante à Insulina-I e promove a sobrevivência de células de Schwann após remoção de soro

A invasão da célula de Schwann pelo *M. leprae*, sem dúvida, representa um ponto-chave na interação patógeno-célula hospedeira e os mecanismos desencadeados a partir desta irão contribuir ou não para o estabelecimento bem sucedido da infecção. Estudos vêm demonstrando que, pelo menos, no início da infecção existe uma relação harmoniosa, onde as CS suportam a multiplicação do *M. leprae* sem evidências de toxicidade celular, entretanto pouco se sabe a respeito dos mecanismos utilizados pelo bacilo para colonizar os nervos periféricos.

Nosso estudo teve início no mestrado que foi concluído em 2005, onde investigamos se, à semelhança do observado na literatura com outros patógenos intracelulares obrigatórios, o *M. leprae* teria um efeito anti-apoptótico sobre a célula hospedeira e, para isto, inicialmente estabelecemos um modelo de indução de apoptose na linhagem de CS humana ST88-14. Como a privação de fatores de crescimento do meio através da remoção de soro é classicamente utilizada em estudos de indução de morte celular por apoptose em CS (Delaney e col., 1999; Syroid e col., 1999; Chuenkova e col., 2001), utilizamos este protocolo com as células ST88-14. Avaliamos a viabilidade das culturas em meio sem soro através de quatro métodos: i) avaliação da capacidade das células viáveis em reduzir o sal metiltetrazólio (MTT) – ensaio colorimétrico; ii) avaliação do potencial da membrana mitocondrial por citometria de fluxo, utilizando o corante iodeto de 3,3-dihexyloxacarbocianina ($DiOC_6$); iii) exclusão de azul de Tripan e iv) avaliação da morfologia nuclear utilizando o corante bis-benzemida. Através destes ensaios demonstramos que o *M. leprae* é capaz de proteger as CS ST88-14 de morte celular induzida por carência de soro e, verificamos, ainda, que fatores solúveis secretados pela célula incubada com *M. leprae* estavam envolvidos nesta proteção, visto que o meio condicionado proveniente de culturas tratadas com a bactéria promovia a sobrevivência das CS. Possíveis candidatos para este efeito protetor seriam os fatores de crescimento semelhantes à Insulina, IGF-I e IGF-II. Confirmamos, então, a capacidade do *M. leprae* induzir a expressão de IGF-I e IGF-II em CS ST88-14 através da técnica de RT-PCR semiquantitativo. Demonstramos também a expressão do receptor IGF-1R nas células ST88-14 e, que a adição de IGF-I recombinante às culturas foi capaz de proteger as CS de morte induzida por remoção de soro (Rodrigues, 2005). Estudos posteriores realizados também em nosso laboratório evidenciaram que o efeito anti-apoptótico sobre as CS ST88-14 é específico, no qual o pré-tratamento das culturas com *Mycobacterium smegmatis* ou *Mycobacterium*

bovis BCG, diferentemente do observado com *M. leprae*, foram incapazes de proteger as CS de morte celular induzida por remoção de soro. Adicionalmente, em ensaios de sobrevivência utilizando anticorpos neutralizantes contra IGF-I, IGF-II e IGF-1R, foi verificado que o efeito anti-apoptótico do *M. leprae* era abolido. Estes dados indicaram que o efeito protetor do *M. leprae* sobre a CS era dependente do sistema IGF. Os estudos foram estendidos às CS primárias humanas, onde foi demonstrada uma capacidade semelhante do *M. leprae* em proteger estas células de apoptose induzida por privação de soro (Maeda, 2008).

Nestes dois estudos, entretanto, ainda não havíamos demonstrado a interferência do *M. leprae* na cascata de ativação de caspases – proteínas-chave na sinalização de apoptose, bem como na secreção de IGF-I pelas CS primárias ou da linhagem ST88-14. Desse modo, no início do doutorado buscamos complementar os resultados previamente obtidos: avaliamos a capacidade proliferativa de CS pré-tratadas com *M. leprae* e mantidas em meio sem soro; confirmamos dados de expressão gênica por RT-PCR quantitativo em CS ST88-14; estendemos a análise às CS primárias e, finalmente, utilizando ensaio imunoenzimático (ELISA) específico, detectamos a secreção de IGF-I em culturas de CS estimuladas com *M. leprae*. O conjunto de dados obtidos ao longo de todo este período originou o artigo a seguir.

Cellular Microbiology (2010) **12**(1), 42–54
doi:10.1111/j.1462-5822.2009.01377.x
First published online 25 September 2009

Mycobacterium leprae induces insulin-like growth factor and promotes survival of Schwann cells upon serum withdrawal

Luciana Silva Rodrigues,[1] Elisa da Silva Maeda,[1] Maria Elisabete Costa Moreira,[2] Antonio Jorge Tempone,[1] Lívia Silva Lobato,[1] Victor Túlio Ribeiro-Resende,[1] Lucineia Alves,[1] Shaila Rossle,[3] Ulisses Gazos Lopes[3] and Maria Cristina Vidal Pessolani[1]*

[1]*Laboratory of Cellular Microbiology, Instituto Oswaldo Cruz, Rio de Janeiro, RJ 21045-900, Brazil.*
[2]*Laboratory of Experimental Medicine, Instituto Nacional do Câncer, Rio de Janeiro, RJ 20230-130, Brazil.*
[3]*Laboratory of Molecular Parasitology, Instituto de Biofísica Carlos Chagas Filho, UFRJ, Rio de Janeiro, RJ 21941-902, Brazil.*

Summary

Peripheral nerve lesions are considered the most relevant symptoms of leprosy, a chronic infectious disease caused by *Mycobacterium leprae*. The strategies employed by *M. leprae* to infect and multiply inside Schwann cells (SCs), however, remain poorly understood. In this study, it is shown that treatment of SCs with *M. leprae* significantly decreased cell death induced by serum deprivation. Not displayed by *Mycobacterium smegmatis* or *Mycobacterium bovis BCG*, the *M. leprae* survival effect was both dose dependent and specific. The conditioned medium (CM) of *M. leprae*-treated cultures was seen to mimic the protective effect of the bacteria, suggesting that soluble factors secreted by SCs in response to *M. leprae* were involved in cell survival. Indeed, by quantitative RT-PCR and dot blot/ELISA, it was demonstrated that *M. leprae* induced the expression and secretion of the SC survival factor insulin-like growth factor-I. Finally, the involvement of this hormone in *M. leprae*-induced SC survival was confirmed in experiments with neutralizing antibodies. Taken together, the results of this study delineate an important strategy for the successful colonization of *M. leprae* in the nerve based on the survival maintenance of the host cell through induction of IGF-I production.

Introduction

Leprosy, one of the oldest recorded diseases, remains an important cause of morbidity with approximately 250 000 new cases per year (http://www.who.int/lep). *Mycobacterium leprae*, the causative agent of leprosy, is an obligate intracellular pathogen. Although, in 1873, *M. leprae* was the first bacterium to be described as a causal agent of a human infectious disease, deciphering the biology of this bacterium has constituted one of the greatest challenges facing microbiologists due to its unique features. Multiple attempts to grow *M. leprae* in axenic or tissue cultures have all been in vain; and, today, infected nine-banded armadillo and athymic nude mouse constitute the major sources of bacteria for biochemical and physiological studies.

It is known that the primary targets of *M. leprae* are Schwann cells (SCs) located in the peripheral nervous system. Nonetheless, the strategies employed by *M. leprae* to infect and multiply inside SCs continue to be poorly understood. Observations have shown that SCs appear to constitute appropriate niches for *M. leprae* survival and replication (Scollard *et al*., 2006). This tissue tropism causes nerve damage, which, in turn, leads to sensorial impairment and permanent disabilities, by far the major problems facing leprosy patients.

But, despite the proven efficiency of antibiotic therapy in killing *M. leprae*, it is unfortunate that treatment is often initiated after nerve damage has begun its course. Moreover, it has been shown that nerve damage continues to evolve even during treatment and subsequent to patient release due, for the most part, to the occurrence of reactional episodes (Sarno and Pessolani, 2001). In light of the above, it is undisputed that there is an urgent need to investigate *M. leprae*–nerve interaction in depth with the objective of developing new strategies for the prevention and treatment of disabilities.

Received 8 June, 2009; revised 21 August, 2009; accepted 24 August, 2009. *For correspondence. E-mail cpessola@ioc.fiocruz.br; Tel. (+55) 21 2598 4467; Fax (+55) 21 2270 9997.

Over the past decade, a substantial body of evidence has pointed to the importance of programmed cell death (apoptosis) as an evolutionarily conserved strategy mechanism for host defence against bacterial and viral infections (Teodoro and Branton, 1997; Hilleman, 2004; Monack *et al*., 2004; Häcker *et al*., 2006). The critical role played by apoptosis during host–pathogen interaction has become even clearer in the context of such intracellular pathogens as *Mycobacterium tuberculosis* (Mtb), the aetiological agent of tuberculosis, which has evolved strong antiapoptotic mechanisms to persist in its host. *In vitro* studies have shown that it is apoptosis, and not necrosis, of mycobacterium-infected macrophages that results in bacterial killing, constituting an effective innate mechanism for reducing the bacterial burden (Molloy *et al*., 1994; Fratazzi *et al*., 1997; Oddo *et al*., 1998; Sly *et al*., 2003). Although a few studies have suggested that, under some conditions, Mtb may induce host cell apoptosis (Rojas *et al*., 1997; Danelishvili *et al*., 2003; Schaible *et al*., 2003), the ability to inhibit macrophage apoptosis has been reported by a number of authors (Kremer *et al*., 1997; Balcewicz-Sablinska *et al*., 1998; Keane *et al*., 2000; Kausalya *et al*., 2001; Riendeau and Kornfeld, 2003; Sly *et al*., 2003; Loeuillet *et al*., 2006; Dhiman *et al*., 2007). It has also been suggested that the capacity to inhibit apoptosis – not found in avirulent species of mycobacteria – is critical for Mtb pathogenesis (Keane *et al*., 2000; Sly *et al*., 2003). In fact, a direct causal relationship between virulence and the mycobacterial ability to inhibit macrophage apoptosis has recently been demonstrated through the identification of the Mtb *nuoG* gene, responsible for the inhibition of apoptosis in infected host cells (Velmurugan *et al*., 2007).

Avoidance of host cell apoptosis is particularly essential for the successful infection of obligate intracellular pathogens, which rely on host cell integrity and metabolic activities to complete their replication cycle. As these microorganisms cannot replicate outside the intracellular environment, apoptosis would probably put an end to the infection and hence be an effective antimicrobial defence. In the present study, we decided to question whether *M. leprae*, similarly to other intracellular pathogens, is able to block host cell apoptosis. Interestingly, our observations disclosed that, to avoid apoptosis/cell death of SC, the leprosy bacillus uses a novel strategy based on its inherent ability to induce insulin-like growth factor-I (IGF-I).

Results and discussion

M. leprae *treatment promotes SC survival in a serum-depleted medium*

Previous studies have reported that SCs undergo apoptosis *in vivo*, i.e. during peripheral nerve development and following injury and disease (Oliveira *et al*., 2003; Jessen and Mirsky, 2005), in addition to apoptosis *in vitro* subsequent to serum withdrawal (Delaney *et al*., 1999; Weiner and Chun, 1999). To investigate the effect of *M. leprae* on host cell survival, the ST88-14 human Schwannoma cell line was used as an *in vitro* model of infection because of its similarity to human primary SCs and its ability to interact with *M. leprae* (Fletcher *et al*., 1991; Marques *et al*., 2000; 2001; Alves *et al*., 2004). In a previous study, active uptake of *M. leprae* by ST88-14 SC was observed and at 24 h, most bacteria were intracellular. Moreover, at the earliest time point (4 h), actin accumulation around individual bacteria was observed and more than 50% of the SCs contained or were associated with at least one bacterium (Alves *et al*., 2004).

ST88-14 cultures were treated with armadillo-derived *M. leprae* and, subsequent to overnight incubation, the cells were starved for 2 days in serum-depleted medium. Cell survival rates were then compared with those of untreated control cultures by monitoring the capacity of the cells to reduce [3-(4, 5-dimethylthiazol-2-yl)-2.5-diphenyltetrazolium bromide] (MTT) (Fig. 1A) and exclude Trypan blue (Fig. 1B).

In Fig. 1A, it is clear that immortalized ST88-14 human SCs have undergone cell death, with more than 50% of the cells dying after 48 h of serum deprivation. Interestingly, SC monolayers treated with *M. leprae* showed significantly higher survival rates than those in the control cultures. This difference, however, was not observed at later incubation times, when cell viability was below 30% in both the treated and control cultures (data not shown). In addition, the survival rates of infected cultures were sometimes even higher than those observed at the time point of serum withdrawal, implying the occurrence of cell proliferation. Since the number of living cells in a culture is a reflection of both cell death and proliferation rates, in subsequent experiments the actual number of dead cells was considered a more reliable measurement of the survival effect of the bacterium on SCs, minimizing the compensatory effect of cell proliferation on living cell numbers.

A similar protective effect was observed when nude mouse-derived instead of armadillo-derived *M. leprae* was used in the survival assay, indicating that this effect was induced by bacterial cell components, not being associated to host tissue contaminants. Indeed, a mock preparation of *M. leprae* from uninfected animals showed no survival effect reinforcing this idea (Fig. S1A).

The ability of *M. leprae*-treated SCs to resist induction of cell death by serum starvation was dose-dependent, exhibiting better protection at a bacteria : cell ratio of 50:1 (Fig. 1B). Overall, these results suggest that *M. leprae* is capable of altering the host cell response towards an apoptotic stimulus and, as such, promotes cell survival.

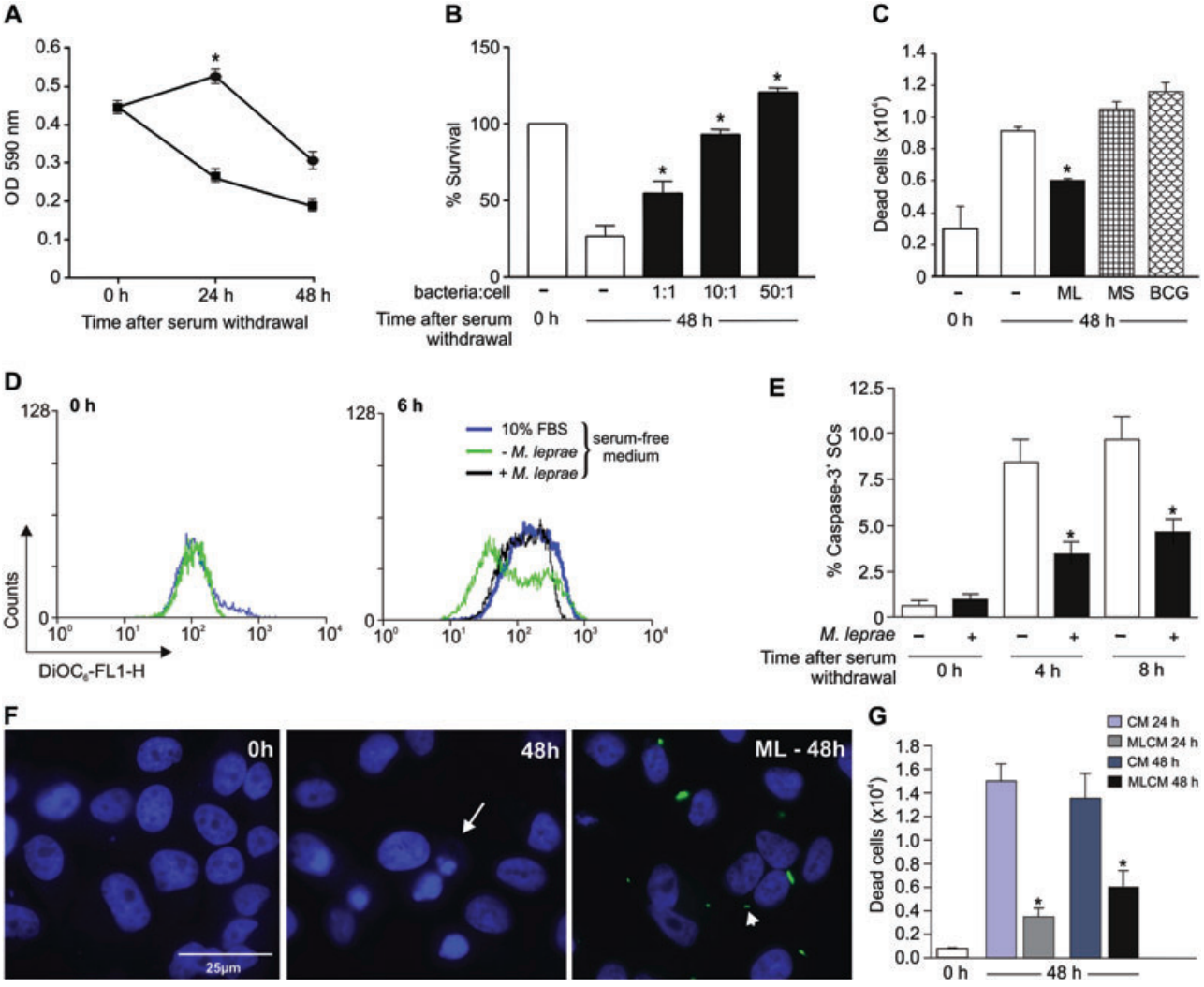

Fig. 1. *M. leprae* promotes survival of SCs in serum-depleted medium. Subconfluent SC monolayers were treated overnight with *M. leprae*. On the following day, cells were switched to serum-free RPMI and the cultures incubated for an additional 48 h.
A. ST88-14 human SCs were treated at a ratio of 5:1 bacteria : cell (●) or not (■) and their viability was assessed by MTT reduction.
B. Dose–response with variable bacteria : cell ratios was obtained, in which viable cells were counted by Trypan blue exclusion.
C. Identical survival assays were also performed on SCs treated with *M. smegmatis* or BCG at a bacteria : cell ratio of 50:1. Dead cells were counted by Trypan blue staining.
D. The cells were harvested at zero and 6 h post serum withdrawal, stained with $DiOC_6$ and analysed by flow cytometry. Codes for lines are: control cultures not treated with *M. leprae* and kept in maintenance medium with 10% FCS (blue); cultures treated (black) or not (green) with *M. leprae* and then switched to serum-free medium.
E. Quantitative analysis of the percentage of active caspase-3.
F. Appearance of SCs kept in medium with 10% FBS; in serum-free medium; or treated with FITC-*M. leprae* (arrowhead) and kept in serum-free medium. The SC monolayers were examined by fluorescence microscopy after staining with bis-benzemide to reveal nuclear morphology and cell-associated bacteria. Scale bar: 25 µm. Arrow – cell with condensed nuclei.
G. SC monolayers were kept for 48 h in media conditioned by *M. leprae*-treated cells maintained in serum-free medium for 24 and 48 h (MLCM). Control cultures were kept in medium conditioned by untreated cells (CM) for identical incubation time. Bars represent the average of three independent experiments ± SEM. An asterisk indicates a statistically significant difference between cultures treated with MLCM and CM ($P < 0.05$). The first bar in the graphics corresponds to culture status at time zero of serum withdrawal.

Specific effect of M. leprae *on SC survival*

Among bacterial pathogens, infection of peripheral nerves is a property unique to *M. leprae*. Nevertheless, mycobacterial species have many components in common, and a number of *in vitro* studies have shown that other species of mycobacteria, including Mtb, BCG and *Mycobacterium smegmatis*, also adhere to and are readily phagocytosed by *in vitro* cultured SCs (Band *et al.*, 1986; Marques *et al.*, 2001). Thus, to evaluate whether this *M. leprae* cell survival effect is shared with other mycobacterial species, SC cultures were treated with

M. smegmatis or *Mycobacterium bovis* BCG under exactly the same conditions described for *M. leprae*, using a bacteria : cell ratio of 50:1. Cell death was measured by Trypan blue staining (Fig. 1C) or by flow cytometry through propidium iodide incorporation (Fig. S1B). As shown in these two figures, *M. smegmatis* and BCG were unable to block SC death induced by serum withdrawal while a slight cytotoxic effect was observed instead. Actually, this cytotoxic effect was minimized by reducing the bacteria : cell ratio to 10:1 and 1:1, although no survival effect was observed, as demonstrated in Fig. S1C. This observation suggests that the perceived SC survival effect is *M. leprae*-specific. A possible explanation for this specificity could be the unique composition of *M. leprae* cell envelope, in the context of both lipid (Vissa and Brennan, 2001) and protein molecules (Marques *et al*., 2008).

M. leprae *treatment prevents reduction of mitochondrial transmembrane potential and delays caspase-3 activation in serum-starved SCs*

Mitochondria play a central role in cell survival and apoptosis. As such, a drop in mitochondrial transmembrane potential has been adopted as an early marker associated with loss of cell viability. Moreover, it is well known that serum withdrawal activates the intrinsic pathway of apoptosis, in which alteration of mitochondria permeability is the starting point (Jaattela and Tschopp, 2003). $DiOC_6$ (3, 3′-dihexyloxacarbocyanine iodide), a fluorescent lipophilic dye, has been largely used to measure mitochondrial transmembrane potential by flow cytometry (Lecoeur *et al*., 2001). Therefore, $DiOC_6$ was used in our survival assays at very early time points after serum withdrawal to detect in a very sensitive way any perturbations in mitochondrial membrane permeability in ST88-14 SCs treated or not with *M. leprae.* Cells stained with $DiOC_6$ were analysed via flow cytometry at 6 h after serum withdrawal. Figure 1D shows that, while untreated control cells exhibited a significant decrease in fluorescence emission as a consequence of the loss of mitochondrial transmembrane potential, *M. leprae*-treated cells exhibited a higher fluorescence emission, similar to that of cells maintained in a RPMI medium supplemented with serum. In fact, the protective effect of *M. leprae* on mitochondrial transmembrane potential was observed as early as 2 h after serum withdrawal (data not show). This finding indicates that *M. leprae* is capable of interrupting cell death pathways at a very early stage.

Caspases are responsible for many of the nuclear hallmarks of apoptosis, including nuclear condensation and DNA fragmentation. It has been previously shown that caspase-3 is rapidly activated in SCs undergoing apoptosis following serum withdrawal (Delaney *et al*., 1999). To determine whether *M. leprae* interferes in caspase activation in our model system, SC cultures treated or not with the bacteria were incubated in serum-free medium for 4 and 8 h and immune labelled with anti-active caspase-3, followed by DAPI counterstaining of SC nuclei. The fluorescence micrographs are shown in Fig. S2. As shown in Fig. 1E, at early time points, the percentage of caspase-3-positive cells was significantly lower in *M. leprae*-treated cultures than the percentage found in the control cultures. This difference, however, was not observed after 24 h of incubation, indicating that *M. leprae* may only be able to sustain SC survival for a relatively brief period of time after serum withdrawal.

M. leprae *survival effect is observed both in bacterium-associated cells and in cells with no bacterium*

Next, to investigate whether the *M. leprae* survival effect described herein was restricted to cells bearing bacteria, ST88-14 SC monolayers were treated or not with FITC-labelled *M. leprae* overnight followed by incubation in serum-free medium for 48 h. Cells were then fixed and the nuclear morphology examined by staining with bisbenzemide. Figure 1F shows that serum-starved SCs displayed typical apoptotic morphology with chromatin condensation. In contrast, in *M. leprae*-treated cultures, most cells exhibited non-condensed chromatin, similarly to cells kept in medium with 10% FBS (data not shown). It is worth noting that nuclear integrity was observed in cells holding (approximately 40%) or not intracellular bacteria, suggesting that soluble factors induced by *M. leprae* and secreted by SCs might be responsible for supporting cell survival.

Media conditioned by M. leprae*-stimulated cultures mimic the survival-promoting activity of* M. leprae

To test the hypothesis that *M. leprae* induces SCs to secrete soluble factors that regulate SC survival, the capacity of the conditioned medium (CM) of *M. leprae*-treated cells to rescue SCs that would otherwise die in serum-depleted medium was examined. As previously described, ST88-14 SC cultures were treated with *M. leprae* and then incubated in a serum-free medium for 24 or 48 h, at which time the CM were collected. The CM (MLCM) was then tested in a 2-day survival assay. As seen in Fig. 1G, both 24 and 48 h MLCM showed the cell death-blocking effect, mimicking the one observed with bacteria. On the other hand, no survival effect was observed when the CM obtained from control cultures (not treated with *M. leprae*) was tested. Taken together, these experiments indicated that *M. leprae*-treated SCs secrete soluble factors capable of preventing their own apoptosis.

M. leprae *induces IGF-I expression and secretion in SCs*

Previous studies have shown that SCs are able to secrete several growth factors such as IGFs, platelet-derived growth factors-BB (PDGF-BB) and neurotrophin-3 (NT-3), which, by acting via an autocrine circuit, inhibit cell death (Meier *et al*., 1999; Syroid *et al*., 1999). In conjunction with the present results, this observation raised the possibility that the survival effect promoted by *M. leprae* could be accounted for by its ability to induce growth factors in the host cell.

To examine this hypothesis, we began by using the OPERON human gene chip to identify potential SC growth factors upregulated by *M. leprae*. SCs, maintained in complete RPMI medium, were treated for 4 and 24 h with *M. leprae*, after which total RNA was extracted and differential gene expression analysis carried out. Preliminary data obtained from these experiments showed that, among the growth factor genes, only IGF-I and IGF-II were found to be significantly upregulated by *M. leprae* with a fold increase of 2.7 and 1.6, respectively, at 24 h post treatment (Fig. S3A). IGF-I induction was confirmed by quantitative RT-PCR (qRT-PCR) analysis. IGF-I seems to be poorly produced by SCs maintained in the presence of serum, which constitutes a good source for this growth factor (Syroid *et al*., 1999). Our results were in agreement with this observation since low levels of IGF-I transcripts were detected in the control cells (Fig. 2A). Strikingly, however, *M. leprae* was able to induce IGF-I transcription even in the presence of serum, as illustrated in Fig. 2A and Fig. S3A. In contrast, no induction of IGF-I expression was observed when SCs were treated with *M. smegmatis* or BCG for 24 h (Fig. S3B). Moreover, a dot-blot analysis with anti-IGF-I of SC supernatants treated for 24 h in complete RPMI medium with three different batches of armadillo-derived *M. leprae* showed stronger positive signals as compared with the supernatant from untreated cells (Fig. 2B), indicating the capacity of *M. leprae* to induce the secretion of IGF-I by SCs.

Experiments were also conducted to analyse the level of IGF-II transcripts in cells infected or not with *M. leprae*. While an initial semi-quantitative RT-PCR suggested *M. leprae* upregulation of this gene post infection, confirming data obtained from the gene array analysis, these results were not sustained by qRT-PCR, which showed no significant alteration in the basal level of IGF-II transcription by *M. leprae* (results not shown). Thus, based on the qRT-PCR results, we decided to focus the remainder of our study on IGF-I.

IGF-I rescues ST88-14 cells from apoptosis induced by serum withdrawal

Previous studies have shown that IGF-I protects SCs from apoptosis induced by serum withdrawal (Delaney *et al*., 1999; Meier *et al*., 1999; Syroid *et al*., 1999). A series of experiments were then performed to investigate whether *M. leprae* sustained SC survival in serum-free conditions via IGF production. First, flow cytometry was used to demonstrate that the type 1 IGF receptor (IGF-1R) serving both IGF-I and IGF-II is well expressed in ST88-14 cells (Fig. S4A). Second, analyses were performed on whether ST88-14, similarly to primary SCs, can be rescued by IGF-I from serum withdrawal-induced cell death, tested by way of the 2-day survival assay in which increasing concentrations of human recombinant IGF-I was added to the cells. As illustrated in Fig. S4B, IGF-I was able to block cell death in a dose-dependent manner. Moreover, at higher IGF-I concentrations, mitogenic effects were observed, mimicking the cell growth seen when serum was added at 10% (data not shown).

IGF-I mediates the survival effect of M. leprae *in SCs*

To further confirm the involvement of IGF-I in the *M. leprae* survival effect, tests were conducted to ascertain whether a pool of blocking antibodies against IGF-I, IGF-II and IGF-1R would interfere with the ability of *M. leprae* to prevent SC death. ST88-14 SCs were treated with *M. leprae* and, after overnight incubation, were starved for 2 days in serum-depleted medium in the presence or not of the blocking antibodies. Cell death was measured by Trypan blue staining. Figure 2C shows that the neutralizing antibodies blocked the ability of *M. leprae* to rescue SCs, which, conversely, was not observed when a normal rabbit IgG was used as a control antibody. At the concentration used, this pool of antibodies was shown to completely block the survival effect of the addition of IGF-I to serum-starved cells at a final concentration of 50 ng ml^{-1} (data not shown). As a whole, these experiments indicated that *M. leprae* survival-promoting activity in SCs could be accounted for by the secretion of IGF, induced upon treatment with the bacteria.

M. leprae *treatment induces cell proliferation in serum-starved SCs*

Cultures were also stained with anti-Ki67 – a good marker for cell proliferation – to measure the proliferation status of cells treated with *M. leprae*. At time zero of serum withdrawal, the percentage of Ki67-positive cells in control cultures was close to 50%, decreasing to around 25% after 24 h of serum withdrawal. In contrast, in cultures pre-treated with *M. leprae*, no decrease in the percentage of Ki67-positive cells was observed, suggesting that the leprosy bacillus exercised a proliferative effect on the SCs (Fig. 2D–E). Due to the well-known proliferative effect of IGF-I on SCs, it is very likely that the *M. leprae* proliferation effect over SCs is mediated by the extra IGF-I pro-

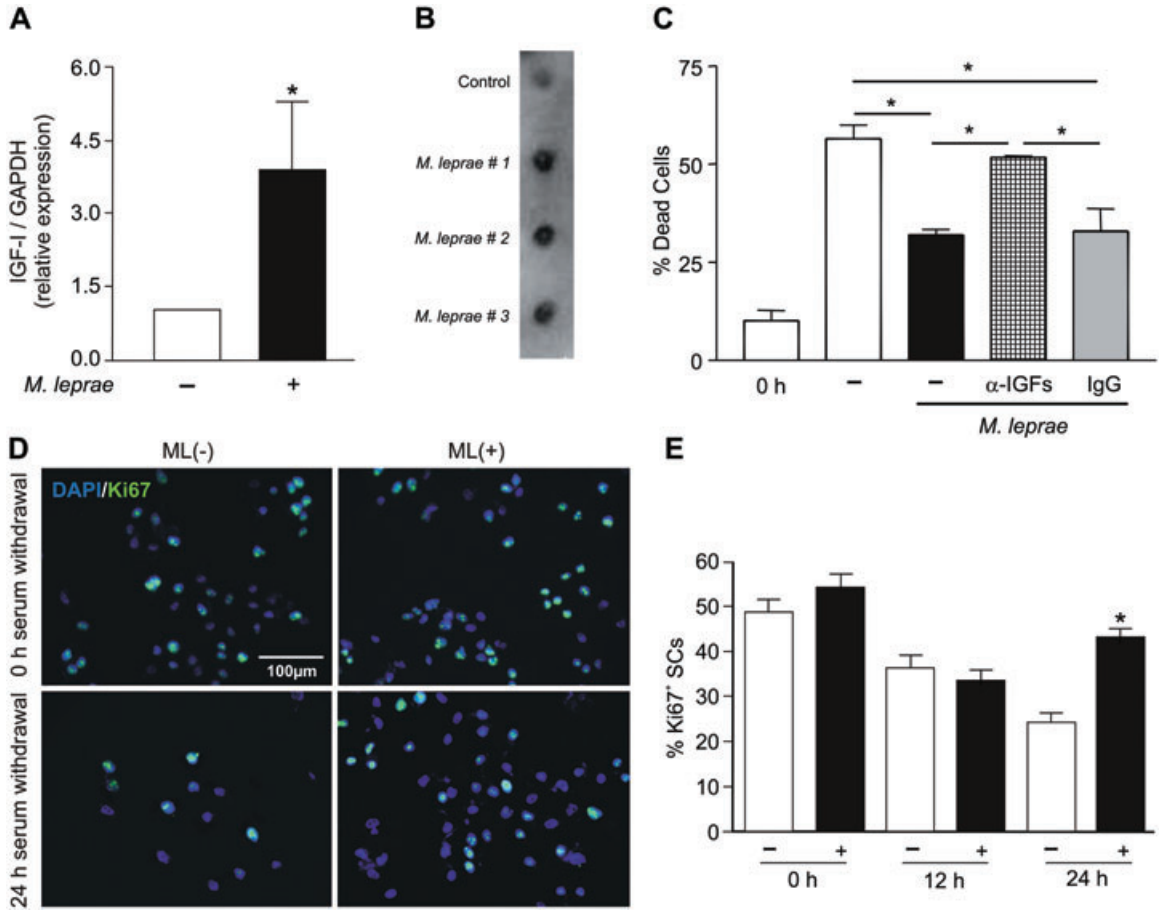

Fig. 2. IGF-I mediates the survival effect of *M. leprae* in SCs.
A. Monolayers of ST88-14 cells in maintenance medium were treated or not with *M. leprae* for 24 h; and total RNA was isolated. IGF-I mRNA levels were verified by qRT-PCR. Bars represent the average of three independent experiments ± SEM (*$P < 0.05$).
B. Dot blot of 24 h supernatants from ST88-14 SCs treated or not with *M. leprae* for IGF-I detection.
C. A pool of anti-IGF-I, -IGF-II and -IGF-1R neutralizing antibodies (α-IGFs; each at 10 μg ml^{-1}) was added to *M. leprae*-treated cells at the moment the maintenance medium was replaced by serum-free medium. Normal goat IgG (30 μg ml^{-1}) was added as a control. After 2 days, the number of dead cells was quantified by Trypan blue staining. The data are expressed as mean ± SD of a representative experiment from three independent ones performed in duplicate (*$P < 0.05$).
D and E. Proliferation analysis by the expression of Ki67. (D) Images captured under epifluorescence microscopy where green dots show the presence of Ki67 in ST88-14 SCs pre-incubated or not with *M. leprae* and 24 h post serum withdrawal. Cell nuclei in blue were counterstained with DAPI. Scale bar: 100 μm. (E) Percentages of positive cells for both markers were calculated considering the total number of DAPI$^+$ cells in the pictures taken as 100% of cells in culture. The data are means ± SEM of two independent experiments performed in duplicate. An asterisk indicates a statistically significant difference in comparison with *M. leprae* untreated cultures ($P < 0.05$).

duced by the host cell upon infection. This *M. leprae* proliferation effect observed early on during infection differs from the recently described growth factor-independent proliferation effect of long-term resident intracellular *M. leprae* on SCs (Tapinos and Rambukkana, 2005).

M. leprae *promotes survival of and induces IGF-I expression in human primary SCs*

ST88-14 cells constitute a Shwannoma tumour cell line, and, consequently, may express altered apoptotic pathways and growth factor production. The next step therefore was to investigate the survival effect of *M. leprae* in cultures of human primary SCs. These cultures were immune stained with anti-S100, a good SC marker, and counterstained with DAPI, showing a purity level higher than 95%. Fibroblasts, the most frequent contaminant of these cultures, are not positive for S100 and can be visualized as isolated DAPI-stained nuclei (data not shown).

After overnight incubation with PI-labelled *M. leprae* (50:1), over 50% of the SCs contained or were associated with more than one bacterium (Fig. 3A, arrowhead). The same *M. leprae* survival effect was observed when human primary cells instead of the ST88-14 cell line were

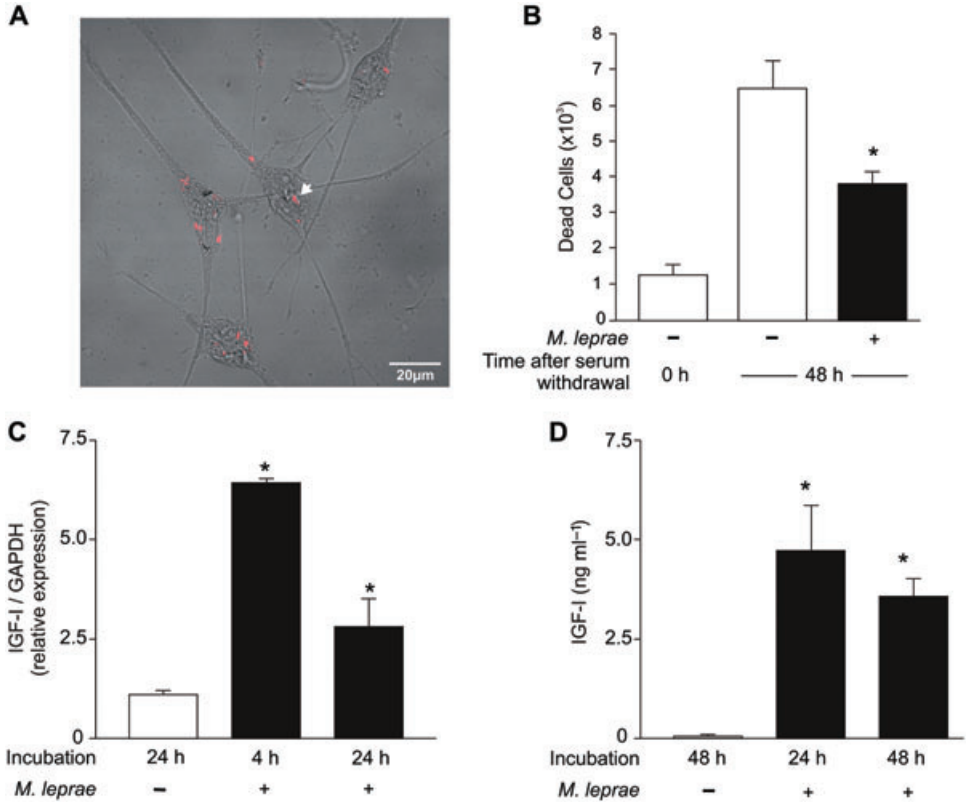

Fig. 3. *M. leprae* promotes survival of and induces IGF-I expression in human primary SCs.
A. Primary SCs were treated overnight with PI-labelled *M. leprae* and the level of bacterium–SC association was analysed by DIC using a confocal microscopy. Arrowhead denotes the bacterium associated with SC. Scale bar: 20 μm.
B. Primary SC culture was treated or not with *M. leprae* and apoptosis induced by serum withdrawal for 48 h. Cellular viability was assessed by Trypan blue exclusion. The data are expressed as mean ± SD of a representative experiment from three independent ones performed in duplicate. An asterisk indicates a statistically significant difference in comparison with *M. leprae* untreated cultures ($P < 0.05$).
C. IGF-I mRNA levels in SCs treated or not with *M. leprae* for 24 h were verified by qRT-PCR.
D. IGF-I protein levels were measured in SC culture supernatants by ELISA. Results are means ± SEM of two different assays carried out in duplicate. *$P < 0.05$, when compared with control cultures.

used in identical 2-day survival assays (Fig. 3B). The number of dead cells was about 40% less in cultures treated with *M. leprae* versus control cells. Moreover, similarly to what was observed in the context of ST88-14 cells, *M. leprae* was able to induce IGF-I expression in primary SCs. Cells kept in medium supplemented with 10% serum were treated with viable nude mouse-derived *M. leprae*; and IGF-I transcripts levels were analysed by qRT-PCR at time points of 4 and 24 h. IGF-I transcription was induced by *M. leprae* as early as 4 h after treatment and persisted at the 24 h time point (Fig. 3C). Contrariwise, no transcripts for IGF-II were detected in control cells or cells treated with *M. leprae* but only in serum-starved cells (data not shown). Finally, IGF-I measurement by a specific sandwich enzyme-like immunosorbent assay (ELISA) in supernatants of SC cultures treated with viable *M. leprae* for 24 and 48 h confirmed the capacity of the bacterium to induce the secretion of IGF-I by human primary SCs (Fig. 3D).

Overall, the present results demonstrate that *M. leprae*-treated human SCs are more resistant to apoptosis induced by serum withdrawal. In this respect *M. leprae* resembles other intracellular pathogens that also display an antiapoptotic effect over their host cells. Many viruses, for example, carry genes whose products have the capacity to block apoptosis of the host cell (Boya *et al*., 2001; Hilleman, 2004). Moreover, strong antiapoptotic mechanisms employed by obligate intracellular bacteria such as *Rickettsia* (Clifton *et al*., 1998) and *Chlamydia* (Fan *et al*., 1998; Coutinho-Silva *et al*., 2001; Rajalingam *et al*., 2001) have been shown to play an important role in their pathogenesis. Additionally, Chuenkova *et al*. (2001) have demonstrated that *Trypanosoma cruzi*, an obligate intracellular protozoan parasite that also infects SCs, suppresses host cell apoptosis. However, although an antiapoptotic effect seems to be a common feature displayed by obligate intracellular microorganisms, our results indicate that *M. leprae* carries this out by way of a novel, previously

undescribed mechanism based on the bacterial capacity to induce IGF-I, a hormone well known for its survival effects in SCs (Campana *et al*., 1999; Delaney *et al*., 1999; Meier *et al*., 1999; Syroid *et al*., 1999).

The data here presented are also reinforced by a recent study showing the capacity of *M. leprae*, but not of *M. bovis* BCG, to inhibit apoptosis of THP-1 monocytes (Hasan *et al*., 2006). The authors of this report showed that *M. leprae* is able to both downregulate the pro-apoptotic genes Bad and Bak and upregulate the anti-apoptotic Bcl-2 family member gene Mcl-1, which results in inhibiting apoptosis. However, whether IGF-I is involved in the survival effect promoted by *M. leprae* in monocytes is certainly a question that deserves attention.

The present findings are also in agreement with the ultrastructure analysis of cutaneous nerve biopsies taken from lepromatous leprosy patients, suggesting that, at the early stages of infection, *M. leprae* favours SC survival over cell death (Job, 1970; 1971). In addition, recent studies have pointed to the absence of any detectable cytotoxic effect of *M. leprae* either in experimentally infected nerves or in infected nerve tissue cultures (Hagge *et al*., 2002; Rambukkana *et al*., 2002; Tapinos and Rambukkana, 2005). However, late in the infection, alterations in the nerve milieu as a consequence of bacterial accumulation may favour SC death, as has been suggested by the degenerative aspect of highly infected cells in nerve biopsies as well as by recent *in vitro* studies in which either a *M. leprae* lipoprotein, *M. leprae*-induced cytokines or high number of bacteria were able to actively induce apoptosis in SCs (Oliveira *et al*., 2003; 2005).

Interestingly, a consistent ultrastructural observation of our group relative to nerves affected by pure neuritic leprosy with inflammatory infiltrates characteristic of lepromatous leprosy is the persistence of numerous denervated SCs, several of which were infected with *M. leprae*, despite the disappearance of most of the myelinated and non-myelinated fibres (S.L. Antunes, pers. comm.). In the absence of axons, the survival of denervated SCs could possibly be maintained by an autocrine loop consisting of several growth factors, including IGF (Meier *et al*., 1999). Thus, the induction of IGF by *M. leprae* infection herein demonstrated may contribute to this survival loop, favouring the preservation of host cell integrity and the metabolic activities essential for an obligate intracellular pathogen such as *M. leprae* to complete its replication cycle. Moreover, the well-known cell proliferation effect of IGF on SCs could be added to the recently described growth factor-independent proliferation effect of long-term resident intracellular *M. leprae* on SCs (Tapinos and Rambukkana, 2005). According to these authors, since *M. leprae* preferentially invades non-myelinating SC, this effect would contribute to leprosy pathogenesis by propagating the favourite cellular niche of the bacterium in the nerve.

Mycobacterium leprae is the only known bacillus to invade peripheral nerves and cause destructive lesions. The immunoinflammatory response elicited by the infection seems to play a major role in this process, which follows a chronic, long-term course, especially in multibacillary patients, despite the accumulation of high numbers of bacilli in the affected nerves. At this point, it is tempting to speculate that, in addition to its antiapoptotic and proliferative effects, the immunomodulatory properties of IGF-I would contribute to tissue homeostasis maintenance during *M. leprae* infection, thereby delaying harmful inflammatory effects on the infected nerves. Indeed, a number of reports have demonstrated the neuroprotective action of IGF-I in both central and peripheral nervous systems in pathologies that are typically associated with overproduction of pro-inflammatory cytokines (for a review, see Venters *et al*., 2000). In conjunction with the anti-inflammatory cytokines IL-10 and IL-4, IGF-I maintains tissue homeostasis and promotes cellular well-being by inhibiting the inflammatory response mediated by the prototypical pro-inflammatory cytokines IL-1 and TNF-α. Additionally, since SCs are able to present *M. leprae* antigens to T cells (Spierings *et al*., 2001), inhibition of SC apoptosis may evade antigen presentation and generation of a specific immune response, as has been shown in the context of tuberculosis (Schaible *et al*., 2003; Fairbairn, 2004; Winau *et al*., 2004; Winau *et al*., 2005; Kaufmann, 2006).

In conclusion, the results of this study delineate an important strategy for the successful colonization of *M. leprae* in the nerve based on the induction of IGF-I production. Interestingly, IGF-I has also been shown to play a role in experimental cutaneous leishmaniasis in favouring infection, acting directly on the promastigote and amastigote forms as a growth factor, but also promoting Leishmania growth/survival within macrophages (Gomes *et al*., 2000; Vendrame *et al*., 2007). The induction of IGF-I by the leprosy bacillus in SCs here described is most probably due to unique *M. leprae* constituents in view of the fact that other mycobacterial species were unable to promote this effect. The identification of these molecules, including their host cell receptors together with the signalling cascade responsible for IGF-I induction, is currently under investigation.

Experimental procedures

Mycobacteria

Armadillo-derived, lethally irradiated *M. leprae* was kindly provided by Dr Patrick J. Brennan (Colorado State University, Fort Collins, CO, USA, under NIH NIAID contract No. 1AI 25469) and *in vivo* grown *M. leprae* (viable and lethally irradiated) derived from the footpads of athymic nu/nu mice provided by J.L. Krahenbuhl (National Hansen's Disease Program Laboratory, Baton

Rouge, LA, USA). Unless otherwise mentioned, lethally irradiated *M. leprae* was used in all bacterium–SC interaction assays. *M. smegmatis* mc^2 155 and *M. bovis* BCG Pasteur strains were grown at 37°C in Middlebrook 7H9 broth (Becton Dickinson, Sparks, MD, USA) supplemented with 0.05% Tween 80 under constant agitation on a magnetic plate. Cultures were harvested in the mid-log phase, counted according to Shepard and McRae (1968), and kept frozen at –70°C until use. FITC- and propidium iodide (PI; Sigma, St. Louis, MO, USA)-labelled *M. leprae* were prepared, as previously described (Smits *et al.*, 1997; Lima *et al.*, 2001). Heat-killed mycobacteria were prepared by incubating aliquots at 80°C for 20 min.

Human SCs

Human primary SCs were isolated from peripheral nerve tissues (a generous gift from Dr Patrick Wood, University of Miami, Miami, FL, USA). These cells were maintained in a DMEM medium (Invitrogen, Eugene, OR, USA) supplemented with 10% of fetal bovine serum (HyClone, Logan, UT, USA), 10 nM heregulin, and 2 μM forskolin in plates previously treated with laminin-1 (Invitrogen). For purity analysis of SC cultures, cells were immunolabelled with anti-S100 (1:500, DAKO, Hamburg, Germany); and nuclei were counterstained with DAPI (4 μg ml^{-1}). The purity percentage of SC cultures was estimated by counting the number of S100-positive SCs over the number of nuclei (total number of cells). Detailed immunofluorescence procedures for S100 are described below. To estimate the level of bacterium–SC association, cultures were incubated with PI-labelled *M. leprae* and analysed by Differential Interference Contrast (DIC) using a confocal microscopy. Fluorescence images were acquired with a LSM 510 Zeiss confocal microscope (Carl Zeiss, Thornwood, NY, USA). The ST88-14 Schwannoma cell line was obtained from Dr Jonathan A. Fletcher (Harvard University, Boston, MA, USA). ST88-14 cells were maintained in RPMI medium 1640 (Invitrogen) supplemented with 10% fetal bovine serum (CULTILAB, Campinas, SP, Brazil), 100 U ml^{-1} penicillin, 100 U ml^{-1} streptomycin and 10 mM HEPES. Cultures were kept at 37°C within a humidified 5% CO_2 atmosphere.

Survival assay

ST88-14 SCs were plated in complete RPMI medium at a density of 20 000 or 30 000 cells in 96- or 24-well plates, respectively, and allowed to attach for 6 h at 37°C with 5% CO_2. Mycobacteria were then added to the cultures and the plates were immediately centrifugated at 400 *g* for 10 min followed by an overnight incubation at 37°C. The next day, wells were washed twice with phosphate-buffered saline (PBS) (pH 7.2) and the cells were switched to serum-free medium and incubated for the time point specified at 37°C. In the particular case of human primary SCs, cells were plated in a DMEM medium with 10% FBS in the absence of heregulin and forskolin. In some wells, recombinant IGF-I (Invitrogen) was added at final concentrations of 5, 10 and 20 ng ml^{-1}. Blocking antibodies were acquired from R&D Systems (Minneapolis, MN, USA) for neutralizing experiments. In these experiments, the goat polyclonal antibodies anti-IGF-I (AF-291-NA), anti-IGF-II (AF-292-NA) and anti-IGF-1R (AF-305-NA), each at a final concentration of 10 μg ml^{-1}, were added as a pool to the cells. In these assays, a normal goat IgG (Santa Cruz Biotechnology, CA, USA) was added at 30 μg ml^{-1}.

Detection of cell death

Cell viability was assessed by three methods: (i) reduction of MTT (Sigma); (ii) cell capability to exclude Trypan blue (Sigma); and (iii) cell permeability to propidium iodide (PI; Sigma). MTT was added to 96-well plate cultures at a concentration of 1 mg ml^{-1}. The cells were then further incubated at 37°C for 1 h. To dissolve the formazan crystals formed in viable, metabolically active cells, 10% SDS (sodium dodecyl sulfate) was added to cultures. The absorbance at OD 590 nm was determined by using an automatic microplate-scanning spectrophotometer (SPECTRAMAX 190; Molecular Devices). For Trypan blue staining, the adherent cells were detached by trypsinization, combined with those present in the supernatant, and collected by centrifugation. Cells were re-suspended in PBS containing 0.2% Trypan blue and immediately counted in a Neubauer camara. Alternatively, cells were re-suspended in PBS containing 0.7 μg ml^{-1} PI and 10 000 cells per sample were analysed via flow cytometer (FACSCalibur; Becton Dickinson) using WinMDI 2.8 software.

Analysis of mitochondrial transmembrane potential

Mitochondrial transmembrane potential was analysed in unfixed SCs using $DiOC_6$ (Molecular Probes, Eugene, OR, USA), a lipophilic dye sequestered into the mitochondrial matrix. Briefly, cells were stained with 10 nM $DiOC_6$ in PBS for 15 min at 37°C in the dark followed by two washes with PBS. The cells were immediately acquired in a FACSCalibur in the FL1-H channel.

Analysis of nuclear morphology and bacteria-bearing cells

Schwann cells were plated in 24-well plates containing glass coverslips covered with 4% silane (Sigma). Cells were allowed to attach for 6 h after which FITC-labelled *M. leprae* was added. Plates were immediately centrifugated at 400 *g* for 10 min followed by an overnight incubation at 37°C. Cells were switched to serum-free RPMI. At zero and 48 h time points, cells were washed with PBS and fixed with 4% paraformaldehyde in PBS for 15 min. Cells were stained with bis-benzemide (1 μg ml^{-1} in PBS) for 15 min, rinsed with PBS, and mounted on glass slides with entellan glue and 90% glycerol in PBS containing 1 mg ml^{-1} p-phenylenediamine. The glass slides were viewed under a led excitation at 470 and 365 nm on an Observer.Z1 Inverted Fluorescence Microscope (Zeiss, Oberkochen, Germany).

Gene chip analysis

A human 14k oligonucleotide set (Operon Biotechnologies) was used to identify differential growth factor gene expression in SCs in response to *M. leprae*. Each oligo element was 70 mer with an approximate melting temperature of 70°C. The arrayer device (ArrayMaker, DeRisi Laboratories) was used to spot the oligo elements on poly-lysine-covered glass slides. ST88-14 SCs were treated with *M. leprae* (10:1) for 4 and 24 h. Reference was the pooled RNA obtained from test plates and untreated controls. Next, cDNA synthesis was carried out as described (http://derisilab.ucsf.edu) and labellled with Cy3 and Cy5 by the indirect method. Hybridization reactions were carried out manually at

70°C for 16 h. Slides were washed and scanned with the AXON 4000B laser scanner. GenePix software was used for image acquisition and spot filtering. Hybridization intensities from each laser channel were obtained, the ratio of intensity from each channel for each element was found (R = Cy5/Cy3), and the background value was deduced. The data were normalized and the R-values were log base 2 converted.

Quantitative RT-PCR (TaqMan)

DNA-free total RNA was extracted from SCs treated or not with *M. leprae* at variable time points using Trizol™ (Invitrogen), according to the manufacturer's instructions. Total RNA was converted to cDNA using random hexamers and Superscript III reverse transcriptase (Invitrogen), as recommended by the manufacturer. Five micrograms of total RNA was reverse transcribed into cDNA and samples were stored at –20°C until further use. qRT-PCR was performed using an ABI Prism 7000 Sequence Detection System (Applied Biosystems, Foster City, CA, USA). TaqMan® Universal PCR Master Mix, human primers IGF-I (Hs01555481_m1), GAPDH (4333764-F) and TaqMan probes were purchased from Applied Biosystems and used according to the manufacturer's instructions. Thermal cycling conditions comprised an initial incubation at 50°C for 2 min, 95°C for 10 min, 40 cycles of denaturation at 95°C for 15 s, and annealing and extension at 60°C for 1 min. To normalize the relative expression of the genes of interest, a human GAPDH gene was used as an endogenous control and the expression values obtained were corrected and quantified by converting the cycle threshold (Ct) value into a numerical value by using the following formula: expression value = $2^{(-\Delta\Delta Ct)}$.

Immunocitochemistry

Schwann cells were fixed in 4% paraformaldehyde (Sigma) for 15 min at 37°C and then washed three times with PBS pH 7.4. Cells were then permeabilized and blocked with PBS plus 0.1% Triton and 5% of normal goat serum (NGS; Invitrogen) for 30 min. Cells were incubated with primary antibody [rabbit polyclonal antibodies anti-S100 (1:500, DAKO), anti-activated capase-3 (1:500, Abcam, Cambridge, MA, USA) or anti-Ki67 antibody (1:100, Abcam)] overnight at 4°C. The cells were washed again thrice 5 min each and incubated for 60 min at room temperature with Alexa 488- or Alexa 555-labelled secondary anti-rabbit IgG (1:250, Molecular Probes; and 1:400, Invitrogen respectively). Nuclei were then stained with DAPI and cells were analysed by epifluorescence microscopy (Axiovert or Apotome, Zeiss) with rodamin, fluorescein and DAPI filters and by confocal microscopy (LSM 510 meta, Zeiss) using 488 and 583 nm lasers as a source of excitation.

IGF-1R expression by flow cytometry

Cells were fixed with 4% paraformaldehyde in PBS for 10 min at room temperature, washed twice with PBS, and incubated with AB human serum (1:1) for 1 min at room temperature. The cells were washed again, permeabilized with 0.1% saponin in PBS (permeabilization solution), and incubated with anti-IGF-1Rβ primary antibodies at a final concentration of 5 μg ml^{-1} in PBS (Santa Cruz Biotechnology) or anti-S100 (1:100, DAKO) for 30 min at room temperature. Cells were washed with a permeabilization solution and incubated with the secondary antibody anti-rabbit IgG conjugated to FITC (1:20, DAKO) for 30 min at room temperature. Finally, cells were washed with a permeabilization solution and re-suspended in 1% paraformaldehyde in PBS. Ten thousand cells were analysed in a FACSCalibur in the FL-1H channel.

IGF-I detection by dot blot

Supernatants from ST88-14 SC cultures maintained in complete RPMI medium were 5× concentrated in an ISS Speed Vac System (Thermo Savant) and 3 μl were spotted onto nitrocellulose membrane strips (Hybound™-C Extra, GE Healthcare, Amershan, UK), which were allowed to dry at room temperature, blocked with 2% BSA (Sigma) in Tris-buffered saline-Tween (TBST) for 30 min, and incubated overnight at 4°C with goat polyclonal antibody anti-IGF-I (1:200; Santa Cruz) TBST-2% BSA containing 0.01% sodium azide. After incubation, the strips were washed by using three changes of TBST and further incubated for 1 h at 37°C with a peroxidase-conjugated secondary antibody anti-goat (1:40 000, Sigma) in TBST-2% non-fat milk. The strips were washed three more times with TBST and the signal was detected by enhanced chemiluminescence and exposure to Hyperfilm™ ECL (GE Healthcare).

Measurement of IGF-I by ELISA

The levels of IGF-I protein in supernatants from SC cultures maintained in complete RPMI medium were determined by ELISA using the Quantikine Immunoassay Human IGF-I (R&D Systems) in accordance with the manufacturer's instructions.

Statistical analysis

To compare three or more groups under differing conditions, a one-way analysis of the variance (ANOVA) test was used followed by the Newmann–Keuls as a post-test. When conducting comparisons between two conditions, a t-test was used. For all analyses, P-values < 0.05 were considered statistically significant.

Acknowledgements

We would like to thank Judy Grevan for editing the text; Dr Flávio Alves Lara, Laboratory of Cellular Microbiology, IOC, for providing the mock preparation of *M. leprae* from nude mouse footpads; Physicians group from Hospital Antônio Pedro/UFF, Dr Osvaldo J.M. Nascimento, Dr Marcos G. de Freitas, Dr Paulo Eduardo Ocke, Dr Daniel Q. Neves and Dr Marcio C. Cardoso for the fundamental technical assistance and Dr Joseph DeRisi, Department of Biophysics, UCSF, for his support and guidance in the microarray experiments. This study was supported by the Conselho Nacional de Desenvolvimento Científico e Tecnológico (CNPq), Brazil. L.S.R. and A.J.T. were awarded a fellowship by the CNPq. E.S.M. was supported by fellowships from the Fundação de Amparo e Apoio à Pesquisa do Rio de Janeiro (FAPERJ) and the Oswaldo Cruz Institute (IOC).

References

Alves, L., de Mendonça Lima, L., da Silva Maeda, E., Carvalho, L., Holy, J., Sarno, E.N., *et al.* (2004) *Mycobacterium leprae* infection of human Schwann cells depends on selective host kinases and pathogen-modulated endocytic pathways. *FEMS Microbiol Lett* **238:** 429–437.

Balcewicz-Sablinska, M.K., Keane, J., Kornfeld, H., and Remold, H.G. (1998) Pathogenic *Mycobacterium tuberculosis* evades apoptosis of host macrophages by release of TNF-R2, resulting in inactivation of TNF-alpha. *J Immunol* **161:** 2636–2641.

Band, A.H., Bhattacharya, A., and Talwar, G.P. (1986) Lack of *Mycobacterium leprae*-specific uptake in Schwann cells. *Int J Lepr Other Mycobact Dis* **54:** 71–78.

Boya, P., Roques, B., and Kroemer, G. (2001) New EMBO members' review: viral and bacterial proteins regulating apoptosis at the mitochondrial level. *EMBO J* **20:** 4325–4331.

Campana, W.M., Darin, S.J., and O'Brien, J.S. (1999) Phosphatidylinositol 3-kinase and Akt protein kinase mediate IGF-I- and prosaptide-induced survival in Schwann cells. *J Neurosci Res* **57:** 332–341.

Chuenkova, M.V., Furnari, F.B., Cavenee, W.K., and Pereira, M.A. (2001) *Trypanosoma cruzi trans*-sialidase: a potent and specific survival factor for human Schwann cells by means of phosphatidylinositol 3-kinase/Akt signaling. *Proc Natl Acad Sci USA* **98:** 9936–9941.

Clifton, D.R., Goss, R.A., Sahni, S.K., van Antwerp, D., Baggs, R.B., Marder, V.J., *et al.* (1998) NF-kappa B-dependent inhibition of apoptosis is essential for host cell survival during *Rickettsia rickettsii* infection. *Proc Natl Acad Sci USA* **95:** 4646–4651.

Coutinho-Silva, R., Perfettini, J.L., Persechini, P.M., Dautry-Varsat, A., and Ojcius, D.M. (2001) Modulation of P2Z/P2X(7) receptor activity in macrophages infected with *Chlamydia psittaci*. *Am J Physiol Cell Physiol* **280:** C81–C89.

Danelishvili, L., McGarvey, J., Li, Y.J., and Bermudez, L.E. (2003) *Mycobacterium tuberculosis* infection causes different levels of apoptosis and necrosis in human macrophages and alveolar epithelial cells. *Cell Microbiol* **5:** 649–660.

Delaney, C.L., Cheng, H.L., and Feldman, E.L. (1999) Insulin-like growth factor-I prevents caspase-mediated apoptosis in Schwann cells. *J Neurobiol* **41:** 540–548.

Dhiman, R., Raje, M., and Majumdar, S. (2007) Differential expression of NF-kappaB in mycobacteria infected THP-1 affects apoptosis. *Biochim Biophys Acta* **1770:** 649–658.

Fairbairn, I.P. (2004) Macrophage apoptosis in host immunity to mycobacterial infections. *Biochem Soc Trans* **32:** 496–498.

Fan, T., Lu, H., Hu, H., Shi, L., McClarty, G.A., Nance, D.M., *et al.* (1998) Inhibition of apoptosis in *Chlamydia*-infected cells: blockade of mitochondrial cytochrome *c* release and caspase activation. *J Exp Med* **187:** 487–496.

Fletcher, J.A., Kozakewich, H.P., Hoffer, F.A., Lage, J.M., Weidner, N., *et al.* (1991) Diagnostic relevance of clonal cytogenetic aberrations in malignant soft-tissue tumors. *N Engl J Med* **324:** 436–442.

Fratazzi, C., Arbeit, R.D., Carini, C., and Remold, H.G. (1997) Programmed cell death of *Mycobacterium avium* serovar 4-infected human macrophages prevents the mycobacteria from spreading and induces mycobacterial growth inhibition by freshly added, uninfected macrophages. *J Immunol* **158:** 4320–4327.

Gomes, C.M.C., Matta, V.L.R., Laurenti, M.D., Gidlund, M., Goto, H., and Corbett, C.E.P. (2000) Insulin-like growth factor (IGF)-I affects parasite growth and host cell migration in experimental cutaneous leishmaniasis. *Int J Exp Pathol* **81:** 249–255.

Häcker, G., Kirschnek, S., and Fischer, S.F. (2006) Apoptosis in infectious disease: how bacteria interfere with the apoptotic apparatus. *Med Microbiol Immunol* **195:** 11–19.

Hagge, D.A., Oby Robinson, S., Scollard, D., McCormick, G., and Williams, D.L. (2002) A new model for studying the effects of *Mycobacterium leprae* on Schwann cell and neuron interactions. *J Infect Dis* **186:** 1283–1296.

Hasan, Z., Ashraf, M., Tayyebi, A., and Hussain, R. (2006) *M. leprae* inhibits apoptosis in THP-1 cells by downregulation of Bad and Bak and upregulation of Mcl-1 gene expression. *BMC Microbiol* **6:** 78.

Hilleman, M.R. (2004) Strategies and mechanisms for host and pathogen survival in acute and persistent viral infections. *Proc Natl Acad Sci USA* **101** (Suppl. 2)**:** 14560–14566.

Jaattela, M., and Tschopp, J. (2003) Caspase-independent cell death in T lymphocytes. *Nat Immunol* **4:** 416–423.

Jessen, K.R., and Mirsky, R. (2005) The origin and development of glial cells in peripheral nerves. *Nat Rev Neurosci* **6:** 671–682.

Job, C.K. (1970) *Mycobacterium leprae* in nerve lesions in lepromatous leprosy. An electron microscopic study. *Arch Pathol* **89:** 195–207.

Job, C.K. (1971) Pathology of peripheral nerve lesions in lepromatous leprosy – a light and electron microscopic study. *Int J Lepr Other Mycobact Dis* **39:** 251–268.

Kaufmann, S.H. (2006) Tuberculosis: back on the immunologists' agenda. *Immunity* **24:** 351–357.

Kausalya, S., Somogyi, R., Orlofsky, A., and Prystowsky, M.B. (2001) Requirement of A1-a for bacillus Calmette-Guerin-mediated protection of macrophages against nitric oxide-induced apoptosis. *J Immunol* **166:** 4721–4727.

Keane, J., Remold, H.G., and Kornfeld, H. (2000) Virulent *Mycobacterium tuberculosis* strains evade apoptosis of infected alveolar macrophages. *J Immunol* **164:** 2016–2020.

Kremer, L., Estaquier, J., Brandt, E., Ameisen, J.C., and Locht, C. (1997) *Mycobacterium bovis Bacillus Calmette Guerin* infection prevents apoptosis of resting human monocytes. *Eur J Immunol* **27:** 2450–2456.

Lecoeur, H., Fevrier, M., Garcia, S., Riviere, Y., and Gougeon, M.L. (2001) A novel flow cytometric assay for quantitation and multiparametric characterization of cell-mediated cytotoxicity. *J Immunol Methods* **253:** 177–187.

Lima, C.S., Ribeiro, M.L., Souza, L.A., Sardella, A.B., Wolf, V.M., and Pessolani, M.C. (2001) Intracellular signals triggered during association of *Mycobacterium leprae* and *Mycobacterium bovis* BCG with human monocytes. *Microb Pathog* **31:** 37–45.

Loeuillet, C., Martinon, F., Perez, C., Munoz, M., Thome, M., and Meylan, P.R. (2006) *Mycobacterium tuberculosis*

subverts innate immunity to evade specific effectors. *J Immunol* **177:** 6245–6255.
Marques, M.A., Mahapatra, S., Nandan, D., Dick, T., Sarno, E.N., Brennan, P.J., and Vidal Pessolani, M.C. (2000) Bacterial and host-derived cationic proteins bind alpha2-laminins and enhance *Mycobacterium leprae* attachment to human Schwann cells. *Microbes Infect* **12:** 1407–1417.
Marques, M.A., Ant nio, V.L., Sarno, E.N., Brennan, P.J., and Pessolani, M.C. (2001) Binding of alpha2-laminins by pathogenic and non-pathogenic mycobacteria and adherence to Schwann cells. *J Med Microbiol* **50:** 23–28.
Marques, M.A., Neves-Ferreira, A.G., da Silveira, E.K., Valente, R.H., Chapeaurouge, A., Perales, J., *et al.* (2008) Deciphering the proteomic profile of *Mycobacterium leprae* cell envelope. *Proteomics* **8:** 2477–2491.
Meier, C., Parmantier, E., Brennan, A., Mirsky, R., and Jessen, K.R. (1999) Developing Schwann cells acquire the ability to survive without axons by establishing an autocrine circuit involving insulin-like growth factor, neurotrophin-3, and platelet-derived growth factor-BB. *J Neurosci* **19:** 3847–3859.
Molloy, A., Laochumroonvorapong, P., and Kaplan, G. (1994) Apoptosis, but not necrosis, of infected monocytes is coupled with killing of intracellular bacillus Calmette-Guerin. *J Exp Med* **180:** 1499–1509.
Monack, D.M., Mueller, A., and Falkow, S. (2004) Persistent bacterial infections: the interface of the pathogen and the host immune system. *Nat Rev Microbiol* **2:** 747–765.
Oddo, M., Renno, T., Attinger, A., Bakker, T., MacDonald, H.R., and Meylan, P.R. (1998) Fas ligand-induced apoptosis of infected human macrophages reduces the viability of intracellular *Mycobacterium tuberculosis*. *J Immunol* **160:** 5448–5454.
Oliveira, R.B., Ochoa, M.T., Sieling, P.A., Rea, T.H., Rambukkana, A., Sarno, E.N., and Modlin, R.L. (2003) Expression of Toll-like receptor 2 on human Schwann cells: a mechanism of nerve damage in leprosy. *Infect Immun* **71:** 1427–1433.
Oliveira, R.B., Sampaio, E.P., Aarestrup, F., Teles, R.M., Silva, T.P., Oliveira, A.L., *et al.* (2005) Cytokines and *Mycobacterium leprae* induce apoptosis in human Schwann cells. *J Neuropathol Exp Neurol* **64:** 882–890.
Rajalingam, K., Al-Younes, H., Muller, A., Meyer, T.F., Szczepek, A.J., and Rudel, T. (2001) Epithelial cells infected with *Chlamydophila pneumoniae* (*Chlamydia pneumoniae*) are resistant to apoptosis. *Infect Immun* **69:** 7880–7888.
Rambukkana, A., Zanazzi, G., Tapinos, N., and Salzer, J.L. (2002) Contact-dependent demyelination by *Mycobacterium leprae* in the absence of immune cells. *Science* **296:** 927–931.
Riendeau, C.J., and Kornfeld, H. (2003) THP-1 cell apoptosis in response to Mycobacterial infection. *Infect Immun* **71:** 254–259.
Rojas, M., Barrera, L.F., Puzo, G., and Garcia, L.F. (1997) Differential induction of apoptosis by virulent *Mycobacterium tuberculosis* in resistant and susceptible murine macrophages: role of nitric oxide and mycobacterial products. *J Immunol* **159:** 1352–1361.
Sarno, E.N., and Pessolani, M.C. (2001) Leprosy. Oldest and most feared disease. *Lancet* **358** (Suppl.)**:** S39.
Schaible, U.E., Winau, F., Sieling, P.A., Fischer, K., Collins, H.L., Hagens, K., *et al.* (2003) Apoptosis facilitates antigen presentation to T lymphocytes through MHC-I and CD1 in tuberculosis. *Nat Med* **9:** 1039–1046.
Scollard, D.M., Adams, L.B., Gillis, T.P., Krahenbuhl, J.L., Truman, R.W., and Williams, D.L. (2006) The continuing challenges of leprosy. *Clin Microbiol Rev* **19:** 338–381.
Shepard, C.C., and McRae, D.H. (1968) A method for counting acid-fast bacteria. *Int J Lepr Other Mycobact Dis* **36:** 78–82.
Sly, L.M., Hingley-Wilson, S.M., Reiner, N.E., and McMaster, W.R. (2003) Survival of *Mycobacterium tuberculosis* in host macrophages involves resistance to apoptosis dependent upon induction of antiapoptotic Bcl-2 family member Mcl-1. *J Immunol* **170:** 430–437.
Smits, E., Burvenich, C., and Heyneman, R. (1997) Simultaneous flow cytometric measurement of phagocytotic and oxidative burst activity of polymorphonuclear leukocytes in whole bovine blood. *Vet Immunol Immunopathol* **56:** 259–269.
Spierings, E., de Boer, T., Wieles, B., Adams, L.B., Marani, E., and Ottenhoff, T.H. (2001) *Mycobacterium leprae*-specific, HLA class II-restricted killing of human Schwann cells by CD4+ Th1 cells: a novel immunopathogenic mechanism of nerve damage in leprosy. *J Immunol* **166:** 5883–5888.
Syroid, D.E., Zorick, T.S., Arbet-Engels, C., Kilpatrick, T.J., Eckhart, W., and Lemke, G. (1999) A role for insulin-like growth factor-I in the regulation of Schwann cell survival. *J Neurosci* **19:** 2059–2068.
Tapinos, N., and Rambukkana, A. (2005) Insights into regulation of human Schwann cell proliferation by Erk1/2 via a MEK-independent and p56Lck-dependent pathway from leprosy bacilli. *Proc Natl Acad Sci USA* **102:** 9188–9193.
Teodoro, J.G., and Branton, P.E. (1997) Regulation of apoptosis by viral gene products. *J Virol* **71:** 1739–1746.
Velmurugan, K., Chen, B., Miller, J.L., Azogue, S., Gurses, S., Hsu, T., *et al.* (2007) *Mycobacterium tuberculosis nuoG* is a virulence gene that inhibits apoptosis of infected host cells. *PLoS Pathog* **3:** e110.
Vendrame, C.M., Carvalho, M.D., Rios, F.J., Manuli, E.R., Petitto-Assis, F., and Goto, H. (2007) Effect of insulin-like growth factor-I on *Leishmania amazonensis* promastigote arginase activation and reciprocal inhibition of NOS2 pathway in macrophage *in vitro*. *Scand J Immunol* **66:** 287–296.
Venters, H.D., Dantzer, R., and Kelley, K.W. (2000) A new concept in neurodegeneration: TNFα is a silencer of survival signals. *Trends Neurosci* **23:** 175–180.
Vissa, V.D., and Brennan, P.J. (2001) The genome of *Mycobacterium leprae*: a minimal mycobacterial gene set. *Genome Biol* **2:** 1023.1–1023.8.
Weiner, J.A., and Chun, J. (1999) Schwann cell survival mediated by the signaling phospholipids lysophosphatidic acid. *Proc Natl Acad Sci USA* **96:** 5233–5238.
Winau, F., Kaufmann, S.H., and Schaible, U.E. (2004) Apoptosis paves the detour path for CD8 T cell activation against intracellular bacteria. *Cell Microbiol* **6:** 599–607.
Winau, F., Hegasy, G., Kaufmann, S.H., and Schaible, U.E. (2005) No life without death-apoptosis as prerequisite for T cell activation. *Apoptosis* **10:** 707–715.

Supporting information

Additional Supporting Information may be found in the online version of this article:

Fig. S1. Specific effect of *M. leprae* on SC survival.
A. ST88-14 SCs were treated with nude mouse-derived *M. leprae* or a mock *M. leprae* preparation at a bacteria : cell ratio of 50:1 and kept for 48 h in serum-free RPMI. Dead cells were counted by Trypan blue staining.
B. Identical survival assays were performed where the SCs were treated with *M. leprae* (ML), *M. smegmatis* (MS) or BCG at a bacteria : cell ratio of 50:1. The percentage of dead cells was assessed by PI staining followed by flow cytometry analysis. Data are representative of two, independently performed experiments.
C. SCs were treated as above with variable bacteria : cell ratios of MS and BCG. Dead cells were then counted by Trypan blue staining. The data are expressed as mean ± SD of a representative experiment performed in triplicate. $*P < 0.05$ when compared with control cultures. The first bar in the graphics corresponds to culture status at time zero of serum withdrawal.
Fig. S2. Apoptosis analysis by the expression of active caspase-3. Images captured under epifluorescence microscopy, where red dots show the presence of active caspase-3 in ST88-14 SCs pre-incubated (B, D and F) or not with *M. leprae* (A, C and E), 4 h (C and D) and 8 h (E and F) post serum withdrawal. Cell nuclei (blue) were counterstained with DAPI. Scale bar in (A)–(F): 100 μm.
Fig. S3. *M. leprae* induces the expression of IGF-I in ST88-14 cells.
A. Fold increase of differentially expressed IGF-I and IGF-II genes in *M. leprae*-treated SCs, as analysed via the OPERON human gene chip.
B. Cell monolayers in maintenance medium were treated or not with *M. leprae*, *M. smegmatis* or BCG (50:1) for 24 h; and total RNA was isolated. IGF-I mRNA levels in SCs were verified by qRT-PCR. Data are representative of two experiments with similar results.
Fig. S4. IGF-I prevented cell death induced by serum withdrawal.
A. ST88-14 cells express the type 1 insulin-like growth factor receptor (IGF-1R) (grey line) and the SC marker S100 (black line), as shown by flow cytometry analysis.
B. SCs were placed in serum-free medium in the absence or presence of increasing concentrations of recombinant IGF-I. After 48 h, the culture survival was estimated by Trypan blue exclusion. Survival percentage is the number of living cells present at the end of the experiment and expressed as the percentage of the number of living cells present at the moment the maintenance medium was switched to serum-free medium.

Please note: Wiley-Blackwell are not responsible for the content or functionality of any supporting materials supplied by the authors. Any queries (other than missing material) should be directed to the corresponding author for the article.

CAPÍTULO 4: Resultados

Circulating Insulin-like Growth Factor-I (IGF-I) and its major binding protein IGFBP-3 indicate disease status and predict reactions at leprosy diagnosis

Luciana Silva Rodrigues[1], Mariana Andrea Hacker[2], Ximena Illarramendi[2], José Augusto da Costa Nery[2], Euzenir Nunes Sarno[3] and Maria Cristina Vidal Pessolani[1] .

[1]Laboratory of Cellular Microbiology, Instituto Oswaldo Cruz, Rio de Janeiro, RJ 21045-900, Brazil; [2]Leprosy Laboratory, Instituto Oswaldo Cruz, Rio de Janeiro, RJ 21045-900, Brazil.

Situação: *submetido*

Níveis circulantes do fator de crescimento semelhante à insulina-I (IGF-I) e de sua principal proteína ligadora (IGFBP-3) em pacientes com hanseníase indicam "status" da doença e predizem o surgimento de episódios reacionais

Embora se saiba que os episódios reacionais estejam associados a uma exacerbação da resposta imune e inflamatória frente a antígenos do *M. leprae*, sua causa e patogenia ainda não foram completamente desvendadas. Sabe-se, no entanto, que estes eventos imuno-inflamatórios são responsáveis pela perda da função motora e nervosa, que leva à incapacidade de inúmeros pacientes. Por isso, um melhor entendimento da fisiopatogenia das reações constitui um tema de grande relevância no campo das pesquisas em hanseníase, já que poderá contribuir para a proposição de tratamentos alternativos mais eficientes e a definição de potenciais biomarcadores de risco para o desenvolvimento das reações, com a consequente prevenção da instalação de incapacidades e deformidades físicas. Neste contexto, vários estudos vêm tentando traçar um perfil imunológico dos pacientes reacionais a partir dos níveis sanguíneos de citocinas – às quais apresentam papel relevante na resposta inflamatória observada na hanseníase e, sobretudo nos episódios reacionais.

Numa primeira abordagem *in vitro*, demonstramos a capacidade do *M. leprae* em induzir a produção de IGF-I e proteger CS de apoptose induzida por privação de soro (Rodrigues e col., 2010). Estes dados indicaram, pela primeira vez, a participação potencial do sistema IGF na infecção pelo *M. leprae*. Um conjunto de dados acumulados da literatura demonstra que processos inflamatórios agudos podem provocar uma diminuição nos níveis circulantes de IGF-I. Além disso, citocinas pró-inflamatórias como o fator de necrose tumoral-alpha (TNF-α), cuja produção é exacerbada durante as reações hansênicas, são capazes de inibir a síntese de IGF-I. Desse modo, numa segunda etapa do doutorado conduzimos um estudo restrospectivo com o objetivo de avaliar possíveis alterações no sistema IGF que pudessem se correlacionar com o surgimento dos episódios reacionais em pacientes com hanseníase. Para atingir este objetivo, avaliamos os níveis séricos de IGF-I, IGFBP-3 e TNF-α em indivíduos sadios e pacientes apresentando as formas multibacilares BL ou LL, e que evoluíram ou não para episódios reacionais do tipo I ou tipo II, respectivamente. Os resultados detalhados se encontram no manuscrito a seguir.

Circulating Insulin-Like Growth Factor-I (IGF-I) and Its Major Binding Protein IGFBP-3 Indicate Disease Status and Predict Reactions at Leprosy Diagnosis

Luciana Silva Rodrigues[1], Mariana Andrea Hacker[2], Ximena Illarramendi[2], José Augusto da Costa Nery[2], Euzenir Nunes Sarno[3] and Maria Cristina Vidal Pessolani[1] .

[1]Laboratory of Cellular Microbiology, Instituto Oswaldo Cruz, Rio de Janeiro, RJ 21045-900, Brazil; [2]Leprosy Laboratory, Instituto Oswaldo Cruz, Rio de Janeiro, RJ 21045-900, Brazil.

Corresponding author:

Maria Cristina Vidal Pessolani

e-mail: cpessola@ioc.fiocruz.br

Fax: 55-21-2270-9997; Tel.: 55-21-2598-4467

Laboratory of Cellular Microbiology

Oswaldo Cruz Institute

Oswaldo Cruz Foundation – FIOCRUZ

Av. Brasil 4365 – Manguinhos

Rio de Janeiro, RJ 21045-900

Brazil

Abstract

Background: Leprosy is an infectious disease caused by *Mycobacterium leprae* (ML). The disease presents a strong immune-inflammatory component, which status dictates both its clinical forms as well as the occurrence of reactional episodes. Nerve damage is still the major problem facing leprosy patients, which progresses gradually during the course of the disease, as well as acutely during reactions. Previous reports have indicated that infection and inflammation cause a serious imbalance in the insulin-like growth factor (IGF) system.

Methodology and principal findings: In the present retrospective study we show significant differences in circulating IGF-I/IGBP-3 levels in leprosy patients at diagnosis according to disease status and occurrence of reaction during or after treatment. Significantly lower levels of circulating IGF-I/IGFBP-3 were found in nonreactional lepromatous leprosy (LL) patients when compared to nonreactional patients with the other clinical forms. Notable, however, were the differences observed in circulating levels at the pre-multidrug therapy stage in patients who developed vs. those who did not develop reaction during or after treatment. Among LL patients, serum IGF-I and IGFBP-3 levels below the normal range were strongly associated with high disease stability. The majority of nonreactional LL patients (82% and 73%, respectively) presented low levels, in contrast to the normal levels observed in patients who suffered type II reaction. The opposite behavior was observed in borderline lepromatous (BL) patients who underwent type I reaction. In this group, the circulating IGF-I/IGFBP-3 levels at diagnosis were significantly lower

(93% and 87%, respectively, with levels below the normal range) in comparison to nonreactional BL patients whose levels were normal.

Major conclusions: Our data revealed important alterations in the IGF system in relation to the status of the host immune-inflammatory response to ML while at the same time pointing to the circulating IGF-I/IGFBP-3 levels as novel predictive biomarkers for leprosy reaction at diagnosis.

Key words: leprosy, IGF-I, IGFBP-3, reaction, *Mycobacterium leprae,* biomarker, neuroendocrine system, immune-inflammatory response

Author Summary

Leprosy is caused by a mycobacterium that has a predilection for nerve cells. Nerve damage may continue during multidrug therapy and even subsequent to patient release, due to the occurrence of acute inflammatory episodes known as leprosy reactions. Reactions constitute a medical emergency, as severe nerve injury may occur rapidly, with subsequent loss of sensation, paralysis and deformity. A priority in leprosy research has been the identification of biomarkers that would predict at disease diagnosis those with high risk of undergoing reactions. So far, most studies have searched for these markers among elements of the immune response, but reliable markers are still missing. The study herein presented extends this analysis to components of the neuroendocrine system. During infectious diseases, the immune and neuroendocrine systems act in concert facilitating host response and homeostasis. In our study, we measured serum levels of the hormone insulin-like growth factor (IGF-I) and IGFBP-3, its major binding protein, at diagnosis in nonreactional vs. reactional patients. Our data indicate that circulating IGF-I and IGFBP-3 levels can be used as predictive biomarkers for leprosy reaction at diagnosis, favoring the development of new strategies for the management of leprosy patients with consequent prevention of reaction and neuropathy.

Introduction

Leprosy, a chronic infectious disease caused by the obligate intracellular bacterium *Mycobacterium leprae* (ML), remains a major source of morbidity in developing countries [1]. The disease principally affects the skin and peripheral nervous system in which the leprosy bacillus is preferentially found inside macrophages and Schwann cells (SC) [2]. This tissue tropism causes nerve damage, which, in turn, leads to sensorial impairment and permanent disabilities, by far the major health concern facing leprosy patients today.

Also known as Hansen´s disease, leprosy manifests as a spectrum of clinical forms in correlation with the nature and magnitude of the innate and adaptive immune responses generated during ML infection [3,4]. At one extreme of the spectrum, individuals with TT leprosy have few lesions and manifest a contained, self-limited infection in which scarce bacilli are detected due to the generation of a strong cellular immune response against ML. At the other extreme, LL is a progressive and disseminated disease characterized by extensive bacterial multiplication within host cells and low cell-mediated immunity (CMI) to the pathogen. Between these two poles are the borderline forms (characterized by their intermediate clinical and immunological patterns), which are referred to as borderline tuberculoid (BT), borderline borderline (BB) and borderline lepromatous (BL), according to their proximity to one pole or the other.

Nerve damage occurs in all clinical forms of the disease, and may continue during multidrug therapy (MDT) and even subsequent to patient release, due, for the most part, to the occurrence of acute immune-inflammatory episodes known as leprosy reactions. The most frequent leprosy reactions are classified as Type 1

(reversal) reaction (RR) and Type 2 reaction, or erythema nodosum leprosum (ENL); and many patients experience multiple, recurrent episodes [5]. Neuritis and cutaneous inflammation are prominent symptoms of both types of reaction with systemic repercussions, as seen in the occurrence of malaise, fever, and inflammation in other tissues. RR predominates in borderline patients with a baciloscopic index (BI) below 3, while ENL only occurs in lepromatous (LL) patients with high bacterial loads [6,7]. Over the past decades numerous studies have been conducted enhancing our knowledge of the epidemiological, clinical and laboratory risk factors for neuropathy and reactions in leprosy. However, our understanding of the physiopathology of reactions remains limited and further research is needed to more clearly define laboratory biomarkers capable of accurately identifying the leprosy patients most at risk of developing reaction.

Interaction between the immune and the neuroendocrine systems plays a critical role in host homeostasis during the adaptive response to stress and pathogens [8,9]. Indeed, an increasing understanding of inflammation control by the neuroendocrine system has contributed to our knowledge of the physiopathology of several immune-inflammatory diseases. Furthermore, evidence has shown that during the immune-inflammatory response to infection, the GH/IGF-I/IGFBP-3 somatotropic axis has a prominent regulatory role [10]. These hormones not only affect cellular metabolism but are likewise able to interact with cytokines and glucocorticoids (GCs) modulating the immune-inflammatory response [11]. IGF-I circulates in relatively high concentration levels in plasma that vary according to age (150-400 ng/mL) [12]. IGFBP-3 binds to 80-90% of circulating IGF in a stable ternary complex with an acid-labile subunit (ALS) serving as the main reservoir for plasma

IGF-I [13]. Most of the IGF-I found in circulation is produced in the liver under growth hormone (GH) regulation.

In leprosy, little, if anything, is known about the interaction between the immune and neuroendocrine systems [14]. Since the disease has a strong immune-inflammatory component, it is hypothesized that the cross-talk taking place between these two systems may have a profound effect on the natural course of ML infection. In the present investigation, a retrospective study was conducted to compare the circulating levels of IGF-I and IGFBP-3 across the spectral clinical forms of leprosy in conjunction with reactional vs. nonreactional LL and BL patients at diagnosis and during reaction. Our results demonstrate significant differences in circulating IGF-I/IGBP-3 in leprosy according to disease status, and indicate that these proteins could be used to identify patients with high risk of developing reactions.

Methods

Study subjects

The sample included 59 patients (26 females, 33 males, aged 19-65) referred to the Souza Araújo Ambulatory (Reference Center for Leprosy Diagnosis and Treatment, Oswaldo Cruz Foundation, Rio de Janeiro, RJ, Brazil) for the diagnosis and treatment of leprosy. Patients were categorized according to the Ridley and Jopling classification scale [3] into borderline tuberculoid (BT), borderline lepromatous (BL), or lepromatous (LL). RR typically developed as an acute inflammatory response in pre-existing lesions while the ENL diagnosis was primarily based on the occurrence of nodular skin lesions together with fever with or without peripheral nerve pain and/or nerve dysfunction. Patients were distributed into the following groups: 13 nonreactional BT; 15 BL who had RR during treatment; 10 nonreactional BL (NR BL); 10 LL that developed ENL during treatment; and 11 nonreactional LL (NR LL) patients. The baseline characteristics of each group of individuals included in the study are shown in Table 1. Blood was collected at the beginning of leprosy treatment. Healthy controls (HC) included 19 individuals (16 females, 3 males, aged 19 - 62).

This study was approved by the Ethics Committee of the Oswaldo Cruz Foundation. Written informed consent was obtained from all patients or their guardians and controls prior to specimen collection. Blood samples were taken from 1995 through 2005; and patient sera were extracted and stored at -20° C until retrieval for analysis.

IGF-I, IGFBP-3, and TNF-α measurements

The serum levels of IGF-I, IGFBP-3, and TNF-α were measured by the IMMULITE 1000 Analyzer (EuroDPC Med Limited, Llanberis, UK). Assays were carried out using the solid phase, enzyme-labeled, chemiluminescent-immunometric method in accordance with the manufacturer´s instructions.

Statistical analysis

Data are expressed as median, mean ± S.D. values. Group comparisons were evaluated by analyzing variance (ANOVA), using age as a covariate. Wilcoxon test was employed to compare cytokine levels before and during reactions. The percentages of individuals with normal and below-normal levels of IGF-I and IGFBP-3 were compared within the groups via Pearson Chi-square (or Fisher) and McNemar (before and during reaction) tests. Bonferroni correction was employed whenever necessary. All statistical calculations were done via the SPSS software program and *p* values lower than 0.05 were considered statistically significant.

Results

Serum IGF-I and IGFBP-3 levels across the spectral clinical forms of leprosy

Evidence in the literature has shown that the somatotropic axis is responsible for modulating the immune system, directly influencing both the humoral and cellular immune responses [15,16]. Since the spectral clinical forms of leprosy occur as a result of the capacity of the host to mount anywhere from low- (LL)-to-high (TT) CMI responses against ML, the serum levels of IGF-I and IGFBP-3 were compared among patients with the different clinical forms. The levels found in leprosy patients were compared with those measured in the healthy controls (HC, n=19). Following analysis in a HC, NR BT, NR BL, and NR LL sequence, a shallow decrease in IGF-I levels was observed, with significant differences between NR LL and HC ($P<0.05$), and between NR LL and NR BT ($P<0.05$) (Figure 1A). A similar decrease in IGFBP-3 was observed, with significant different between NR LL and HC ($P<0.05$), NR LL and NR BT ($P<0.001$), NR BL and HC ($P<0.001$), and between NR BL and NR BT ($P<0.05$) (Figure 1B). As depicted in Fig. 1C and D, there was a significant difference between the NR LL and all other groups when the percentage of individuals in each group with a below-normal IGF-I/IGFBP-3 range was calculated.

Circulating IGF-I and IGFBP-3 levels were significantly higher at the pre-MDT stage in LL patients that presented ENL episodes during treatment

Serum IGF-I and IGFBP-3 levels in nonreactional and reactional LL patients were then investigated. For this purpose, LL patients (n=21) who suffered ENL episodes or not during MDT were enrolled in the study. For the LL patients without

reaction (referred to as NR LL, n=11), serum samples were obtained at the onset of MDT. For reactional patients (n=10), serum samples were obtained at two different time points: i) at the outset of MDT, when no signs of reaction were detected (referred to as R $LL_{t=0}$); and ii) during reactions (referred to as R LL_{ENL}) taking place between 3 weeks and 2 years after the beginning of treatment (mean average of 11.5 ± 9.3 months). IGF-I and IGFBP-3 displayed identical level patterns in these 3 different sets of serum samples, as shown in the box plots of Figure 2A and B, respectively. Interestingly, the R $LL_{t=0}$ samples presented significantly higher levels of IGF-I and IGFBP-3 in comparison with the NR LL group ($P<0.001$ and $P=0.007$, respectively). However, during reaction, these levels decreased significantly (R LL_{ENL}; $P<0.05$), reaching similar values to those detected in the NR LL group.

TNF-α was also quantified in the same serum samples due to the well-established role of this pro-inflammatory cytokine in leprosy reaction [17,18] and its antagonistic activity on IGF-I [19]. Similar range levels of TNF-α were observed in NR LL and R $LL_{t=0}$ serum samples (Figure 2C). However, TNF-α levels were much higher during ENL ($P < 0.05$) in comparison to the ones measured prior to reaction. When the IGF-I/TNF-α and IGFBP-3/TNF-α ratios for each individual were calculated and compared before and during ENL, remarkably homogeneous behavior was observed in most patients, registering a significant drop in both ratios during reaction (Figure 2D and E).

Table 2 shows the percentage of serum samples in the LL groups having below-reference range IGF-I and IGFBP-3 levels according to age. The difference in the IGF-I and IGFBP-3 levels in NR LL versus R $LL_{t=0}$ is best represented in the pie diagram shown in Figure 3. Among NR LL patients, the IGF-I levels of 81.8% (9 out of 11) were below the reference range, in contrast to only 20% (2 out of 10) of the R

$LL_{t=0}$ serum samples. Again, while the IGFBP-3 levels of 72.7% (8 out of 11) of the NR LL patients were below the reference range, the same occurred in only 20% (2 out of 10) of the R $LL_{t=0}$ serum samples.Taken together, these results demonstrate that the IGF-I and IGFBP-3 circulating levels were significantly higher in the LL patients presenting ENL than among the LL patients that did not experience reaction. During ENL, however, these levels tended to decrease, attaining the same levels as the NR LL patients.

Circulating IGF-I and IGFBP-3 levels were significantly lower at the pre-MDT stage in reactional BL patients that presented RR episodes during treatment

The investigation of IGF-I and IGFBP-3 levels in the context of RR episodes followed. This type of reaction affects approximately one third of all borderline patients [20]. A group of BL patients categorized as nonreactional (referred to as NR BL; n=10) and reactional BL (or R BL; n=15) was included in this analysis. For the NR BL group, blood samples were taken upon initiation of MDT. Serum samples from reactional patients were obtained at 2 different time points: i) at the beginning of MDT when no signs of reaction were detected (R $BL_{t=0}$); and ii) during reaction (R BL_{RR}) occurring between 2 weeks and 18 months after the beginning of treatment (mean average of 6.6 ± 4.8 months). IGF-I and IGFBP-3 displayed identical level patterns in these 3 different sets of serum samples, as can be seen in the box plots of Figure 4A and B, respectively. Notably, the R $BL_{t=0}$ samples showed lower IGF-I/IGFBP-3 levels than the NR BL ones. Nevertheless, IGF-I rose significantly during reaction (R BL_{RR} samples) ($P<0.014$).

In parallel, TNF-α levels were quantified in the same serum samples. In contrast to the differences observed in IGF-I/IGFBP-3, a similar range of TNF-α serum concentrations was observed in BL patients regardless of disease status (Figure 4C). Figure 4D and E show the IGF-I/TNF-α and IGFBP-3/TNF-α serum ratios calculated before and during RR for each BL patient. Both ratios increased in 13 of the 15 patients during RR as a consequence of the higher IGF-I/IGFBP-3 levels during these episodes.

Table 2 shows the percentage of serum samples in each group, with IGF-I and IGFBP-3 levels below the reference range according to age in all groups analyzed. Accordingly, 93.3% (14 out of 15) of the R $BL_{t=0}$ patients showed IGF-I levels below the reference range, in contrast to 10% (1 out of 10) of the NR BL patients. Again, while 86.6% (13 out of 15) of the R $BL_{t=0}$ patients displayed IGFBP-3 levels below the reference range, the same was true in only 20% (2 out of 10) of the NR BL individuals. A clearer representation of the different patterns in the IGF-I/IGFBP-3 levels observed in NR BL vs. R $BL_{t=0}$ can be found in Figure 5.

Taken together, the results presented in this section of our study demonstrate that, at diagnosis, the IGF-I and IGFBP-3 circulating levels were significantly lower in BL patients presenting RR, as compared to the BL patients that did not experience these episodes, and that these levels tended to increase during RR, attaining the same levels as the NR BL group.

Discussion

The interplay between the immune and neuroendocrine systems exerts a critical role in the maintenance of host homeostasis during infection. The neuroendocrine system not only favors the building of an effective immune response against the pathogen, but also controls its intensity, thus avoiding extensive tissue damage [8].

Leprosy is an infectious disease with a strong immune-inflammatory component, whose status dictates both the clinical form of the disease as well as the occurrence of reaction. This particular characteristic makes this disease a very attractive model for studying immunoneuroendocrine interactions, allowing for a broader understanding of the interplay among hormones, cytokines, and GCs during chronic inflammation in combination with acute inflammatory episodes in response to mycobacterial antigens.

One of the many players involved in this interaction is the hormone IGF-I, previously shown to suffer a serious imbalance during [8,10]. In the present study, the IGF system was analyzed for the first time during the course of disease by measuring the circulating levels of IGF-I and IGFBP-3 in patients representing status variations with regard to the immune-inflammatory response to ML infection. Circulating IGF-I/IGFBP-3 was initially examined across the leprosy spectrum. Interestingly, while no significant difference was observed between BT and HC (perhaps due to the low number of BT patients included in this study), both the nonreactional, clinically-stable BL and, to a greater extent, LL patients showed decreased levels of IGF-I/IGFBP-3. It is worth noting that the IGF-I/IGFBP-3 levels across the leprosy spectrum appeared to follow a trend similar to the one observed

in serum IFN-γ [21,22] according to the magnitude of the specific cellular immune response mounted by the host in reacting to infection (higher at the TT pole). These results, however, were diametrically opposed to what was found with respect to the circulating levels of the pro-inflammatory cytokines IL-1-β, IL-6, and TNF-α [17,18,23,24] (higher at the LL pole). A possible interpretation for our findings is that, under the emergence of the cell-mediated immunity in response to ML infection, a scenario of immune-neuroendocrine interaction is established with the participation of Th1-type cytokines. We hypothesize that the somatotropic axis remains undisturbed in this scenario while, in most individuals, circulating IGF-I and IGFBP-3 continue their normal-range levels. At the LL pole, on the other hand, an important imbalance in the somatotropic axis emerges, with most individuals presenting a below-normal range IGF-I/IGFBP-3 together with high levels of pro-inflammatory cytokines. Actually, as will be discussed later, the low levels of IGF-I/IGFBP-3 at the LL pole and the normal levels observed in BT-BL patients have proven to be, respectively, reliable indicators of a controlled immune-inflammatory response to ML across the spectral forms of leprosy.

The systemic low IGF levels in patients with high bacterial loads as reported herein is not in conflict with our previous data indicating the induction of IGF expression by ML in infected SC [25]. The locally-produced IGF may still favor host-cell survival after ML infection without any major repercussions affecting the systemic concentration of this hormone, largely produced by the liver in response to GH.

Several previous reports have demonstrated the importance of maintaining the delicate balance between circulating IGF-I and cytokines during inflammatory diseases. It has been observed that, in patients with chronic obstructive pulmonary

disease, higher concentrations of TNF-α, IL-1β, IL-6, and IL-8 are accompanied by a significant decrease in circulating IGF-I [26]. In Alzheimer´s disease, for example, TNF-α levels correlate negatively to IGF-I [27]. In Henoch-Schonlein Purpura, the most common systemic vasculitis in children, increased serum levels of IGF-I are found [28]. Moreover, in the context of other infectious diseases, it has been reported that HIV patients with wasting syndrome and children with Failure to Thrive have reduced IGF-I serum levels [29,30]. In addition, in patients infected with *Helicobacter pylori*, a reduction in circulating IGF-I levels in comparison what is seen in HC has been observed [31].

The low circulating levels of IGF-I/IGFBP-3 found in NR LL patients (~75% with below-normal levels) were in parallel with those found in critical illnesses like sepsis [32,33]. It is known that the inflammatory response to sepsis is followed by the development of a hypo-inflammatory and immunosuppressive state, which is unable to eradicate the infection [34]. The low IGF-I/IGFBP-3 levels found in the chronic phase of sepsis are the result of overactivation of the HPA axis by the excessive and prolonged production of pro-inflammatory cytokines, leading to the subsequent peripheral secretion of GCs and inhibition of IGF synthesis by the liver [8].

LL and sepsis share this immunosuppressive state. In LL patients, the absence of a CMI response against ML allows the pathogen to proliferate indiscriminately, reach high numbers, and disseminate systemically throughout the bloodstream. Although presenting high bacteremia, approximately 50% of LL patients are clinically stable, evidence of a controlled, finely-regulated immune-inflammatory response due to the activation of anti-inflammatory loops that prevent over-inflammation and subsequent immune-mediated tissue damage. It is

reasonable to speculate that HPA, considered the main physiological feedback loop in inflammation, is activated in these patients, playing a critical role in maintaining homeostasis. HPA activation in these patients is expected, based on the high circulating levels of the pro-inflammatory cytokines such as the IL-1β, IL-6, and TNF-α detected in LL [17,18,23,24]. However, to date, evidence concerning the circulating levels of cortisol and the adrenal functional status in leprosy has been conflicting [14]. Additionally, intrinsic anti-inflammatory mechanisms such as the high production of IL-10 observed in these patients [35] may complement the immune-suppressive effects of GCs, making possible a controlled immune-inflammatory response in a scenario of hyper-stimulation of the host immune system resulting from accumulated concentrations of mycobacterial antigens.

Notably, the LL patients who underwent ENL during treatment showed significantly higher levels of IGF-I/IGFBP-3 at the pre-MDT stage (up to 2 years before reaction), suggesting that changes in these proteins reflect the delicate balance between the pro- and anti-inflammatory responses in these patients and, consequently, the risk of initiating an uncontrollable inflammatory event. In these patients, very low levels of IGF-I/IGFBP-3 might, then, be reflective of high immune-suppression levels, a controlled immune-inflammatory response, and high clinical stability. In contrast, LL patients with higher IGF-I/IGFBP-3 may be the result of insufficient anti-inflammatory feedback, which is necessary for the maintenance of homeostasis in the presence of high concentrations of ML antigens.

During ENL, previous data indicating high systemic production of TNF-α [17] were confirmed. Also observed was a reduction in IGF-I/IGFBP-3 levels as an attempt to reach the low levels observed in NR LL, most likely as the result of the activation of an anti-inflammatory loop such as the release of GCs in response to the

presence of high levels of pro-inflammatory cytokines. When the IGF-I/TNF-α and IGFBP-3/TNF-α ratios were calculated before and during ENL, a significant decrease was observed during reaction in these individuals. These lower ratios, which may also contribute to the nerve injuries observed during ENL, may at least partially explain the enhanced rate of spontaneous apoptosis *ex vivo* demonstrated in the CD 14^+ cells (PBMC) of ENL patients [36].

Indeed, a number of reports have demonstrated the neuroprotective activity of IGF-I both in the peripheral (PNS) and central nervous systems (CNS) in pathologies typically associated with the overproduction of pro-inflammatory cytokines [19]. IGF-I is able to maintain tissue homeostasis and promote cellular well-being in conjunction with the anti-inflammatory cytokines IL-10 and IL-4 by inhibiting the inflammatory response mediated by the prototypical, pro-inflammatory cytokines IL-1β and TNF-α. In this regard, Laue and coworkers [30] has reported that the degree of neurodegeneration in patients with HIV-associated dementia correlated with high TNF-α production and IGF-I reduction. In sepsis, a decrease in IGF-I [32] also accompanies the increase of TNF-α and IL-1β serum levels, which, in turn, correlates with organ injury and the severity of disease [37,38]. Furthermore, IGF-I treatment is known to improve the chances of survival in murine sepsis [33].

It should be highlighted that whenever a group of BL patients was analyzed, very interesting but opposing findings were observed in the context of changes in circulating IGF-I/IGFBP-3 according to the immunological stability of the patients. Differently from the anergic state of LL patients, BL patients are known to build a weak CMI response against ML [21,22]. RR is associated with increased CMI, which may occur subsequent to ML antigen release during MDT [39]. RR is characterized by an increase in Th1 response to ML antigens that is capable of rapidly triggering

the production of nerve damage [40]. The IGF-I/IGFBP-3 levels in NR BL vs. HC were only marginally lower. In fact, most individuals (~85%) presented normal levels. In contrast, the BL group that manifested RR during MDT displayed significantly lower levels of IGF-I/IGFBP-3 (~90% below the normal range) at the pre-MDT stage.

All together, these data suggest that, in BL patients, the IGF-I/IGFBP-3 levels and/or factors that are able to maintain their normal activity are crucial in controlling the immune-inflammatory response since their reduction in circulation below the normal range leads to homeostasis disruption and the emergence of RR. Significantly, during RR in BL patients, an increase in IGF-I/IGFBP-3 was observed as an attempt to reach normal levels. Actually, based on the capacity of IGF-I to stimulate the secretion of IL-10 by activated T cells [16], it is tempting to speculate an anti-inflammatory role for this hormone by dampening local inflammation in the skin and nerves in nonreactional BL patients and during RR. Thus, IGF-I could act as an anti-inflammatory cytokine, contributing to the re-establishment of homeostasis. Consistent with the studies of Anderson and colleagues [41], no changes in the TNF-α serum levels of BL patients were detected during RR. When the IGF-I/TNF-α and IGFBP-3/TNF-α ratios were calculated at the pre-MDT stage and during RR, a significant increase was observed during reaction in most of the affected individuals.

In conclusion, our data revealed important alterations in the IGF system in relation to the status of the host immune-inflammatory response to ML. These findings support the hypothesis that immune-neuroendocrine interactions play a critical role during the natural course of ML infection, contributing to a controlled CMI response across the spectral clinical forms of leprosy. Disruption of immune neuroendocrine homeostasis seems to be associated with acute, uncontrolled

inflammatory episodes. Of note, our data indicate that circulating IGF-I and IGFBP-3 levels can be used as predictive biomarkers for leprosy reaction at diagnosis, favoring the development of new strategies for the management of leprosy patients and the prevention of reaction and neuropathy.

Acknowledgments

We would especially like to thank Judy Grevan for editing the text; Dr. Geraldo Pereira for his constructive comments; Dr. Maria Fernanda Miguens Castelar Pinheiro of the Sérgio Franco Laboratory for the quantification of IGFs and TNF-α and her important technical assistance; and the medical (all) staff of the Souza Araújo Ambulatory, Oswaldo Cruz Institute, for their hard work and dedication.

References

1. WHO. Global Leprosy Situations, beginning of 2009 (2009) Weekly Epidemiol Rec 84: 333-340.
2. Kaplan G, Cohn ZA (1986) Regulation of cell-mediated immunity in lepromatous leprosy. Lepr Rev 57 (2):199-202.
3. Ridley DS, Jopling WH (1966) Classification of leprosy according to immunity. A five-group system. Int J Lepr Other Mycobact Dis 34(3): 255-273.
4. Bloom BR, Mehra V (1984) Immunological unresponsiveness in leprosy. Immunol Rev 80: 5-28.
5. Ridley DS (1969) Reactions in Leprosy. Lepr Rev 40: 77-81.
6. Van Brakel WH, Khawast IB, Lucas SB (1994) Reactions in leprosy: a epidemiological study of 386 patients in West Nepal. Lepr Rev 65: 190-203.
7. Nery JA, Vieira LM, de Mattos HJ, Sarno EN (1998) Reactional states in multibacilary Hansen disease patients during multidrug therapy. Rev Inst Med Trop São Paulo 40: 363-370.
8. Borghetti P, Saleri R, Mocchegiani E, Corradi A, Martelli P (2009) Infection, immunity and the neuroendocrine response. Vet Immunol Immunopathol 130: 141-162.
9. Pérez AR, Bottasso O, Savino W (2009) The impact of infectious diseases upon neuroendocrine circuits. Neuroimmunomodulation 16: 96-105.
10. Mesotten D, Van den Berghe G (2006) Changes within the growth hormone/insulin-like growth factor I/IGF binding protein axis during critical illness. Endocrinol Metab Clin North Am 35: 793-805.

11. Agha A, Monson JP (2007) Modulation of glucocorticoid metabolism by growth hormone – IGF-1 axis. Clin Endocrionol 66: 459-465.
12. Clemmons DR (2007) Modifying IGF1 activity: an approach to treat endocrine disorders, atherosclerosis and cancer. Nature 6: 821-833.
13. Baxter RC (2000) Insulin-like growth factor (IGF)-binding proteins: interactions with IGFs and intrinsic bioactivities. Am J Physiol Endocrinol Metab 278: 967-976.
14. Leal AM, Foss NT (2009) Endocrine dysfunction in leprosy. Eur J Clin Microbiol Infect Dis 28: 1-7.
15. Van Buul-Offers SC, Kooijman R (1998) The role of growth hormone and insulin-like growth factors in the immune system. Cell Mol Life Sci 54: 1083-1094.
16. Kooijman R, Coppens A (2004) Insulin-like Growth Factor-I stimulates IL-10 production in human T cells. J Leukoc Biol 76: 862-867.
17. Sarno EN, Grau GE, Vieira LMM, Nery JA (1991) Serum levels of tumor necrosis factor-alpha and interleukin-1β during leprosy reactional states. Clin Exp Immunol 84: 103-108.
18. Lyer A, Hatta M, Usman R, Luiten S, Oskam L, Faber W, Geluk A, Das P (2007) Serum levels of interferon-gamma, tumour necrosis factor-alpha, soluble interleukin-6R and soluble cell activation markers for monitoring response to treatment of leprosy reactions. Clin Exp Immunol 150: 210-216.
19. Venters HD, Dantzer R, Kelly KW (2000) A New Concept in Neurodegeneration: TNF-α is a Silencer of Survival Signals. T Neurosci 23: 175-180.

20. Lienhardt C, Fine PE (1994) Type 1 reaction, neuritis and disability in leprosy. What is the current epidemiological situation? Lepr Rev 65: 9-33.
21. Nogueira N, Kaplan G, Levy E, Sarno EN, Kushner P, Granelli-Piperno A, Vieira L, Colomer Gound V, Levis W, Steinman R, Yip YK, Cohn ZA (1983) Defective interferon production in leprosy. J Exp Med 158: 2165-2170.
22. Godal T, Myrvang B, Samuel DR, Foss WF, Lofgren M (1973) Mechanisms of “reactions” in borderline tuberculoid (BT) leprosy. A preliminary report. Acta Pathol Microbiol Scand A 236: 45-53.
23. Moubasher AD, Kamel NA, Zedan H, Raheem DD (1998) Cytokines in leprosy, I. Serum cytokine profile in leprosy. Int J Dermatol 37: 733-740.
24. Belgaumkar VA, Gokhale NR, Mahajan PM, Bharadwaj R, Pandit DP, Deshpande S (2007) Circulating cytokine profile in leprosy patients. Lepr Rev 78: 223-230.
25. Rodrigues LS, da Silva Maeda E, Moreira ME, Tempone AJ, Lobato LS, Ribeiro-Resende VT, Alves L, Rossle S, Lopes UG, Pessolani MC (2010) *Mycobacterium leprae* induces insulin-like growth factor and promotes survival of Schwann cells upon serum withdrawal. Cell Microbiol 12: 42-54.
26. Kythreotis P, Kokkini A, Avgeropoulou S, Hadjioannou A, Anastasakou E, Rasidakis A, Bakakos P (2009) Plasma leptin and insulin-like growth factor I levels during acute exacerbations of chronic obstructive pulmonary disease. BMC Pulm Med 5: 9-11.
27. Alvarez A, Cacabelos R, Sanpedro C, García-Fantini M, Aleixandre M (2007) Serum TNF-alpha levels are increased and correlate negatively with free IGF-I in Alzheimer disease. Neurobiol Aging 28: 533-536.

28. Yildiz B, Kural N, Aydin B, Colak O (2008) Increased serum levels of insulin-like growth factor (IGF)-1 and IGF-binding protein-3 in Henoch-Schonlein purpura. Tohoku J Exp Med 214: 333-340.
29. Jain S, Golde DW, Balley R, Geffner ME (1998) Insulin-like growth factor-I resistence. Endocr Rev 19: 625-646.
30. Laue L, Pizzo PA, Butler K, Cutler Jr GB (1990) Growth and neuroendocrine dysfunction in children with acquired immunodeficiency syndrome. J Pediatr 117: 541-545.
31. BariceviæI, NediæO, NikoliæJA, BojiæB, JojiæN (2004) Circulating insulin-like growth factors in patients infected with *Helicobacter pylori*. Clin Biochem 37: 997-1001.
32. Karinch AM, Pan M, Lin CM, Strange R, Souba WW (2001) Glutamine metabolism in sepsis and infection. J Nutr 131: 2535S-2538S. [Discussion, 2550S-2551S].
33. Ashare A, Nymon AB, Doerschug KC, Morrison JM, Monick MM, Hunninghake GW (2008) Insulin-like growth factor-1 improves survival in sepsis via enhanced hepatic bacterial clearance. Am J Respir Crit Care Med 178: 149-157.
34. Hotchkiss RS, Nicholson DW (2006) Apoptosis and caspases regulate death and inflammation in sepsis. Nat Rev Immunol 6: 813-822.
35. Lima MC, Pereira GM, Rumjanek FD, Gomes HM, Düppre N, Sampaio EP, Alvim IM, Nery JA, Sarno EM, Pessolani MC (2000) Immunological cytokine correlates of prospective immunity and pathogenesis in leprosy. Scand J Immunol 51: 419-428.

36. Hernandez MO, Neves JR, Sales JS, Carvalho DS, Sarno EN, Sampaio EP (2003) Induction of apoptosis in monocytes by *Mycobacterium leprae in vitro*: a possible role for tumour necrosis factor-α. Immunol 109: 156-164.
37. Martin C, Boisson C, Haccoun M, Thomachot L, Mege JL (1997) Patterns of cytokine evolution (tumor necrosis factor-alpha and interleukin-6) after septic shock, hemorrhagic shock, and severe trauma. Crit Care Med 25: 1813-1819.
38. Meduri GU, Headley S, Kohler G, Stentz F, Tolley E, Umberger R, Leeper K (1995) Persistent elevation of inflammatory cytokines predicts a poor outcome in ARDS. Plasma IL-1 beta and IL-6 levels are consistent and efficient predictors of outcome over time. Chest 107: 1062-1073.
39. Lockwood DN, Vinayakumar S, Stanley JN, McAdam KP, Colston MJ (1993) Clinical features and outcome of reversal (type 1) reactions in Hyderabad, India. Int J Lepr Other Mycobact Dis 61: 8-15.
40. Yamamura M, Wang XH, Ohmen JD, Uyemura K, Rea TH, Bloom BR, Modlin RL (1992) Cytokine patterns of immunologically mediated tissue damage. J Immunol 149: 1470-1475.
41. Anderson AK, Chaduvula M, Atkinson SE, Khanolkar-Young S, Jain S, Suneetha L, Suneetha S, Lockwood DN (2005) Effects of prednisolone treatment on cytokine expression in patients with leprosy type 1 reactions. Infect Immun 73: 3725-3733.

Figure Legends

Figure 1. Serum IGF-I and IGFBP-3 levels along the spectrum of leprosy clinical forms. Box-plots represent the serum levels of IGF-I (A) and IGFBP-3 (B) assessed in healthy controls (HC, n=19), and nonreactional borderline tuberculoid patients (NR BT, n=13), borderline lepromatous leprosy patients (NR BL, n=10), and lepromatous leprosy patients (NR LL, n=11) before polychemotherapy treatment. Median values are indicated by line (-). Statistical differences between the groups were evaluated by ANOVA, using age as a covariate. C and D represent the percentage of individuals in each group with below-normal IGF-I and IGFBP-3 serum levels, respectively. Statistical differences were compared within the groups via Pearson Chi-square (or Fisher). *, statistically significant when compared to all other groups.

Figure 2. Circulating IGF-I and IGFBP-3 levels change according to disease status in LL patients. Box-plots represent the serum levels of IGF-I (A), IGFBP-3 (B), and TNF-α (C) assessed in nonreactional (NR LL, n=11) and reactional LL patients (n=10) at the pre-MDT stage (R $LL_{t=0}$) and during ENL (R LL_{ENH}). Median values are indicated by line (-). Statistical differences between the groups were evaluated by ANOVA, using age as a covariate. D and E represent the IGF-I/TNF-α and IGFBP-3/TNF-α ratios, respectively. Each line represents one patient. Wilcoxon test was used for statistical analysis.

Figure 3. IGF-I and IGFBP-3 at diagnosis discriminate LL patients with high risk of developing ENL. Pie diagram showing the percentage of individuals with

normal- and reduced-circulating levels of IGF-I and IGFBP-3 in nonreactional (NR LL) and reactional LL (R $LL_{t=0}$) at leprosy diagnosis.

Figure 4. Circulating IGF-I and IGFBP-3 levels change according to disease status in BL patients. Comparison of the IGF-I (A), IGFBP-3 (B), and TNF-α (C) serum levels among nonreactional (n=10) and reactional BL patients (n=14) at the pre-MDT stage (R $BL_{t=0}$) and during RR (R BL_{RR}). Median values are indicated by line (-) in the box-plots. Statistical differences between the groups were evaluated by ANOVA, using age as a covariate. D and E represent the IGF-I/TNF-α and IGFBP-3/TNF-α ratios, respectively. Each line represents one patient. Wilcoxon test was used for statistical analysis

Figure 5. IGF-I and IGFBP-3 at diagnosis discriminate BL patients with high risk of developing RR. Pie diagram showing the percentage of individuals with normal- and reduced-circulating levels of IGF-I and IGFBP-3 in nonreactional (NR BL) and reactional BL (R $BL_{t=0}$) at leprosy diagnosis.

Table 1

Table 1. Baseline characteristics of leprosy patients and healthy controls.

Characteristics	HC	NR BT	NR BL	RR BL	NR LL	ENL LL
Individuals (n)	19	13	10	15	11	10
Sex						
Female	16	8	2	9	3	4
Male	3	5	8	6	8	6
Age (median ± SD)	36.9 ± 13.9	35.8 ± 16.2	37.4 ± 19.9	37.2 ± 18.2	36.9 ±12.8	39.3 ± 19.5
Baciloscopic Index (median ± SD)	------	0.08 ± 0.2	2.4 ± 1.3	1.7 ± 1.2	3.4 ± 0.5	4.5 ± 0.5

Groups included in this study: HC, healthy controls; NR BT, nonreactional BT patients; NR BL, nonreactional BL patients; RR BL, reversal reaction cases of BL patients; NR LL, nonreactional LL patients; ENL LL, erythema nodosum leprosum cases of LL patients.

597 Table 2

598

Table 2. Individuals with below-normal IGF-I and IGFBP-3 serum levels.

	HC	NR BT	NR BL	BL t=0	RR BL	NR LL	LL t=0	ENL LL
IGF-I	3/19	1/13	1/10	14/15	11/15	9/11	2/10	4/10
(%)	(15.7)	(7.7)	(10)	(93.3) [a,b,c,d]	(73.3) [a,c]	(81.8) [a]	(20) [b,d]	(40)
IGFBP-3	4/19	2/14	2/10	13/15	11/15	8/11	2/10	6/10
(%)	(21)	(15.3)	(20)	(86.6) [a,b,c,d]	(73.3) [a,c]	(72.7)	(20) [d]	(60)

a, b, c and d represent comparisons with significant values when compared: (a) to the HC group; (b) to the NR group with the same clinical form; (c) to the reactional group with the same clinical form; (d) t=0 between BL and LL groups.

599

600 Figure 1

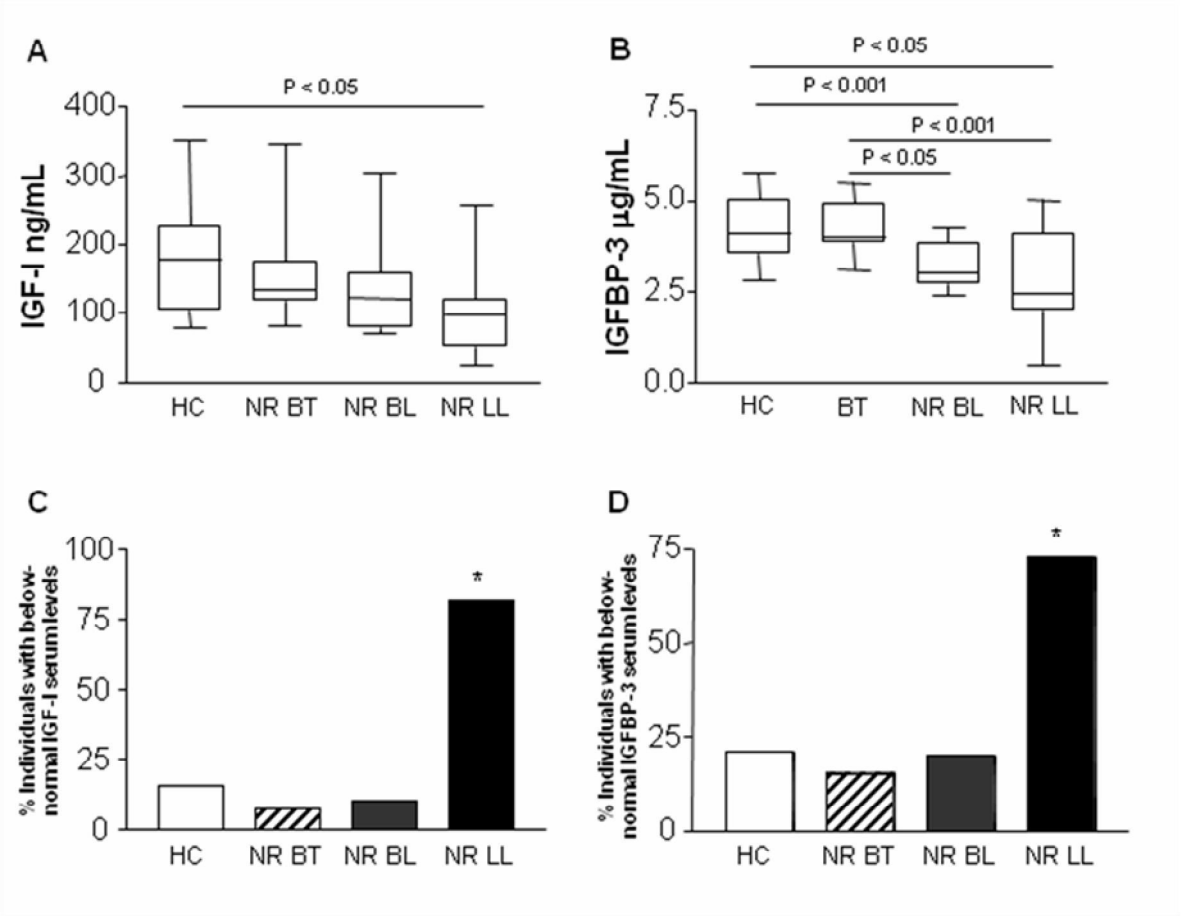

601

602 Figure 2

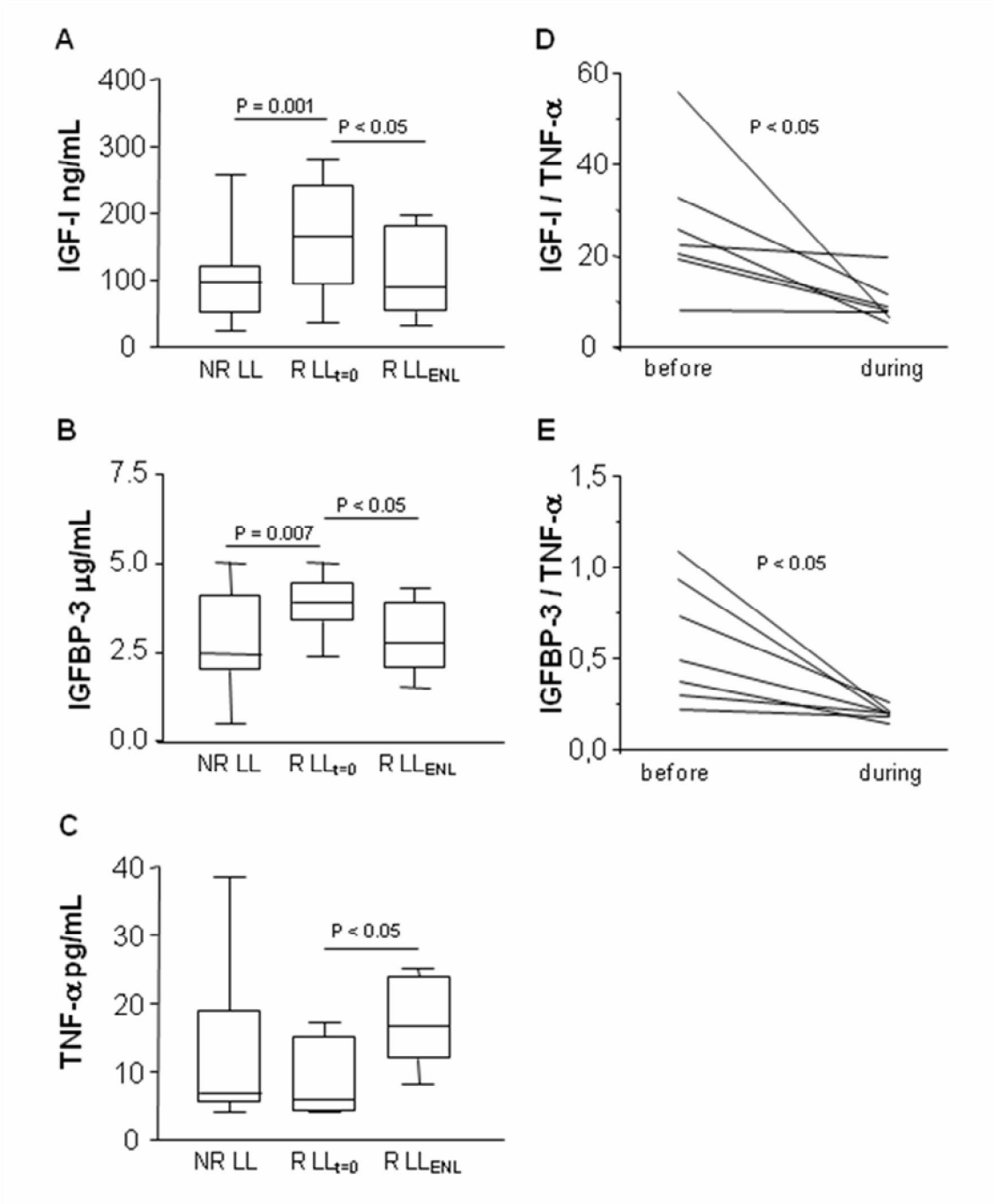

603

604 Figure 3

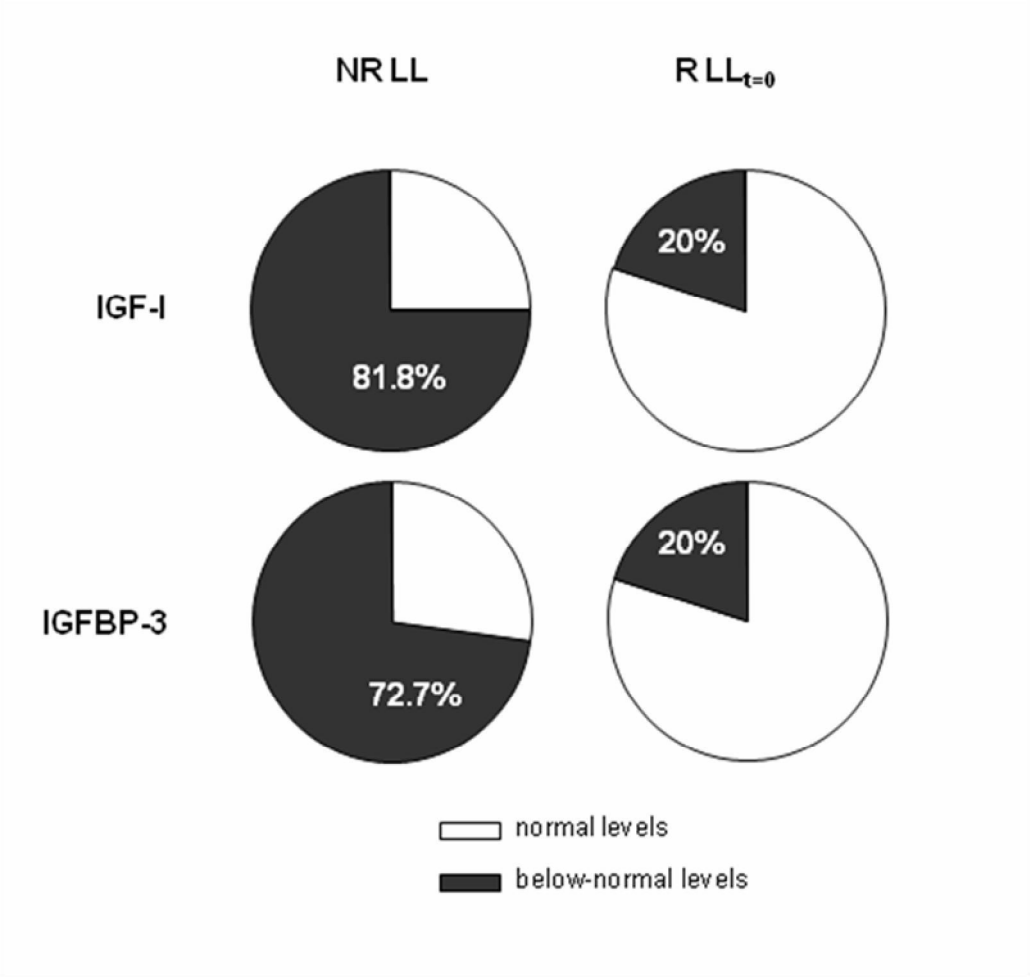

605

606 Figure 4

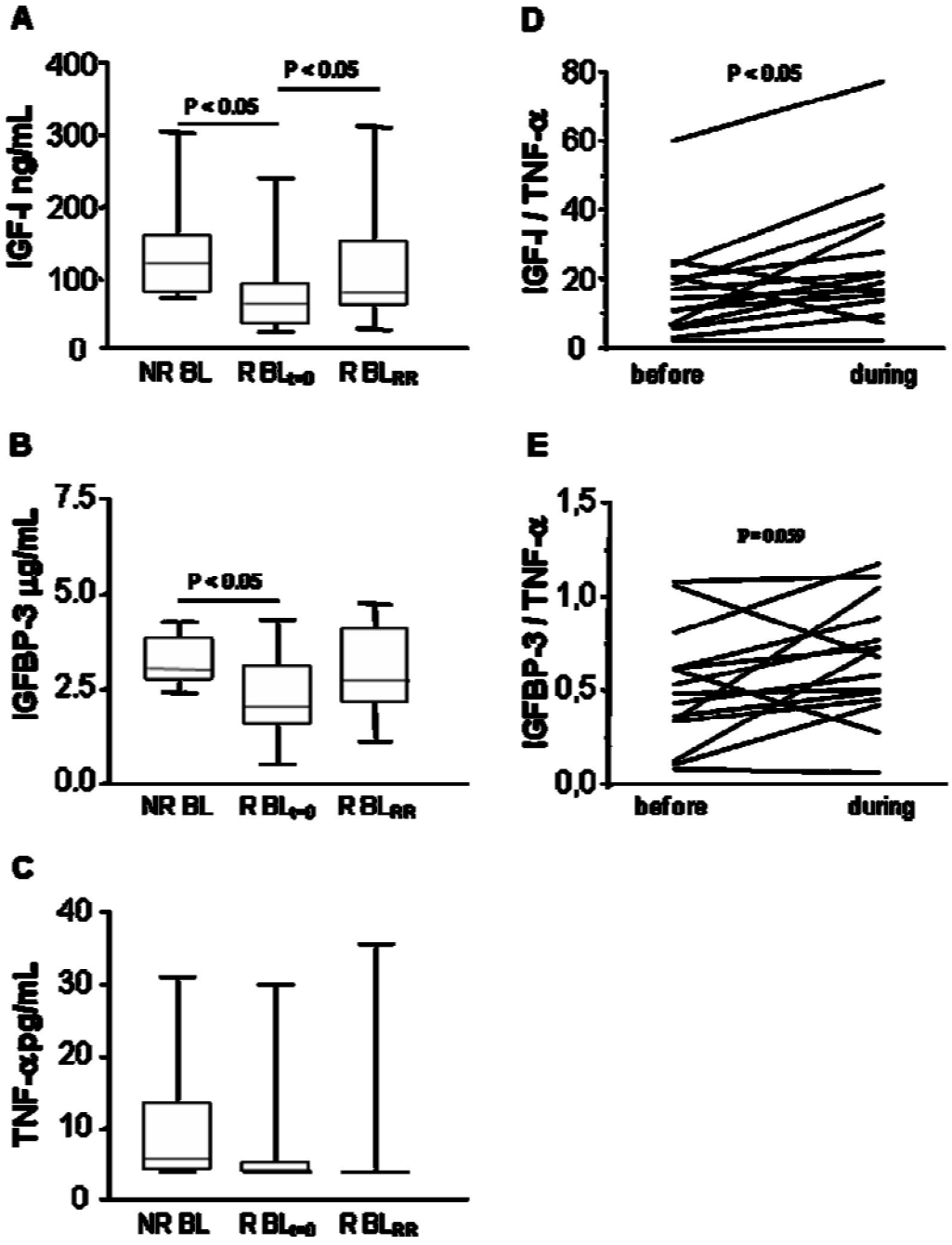

607

608 Figure 5

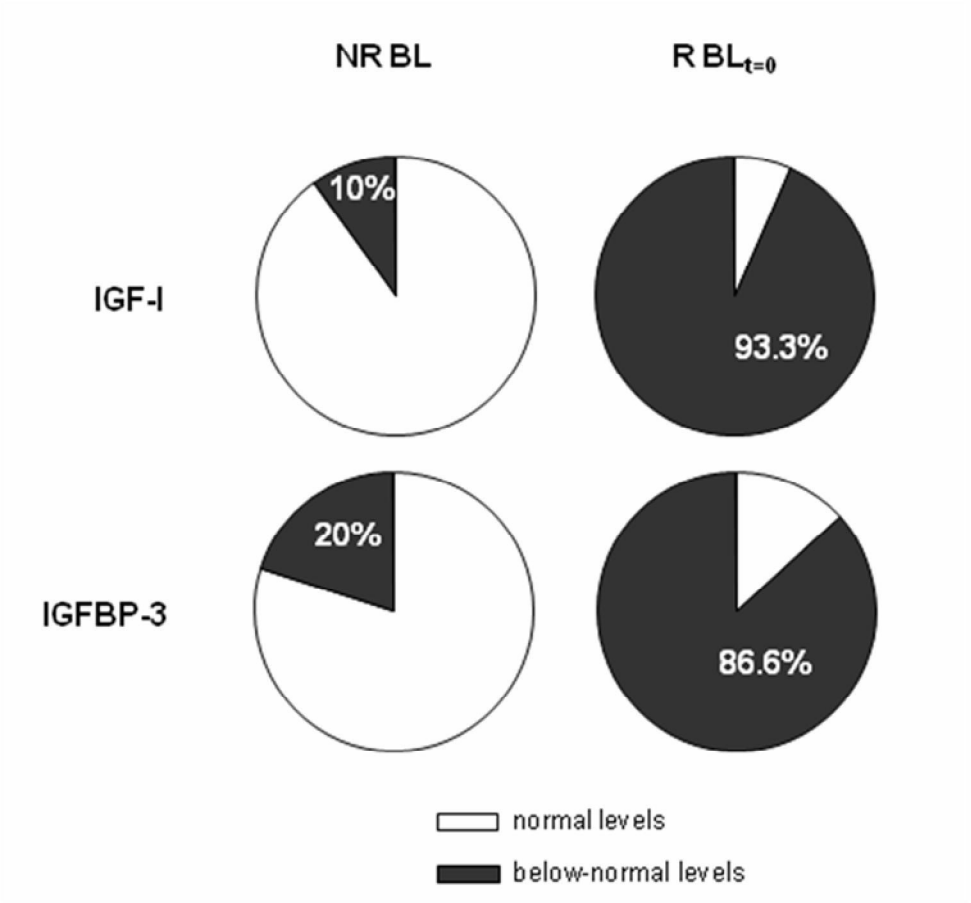

609

CAPÍTULO 5: Discussão

A grande maioria dos indivíduos expostos ao *M. leprae* não desenvolvem a doença e, uma minoria susceptível – possivelmente devido à associação de fatores genéticos e condições sócio-econômicos – manifesta a doença dentro de um espectro de formas clínicas variáveis de acordo com a resposta imunológica montada frente ao bacilo. Desta forma, a hanseníase se apresenta como um excelente modelo de estudo dos processos envolvidos na resposta imunológica do indivíduo frente a uma infecção. O tropismo do *M. leprae* pela CS leva à inflamação, fibrose, desmielinização e degeneração dos nervos periféricos – embora estudos demonstrem uma relação harmoniosa entre o bacilo e sua célula hospedeira preferencial. Sabe-se também que ao longo do curso crônico da hanseníase, os pacientes podem apresentar abruptos episódios imuno-inflamatórios, como resultado de uma reativação da resposta imunológica do indivíduo. Estes episódios são conhecidos como reações hansênicas e são responsáveis pelo agravamento da doença, podendo levar à instalação de incapacidades físicas importantes. Numa tentativa de contribuir para uma melhor compreensão dos mecanismos adotados pelo bacilo de Hansen na colonização bem sucedida do nervo, o presente estudo teve como principal objetivo investigar a participação do IGF-I durante a interação do *M. leprae* com a CS humana e, ainda, durante a evolução natural da doença, sobretudo, durante os episódios reacionais.

Inicialmente, numa abordagem *in vitro*, demonstramos que o *M. leprae* é capaz de inibir a apoptose de CS humanas primárias e da linhagem ST88-14 mantidas em condições livres de soro. Este efeito anti-apoptótico mostrou ser dose-dependente e específico ao *M. leprae*, visto que o tratamento das células com *Mycobacterium bovis* BCG ou *Mycobacterium smegmatis* foram ineficazes na proteção contra a apoptose das CS (Rodrigues e col., 2010). A capacidade de patógenos intracelulares obrigatórios inibirem a apoptose da célula hospedeira é bem descrita e constitui um fator-chave para o sucesso da infecção (Gao e Kwaik, 2000; Hacker e col., 2005). Estes patógenos podem manipular as vias apoptóticas da célula hospedeira interferindo em vias de sinalização que, de alguma forma, regulam o delicado equilíbrio entre fatores apoptóticos e anti-apoptóticos no interior da célula, alterando assim a susceptibilidade da mesma aos inúmeros insultos que venha a receber. De forma bastante interessante, Chuenkova e colaboradores (2001; 2009) demonstraram que o *Trypanosoma cruzi* – um protozoário intracelular com capacidade de invadir diversos tecidos – inibe a apoptose de CS induzida por privação de soro ou pelo estímulo de TNF-α em associação com

TGF-β. Os autores demonstraram ainda, que o parasita ativa diretamente a via PI 3-k através da fosforilação da proteína Akt no interior da célula para inibir a apoptose.

Os efeitos não tóxicos do *M. leprae* já haviam sido previamente descritos por outros autores (Antia e Mukherje, 1985; Hagge e col., 2002; Rambukkana e col., 2002; Tapinos e Rambukkana, 2005) e o efeito anti-apoptótico do *M. leprae* sobre a CS, observado em nosso trabalho complementa estas observações encontradas na literatura. Mais recentemente, foi demonstrado que a infecção de macrófagos com *M. leprae* viável purificado de camundongos *nude* não foi capaz de induzir apoptose destas células (Lahiri e col., 2010). Em outro trabalho, o *M. leprae* parece regular negativamente genes pró-apoptóticos como Bad e Bak e induzir membros anti-apoptóticos da família Bcl-2, como Mcl-1 para inibir a apoptose de células THP-1 (Hasan e col., 2006). Já no estudo de Silva e colaboradores (2008) foi verificado que o bacilo pode induzir baixos níveis de apoptose em CS da linhagem ST88-14, e a lipoproteína 16 kDa do *M. leprae* ou alta infecção foram capazes de induzir apoptose em CS (Oliveira e col., 2003; 2005).

A tecnologia de microarranjos de DNA nos foi muito útil na identificação de um suposto candidato para explicar o mecanismo utilizado pelo *M. leprae* para a proteção da sobrevivência da CS. Utilizando esta metodologia verificamos a regulação positiva de genes da família de fatores de crescimento semelhante à insulina (IGF-I e IGF-II) em CS estimuladas com *M. leprae*. Somente a indução da expressão de RNAm para IGF-I, pelo *M. leprae*, foi confirmada através de RT-PCR quantitativo (em Tempo Real), tanto em CS primárias quanto no Schwanoma ST88-14 e, a proteína detectada no sobrenadante das culturas (Rodrigues e col., 2010). Este fator de crescimento é amplamente descrito como potente inibidor de apoptose de CS, além de participar no estabelecimento de um circuito autócrino e parácrina para promover a sobrevivência de CS na ausência de axônio (Meier e col., 1999). Ainda em 1999, Delaney e seus colaboradores descreveram o efeito anti-apoptótico de IGF-I mediado pela inibição da ativação de caspase-3. Eles utilizaram CS provenientes de nervo ciático de ratos e induziram a apoptose pela retirada de soro do meio por até 72h. O tratamento das culturas com IGF-I foi, contudo, capaz de proteger significativamente as CS de apoptose. Em nosso trabalho, mostramos experimentos similares com a CS ST88-14, onde a incubação com 5-20 ng/mL de IGF-I recombinante protegeu de maneira dose-dependente a apoptose de células incubadas em meio sem soro (Rodrigues e col., 2010). Estes dados sugerem a indução de IGF-I pelo *M. leprae* seria uma provável estratégia para inibir vias apoptóticas na CS de forma a garantir sua sobrevivência.

Na literatura encontramos relatos da participação do IGF-I na infecção por *Leishmania amazonensis*, onde IGF-I atua diretamente como um fator de crescimento para formas pro e

amastigotas do parasita (Goto e col., 1998; Gomes e col., 2001). Estudos adicionais *in vitro* demonstraram que o pré-tratamento de formas proamastigotas de *L. amazonensis* com IGF-I causa um aumento no tamanho das lesões cutâneas de camundongos infectados e aumenta o número de parasitos (Gomes e col., 2000), contribui no bloqueio da ativação de macrófagos e pode, ainda, modular a resposta inflamatória local, favorecendo a sobrevivência e perpetuação do parasita no hospedeiro (Vendrame e col., 2007).

No sistema nervos central (SNC), o papel anti-inflamatório e imunomodulador do IGF-I tem sido bastante estudado. Neste contexto é sabido que o TNF-α contribui significativamente para a morte de neurônios após injúria (derivada de esquemia ou infecção por HIV, por exemplo) e a sinalização através do receptor IGF-1R foi vista antagonizando os efeitos neurodegenerativos provocados pelo TNF-α e, ainda, contribuindo na diferenciação de neurônios (Wang e col., 2003). IGF-I protege neurônios frente a uma variedade de patologias do SNC que estão, tipicamente, associadas com a produção maciça de citocinas pró-inflamatórias (Dore e col., 1997; Feldman, 1997; Torres-Aleman, 1999). Foi visto ainda, que o tratamento de oligodendrócitos com IGF-I previne a apoptose induzida por TNF-α (Ye e D´Ercole, 1999). Outros trabalhos igualmente reforçam que o efeito apoptótico do TNF-α é bloqueado pela sinalização de IGF-I (Wu e col., 1996; Remancle-Bonnet e col., 2000). Outro dado interessante é que após injúria da medula óssea, por exemplo, foi demonstrado que macrófagos residentes (microglia) e monócitos vindos da circulação expressam altos níveis de IGF-I no sítio da lesão como um auxílio no reparo tecidual (Rolls e col., 2008). Na regeneração do sistema nervoso periférico (SNP), IGF-I parece ser um dos principais fatores de crescimento por suas ações pleiotrópicas que promovem sobrevivência, crescimento (proliferação) e diferenciação (revisto por Rabinovsky, 2004).

Em vista das propriedades anti-apoptóticas e, ainda, anti-inflamatórias do IGF-I já mencionadas (Venters e col., 2000; Kooijman, 2006), a indução deste fator crescimento pelo *M. leprae* representa uma excelente estratégia que contribui para a sobrevivência da célula hospedeira e garante um nicho adequado para a replicação do bacilo, especialmente em pacientes multibacilares onde são encontradas CS altamente infectadas e sem indícios de toxicidade ou morte celular (Mukherjee e Antia, 1985; Antia e Shetty, 1997; Hagge e col., 2002). A indução de IGF-I pelo *M. leprae* poderia, ainda, favorecer o caráter crônico da hanseníase por manter um micro-ambiente regulado por alças anti-inflamatórias (Figura 9), evidenciado pela capacidade deste hormônio em induzir citocinas deste perfil, como IL-10 (Kooijman e Coppens, 2004).

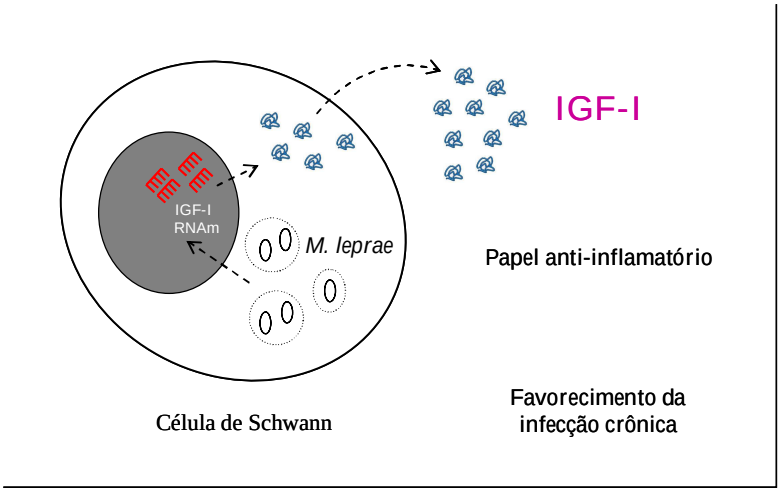

Figura 9: Possível papel do IGF-I na interação do *M. leprae* com a CS. O bacilo é capaz de proteger CS de apoptose através da indução da expressão e produção de IGF-I, que de maneira autócrina e parácrina atua na sobrevivência celular. O efeito anti-apoptótico, aliado as suas propriedades anti-inflamatórias podem representar uma estratégia utilizada para a colonização bem sucedida do nervo periférico e favorecer o caráter crônico da doença.

O sistema imune interage ativamente com o sistema endócrino na regulação de processos adaptativos, que de maneira bi-direcional atuam para garantir a manutenção da homeostasia durante a infecção. Tem sido muito bem descrito que o sistema imune interage com o SNC e assim, a resposta imune-inflamatória deflagrada por infecção viral ou bacteriana pode ser modulada pelo sistema endócrino através da ativação do eixo hipotálamo-pituitária-adrenal (HPA), que por sua vez interfere no eixo somatotrófico, constituído por GH/IGF-I (revisto por O´Connor e col., 2008; Borghetti e col., 2009). De fato, a exacerbada produção de citocinas pró-inflamatórias ativa o eixo HPA, resultando na secreção de potentes hormônios anti-inflamatórios e imunosupressores. Após estímulo inflamatório, células do núcleo paraventricular do hipotálamo expressam o hormônio liberador de corticotrofina (CRH) para estimular a porção anterior da glândula pituitária a liberar o hormônio adrenocorticotrófico (ACTH) na circulação. Na glândula adrenal, o ACTH estimula a síntese e liberação de glicocorticóides (GCs), como o cortisol, na tentativa de retornar a homeostasia (Webster e Sternberg, 2004).

Na hanseníase, as citocinas têm um papel relevante na evolução natural da doença, sobretudo durante o aparecimento dos episódios reacionais, onde a reativação da resposta imune do indivíduo reflete no painel de citocinas pró-inflamatórias expressas pelos pacientes, tanto a nível local quanto sistêmico (Yamamura e col., 1992; Sarno e col., 1991; Moraes e

col., 1999; Little e col., 2001; Lyer e col., 2007; Stefani e col., 2009). Entretanto pouco se sabe sobre a influência da infecção pelo *M. leprae* na atividade do eixo HPA. Na literatura, encontramos o trabalho de Anderson e colaboradores (2007) que apresenta evidências do aumento da secreção de cortisol em pacientes que desenvolveram reação tipo I, dada pela regulação negativa da expressão da enzima 11βHSD (11-beta dehidrogenase hidroxi-esteróide, responsável pela conversão do cortisol ativo em cortisona) em biópsias de pele. Entretanto, estudos que relacionam a atividade do eixo HPA, através da secreção de hormônios pelas glândulas pituitária ou adrenal, com a resposta imune observada nos pacientes com hanseníase são, contudo, escassos ou controversos (revisto por Leal e Foss, 2009). Sendo assim, numa segunda etapa do nosso trabalho, investigamos as alterações do IGF-I e também de IGFBP-3 no soro de pacientes com hanseníase que desenvolveram ou não episódios reacionais do tipo I ou II.

Numa comparação inicial entre indivíduos sadios e pacientes não-reacionais apresentando as formas clínicas BT, BL e LL, curiosamente cerca de 70 a 80% dos pacientes LL não-reacionais (NRLL) foram encontrados com os níveis de IGF-I e IGFBP-3 abaixo da faixa de normalidade para a idade. De forma interessante, à medida que a forma clínica avança para o pólo tuberculóide – caracterizado pela capacidade de montar uma resposta mais efetiva frente a antígenos do *M. leprae* – os níveis séricos de IGF-I e IGFBP-3 pareceram acompanhar os níveis observados em indivíduos sadios. Os pacientes BT e BL não-reacionais apresentaram níveis de IGF-I bastante similares entre si e também em comparação com indivíduos sadios. A capacidade destes pacientes (BT e BL) em elaborar uma resposta imune celular frente à infecção é, comprovadamente, superior àquela produzida por pacientes lepromatosos polares (revisto por Scollard e col., 2006) e, este fato pode estar relacionado às alterações observadas no eixo GH/IGF-I.

Embora IGF-I tenha um papel anti-inflamatório amplamente descrito, paralelamente atua na diferenciação e proliferação tanto de células mielóides quanto linfóides (Lin e col., 1997; van Buul-Offers e Kooijman, 1998). Ratos que foram submetidos à remoção cirúrgica da glândula pituitária foram incapazes de conter a infecção por *Salmonella typhimurium* e, em contrapartida, o tratamento com GH recombinante aumentou a sobrevida dos animais e restabeleceu a capacidade de matar a bactéria (Edwards e col., 1991). É possível, assim, que o IGF-I, mantido em níveis normais nos pacientes *borderline*, contribua para o "status" imuno-inflamatório destes indivíduos favorecendo alguma estabilidade associada à geração de resposta imune celular. Os pacientes NRLL contrastaram com aqueles que desenvolveram ENH (R $LL_{t=0}$), onde no momento do diagnóstico, apenas 20% apresentaram IGF-I e IGFBP-3 abaixo do normal. Imaginamos que a dinâmica obedecida por estes pacientes (reacionais ou

não) seja explicada pela sua resposta imunológica e que os níveis de IGF-I e IGFBP-3 sejam um reflexo deste estado. Nossa hipótese, no caso dos pacientes LL, é que aqueles que não evoluem para reação encontram-se num estado de imunosupressão, onde o paciente não consegue conter a proliferação do bacilo e apresenta alto índice baciloscópico (IB).

A expressão crônica de citocinas inflamatórias é incapaz de auxiliar no combate à infecção, entretanto ativa o eixo HPA provocando a secreção de GCs para inibir processos inflamatórios e manter a homeostasia que suporte a infecção. Em paralelo, o eixo GH/IGF-I é afetado, com conseqüente diminuição da função hepática para produzir IGF-I (revisto por Borghetti e col., 2009). Dados da literatura que demonstram a alta capacidade de produção de IL-10 por estes pacientes (Lima e col., 2000), aliada aos nossos achados de que a grande maioria dos NRLL se encontrem com os níveis de IGF-I e IGFBP-3 abaixo do normal, suportam nossa hipótese do estado de imunosupressão em que estes pacientes se encontram (Figura 10). Os pacientes que desenvolveram reação, no momento do diagnóstico apresentaram níveis de IGF-I e IGFBP-3 dentro da faixa de normalidade e, talvez isto possa ser explicado por sua capacidade de evoluir para o processo reacional e apresentarem uma reativação da resposta Th1 com a expressão de IFN-γ, TNF-α e IL-12, conforme discutem alguns autores (Yamamura e col., 1992; Sreenivasan e col., 1998). Entretanto a produção crônica destas citocinas contribui para a queda dos níveis de IGF-I e IGFBP-3, conforme evidenciados em nosso estudo durante a reação. Os baixos níveis de IGF-I poderiam explicar o aumento do grau de apoptose espontânea, observada *ex vivo*, em células CD14+ derivadas de PBMC de pacientes multibacilares com ENH (Hernandez e col., 2003).

Traçando um paralelo com nossos dados iniciais, onde mostramos a capacidade do *M. leprae* induzir a produção de IGF-I em CS (Rodrigues e col., 2010), imaginamos que não necessariamente deveríamos esperar que pacientes lepromatosos não-reacionais apresentassem níveis circulantes de IGF-I normais ou mais elevados. A explicação para isto reside no fato de que o IGF-I circulante tem origem no fígado sob a regulação do GH e atua de maneira endócrina no crescimento e metabolismo. Mas sabemos que diferentes tecidos podem produzir IGF-I e, localmente, este pode agir de maneira autócrina e parácrina na sobrevivência, proliferação, diferenciação e garantia da homeostasia tecidual. Sabemos, ainda, que o IGF-I local pode não ser o reflexo do IGF-I hepático. Por isso, como perspectivas deste estudo, pretendemos avaliar a expressão de IGF-I em lesões de pacientes apresentando as formas polares da doença, bem como durante o aparecimento dos quadros reacionais. Desta forma, poderíamos traçar um perfil do papel do IGF-I no sítio da inflamação.

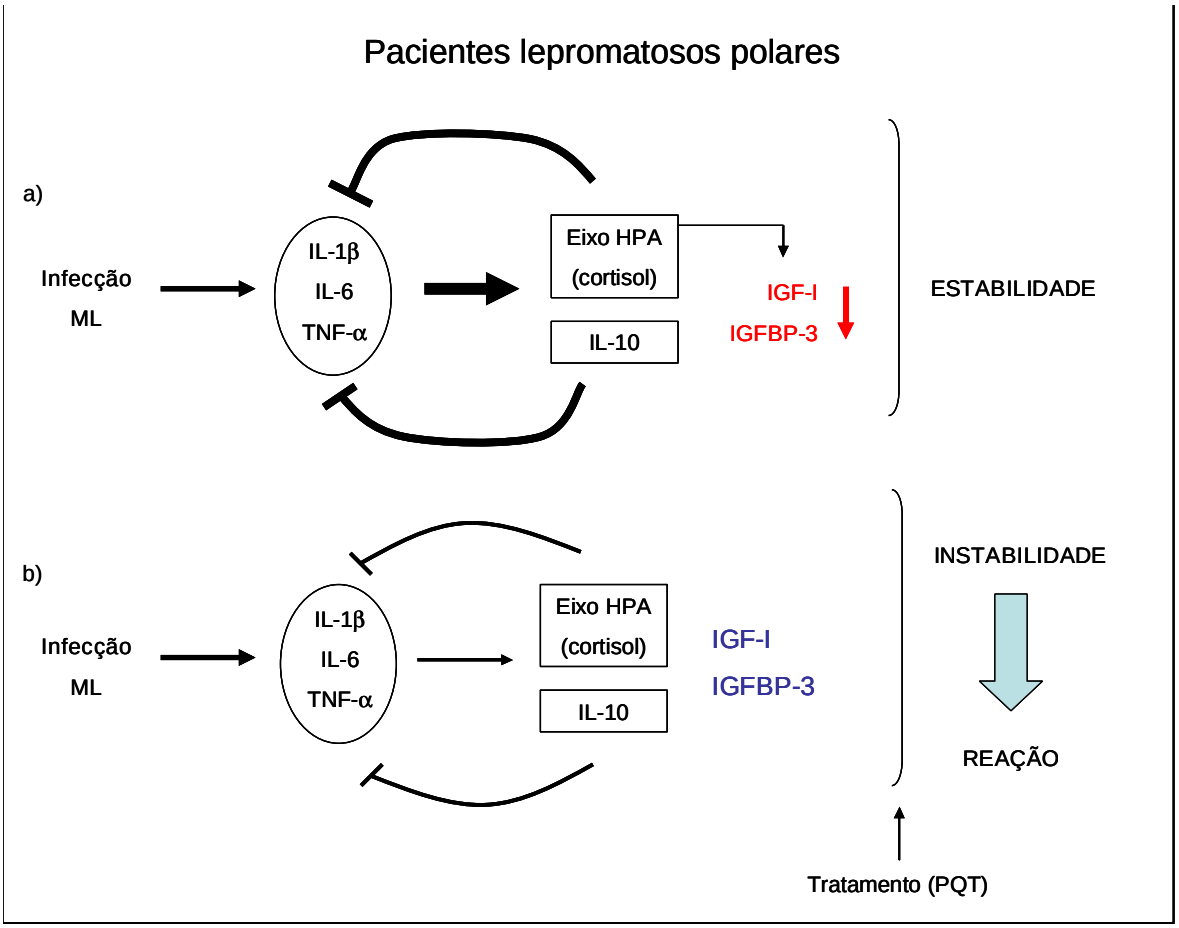

Figura 10: Hipótese para a dinâmica das alterações de IGF-I e IGFBP-3 em pacientes com a forma LL que evoluíram ou não para a reação tipo II. a) Os pacientes LL não reacionais apresentam um estado imunossupressor caracterizado pela expressão de IL-10, que mantém um ambiente favorável à replicação do *M. leprae*, e ativação do eixo HPA (secreção de glicocorticóides) por citocinas inflamatórias como IL-6, por exemplo. Neste cenário, os níveis de IGF-I e IGFBP-3 se encontram abaixo da faixa normal, indicando estabilidade. b) Níveis normais de IGF-I e IGFBP-3, em pacientes LL reacionais, podem indicar um menor grau de imunosupressão e, consequentemente, maior instabilidade.

A sepse – resposta ao alto grau de infecção sistêmica – compartilha com a hanseníase lepromatosa o quadro de imunosupressão apresentado pelos pacientes. Não fossem estas alças moduladoras da resposta imune, fatalmente levariam rapidamente ao óbito pela superprodução sistêmica de citocinas inflamatórias e incapacidade do indivíduo em controlar a infecção. A evolução da sepse está associada a um aumento prolongado de TNF-α no fígado, causando a apoptose das células de Kupffer e levando à disfunção hepática (revisto por Ashare e col., 2006). Em consequência, os níveis circulantes de IGF-I encontram-se

diminuídos na sepse grave (Karinch e col., 2001; Ashare e col., 2008). Outros trabalhos igualmente mostram que a expressão de citocinas pró-inflamatórias pode interferir no eixo GH/IGF-I. Para algumas patologias como a sepse, a tuberculose e caquexia relacionada à infecção por HIV, especula-se a que a razão para a queda dos níveis de IGF-I circulante seja o estabelecimento de quadros de resistência ao GH, caracterizados pela supressão do eixo somatotrófico (revisto por Mesothen e Van den Berghe, 2006). Os efeitos dessa supressão se refletem nas alterações clínicas observadas nestes pacientes, tais como: perda peso e mal estar geral.

Pacientes infectados com *Helicobacter pylori* apresentam elevados níveis de cortisol (confirmando a ativação do eixo HPA através de citocinas pró-inflamátórias) e, em contrapartida, os níveis circulantes de IGF-I encontram-se reduzidos (Bariceviæe col., 2004). Em pacientes com HIV, o grau de neurodegeneração em consequência da elevada produção de TNF-α foi correlacionado, também, à redução dos níveis séricos de IGF-I (Jain e col., 1998; Laue e col., 1990). Em pacientes com Alzheimer, os níveis séricos de TNF-α são elevados e negativamente correlacionados com IGF-I (Alvarez e col., 2007). Foram observados níveis plasmáticos elevados de TNF-α, IL-1β, IL-6 e IL-8 em pacientes com doença obstrutiva pulmonar crônica, enquanto os níveis de IGF-I encontravam-se diminuídos durante a fase a aguda da doença (Kythreotis e col., 2009).

De maneira bastante interessante, os dados obtidos a partir da análise do comportamento dos pacientes BL foram exatamente opostos aos observados com pacientes LL. Diferentemente dos pacientes NRLL, apenas 10% dos pacientes NRBL que não sofreram reação apresentaram IGF-I abaixo do normal, próximo aos indivíduos sadios (15.7%). Por outro lado, 93.3% dos pacientes BL que evoluíram para a reação tipo I (R $BL_{t=0}$) apresentaram níveis de IGF-I abaixo do normal. Mais uma vez, a avaliação dos níveis de IGF-I e IGFBP-3 foi capaz de distinguir grupos de pacientes, agora com a forma BL, que sofreram ou não episódio reacional tipo I. Além disso, estes dados reforçam a organização da doença em formas clínicas proposta por Ridley e Jopling (1966), no que diz respeito ao perfil diferenciado em que se encontram, embora sejam agrupadas como multibacilares, conforme proposto pela OMS (1982) com fins terapêuticos. É interessante argumentar, porém, o que faz um paciente BL evoluir para reação tipo I ou tipo II, por exemplo – sendo estes episódios diferentes entre si.

Embora os níveis de IGF-I aumentem significativamente durante a reação reversa, a maioria dos indivíduos avaliados não conseguiu alcançar os níveis normais. De fato, houve uma queda no percentual de indivíduos com níveis de IGF-I baixos durante a reação (73.3%, contrastando com 93.3% no momento do diagnóstico). Esta tentativa de alcançar níveis

normais possa se dar como uma estratégia ou desenvolvimento de um processo adaptativo, no qual o organismo busque ativar uma alça anti-inflamatória para conseguir alcançar a homeostasia (Figura 11). Esta capacidade adaptativa, mais uma vez, poderia ser explicada pela diferença entre pacientes BL e LL em elaborar uma resposta imune Th1.

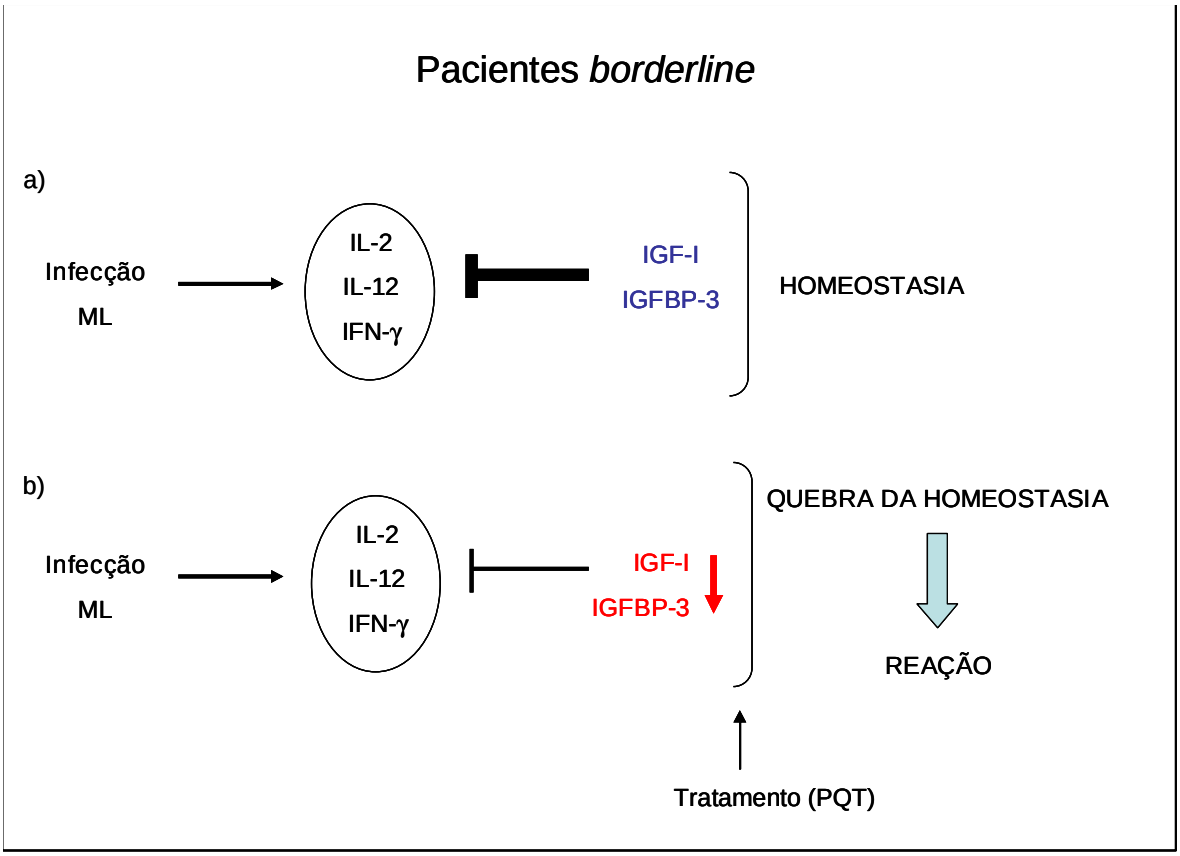

Figura 11: Hipótese para a dinâmica das alterações de IGF-I e IGFBP-3 em pacientes com a forma BL com evolução ou não para a reação tipo I. Embora considerados multibacilares, os pacientes BL apresentam alguma capacidade de resposta imune frente a antígenos do *M. leprae*, superior em relação aos lepromatosos polares. a) Na presença de resposta celular, citocinas de perfil Th1, como IL-2, IL-12 e IFN-γ, passam a ser produzidas, gerando um novo cenário imune-inflamatório onde a manutenção de níveis normais de IGF-I indica uma situação de controle da inflamação e homeostasia. b) Ao contrário, níveis baixos de IGF-I, neste cenário, refletem num alto risco de desenvolvimento de reação.

A partir do conjunto de dados expostos, demonstramos a interação do sistema imune com o sistema endócrino na hanseníase, no qual o IGF-I parece ter um papel importante não só na interação direta do *M. leprae* com a CS, mas também a nível sistêmico, durante a evolução natural da doença. Esperamos que nosso estudo possa contribuir principalmente

como um auxílio no desenvolvimento de ferramentas que possam refletir no controle da doença e no prognóstico dos episódios reacionais.

Como perspectivas, pretendemos conduzir um estudo prospectivo para uma análise mais ampla das alterações do eixo HPA e somatotrófico (GH/IGF-I) em pacientes com hanseníase que apresentarem ou não episódios reacionais tipo I ou II. Imaginamos que possa existir uma correlação entre a expressão de citocinas inflamatórias e a alteração do eixo GH/IGF-I, que suportem a indicação deste hormônio como fatores preditivos dos episódios reacionais. Seguem algumas metas inicialmente traçadas:

i) Determinar os níveis circulantes do hormônio adrenocorticotrófico (ACTH), GH, IGF-I, IGFBP-3 e cortisol, bem como das citocinas pró-inflamatórias IL-1β, IL-6, TNF-α e IFN-γ;
ii) Verificar a associação das alterações no eixo GH/IGF com o quadro clínico apresentado pelos pacientes durante os episódios reacionais;
iii) Analisar a expressão dos receptores para IGF-I, GH e glicocorticóides em lesões de pele de pacientes;
iv) Avaliar o grau de apoptose e a produção espontânea de IGF-I em células mononucleares de sangue periférico (PBMC);
v) Quantificar a produção *in vitro* de IGF-I em PBMC de pacientes estimulados com GH e frações purificadas do *M. leprae*.

CAPÍTULO 6: Conclusões

A partir dos dados obtidos durante o desenvolvimento deste trabalho podemos concluir que:

1. *M. leprae* inibe a ativação de caspase-3 em CS da linhagem ST88-14, como um mecanismo de prevenir a apoptose induzida por privação de soro;

2. *M. leprae* induz a expressão de RNAm e produção de IGF-I em CS da linhagem ST88-14;

3. Culturas de CS da linhagem ST88-14 estimuladas com *M. leprae* e cultivadas em meio sem soro apresentaram maior grau de proliferação comparado às culturas não estimuladas;

4. A estimulação com *M. leprae* foi capaz de induzir a expressão de RNAm e produção de IGF-I em CS humanas primárias e da linhagem ST88-14;

5. A quantificação dos níveis circulantes de IGF-I e IGFBP-3 em pacientes com hanseníase com as diferentes formas clínicas, e em pacientes reacionais e não reacionais mostrou alterações significativas no eixo somatotrófico durante o curso da infecção pelo *M. leprae*. Estas alterações se correlacionaram com a forma clínica, assim como, com a estabilidade da resposta imuno-inflamatória do hospedeiro contra os antígenos micobacterianos, assim resumidas:

- Verificamos que pacientes não reacionais com a forma LL apresentaram níveis circulantes reduzidos de IGF-I e IGFBP-3 quando comparados aos indivíduos sadios;

- Os pacientes não reacionais com a forma LL apresentaram níveis circulantes de IGF-I e IGFBP-3 reduzidos em comparação com pacientes com a mesma forma clínica que desenvolveram reação tipo II;

- Durante a reação tipo II os níveis séricos de TNF-α encontraram-se aumentados em relação aos níveis observados no momento do diagnóstico da hanseníase e aos indivíduos sadios;

- Os pacientes não reacionais com a forma BL apresentaram níveis circulantes de IGF-I comparáveis aos indivíduos sadios, entretanto a maioria dos pacientes que desenvolveram reação tipo I apresentou níveis de IGF-I e IGFBP-3 abaixo da faixa de normalidade;

- Durante ambos os tipos de reação, os níveis circulantes de IGF-I e IGFBP-3 tentam alcançar os níveis observados nos pacientes não reacionais.

Com base nas conclusões acima, nossos dados sugerem fortemente o envolvimento do sistema IGF na interação do *M. leprae* com sua célula hospedeira preferencial no nervo periférico, a CS, bem como sua participação sistêmica durante a evolução natural da doença e, indicam a avaliação dos níveis séricos de IGF-I e sua principal proteína ligante, a IGFBP-3 com potenciais candidatos na identificação do grau de risco para o desenvolvimento de episódios reacionais em pacientes com hanseníase.

Referências Bibliográficas

Alcais A, Alter A, Antoni G, Orlova M, Van Thuc N, Singh M, Vanderborght PR, Katoch K, Mira MT, Thai VH, Huong NT, Ba NN, Moraes M, Mehra N, Schurr E, Abel L. Stepwise replication identifies a low-producing lymphotoxin-[alpha] allele as a major risk factor for early-onset leprosy. Nat Genet 2007; 39: 517–522.

Alvarez A, Cacabelos R, Sanpedro C, García-Fantini M, Alexandre M. Serum TNF-alpha levels are increased and correlate negatively with free IGF-I in Alzheimer disease. Neurobiol Aging 2007; 28: 533-536.

Alves L, de Mendonça Lima L, da Silva Maeda E, Carvalho L, Holy J, Sarno EN, Pessolani MC, Barker LP. *Mycobacterium leprae* infection of human Schwann cells depends on selective host kinases and pathogen-modulated endocytic pathways. FEMS Microbiol Lett 2004; 238: 429-437.

Anderson Ak, Atkinson SE, Khanolkar-Young S, Chaduvula MV, Jain S, Suneetha L, Suneetha S, Lockwood DNJ. Alterations of the cortisol-cortisone shuttle in leprosy type I reactions in leprosy patients in Hyderabad, Índia. Immunol Lett 2007; 109: 72-75.

Anderson AK, Chaduvula MV, Atkinson SE, Khanolkar-Young S, Jain S, Suneetha L, Suneetha S, Lockwood DNJ. Effects of prednisolone treatment on cytokine expression in patients with leprosy type I reactions. Infect Immun 2005; 73(6): 3725-3733.

Antia NH, Shetty VP. The peripheral nerve in leprosy and other neuropathies. Pathology of nerve damage in leprosy. In Oxford University Press 1997; p. 79-137.

Ashare A, Monick MM, Powers LS, Yarovinsky T, Hunninghake GW. Severe bacteremia results in a loss of hepatic bacterial clearance. Am J Respir Crit Care Med 2006; 173: 644-652.

Ashare A, Nymon AB, Doerschug KC, Morrison JM, Monick MM, Hunninghake GW. Insulin-like growth factor-1 improves survival in sepsis via enhanced hepatic bacterial clearance. Am J Respir Crit Care Med 2008; 178 (2):149-157.

Ashkenazi A, Dixit VM. Death receptors: signaling and modulation. Science 1998; 281(5381): 1305-1308.

Atkinson SE, Khanolkar-Young S, Marlowe S, Jain S, Reddy RG, Suneetha S, Lockwood DN. Detection of IL-13, IL-10, and IL-6 in the leprosy skin lesions of patients during prednisolone treatment for type 1 (T1R) reactions. Int J Lepr Other Mycobact Dis 2004; 72(1):27-34.

BaricevićI, NedićO, NikolićJA, BojićB, JojićN. Circulating insulin-like growth factors in patients infected with *Helicobacter pylori*. Clin Biochem 2004; 37 (11): 997-1001.

Barnetson RS, Bjune G, Pearson JM, Kronvall G. Cell mediated and humoral immunity in "reversal reactions". Int J Lepr Other Mycobact Dis 1976; 44: 267-274.

Baxter, R.C. Insulin-like growth factor (IGF)-binding proteins: interactions with IGFs and intrinsic bioactivities. Am J Physiol Endocrinol Metab 2000; 278 (6): 967-976.

Becx-Bleumink M, Berhe D. Occurrence of reactions, their diagnosis and management in leprosy patients treated with multidrug therapy; experience in the leprosy control program of the all Africa Leprosy and Rehabilitation Training Center (ALERT) in Ethiopia; practical difficulties with diagnosing relapses; operational procedures and criteria for diagnosing relapses. Int J Lepr Other Mycobact Dis 1992; 60: 421-435.

Bloom B. Learning from leprosy: a perspective on immunology a the third world. J Immunol 1986; 131:1-10.

Borghetti P, Saleri R, Mocchegiani E, Corradi A, Martelli P. Infection, immunity and the neuroendocrine response. Vet Immunol Immunopathol 2009; 130: 141-162.

Britton WJ, Lockwood DNJ. Leprosy. The Lancet 2004; 363: 1209-1219.

Browne SG. Erythema nodosum in leprosy. J Chron Dis 1963; 16: 23-30.

Bunge RP. Expanding roles for the Schwann cell: ensheathment, myelination, trophism and regeneration. Cur Opin Neurobiol 1993; 3: 805-809.

Butler AA, Yakar S, Gewolb IH, Karas M, Okubo Y, Leroith D. Insulin-Like Growth Factor-I Receptor signal transduction: at the interface between physiology and cell biology. Comparative Biochem Physiol 1998; 121:19-26.

Chan JM, Stampfer MJ, Giovannucci E, Gann PH, Ma J, Wilkinson P, Hennekens CH, Pollak M. Plasma insulin-like growth factor-I and prostate cancer risk: a prospective study. Science 1998; 23;279(5350):563-566.

Cheng HL, Russel JW, Feldman EL. IGF-I promotes Peripheral Nervous system Myelination. Ann N Y Acad Sci 1999; 883: 124-130.

Chernousov MA, Carey DJ. Schwann cell extracellular matrix molecules and their receptors (review). Histol Histopathol 2000; 15: 593-601.

Cho SN, Cellona RV, Villahermosa LG, Fajardo TT Jr, Balagon MV, Abalos RM, et al. Detection of phenolic glycolipid I of *Mycobacterium leprae* in sera from leprosy patients before and after start of multidrug therapy. Clin Diagn Lab Immunol 2001; 8(1): 138-142.

Chopra NK, Agrawal JS, Pandya PG. Reactions in leprosy – A study of 250 patients in multidrug therapy project. Baroda District, Gurajat, Índia. Int J Dermatol 1990; 29: 490-493.

Chuenkova MV, PereiraPerrin M. Trypanosoma cruzi targets Akt in host cells as an intracellular antiapoptotic strategy. Sci Signal 2009; 17;2(97):ra74.

Chuenkova, M.V., F.B. Furnari, W.K. Cavenee And M.A. Pereira. 2001. *Trypanosoma cruzi* trans-sialidase: A potent and specific survival factor for human Schwann cells by means phosphatidylinositol 3-kinase/Akt signaling. PNAS. 98:9936-9941.

Clemmons DR. Modifying IGF1 activity: an approach to treat endocrine disorders, atherosclerosis and cancer. Nat Rev Drug Discov 2007; 6(10): 821-833.

Clifford J R, Pollak M. Circulating IGF-I: New perspectives for a new contury. TEM 1999; 10(4): 136-141.

Clifton DR, Goss RA, Sahni SK, Van Antwerp D, Baggs RB, Marder VJ, Silverman DJ, Sporn LA. NF-κB-dependent inhibition of apoptosis is essencial for host cell survival during *Rickettsia rickettsii* infection. Proc Natl Acad Sci 1998; 95: 4646-4651.

Cole ST, Eiglemeir J, Parkhill KD, James NR, Thomson PR, Wheeler PR, Honore N, Garnier T, Churcher C, Harris D, Mungall K, Basham D, Brown D, Chillingworth T, Connor R, Davies RM, Devlin K, Duthoy S, Feltwell T, Fraser A, Hamlin N, Holroyd S, Hornsby T, Jagels K, Lacroix C, Maclean J, Moule S, Murphy L, Oliver K, Quail MA, Hajandream MA, Rutherford KM, Rutter S, Seeger K, Simon S, Simmonds M, Skelton J, Squares R, Stevens K, Taylor K, Whitehead S, Woodward JR, Barrell BG. Massive gene decay in the leprosy bacillus. Nature 2001; 409:1007-1011.

Convit J, Ulrich M, Aranzazu N, Castellanos PL, Pinardi ME, Reyes O. The development of a vaccination model using two microorganisms and its application in leprosy and leishmaniasis. Lepr Rev 1986; 57(Suppl 2): 263-273.

Coombs RRA, Gell PGH. The classification of allergic reactions underlying disease in clinical aspects of immunology. Davis, Philadelphia, 1963.

Coutinho-Silva R, Perfettini JL, Persechini PM, Dautry-Varsat A, Ojcius DM. Modulation of P2Z/P2X(7) receptor activity in macrophages infected with *Chlamydia psittaci*. Am J Physiol 2001; 280: C81-C89.

Croft RP, Richardus JH, Nicholls PG, Smith WC. Nerve function impairment in leprosy: design, methodology, and intake status of a prospective cohort study of 2664 new leprosy cases in Bangladesh (The Bangladesh Acute Nerve Damage Study). Lepr Rev 1999; 70: 140-159.

Cuevas J, Rodriguez-Peralto JL, Carrillo R, Contreras F. Erythema nodosum leprosum: reactional leprosy. Semin Cutan Med Surg 2007; 26(2): 126-130.

Delaney CL, Cheng HL, Feldman EL. Insulin-like growth factor-I prevents caspase-mediated apoptosis in Schwann cells. J Neurobiol 1999; 41: 540-548.

Denley A, Cosgrove LJ, Booker GW, Wallace JC, Forbes BE. Molecular interactions of the IGF system. Cytokine Growth Factor Rev 2005; 16: 421-439.

Dore S, Kar S, Quirion R. Rediscovering an old friend, IGF-I: potential use in the treatment of neurodegenerative diseases. Trends Neurosci 1997; 20: 326-331.

Douglas JT, Cellona RV, Fajardo Jr, Abalos RM, Balagon MVF, Klatser PR. Prospective study of serological conversion as a risk factor for development of leprosy among household contacts. Clin Diagn Lab Immunol 2004; 11(5): 897-900.

Dudek H, Datta SR, Franke TF, et al. Regulation of neuronal survival by the serine-threonine protein kinase Akt. Science 1997; 27: 661-665.

Duncan ME, Pearson JM. Neuritis in pregnancy and lactation. In J Lepr Other Mycobact Dis 1982; 50: 31-38.

Düppre NC, Camacho LA, da Cunha SS, Struchiner CJ, Sales AM, Nery JA, Sarno EN. Effectiveness of BCG vaccination among leprosy contacts: a cohort study. Trans R Soc Trop Med Hyg 2008; 102(7): 631-638.

Edwards III CK, Yunger LM, Lorence RM, Dantzer R, Kelley KW. The pituitary gland is required for protection against lethal effects of Salmonella typhimurium. Proc Natl Acad Sci 1991; 88: 2274-2277.

Espig AF, Slomp AA, Campagnolo AQ, Rockenbach DM, Silva BD, Pomblum VJ. Neurofibromatosis Type 1: Update. Rev Bras Clin Med 2008; 6:243-249.

Faber WR, Lyer AM, Fajardo TT, Dekker T, Villahermosa LG, Abalos RM, Das PK. Serial measurement of serum cytokines, cytokine receptors and neopterin in leprosy patients with reversal reactions. Lepr Rev 2004; 75(3): 274-281.

Fan T, Lu H, Hu H, Shi L, MacClarty GA, Nance DM, Greenberg AH, Zhong G. Inhibition of apoptosis in *Chlamydia*-infected cells: blockade of mitochondrial citochrome c release and caspase activation. J Exp Med 1998; 187: 487-496.

Feldman EL, Sullivan KA, Kim B, Russel JW. Insulin-like growth factors regulate neuronal differentiation and survival. Neurobiol Dis 1997; 4: 201-214.

Fletcher JA, Kozakewich HP, Hoffer FA, Lage JM, Weidner N, Tepper R, Pinkus GS. Diagnostic relevance of clonal cytogenetic aberrations in malignant soft-tissue tumors. N England J Med 1991; 324: 436-442.

Foss NT. Episódios reacionais na hanseníase. Medicina, Ribeirão Preto 2003; 36: 453-459.

Fratti RA, Chua J, Vergne I, Deretic V. *Mycobacterium tuberculosis* glycosylated phosphatidylinositol causes phagosome maturation arrest. PNAS 2003; 100: 5437-5442.

Gao LY, Kwaik YA. The modulation of host cell apoptosis by intracellular bacterial pathogens. Trends Microbiol 2000; 8(7): 306-313.

Gillis W. Leprosy at a turning point? Int J Lepr 2000; 68: 312-318.

Godal I. Leprosy immunology – some aspects of the role of the immune system in the pathogenesis of disease. Lepr Rev 1984; 55(4): 407-414.

Godal T, Myrvang B, Samuel DR, Foss WF, Lofgren M. Mechanisms of “reactions” in borderline tuberculoid (BT) leprosy. A preliminary report. Acta Pathol Microbiol Scand A 1973; 236:45-53.

Gomes CM, Goto H, Magnanelli AC, Monteiro HP, Soares RP, Corbett CE, Gidlund M.Characterization of the receptor for insulin-like growth factor on Leishmania promastigotes. Exp Parasitol 2001; 99(4): 190-197.

Gomes CMC, Goto H, Matta VLR, Laurenti MD, Gidlund M, Corbett CEP. Insulin-like growth factor-I affects parasite growth and host cell migration in experimental cutaneous leishmaniasis. Int J Exp Path 2000; 81:249-255.

Goto H, Gomes CM, Corbett CE, Monteiro HP, Gidlund M. Insulin-like growth factor I is a growth-promoting factor for *Leishmania* promastigotes and amastigotes. Proc Natl Acad Sci USA 1998; 27;95(22):13211-13216.

Goulart IMB, Penna GO, Cunha G. Immunopathology of leprosy: the complexity of the mechanisms of host immune response to *Mycobacterium leprae*. Rev Soc Bras Med Trop 2002; 35(4): 365-375.

Grivicich I, Regner A, Rocha AB. Apoptosis: Programmed cell death. Rev Bras Cancerol 2007; 53(3): 335-343.

Guerra JG, Penna GO, de Castro LCM, Martelli CMT, Stefani MMA, Costa MB. Erythema nodosum leprosum case series report: clinical profile, immunological basis and treatment implemented in health services. Rev Soc Bras Med Trop 2004; 37(5): 384-390.

Guimarães CA, Linden R. Programmed cell death. Apoptosis and alternative deathstyles. Eur J Biochem 2004; 271: 1638-1650.

Häcker G, Kirschnek S, Fisher SF. Apoptosis in infectious disease: how bacteria interfere with the apoptotic apparatus. Medical Microbiol. and Immunol. 2005; 195(1): 11-19.

Hagge DA, Oby Robinson S, Scollard D, McCormick G, Williams DL. A new model for studying the effects of *Mycobacterium leprae* on Schwann cell and neuron interactions. J Infect Dis 2002; 186: 1283-1296.

Hasan Z, Ashraf M, Tayyebi A, Hussain R. *M. leprae* inhibits apoptosis in THP-1 cells by downregulation of Bad and Bak and upregulation of Mcl-1 gene expression. BMC Microbiol 2006; 6: 78.

Hengartner MO. The biochemistry of apoptosis. Nature 2000; 405: 770-776.

Hernandez MO, Neves JR, Sales JS, Carvalho DS, Sarno EN, Sampaio EP. Induction of apoptosis in monocytes by *Mycobacterium leprae in vitro*: a possible role for tumour necrosis factor-α. Immunol 2003; 109: 156-164.

Holdenrieder S, Stieber P. Apoptotic markers in cancer. Clin Biochem 2004; 37:605-617.

Hunter SW, Brennan PJ. A novel phenolic glycolipid from *Mycobacterium leprae* possibly is involved in immunogenecity an pathogenicity. J Bacteriol 1981; 147: 728-735.

Jain S, Golde DW, Balley R, Geffner ME. Insulin-like growth factor-I resistence. Endocr Rev 1998; 19(5): 625-646.

Jessen KR, Mirsky R. Schwann cells and their precursors emerge as major regulators of nerve development. Trends Neurosci 1999; 22: 402-410.

Jessen KR, Mirsky R. The origin and development of glial cells in peripheral nerves. Nat Rev Neurosci 2005; 6(9): 671-682.

Job CK. Pathology of leprosy. In: Hastings RC, editor. Leprosy. 2nd ed. Edinburgh: Churchill Livingstone 1994, p. 193-234.

Jones JI, Clemmons DR. Insulin-like growth factors and their binding proteins: biological actions. Endocr Rev 1995; 1: 3-34.

Kaplan G, Cohn ZA. Regulation of cell-mediated immunity in lepromatous leprosy. Lepr Rev 1986; 57(2):199-202.

Karinch AM, Pan M, Lin CM, Strange R, Souba WW. Glutamine metabolism in sepsis and infection. J Nutr 2001; 131 (9, suppl): 2535S-2538S. [Discussion, 2550S-2551S].

Kerr JFR, Wyllie AH, Currie AR. Apoptosis: a basic biological phenomenon with wide-raging implications in tissue kinetics. Br J Cancer 1972; 26: 239-257.

Khanolkar-Young S, RAyment N, Brickell PM, Katz DR, Vinayakumar S, Colston MJ, et al. Tumor necrosis factor-alpha (TNF-alpha) synthesis is associated with the skin and peripheral nerve pathology of leprosy reversal reactions. Clin Exp Immunol 1995; 99(2): 196-202.

Kirchheimer WF, Storrs EE. Attempts to establish the armadillo (*Dasypus novencinctus*, Linn.) as a modelfor the leprosy. Int J Lepr 1971; 39:693-703.

Kirkaldy AA, Musonda AC, Khanolkhar-Young S, Suneetha S, Lockwood DN. Expression of CC and CXC chemokines and chemokyne receptors in human leprosy skin lesions. Clin Exp Immunol 2003; 134:447-453.

Knodler LA, Finlay BB. *Salmonella* and apoptosis: to live or let die? Microb Infect 2001; 3: 1321-1326.

Kooijman R, Coppens A. Insulin-like Growth Factor-I stimulates IL-10 production in human T cells. J Leukoc Biol 2004; 76(4): 862-867.

Kooijman R. Regulation of apoptosis by insulin-like growth factor (IGF)-I. Cytokine Growth Factor Rev 2006; 17: 305-323.

Kulik G, Klippel A, Weber, MJ. Antiapoptotic signaling by the insulin-like growth factor I receptor, phosphatidylinositol 3-kinsase, and Akt. Mol Cell Biol 1997; 17: 1595-1606.

Kumar B, Dogra S, Kaur I. Epidemiological characteristics of leprosy reactions: 15 years experience from north Índia. Int J Lepr Other Mycobact Dis 2004; 72:125-133.

Kwaik YA. Fatal attraction of mammalian cells to *Legionella pneumophila*. Mol Microbiol 1998; 30: 689-696.

Kythreotis P, Kokkini A, Avgeropoulou S, Hadjioannou A, Anastasakou E, Rasidakis A, Bakakos P. Plasma leptin and insulin-like growth factor I levels during acute exacerbations of chronic obstructive pulmonary disease. BMC Pulm Med 2009; 5 (9):11-20.

Lahiri R, Randhawa B, Krahenbuhl JL. Infection of mouse macrophages with viable *Mycobacterium leprae* does not induce apoptosis. J Infect Dis 2010; 201(11):1736-1742.

Laue L, Pizzo PA, Butler K, Cutler Jr GB. Growth and neuroendocrine dysfunction in children with acquired immunodeficiency syndrome. J Pediatr 1990; 117 (4): 541-545.

Leal AMO, Foss NT. Endocrine dysfunction in leprosy. Eur J Clin Microbiol Infect Dis 2009; 28: 1-7.

Lefford MJ, Huneg Naw M, Siwik E. The value of IgM antibodies to PGL-1 in the diagnosis of leprosy. Int J Lepr 1991; 59(3): 432-440.

Lienhardt C, Fine PE. Type 1 reaction, neuritis and disability in leprosy. What is the current epidemiological situation? Lepr Rev 1994; 65: 9-33.

Lima MC, Pereira GM, Rumjanek FD, Gomes HM, Düppre N, Sampaio EP, Alvim IM, Nery JA, Sarno EM, Pessolani MC. Immunological cytokine correlates of prospective immunity and pathogenesis in leprosy. Scand J Immunol 2000; 51(4): 419-428.

Lin B, Kinochita Y, Haoto F, Tsuji Y. Enhancement of DNA synthetic activity of thymic lymphocytes by the culture supernatant of thymus epithelial cells stimulated by growth hormone. J Biol Regul Homeost Agents 1997; 11: 154-156.

Little D, Khanolkar-Young S, Coulthart A, Suneetha S, Lockwood DN. Immunohistochemical analysis of cellular infiltrate and gamma interferon, interleukin-12, and inducible nitric oxide synthase expression in leprosy type 1 (reversal) reactions before and during prednisolone treatment. Infect Immun 2001; 69(5): 3413-7.

Lockwood DN, Sinha HH. Pregnancy and leprosy: a comprehensive literature review. Int J Lepr Other Mycobact Dis 1999; 67:6-12.

Lockwood DN, Vinayakumar S, Stanley JN, Mcadam KP, Colston MJ. Clinical features and outcome of reversal (type 1) reactions in hyderabad, india. Int J Lepr other Mycobact Dis 1993; 61(1), 8-15.

Lockwood DN. The management of erythema nodosum leprosum: current and future options. Lepr Rev 1996; 67: 253-259.

Lyer A, Hatta M, Usman R, Luiten S, Oskam L, Faber W, Geluk A, Das P. Serum levels of interferon-gamma, tumour necrosis factor-alpha, soluble interleukin-6R and soluble cell

activation markers for monitoring response to treatment of leprosy reactions. Clin Exp Immunol 2007; 150 (2): 210-216.

Maeda ES. Estudo do efeito de sobrevivência promovido pelo Mycobacterium leprae sobre as células de Schwann: análise do envolvimento dos fatores semelhantes à insulina (IGFs) e da via PI 3-k/Akt. Dissertação de Mestrado, Instituto Oswaldo Cruz, 2008.

Maiti D, Bhattacharyya A, Basu J. Lipoarabinomannan from *Mycobacterium tuberculosis* promotes macrophage survival by phosphorylating Bad through a phosphatidylinositol 3-kinase/Akt pathway. J Biol Chem 2001; 276: 329-333.

Malik ZA, Thompson CR, Hashimi S, Porter B, Iyer SS, Kusner DJ. *Mycobacterium tuberculosis* blocks Ca^{2+} signaling and phagosome maturation in human macrophages via specific inhibition of sphingosine. Kinase. J Immunol 2003; 170: 2811-2815.

Manandhar R, LeMaster JW, Roche P. Risk factors for erythema nodosum leprosum. Int J Lep 1999; 67: 270-278.

Marques MA, Antônio VL, Sarno EN, Brennan PJ, Pessolani MC. Binding of alpha2-laminins by pathogenic and non-pathogenic mycobacteria and adherence to Schwann cells. J Med Microbiol 2001; 50: 23-28.

Marques MA, Mahapatra S, Nandan D, Dick T, Sarno EN, Brennan PJ, Pessolani MCV. Bacterial and host-derived cationic proteins bind α2-laminins and enhance *Mycobacterium leprae* attachment to human Schwann cells. Microb Infec. 2000; 2: 1407-1471.

Marte BM, Downward J, Deprez J, et al. PKB/Akt: connecting phosphoionositide 3-kinase to cell survival and beyond. Phosphorylation and activation of heart 6-phosphofructo-2-kinase by protein kinase B and other kinases of the insulin signalling cascade. Trends Biochem Sci 1997; 22: 355-358.

Martinvalet D, Zhu P, Liberman J. Granzyme A induces caspase-independent mitochondrial damage, a required first step for apoptosis. Immunity 2005; 22: 355-370.

Meier C, Parmantier E, Brennan A, Mirski RD, Jessen KR. Developing Schwann Cells acquire the ability to survive without axons by establishing an autocrine circuit involving insulin-like growth factor, neurotrophin-3 and platelet-derived growth factor-BB. J Neurosci 1999; 19: 3847-3859.

Mesotten D, Van den Berghe. Changes within the growth hormone/Insulin-like growth factor/IGF binding protein axis during critical illness. Endocrinol Metab Clin N Am 2006; 35: 793-805.

Mills SD, Boland A, Sory MP, Van Der Smissen P, Derbourch C, Finlay BB, Cornelis GR. *Yersinia* enterocolitica induces apoptosis in macrophages by a process requiring functional tipe III secretion and translocation mechanisms and involving YopP, presumably acting as an effector protein. Proc Natl Acad Sci 1993; 94: 12638-12643.

Ministério da Saúde. Boletim da Secretaria de Vigilância em Saúde. Coordenação geral de doenças endêmicas. Área técnica de dermatologia sanitária. Brasília, 2008.

Ministério da Saúde. Guia de controle da hanseníase. CNDS/CENEPI/FNS/Ministério da Saúde-Brasil. 2ª ed, Brasília: Ministério da Saúde 1994; p. 11-59.

Mira MT, Alcais A, Nguyen VT, Moraes MO, Di Flumeri C, Vuht Mai CP, Nguyen TH, Nguyen NB, Pham XK, Sarno EN, Alter A, Montpetit A, Moraes ME, Moraes JR, Dore C, Gallant CJ, Lepage P, Werner A, Van De Vosse E, Hudson TJ, Abel L, Schurr E. Susceptibility to leprosy is associated with PARK2 and PACRG. Nature 2004; 427(6975): 636-640.

Mira MT. Genetic host resistance and susceptibility to leprosy. Microb and Infect 2006; 8: 1124-1131.

Misra N, Murtaza A, Walker B, Narayan NP, Misra RS, RAmesh V, Singh S, Colston MJ, Nath I. Cytokine profile of circulating T cells of leprosy patients reflects both indiscriminate and polarized T-helper subsets: T-helper phenotype is stable and uninfluenced by related antigens of Mycobacterium leprae. Immunol 1995; 86(1): 97-103.

Montestruc E. Reactions in arrested cases after BCG vaccination (letter). Int J Lepr Other Mycobact Dis 1960; 28: 183-184.

Moraes MO, Cardoso CC, Vanderborght PR, Pacheco AG. Genetics of host response in leprosy. Lepr Rev 2006; 77:189-202.

Moraes MO, Pacheco AG, Schonkeren JJ, Vanderborght PR, Nery JA, Santos Ar, Moraes ME, Moraes JR, Ottenhoff TH, Sampaio EP, Huizinga TW, Sarno EN. Interleukin-10 promoter single-nucleotide polymorphisms as markers for disease susceptibility and disease severity in leprosy. Genes Immun 2004; 5(7): 592-595.

Moraes MO, Sarno EN, Almeida AS, Saraiva BC, Nery JA, Martins RC, Sampaio EP. Cytokine mRNA expression in leprosy: a possible role for interferon-gamma and interleukin-12 in reactions (RR and ENL). Scand J Immunol 1999; 50(5):541-9.

Morrissey TK, Kleitman N, Bunge RP. Isolation and functional characterization of Schwann cells derived from adult peripheral nerve. J Neurosci 1991; 11: 2433-2442.

Moubasher AD, Kamel NA, Zedan H, Raheem DD. Cytokines in leprosy, I. Serum cytokine profile in leprosy. Int J Dermatol 1998; 37(10): 733-740.

Mukherjee R, Antia NH. Intracellular Multiplication of Leprosy-Derived Mycobacteria in Schwann Cells of Dorsal Root Ganglion Cultures. J Clin Microbiol 1985; 21: 808-814.

Muller A, Hacker J, Brand BC. Evidence for apoptosis of human macrophage-like HL-60 cells by *Legionella pneumophila* infection. Infect Immun 1996; 64: 4900-4906.

Naafs B. Bangkok Workshop on Leprosy Research. Treatment of reactions and nerve damage. In J Lepr Other Mycobact Dis 1996; 64 (4 Suppl): S21-28.

Nery JA, Vieira LM, de Mattos HJ, Sarno EN. Reactional states in multibacilary Hansen disease patients during multidrug therapy. Rev Inst Med Trop São Paulo 1998; 40(6): 363-370.

Nery JAC, Perisse ARS, Sales AM, Vieira LMM, Souza RV, Sampaio EP, Sarno EN. The use of pentoxifinlin in the treatment of type 2 reactional episodes in leprosy. Indian J Lepr 2000; 77: 29-39.

Nery JAC, Sales AM, llarramendi X, Duppre NC, Jardim MR, Machado AM. Contribution to diagnosis and management of reactional states: a practical approach. An Bras Dermatol 2006; 81(4):367-75.

Ng, V, Zanazzi G, Timpl R, Talts J, Salzer JL, Brennan PJ, Rambukkana A. Role of the cell wall phenolic glycolipid-1 in the peripheral nerve predilection of *Mycobacterium leprae*. Cell 2000; 103: 511-529.

Nicholson DW, Thornberry NA. Caspases killer proteases. Trends Biochem Sci 1997; 22: 299-306.

Nogueira N, Kaplan G, Levy E, Sarno EN, Kushner P, Granelli-Piperno A, Vieira L, Colomer Gound V, Levis W, Steinman R, Yip YK, Cohn ZA. Defective γ interferon production in leprosy. J Exp Med 1983; 158:2165-2170.

O'Connor JC, McCusker RH, Strle K, Johnson RW, Dantzer R, Kelley KW. Regulation of IGF-I function by proinflammatory cytokines: at the interface of immunology and endocrinology. Cell Immunol 2008; 252(1-2): 91-110.

Oliveira RB, Ochoa MT, Sieling PA, Rea TH, Rambukkana A, Sarno EN, Modlin RL. Expression of Toll-like receptor 2 on human Schwann cells: a mechanism of nerve damage in leprosy. Infect Immun 2003; 71: 1427-1433.

Oliveira RB, Sampaio EP, Aarestrup F, Teles RM, Silva TP, Oliveira AL, *et al.* Cytokines and *Mycobacterium leprae* induce apoptosis in human Schwann cells. J Neuropathol Exp Neurol 2005; 64: 882-890.

Orrenius S. Mitochondrial regulation of apoptotic cell death. Toxicol Lett 2004; 149:19-23.

Pessolani MCV, Marques MA, Reddy VM, Locht C, Menozzi TD. Systemic dissemination in tuberculosis and bacterial adhesins play a role? Microb Infec 2003; 5: 677-684.

Pimentel MIF, Nery JAC, Borges E, Rolo R, Sarno EN. Silent neuritis in multibacillary leprosy evaluated through the development of disabilities before, during and after multidrug therapy. An Bras Dermatol 2004; 79(2): 169-179.

Pocaterra L, Jain S, Reddy R, et al. Clinical course of erythema nodosum leprosum: a 11-year cohort study in Hyderabad, Índia. Am J Trop Med Hyg 2006; 74: 868-879.

Rabinovsky ED. The multifunctional role of IGF-1 in peripheral nerve regeneration. Neurological Res 2004; 26: 204-210.

Rajalingam K, Al-Younes H, Muller A, Meyer TF, Szczepek AJ, Rudel T. Epithelial cells infected with *Chlamydophila pneumoniae* (*Chlamydia pneumoniae*) are resistant to apoptosis. Infect Immun 2001; 69: 7880-7888.

Rambukkana A, Salzer JL, Yurchenco PD, Tuomanen EI. Neural targeting of *Mycobacterium leprae* mediated by the G domain of the lamin-α2 chain. Cell 1997; 88: 811-821.

Rambukkana A, Yamada H, Zanazzi G, Mathus T, Salzer JL, Yurchenco PD, Campebell KP, Fischetti VA. Role of α-dystroglycan as a Schwann cell receptor for *Mycobacterium leprae*. Science. 1998; 282: 2076-2081.

Rambukkana A, Zanazzi G, Tapinos N, Salzer JL. Contact-Dependent Demyelination by *Mycobacterium leprae* in the Absence of Immune Cells. Science 2002; 296: 927-931.

Ranque B, Nguyen VT, Vu HT, Nguyen TH, Nguyen NB, Pham XK, e col., Age is an important risk factor for onset and sequelae of reversal reactions in Vietnamese patients with leprosy. Clin Infect Dis 2007; 44(1): 33-40.

Remancle-Bonnet MM, Garrouste FL, Heller S, Andre F, Marvaldi JL, Prommier GJ. Insulin-like growth factor I protects colon cancer cells from death factor-induced apoptosis by potentiating tumor necrosis alpha-induced mitogen-activated protein kinase and nuclear factor kappaB signaling pathways. Cancer Res 2000; 60: 2007-2017.

Ridley DS, Jopling WH. Classification of leprosy according to immunity. A five-group system. Int J Lepr other Mycobact Dis 1966; 34(3): 255-273.

Ridley DS. Reactions in Leprosy. Lepr Rev 1969; 40:77.

Ridley DS. Skin biopsy in leprosy. Documenta Geigy, 3rd edition. CIBA-GEIGY Limited. Basle, Switzerland, 1990.

Roche PW, Britton WJ, Failbus SS, Williams D, Pradhan HM, Theuyenet WJ. Operational value of serological measurements in multibacillary leprosy patients: clinical and bacteriological correlates of antibody responses. Int J Lepr 1990; 58:480–490.

Roche PW, Le Master J, Butlin R. Risk factors for type 1 reactions in leprosy. Int J Lepr 1997; 65(4): 450-455.

Rodrigues LS. Estudo do efeito anti-apoptótico do Mycobacterium leprae em células de Schwann humanas. Dissertação de Mestrado, Instituto Oswaldo Cruz, 2005.

Rodrigues LS, da Silva Maeda E, Moreira ME, Tempone AJ, Lobato LS, Ribeiro-Resende VT, Alves L, Rossle S, Lopes UG, Pessolani MC. *Mycobacterium leprae* induces insulin-like growth factor and promotes survival of Schwann cells upon serum withdrawal. Cell Microbiol 2010; 12(1): 42-54.

Rolls A, Shechter R, London A, Jacob-Hirsch J, Amariglio N, Rechavi G, Schwartz M. Two faces a chondroitin sulfate proteoglycan in spinal cord repair: a role in microglia/macrophage activation. PLOS Med 2008; 5(8): 1262-1277.

Rosen CJ, Conover C. GH/IGF-I axis in aging: a summary of a NIA-sponsored symposium. J Clin Endocrinol Metab 1997; 82: 3919-3922.

Rosen CJ, Dimai HP, Vereault D, Donahue LR, Beamer WG, Farley J, Linkhart S, Linkhart T, Mohan S, Baylink DJ. Circulating and skeletal insulin-like growth factor-I (IGF-I) concentrations in two inbred strains of mice with different bone mineral densities. Bone. 1997; 21(3): 217-223.

Rosen CJ, Kurland ES, Vereault D, Adler RA, Rackoff PJ, Craig WY, Witte S, Rogers J, Bilezikian JP. Association between serum insulin growth factor-I (IGF-I) and a simple

sequence repeat in IGF-I gene: implications for genetic studies of bone mineral density. J Clin Endocrinol Metab1998; 83(7): 2286-2290.

Rosen CJ, Pollak M. Circulating IGF-I: New Perspectives for a New Century. Trends Endocrinol Metab 1999; 10(4): 136-141.

Rudman D, Feller AG, Nelgrag HS. Effect of human GH in men over age 60. New Engl J Med 1990; 323: 52-60.

Russo VC, Gluckman PD, Feldman EL, Werther GA.The insulin-like growth factor system and its pleiotropic functions in brain. Endocr Rev 2005; 26(7): 916-943.

Rutkowski JL, Tennekoon GI, McGillicuddy JE. Selective culture of mitotically active human Schwann cells from adult sural nerves. Ann Neurol 1992; 31: 580-586.

Ryan JJ, Klein KA, Neuberg TJ, Leftwich JA, Westin EH, Kauma S, Fletcher JA, Devries GH, Huff TF. Role for the stem cell factor/kit complex in Schwann cell neoplasia and mast cell proliferation associated with neurofibromatosis. J Neurosci Res 1994; 37: 415-432.

Sampaio EP, Moreira AL, Kaplan G, Alvim MF, Düppre NC, Miranda CF, Sarno EM. *Mycobacterium leprae* – induced interferon-gamma production by household contacts of leprosy patients: association with the development of active disease. J Infect Dis 1991; 164(5): 990-993.

Sampaio EP, Moreira AL, Sarno EN, Malta AM, Kaplan G. Prolonged treatment with recombinant interferon gamma induces erythema nodosum leprosum in lepromatous leprosy patients. J Exp Med 1992; 175(6): 1729-1737.

Sampaio EP, Oliveira RB, Warwick-Davies J, Faria Neto RB, Griffin GE, Shattock RJ. T cell-monocyte contact enhances TNFα production in response to *M leprae in vitro*. J Infect Dis 2000; 182: 1463-1472.

Sampaio EP, Pereira GMB, Pessolani MCV, Sarno EN. Interaction of the leprosy bacillus and the human host: Relevant components and mechanism of disease. Ciência & Cultura 1994; 46: 462-471.

Sampaio EP, Sarno EN, Galilly R, Cohn ZA, Kaplan. Thalidomide selectively inhibits tumor necrosis factor-alpha production by stimulated human monocytes. J Exp Med 1991; 699-703.

Santos AR, Suffys PN, Vanderborght PR, Moraes MO, Vieira LM, Cabello PH, Bakker AM, Matos HJ, Huizinga TW, Ottenhoff TH, Sampaio EP, Sarno EN. Role of tumor necrosis factor-alpha and interleukin-10 promoter gene polimorphisms in leprosy. J Infect Dis 2002; 186: 1687-1691.

Sarno EN, Grau GE, Vieira LMM, Nery JA. Serum levels of tumor necrosis factor-alpha and interleukin-1β during leprosy reactional states. Clin Exp Immunol 1991; 84:103-108.

Schlesinger LS, Horwitz MA. Phenolic glycolipid-1 of *Mycobacterium leprae* binds complement component C3 in serum and mediates phagocytosis by human monocytes. J Exp Med 1991; 174: 1031-1038.

Scollard DM, Adams LB, Gillis TP, Krahenbuhl JL, Truman RW, Williams DL. The continuing challenges of leprosy. Clin Microbiol Rev 2006; 19(2): 338-381.

Sehgal VN, Sharma V. Reactions in Leprosy – A prospective study of clinical, bacteriological, immunological and histopathological parameters in thirty-five Indians. J Dermatol 1988; 15: 412-419.

Shaw MA, Donaldson IJ, Collins A, Peacock CS, Lins-Lainson Z, Shaw JJ, Ramos F, Silveira F, Blackwell JM. Association and linkage of leprosy phenotypes with HLA class II and tumor necrosis factor genes. Genes Immun 2001; 2: 196-204.

Shepard CC, Chang YT. Effect of several anti-leprosy drugs on the multiplication of human leprosy bacilli in footpads of mice. Proc Soc Exp Biol Med 1962; 109: 636-638.

Shepard CC. Multiplication of *Mycobacterium leprae* in the foot-pad of the mouse. Int J Lepr 1962; 3: 291-306.

Shepard CC. The experimental disease that follows the injection of human leprosy bacilli into footpads of mice. J. Exp. Med 1960; 112:445-454.

Shimoji Y, Ng V, Matsumura K, Fischetti VA, Rambukkana A. A 21-kDa surface protein of *Mycobacterium leprae* binds peripheral nerve laminin-2 and mediates Schwann cell invasion. Proc Natl Acad Sci 1999; 96: 9857-9862.

Silva TP, Silva AC, Baruque MG, Oliveira RB, Machado MP, Sarno EN. Morphological and functional characterizations of Schwann cells stimulated with *Mycobacterium leprae*. Mem Inst Oswaldo Cruz 2008; 103(4): 363-369.

Silva SR, Tempone AJ, Silva TP, Costa MR, Pereira GM, Lara FA, Pessolani MC, Esquenazi D. *Mycobacterium leprae* downregulates the expression of PHEX in Schwann cells and osteoblasts. Mem Inst Oswaldo Cruz 2010; 105(5): 627-632.

Souza ALOM, Stefani MMA, Pereira GAS, Costa MB, Rebello PF, Gomes MK, Narahashi K, Gillis TP, Krahenbuhl JL, Martelli CMT. *Mycobacterium leprae* DNA associated with type 1 reactions in single lesion paucibacillary leprosy treated wih single dose rifampin, ofloxacin and minocycline. Am J Trop Med Hyg 2007; 77(5): 829-833.

Spinola-Castro AM, Siviero-Miachon AA, da Silva MTN, Guerra-Junior G. O papel do hormônio de crescimento e tratamento dos distúrbios endócrino-metabólicos do paciente com a síndrome da imunodeficiência adquirida (Aids). Arq Bras Endocrinol Metab 2008; 52(5): 818-832.

Sreenivasan P, Misra RS, Wilfred D, Nath I. Lepromatous leprosy patients show T helper 1-like cytokine profile with differential expression of interleukin-10 during type 1 and 2 reactions. Immunol 1998; 95 (4):529-536.

Stefani MM, Guerra JG, Sousa AL, Costa MB, Oliveira ML, Martelli CT, Scollard DM. Potential plasma markers of Type 1 and Type 2 leprosy reactions: a preliminary report. BMC Infect Dis 2009; 9: 75.

Svoboda ME, Van Wyk JJ, Klapper DG, Fellows RE, Grissom FE, Schlueter RJ. Purification of somatomedin-C from human plasma: chemical and biological properties, partial sequence analysis, and relationship to other somatomedins. Biochem 1980; 19: 790 - 797.

Syroid DE, Zorick TS, Arbet-Engels C, Kilpatrick TJ, Eckhart W, Lemke G. A role for insulin-like growth factor-I in the regulation of Schwann cell survival. J Neurosci 1999; 19: 2059-2068.

Tapinos N, Rambukkana A. Insights into regulation of human Schwann cell Proliferation by Erk1/2 via a MEK-independent and p56Lck-dependent pathway from leprosy bacilli. Proc Natl Acad Sci 2005; 102: 9188-9193.

Teles RM, Moraes MO, Geraldo NT, Salles AM, Sarno EN, Sampaio EP. Differential TNFalpha mRNA regulation detected in the epidermis of leprosy patients. Arch Dermatol Res 2002; 294: 355-362.

Torres-Aleman I. Insulin-like growth factors as mediators of functional plasticity in the adult brain. Horm Metab Res 1999; 31: 114–119.

Trao VT, Long HT, Quyen ND, Ly HM, Hong ND, Hang, LT, Khang DD, Due LK, Hendriks JT, Wrigert P. Long term evaluation of the immune status in leprosy patients undergoing multiple drug therapy. Int J Lepr 62: 365-373.

Triccas JA, Roche PW, Winter N, Feng CG, Butlin CR, Britton WJ. A 35 kDa protein is a major target of the human immune response to *Mycobacterium leprae*. Infect Immun 1996; 64: 5171-5177.

Truman RW, Krahenbuhl JL. Viable *M. leprae* as a research reagent. Int J Lepr Other Mycobact Dis 2001; 69:1-12.

Tung KS, Umland E, Matzner P, Nelson K, Schauf V, Rubin L, Wagner D, Scollard D, Vithayasai P, Vithayasai V, *et al*. Soluble serum interleukin 2 receptor levels in leprosy patients. Clin Exp Immunol 1987; 69(1):10-15.

Van Brakel WH, Khawas IB, Lucas SB. Reactions in leprosy: a epidemiological study of 386 patients in West Nepal. Lepr Rev 1994; 65(3): 190-203.

Van Buul-Offers SC, Kooijman R. The role of growth hormone and insulin-like growth factors in the immune system. Cell Mol Life Sci 1998; 54: 1083-1094.

Velmurugan K, Chen B, Miller JL, Azogue S, Gurses S, Hsu T. *Mycobacterium tuberculosis* nuoG is a virulence gene that inhibits apoptosis of infected host cells. PLoS Pathog 2007; 3: e110.

Vendrame CM, Carvalho MD, Rios FJ, Manuli ER, Petitto-Assis F, Goto H. Effect of insulin-like growth factor-I on Leishmania amazonensis promastigote arginase activation and reciprocal inhibition of NOS2 pathway in macrophage *in vitro*. Scand J Immunol 2007; 66: 287-296.

Venters HD, Dantzer R, Kelly KW. A New Concept in Neurodegeneration: TNF-α is a Silencer of Survival Signals. T Neurosci 2000; 23: 175-180.

Vergne I, Chua J, Deretic V. Tuberculosis toxin blocking phagosome maturation inhibits a novel Ca^{2+}/calmodulin-PI 3-K hVPS34 cascade. J Exp Med 2003; 4: 653-659.

Verhagen CE, Wierenga EA, Buffing AA, Chand MA, Faber WR, Das PK. Reversal reaction in borderline leprosy is associated with a polarized shift to type 1-like *Mycobacterium leprae* T cell reactivity in lesional skin: a follow-up study. J Immunol 1997; 159(9): 4474-4483.

Vermes I, Haanen C, Reutelingsperger. Flow cytometry of apoptotic cell death. J Immunol Meth 2000; 243:167-190.

Vissa VD, Brennan PJ. Impact of the *Mycobacterium leprae* genome sequence on leprosy research. Genomics of G-C Rich Gram-positive Bacteria. Caister Acad Press. Wymondham, U.K. 2002; p. 85-117.

Walker SL, Lockwood DN. The clinical and immunological features of leprosy. Br Med Bull 2006; 77-78: 103-121.

Wallach D, Varfolomeev EE, Malinin NL, Goltsev YV, Kavalenko AV, Boldin MP. Tumor necrosis factor and Fas signaling mechanism. Annu Rev Immunol 1999; 17: 331-367.

Wang JY, Peruzzi F, Lassak A, Valle LD, Radhakrishnan S, Rappaport J, Khalili K, Amini S, Reiss K. Neuroprotetive effects of IGF-I against TNF-α-induced neuronal damage in HIV-associated Dementia. Virol 2003; 305: 66-76.

Waters MFR. Treatment of reactions in leprosy. Lepr Rev 1974; 45: 337-340.

Webster JI, Sternberg EM. Role of hypothalamic-pituitary-adrenal axis, glicocorticoids and glucocorticoids receptors in toxic sequelae of exposure to bacterial and viral products. J Endocrinol 2004; 181: 207-221.

Wemambu SNC, Turk JL, Waters SNC, Rees RJW. Erythema Nodosum Leprosum: a clinical manifestation of Arthus phenomenon. Lancet 1969; 2:933-935.

WHO. Expert Comitee on Leprosy. Seventh Report. World Health Organization, Genova

WHO. Global Leprosy Situations, beginning of 2009. Weekly Epidemiol Rec 2009; 84: 333-340.

WHO. Laboratory Techniques for Leprosy. 1987; p. 62

Wu Y, Tewari M, Cui S, Rubin R. Activation of the insulin-like growth factor-I receptor inhibits tumor necrosis factor-induced cell death. J Cell Physiol 1996; 168(3): 499-509.

Yamamura M, Uyemura K, Deans RJ, Weinberg K, Rea TH, Bloom BR, Modlin RL. Defining protective responses to pathogens: Cytokine profiles in leprosy lesions. Science 1991; 254: 277-279.

Yamamura M, Wang XH, Ohmen JD, Uyemura K, Rea TH, Bloom BR, Modlin RL. Cytokine patterns of immunologically mediated tissue damage. J Immunol 1992; 149(4): 1470-1475.

Yan N, Ricca C, Fletcher J, Glover T, Seizinger BR, Manne V. Farnesyltransferase inhibitors block the neurofibromatosis type 1 (NF1) malignant phenotype. Cancer Res 1995; 55: 3569-3575.

Ye P, D`Ercole AJ. Insulin-Like Growth Factor I Protects Oligodendrocytes from Tumor Necrosis Factor-α-Induced Injury. Endocrinol 1999; 140 (7): 3063-3072.

Zhang Nu, Hartig H, Dzhagalov I, Draper D, He YW. The role of apoptosis in the development and function of T lymphocytes. Cell Research 2005; 15(10: 749-769.

Anexos – Artigos em colaboração

Artigo 1:

Katherine A. Mattos, Heloisa D'Avila, Luciana S. Rodrigues, Viviane G. C. Oliveira, Euzenir N. Sarno, Georgia C. Atella, Geraldo M. Pereira, Patricia T. Bozza, Maria Cristina V. Pessolani. Lipid droplet formation in leprosy: Toll-like receptor-regulated organelles involved in eicosanoid formation and *Mycobacterium leprae* pathogenesis. J Leukoc Biol 2010; 87(3): 371-384.

Artigo 2:

Katherine A. Mattos, Flavio A. Lara, Viviane G.C. Oliveira, Luciana S. Rodrigues, Heloisa D'Avila, Rossana C. N. Melo, Pedro P. A. Manso, Euzenir N. Sarno, Patricia T. Bozza and Maria Cristina V. Pessolani. Modulation of lipid droplet by *Mycobacterium leprae* in Schwann cells: a putative mechanism for host lipid acquisition and bacterial survival in phagosomes. Cel Microbiol *in press*
Situação: aceito para publicação

Artigo 3:

Mattos, K.A, Oliveira, V.G.C, Rodrigues, L.S., D'Avila, H., Olmo, R.P, Sarno, E. N., Bozza, P.T. and Pessolani, M.C.V. Metabolic consequences of stored neutral lipid in leprosy: linking the lipid metabolism and immune system by lipid droplets organelles regulation through new Toll like receptor 6 signaling pathway in Schwann cells.
Situação: em preparação

Health and Human Services nor does mention of trade names, commercial products, or organizations imply endorsement by the U.S. government.

REFERENCES

1. Naldini, A., Morena, E., Pucci, A., Pellegrini, M., Baldari, C. T., Pelicci, P. G., Presta, M., Ribatti, D., Carraro, F. (2009) The adaptor protein p66shc is a positive regulator in the angiogenic response induced by hypoxic T cells. *J. Leukoc. Biol.* **87,** 367–371.
2. Carraro, F., Pucci, A., Pellegrini, M., Pelicci, P. G., Baldari, C. T., Naldini, A. (2007) p66Shc is involved in promoting HIF-1α accumulation and cell death in hypoxic T cells. *J. Cell. Physiol.* **211,** 439–447.
3. Semenza, G. L. (2009) Regulation of oxygen homeostasis by hypoxia-inducible factor 1. *Physiology (Bethesda)* **24,** 97–106.
4. Chan, D. A., Giaccia, A. J. (2007) Hypoxia, gene expression, and metastasis. *Cancer Metastasis Rev.* **26,** 333–339.
5. Migliaccio, E., Giorgio, M., Mele, S., Pelicci, G., Reboldi, P., Pandolfi, P. P., Lanfrancone, L., Pelicci, P. G. (1999) The p66shc adaptor protein controls oxidative stress response and life span in mammals. *Nature* **402,** 309–313.
6. Pouyssegur, J., Dayan, F., Mazure, N. M. (2006) Hypoxia signaling in cancer and approaches to enforce tumor regression. *Nature* **441,** 437–443.
7. Jung, F., Haendeler, J., Hoffmann, J., Reissner, A., Dernbach, E., Zeiher, A. M., Dimmeler, S. (2002) Hypoxic induction of the hypoxia-inducible factor is mediated via the adaptor protein Shc in endothelial cells. *Circ. Res.* **91,** 38–45.
8. Sitkovsky, M., Lukashev, D. (2005) Regulation of immune cells by local-tissue oxygen tension: HIF1 α and adenosine receptors. *Nat. Rev. Immunol.* **5,** 712–721.
9. Melillo, G. (2007) Targeting hypoxia cell signaling for cancer therapy. *Cancer Metastasis Rev.* **26,** 341–352.

KEY WORDS:
adaptive immunity · cancer · transcription factors · angiogenesis · HIF-1

Editorial: **Lepromatous leprosy, lipids, and lessons in immunology: what we can learn by using modern methods to study an ancient disease**

Mitchell P. Fink[1]

Departments of Critical Care Medicine, Surgery and Pharmacology, University of Pittsburgh School of Medicine, Pittsburgh, Pennsylvania, USA

RECEIVED OCTOBER 19, 2009; REVISED NOVEMBER 8, 2009; ACCEPTED NOVEMBER 11, 2009. DOI: 10.1189/jlb.1009685

SEE CORRESPONDING ARTICLE ON PAGE 371

Leprosy, also sometimes called Hansen's disease, is a chronic infectious disease caused by *Mycobacterium leprae*, a slow-growing obligate intracellular bacterial pathogen. Leprosy has been an affliction of mankind for millenia; skeletal remains from a middle-aged adult male, who was buried inside a stone enclosure at Balathal in India sometime between 2500 and 2000 B.C., show pathological changes that are highly indicative of the diagnosis of leprosy [1]. According to the World Health Organization, 407,791 new cases of leprosy were detected worldwide in 2004 [2]. Fortunately, leprosy is a completely curable illness. Therapy consists of a combination of three antimicrobial agents (rifampicin, clofazimine, and dapsone). The World Health Organization provides these drugs, packaged in convenient blister packs, free of charge in all countries where the disease is endemic.

Leprosy can present as a "tuberculoid" ("paucibacillary") form, which is characterized by the presence of one or at most, a few well-delineated skin lesions, limited nerve involvement, absence of histologically detectable acid-fast bacilli in skin and nerves, and the local production of type 1 cytokines (IFN-γ, IL-2, IL-7, IL-12, IL-15, and IL-18) [3]. Leprosy also can present as a disfiguring "lepromatous" ("multibacillary") form, which is characterized by cutaneous nodules and extensive areas of dermal thickening. In lepromatous leprosy, the skin lesions are infiltrated heavily by foamy macrophages, easily detectable leprosy bacilli within macrophages and nerves, and the production of type 2 cytokines (IL-4, IL-5, and IL-10) [3].

The tuberculoid and lepromatous forms of leprosy represent two extremes of a spectrum of disease manifestations; intermediate forms of the disease are common. The immunological response mounted by the host dictates the clinical phenotype that develops. In patients with tuberculoid disease, the immune response is polarized in the Th1 direction, whereas in cases of lepromatous leprosy, the immune response is polarized in the Th2 direction [4].

In some countries, leprosy remains an important public health problem. This fact alone is sufficient to promote ongoing research related to the responses of immune cells, particularly macrophages, to *M. leprae*. However, even if leprosy is successfully eliminated as a public health problem worldwide (and elimination is the goal of the World Health Organization), studies of the interac-

Abbreviations: ADRP=adipose differentiation-related protein, COX-2=cyclooxygenase 2, LD=lipid droplet, LT=leukotriene, LX=lipoxin, NSAID=nonsteroidal anti-inflammatory drug, PAMP=pathogen-associated molecular pattern, PLA_2=phospholipase A_2

1. Correspondence: University of Pittsburgh, Departments of Critical Care Medicine, Surgery and Pharmacology, 10801 National Blvd., Pittsburgh, PA, USA. E-mail: finkmp@ccm.upmc.edu

tion of *M. leprae* with macrophages will still be relevant, as the results obtained are likely to provide broader insights into the complex factors that regulate responses of the innate immune system to pathogens and PAMP molecules.

In this issue of the *Journal of Leukocyte Biology*, Mattos and co-workers [5] present the results of a series of experiments that focused on the accumulation of lipids in macrophages associated with the cutaneous lesions of lepromatous leprosy. These foamy-appearing, lipid-laden cells, which were described first by the great pathologist Rudolph Virchow, are a hallmark of lepromatous leprosy and bear strong resemblance to the foam cells commonly seen in histopathological sections of atheromatous vascular lesions. Using immunohistochemical methods, Mattos et al. [5] showed that the foamy cells in tissue sections of lepromatous leprosy lesions stained with an antibody that recognizes the LD (see next paragraph) marker, ADRP, also known as adipophilin. These same cells also stained positively for CD68, confirming that they were macrophages. Increased expression of ADRP has been shown to be a sensitive marker for lipid-loading (foam cell formation) by macrophages [6].

LDs, also called lipid storage droplets, are cytoplasmic structures, which are surrounded by a phospholipid-containing monolayer, and store neutral lipids in their core. In most tissues, triglycerides and sterol esters are the most abundant constituents of the LD core, but other endogenous neutral lipids, such as free cholesterol, can also be present [7]. LDs are found in most mammalian cell types, including adipocytes, hepatocytes, fibroblasts, and macrophages. Relevant to the paper under discussion here, previously reported results from a study of fetal membranes showed that key enzymes involved in the synthesis of PGs, such as PLA_2, COX-2, and microsomal-associated PGE synthase-1, can be localized to LDs [8].

By studying macrophages obtained from wild-type as well as TLR2- and TLR6-deficient mice, Mattos et al. [5] obtained evidence in support of the view that both of these pattern recognition receptors play a role in triggering macrophages to form LDs following exposure to *M. leprae*. Moreover, these authors showed that macrophages infected with *M. leprae* are stimulated to secrete one or more soluble factors, which promote LD formation in uninfected cells. The soluble factor(s) that are responsible for this paracrine phenomenon remain to be identified. Perhaps most importantly, Mattos and co-workers [5] showed that the accumulation of LDs in macrophages exposed to *M. leprae* is associated with increased secretion of the potent immunomodulating lipid mediator, PGE_2. Experimental conditions that inhibited *M. leprae*-induced LD formation also down-regulated *M. leprae*-induced PGE_2 secretion, supporting the notion that LDs are important for PGE_2 biosynthesis by *M. leprae*-infected cells.

Conventional NSAIDs, such as naproxen, or COX-2-selective inhibitors, such as celecoxib, are thought to exert their salutary pharmacological effects—reduction in the pain, redness, and swelling of joints affected by rheumatoid arthritis, for example—by down-regulating production of PGE_2 (and perhaps other related PGs). These pharmacological observations support the notion that PGE_2 is a "proinflammatory" mediator. However, the dichotomous characterization of mediators as being proinflammatory or "anti-inflammatory" is often too simplistic. Yes, there is abundant evidence that PGE_2 elicits some of the cardinal features of inflammation; i.e., it is proinflammatory. By the same token, however, it is also clear that PGE_2 is a potent inhibitor of many aspects of innate and adaptive immune system function [9, 10].

In accordance with this latter concept, some studies suggest that the ability of macrophages to kill bacteria is down-regulated by PGE_2 [11]. Furthermore, it has been known for many years that *M. leprae*-burdened macrophages tend to be unresponsiveness to activation induced by IFN-γ, and this effect can be abrogated by treating the cells with the NSAID indomethacin to block PG production [12]. Moreover, feeding mice an essential fatty acid-deficient diet (a classical way to inhibit synthesis of PGE_2 and other eicosanoids) has been shown to promote in vivo killing of *M. leprae* [13]. Thus, armed with the new data reported in this issue of the *Journal of Leukocyte Biology* by Mattos et al. [5], it is not too big a stretch to propose that LD formation in macrophages is not only a characteristic feature of lepromatous leprosy but also is a key pathophysiological mechanism that inhibits development of a robust Th1 response and eradication of the pathogen.

When arachidonic acid is liberated from phospholipids by the enzyme PLA_2, three main classes of downstream products (eicosanoids) can be produced: PGs, such as PGE_2; LTs, such as LTB_4; and LX, such as LXA_4. As noted above, LD-dependent PGE_2 synthesis might account for the persistence of *M. leprae* in infected macrophages. However, it is also conceivable that an eicosanoid, belonging to an entirely different class, might be responsible. This notion is suggested by recently reported data, showing that virulent (but not avirulent) strains of *Mycobacterium tuberculosis* induce production of LXA_4 by infected macrophages [14]. According to this view (and in contradistinction to the concept presented in the previous paragraph), PGE_2 production limits bacterial replication in macrophages infected with *M. tuberculosis* by promoting apoptosis of these cells. LXA_4 production inhibits PGE_2 synthesis and thereby promotes evasion by the pathogen of macrophage-mediated defenses [15]. Thus, at first glance, the role of PGE_2 as a modulator of bacterial clearance seems like it might be at polar extremes for infections caused by two different mycobacterial pathogens: *M. leprae* on the one hand and *M. tuberculosis* on the other. At a minimum, it would be simpler and hence, more satisfying intellectually if a more-unifying hypothesis to explain these phenomena can be formulated. Further studies are clearly necessary to sort out the relationships in these infections among the formation of LDs, bacterial persistence in macrophages, and the production of the eicosanoids, PGE_2 and/or LXA_4.

There is widespread consensus that genetic factors determine the susceptibility of humans to infection with *M. leprae* [16, 17]. Genetic factors almost

certainly also play a key role in determining whether infection leads to the tuberculoid form of the disease, the lepromatous form of the disease, or an intermediate manifestation. Given the importance of TLR-mediated signaling for host resistance to microbial pathogens, much of the research into the influence of genetic background on leprosy has focused on polymorphisms in various TLR genes [16, 18] or other PAMP receptors [19]. In view of the findings presented by Mattos et al. [5], it would not be surprising, however, to learn that genetic variations in the tendency to form LDs in macrophages might also be quite important. By extension, one also has to wonder about the role of LDs in modulating the responses of macrophages to pathogens other than *M. leprae*.

REFERENCES

1. Robbins, G., Tripathy, V. M., Misra, V. N., Mohanty, R. K., Shinde, V. S., Gray, K. M., Schug, M. D. (2009) Ancient skeletal evidence for leprosy in India (2000 B.C.). *PLoS One* **4,** e5669.
2. World Health Organization (2005) Global leprosy situation. *Wkly. Epidemiol. Rec.* **80,** 289–295.
3. Britton, W. J., Lockwood, D. N. (2004) Leprosy. *Lancet* **363,** 1209–1219.
4. Modlin, R. L. (1994) Th1-Th2 paradigm: insights from leprosy. *J. Invest. Dermatol.* **102,** 828–832.
5. Mattos, K. A., D'Avila, H., Rodrigues, L. S., Oliveira, V. G. C., Sarno, E. N., Atella, G. C., Pereira, G. M., Bozza, P. T., Pessolani, M. C. V. (2009) Lipid droplet formation in leprosy: 1 Toll-like receptor-regulated organelles involved in eicosanoid formation and *Mycobacterium leprae* pathogenes. *J. Leukoc. Biol.* **87,** 373–385.
6. Buechler, C., Ritter, M., Duong, C. Q., Orso, E., Kapinsky, M., Schmitz, G. (2001) Adipophilin is a sensitive marker for lipid loading in human blood monocytes. *Biochim. Biophys. Acta* **1532,** 97–104.
7. Thiele, C., Spandl, J. (2008) Cell biology of lipid droplets. *Curr. Opin. Cell Biol.* **20,** 378–385.
8. Meadows, J. W., Pitzer, B., Brockman, D. E., Myatt, L. (2005) Expression and localization of adipophilin and perilipin in human fetal membranes: association with lipid bodies and enzymes involved in prostaglandin (PG) synthesis. *J. Clin. Endocrinol. Metab.* **90,** 2344–2350.
9. Weissmann, G. (1993) Prostaglandins as modulators rather than mediators of inflammation. *J. Lipid Mediat.* **6,** 275–286.
10. Dooper, M. M., Wassink, L., M'Rabet, L., Graus, Y. M. (2002) The modulatory effects of prostaglandin-E on cytokine production by human peripheral blood mononuclear cells are independent of the prostaglandin subtype. *Immunology* **107,** 152–159.
11. Serezani, C. H., Chung, J., Ballinger, M. N., Moore, B. B., Aronoff, D. M., Peters-Golden, M. (2007) Prostaglandin E2 suppresses bacterial killing in alveolar macrophages by inhibiting NADPH oxidase. *Am. J. Respir. Cell Mol. Biol.* **37,** 562–570.
12. Sibley, L. D., Krahenbuhl, J. L. (1988) Induction of unresponsiveness to γ interferon in macrophages infected with *Mycobacterium leprae*. *Infect. Immun.* **56,** 1912–1919.
13. Adams, L. B., Gillis, T. P., Hwang, D. H., Krahenbuhl, J. L. (1997) Effects of essential fatty acid deficiency on prostaglandin E2 production and cell-mediated immunity in a mouse model of leprosy. *Infect. Immun.* **65,** 1152–1157.
14. Chen, M., Divangahi, M., Gan, H., Shin, D. S., Hong, S., Lee, D. M., Serhan, C. N., Behar, S. M., Remold, H. G. (2008) Lipid mediators in innate immunity against tuberculosis: opposing roles of PGE2 and LXA4 in the induction of macrophage death. *J. Exp. Med.* **205,** 2791–2801.
15. Divangahi, M., Chen, M., Gan, H., Desjardins, D., Hickman, T. T., Lee, D. M., Fortune, S., Behar, S. M., Remold, H. G. (2009) *Mycobacterium tuberculosis* evades macrophage defenses by inhibiting plasma membrane repair. *Nat. Immunol.* **10,** 899–906.
16. Alcais, A., Mira, M., Casanova, J-L., Schurr, E., Abel, L. (2005) Genetic dissection of immunity in leprosy. *Curr. Opin. Immunol.* **17,** 44–48.
17. Casanova, J-L., Abel, L. (2002) Genetic dissection of immunity to mycobacteria: the human model. *Annu. Rev. Immunol.* **20,** 581–620.
18. Schuring, R. P., Hamann, L., Faber, W. R., Pahan, D., Richardus, J. H., Schumann, R. R., Oskam, L. (2009) Polymorphism N248S in the human Toll-like receptor 1 gene is related to leprosy and leprosy reactions. *J. Infect. Dis.* **199,** 1816–1819.
19. De Messias-Reason, I., Kremsner, P. G., Kun, J. F. (2009) Functional haplotypes that produce normal ficolin-2 levels protect against clinical leprosy. *J. Infect. Dis.* **199,** 801–804.

KEY WORDS:
primary cells · rodent · secreted regulatory products · Toll-like receptors

JLB

Article

Lipid droplet formation in leprosy: Toll-like receptor-regulated organelles involved in eicosanoid formation and *Mycobacterium leprae* pathogenesis

Katherine A. Mattos, Heloisa D'Avila,† Luciana S. Rodrigues,* Viviane G. C. Oliveira,* Euzenir N. Sarno,‡ Georgia C. Atella,§ Geraldo M. Pereira,*,|| Patricia T. Bozza,†,1 and Maria Cristina V. Pessolani*,1,2*

Laboratórios de *Microbiologia Celular, †Imunofarmacologia, and ‡Hanseniase, Instituto Oswaldo Cruz, FIOCRUZ, Rio de Janeiro, Brazil; §Laboratório de Bioquímica de Lipídeos e Lipoproteínas, Instituto de Bioquímica Médica, Universidade Federal do Rio de Janeiro, Brazil; and ||Laboratório de Imunopatologia, Faculdade de Ciências Médicas, Universidade do Estado do Rio de Janeiro, Rio de Janeiro, Brazil

RECEIVED JUNE 25, 2009; REVISED SEPTEMBER 11, 2009; ACCEPTED OCTOBER 5, 2009. DOI: 10.1189/jlb.0609433

ABSTRACT

A hallmark of LL is the accumulation of Virchow's foamy macrophages. However, the origin and nature of these lipids, as well as their function and contribution to leprosy disease, remain unclear. We herein show that macrophages present in LL dermal lesions are highly positive for ADRP, suggesting that their foamy aspect is at least in part derived from LD (also known as lipid bodies) accumulation induced during ML infection. Indeed, the capacity of ML to induce LD formation was confirmed in vivo via an experimental model of mouse pleurisy and in in vitro studies with human peripheral monocytes and murine peritoneal macrophages. Furthermore, infected cells were shown to propagate LD induction to uninfected, neighboring cells by generating a paracrine signal, for which TLR2 and TLR6 were demonstrated to be essential. However, TLR2 and TLR6 deletions affected LD formation in bacterium-bearing cells only partially, suggesting the involvement of alternative receptors of the innate immune response besides TLR2/6 for ML recognition by macrophages. Finally, a direct correlation between LD formation and PGE_2 production was observed, indicating that ML-induced LDs constitute intracellular sites for eicosanoid synthesis and that foamy cells may be critical regulators in subverting the immune response in leprosy. *J. Leukoc. Biol.* 87: 371–384; 2010.

Abbreviations: ADRP=adipose differentiation-related protein, B6 mice=C57BL/6J mice, BCG=bacillus Calmette-Guerin, BP=Bodipy (4,4-difluoro-1,3,5,7,8-pentamethyl-4-bora-3a,4a-diaza-s-indacene), CHO=cholesterol, CHOE=CHO ester, CM=conditioned medium, COX-2=cyclooxygenase type 2, Cyt B=cytochalasin B, DAPI=4′,6-diamino-2-phenylindole, EIA=enzyme immunoassay, FL=fluorescence channel, HPTLC=high-performance thin-layer chromatography, i.pl.=intrapleurally, LD=lipid droplet, LL=lepromatous leprosy, MFI=mean fluorescence intensity, ML=*Mycobacterium leprae*, MOI=multiplicity of infection, NIH=National Institutes of Health, NS-398=N-(2-cyclohexyloxy-4-nitrophenyl) methane sulfonamide, PI=propidium iodide, $TLR^{-/-}$=TLR-signaling deficient, TT=tuberculoid leprosy, WT=wild-type

Introduction

Leprosy, a chronic, infectious disease caused by the obligate intracellular bacterium ML, is still a major source of morbidity in developing countries [1]. The disease principally affects the skin and the peripheral nervous system, in which the leprosy bacillus is found preferentially inside macrophages and Schwann cells [2–4].

Leprosy manifests as a spectrum of clinical forms in correlation with the nature and magnitude of the innate and adaptive immune response generated during ML infection [3, 5, 6]. At one extreme of the spectrum, individuals with TT have few lesions and manifest a contained and self-limited infection in which scarce bacilli are detected as a result of the generation of a strong cellular immune response against ML. At the other end, LL is a progressive and disseminated disease characterized by extensive bacterial multiplication within host cells and low cell-mediated immunity to the pathogen. Although major advances have been made, the mechanisms responsible for the permissive infection observed in individuals with LL remain only partially understood.

The first line of defense against microbial pathogens is composed of macrophages, so that their innate responses are critical in the early containment of infection. Their capacity to engulf and expose microbes to the acidic and hydrolytically active environment of the phagosome is in most cases sufficient to bring about the demise of these microbes [7, 8]. In addition, macrophages are equipped with a full

1. These senior authors equally contributed to the study.

2. Correspondence: Laboratório de Microbiologia Celular, Instituto Oswaldo Cruz, Avenida Brasil, 4365, Rio de Janeiro, 21040-360, Brazil. E-mail: cpessola@ioc.fiocruz.br

range of TLRs and other pattern-recognition receptors capable of sensing the microbial presence [9–13]. The stimulation of TLR signals triggers inflammation and induces macrophage transition to immune effector cells, which by antigen presentation, costimulatory activity, and production of cytokines and chemokines, will dictate the nature of the adaptive immune response to the pathogen. Macrophages are also essential players in mycobacterial infection [11, 13–16]. However, mycobacteria may persist and replicate in macrophages, whether in part by modulating the phagosomal compartment [16–18] or by inducing macrophage deactivation [16, 19].

The clinico-pathological bipolarity observed in leprosy may stem from the dual responses of monocytes and macrophages to ML in LL and TT patients [20]. Indeed, a histopathological hallmark of LL not seen in TT lesions is the presence of large collections of highly infected macrophages, in which bacilli are allowed to multiply and form *globis*. In 1863, Virchow [21] described these macrophages originally, also referred to as Virchow or Lepra cells and often characterized as foamy or lipid-laden cells. These cells accumulate large amounts of lipids, but the mechanisms that regulate this lipid accumulation, as well as whether they are bacterial and/or cell host products remain nebulous [22]. These lipids, including phospholipids and fatty acids, were thought initially to be derived from ML [22]. Very recently, however, a more detailed analysis of the lipid metabolism in LL lesions indicated the accumulation of host-derived, oxidized phospholipids in these cells [23]. Moreover, the same study showed that these lipids are able to down-regulate the innate immune response, suggesting that their accumulation in infected cells may favor bacterial growth and persistence in the host.

In parallel with this information, studies have shown recently that leukocytes are able to accumulate lipids in response to infection and inflammation and that these lipids are organized in nonmembrane-bound cytoplasmic organelles known as LDs or lipid bodies [24, 25]. Consistent with the role of leukocytes in inflammation, the LDs formed by these cells constitute production sites of inflammatory mediators, enriched by arachidonate esterified in neutral lipids, phospholipids, and eicoisanoid-forming enzymes [25–27].

In terms of mycobacterial infections, we have shown recently that *Mycobacterium bovis* BCG, but not *Mycobacterium smegmatis*, a saprophytic bacterium, induced a time- and dose-dependent increase in LD formation and that this induction was mediated through BCG recognition by TLR2 [24, 28]. Moreover, we have also demonstrated that the newly formed LDs were the predominant PGE_2 production sites in BCG-activated macrophages [28]. These data provide evidence that leukocyte LDs may play a critical role in immunity and inflammation.

LD structure consists of a neutral core composed of triacylglycerol, CHOE, and diacylglycerol surrounded by a half-unit membrane of a complex variety of phospholipids [29, 30]. One of the major proteins found on the LD surface is the ADRP (adipophilin), which has been implicated in LD biogenesis and assembling [25, 31]. Besides ADRP and eicosanoid-forming enzymes, other proteins present in LDs include enzymes involved in the biosynthesis and degradation of other lipid molecules, caveolin, proteins of the Rab family [32, 33], protein kinases [34, 35], and cytokines [28, 36], all of which are essentially pointing to a multifunctional role for these organelles in several cellular processes.

In the present study, we detected LDs inside macrophages present in the dermal lesions of LL patients and investigated the mechanisms involved in ML-induced LD formation. The data presented show that LD formation is induced during ML infection and suggest the involvement of these organelles in PGE_2 biosynthesis and leprosy pathogenesis.

MATERIALS AND METHODS

ML

James Krahenbuhl (National Hansen's Disease Program, Laboratory Research Branch, Louisiana State University, Baton Rouge, LA, USA), through National Institute of Allergy and Infectious Diseases/NIH (Bethesda, MD, USA), Contract No. 155262, kindly provided ML, prepared from footpads of athymic *nu/nu* mice. Part of the ML suspension was killed by γ-irradiation [37]. Prior to interactive assays with macrophages, dead bacteria were stained with PI (Sigma Chemical Co., St. Louis, MO, USA) and live bacteria with PKH26 Red Fluorescence cell linker kit (Sigma Chemical Co.). Equal volumes of dead bacterial suspension (1×10^9 ml^{-1} in 10 mM PBS, pH 7.2) and PI solution (100 μg ml^{-1} in PBS) were mixed by rotation for 15 min at room temperature. The PI-labeled bacteria were washed three times in PBS and finally suspended in RPMI 1640 at 1×10^9 bacilli ml^{-1} [38]. Alternatively, live ML was prelabeled with a PKH26, according to the manufacturer's instructions. Aliquots were stored at −20°C and thawed immediately before use. The quality of labeling was checked by fluorescence microscope.

Animals

B6 mice were obtained from the Oswaldo Cruz Foundation Breeding Unit (Rio de Janeiro, RJ, Brazil). Shizuo Akira (Osaka University, Osaka, Japan) donated TLR2 and TLR6 knockout mice in a homogeneous B6 background. Animals were caged with free access to food and fresh water in a room at 22–24°C and a 12-h light-dark cycle. Animal protocols were in agreement with the animal care guidelines of the NIH and were approved by the Animal Welfare Committee of the Oswaldo Cruz Foundation.

Isolation and treatment of mononuclear phagocytes with ML

Mouse resident peritoneal macrophages were recovered from unstimulated mice after peritoneal washings with RPMI medium as described previously [39]. Cells were plated at a density of 1×10^6 cells in 1 ml medium (RPMI 1640 supplemented with 2% heat-inactivated FBS and 1% penicillin-streptomycin; Invitrogen, Eugene, OR, USA)/well in a 24-well tissue-culture plate. For microscope visualization, cells were plated in tissue-culture dishes containing glass coverslips. Peritoneal macrophages were allowed to adhere for 2 h at 37°C in a 5% CO_2 atmosphere and subsequently washed with PBS to remove nonadherent cells. ML was added to the culture at a MOI of five bacilli/cell (5:1) for 1 h. In some experiments, cells infected with BCG (MOI=5) or *M. smegmatis* (MOI=5) or stimulated with LPS (500 ng ml^{-1}) were included as controls. Cultures were then washed three times with PBS and incubated for 24, 48, and 72 h at 37°C in 5% CO_2. Alternatively, mice were i.pl.-injected with ML (5×10^6 bacilli/cavity) in 100 μl sterile saline. Control animals received the same volume of sterile saline only. After 24 and 48 h, the animals were killed by CO_2 inhalation, and their thoracic cavities were washed with 1 ml heparinized PBS (10 UI ml^{-1}).

Human PBMCs were isolated from fresh heparinized blood withdrawn from healthy volunteers and prepared by way of Ficoll-Hypaque density gradient centrifugation (Sigma Chemical Co.). Monocytes were isolated from PBMC by exploiting their ability to adhere to plastic surfaces. The cells were allowed to adhere for 2 h in serum-free medium

and then washed to remove the nonadherent cells. Monocytes were treated with ML as described above.

In the inhibitory studies, cells were pretreated with Cyt B (20 μM, Sigma Chemical Co.) or the nonesteroidal drug NS-398 (1 μM, Biomol, Plymouth Meeting, PA, USA) for 30 min at 37°C. As mentioned previously, after two washings with RPMI medium, cells were treated with ML. The supernatants were collected after 48 h, centrifuged for 5 min at 3000 *g*, filtered (0.2 μm), and then frozen until testing for biological effects.

LD evaluation by microscopy

Cells adhering to coverslips were fixed in 3.5% paraformaldehyde in Ca^{2+}/Mg^{2+}-free HBSS, pH 7.4, for 10 min and stained by osmium tetroxide or BP [40, 41]. Briefly, slides were rinsed in 0.1 M cacodylate buffer (pH 7.4), stained in 1.5% osmium tetroxide (30 min), rinsed in water, immersed in 1.0% thiocarbohydrazide (5 min), rinsed in water, rinsed in 0.1 M cacodylate buffer, restained in 1.5% osmium tetroxide (3 min), rinsed in water, dried, and mounted. For fluorescent LD-labeling, cells were incubated with BP 493/503 dye (Molecular Probes, Eugene, OR, USA) at a final concentration of 1 μM for 45 min at 37°C in PBS, pH 7.8. The slides were stained with 2 μM DAPI (Invitrogen) at room temperature for 5 min. The coverslips were then mounted in 20% glycerol and 1% n-propyl gallate in PBS. Preparations were examined using an Olympus BX-FLA microscope equipped with a Plan Apo 100× 1.4 Ph3 objective (Olympus Optical, Japan) and CoolSNAP-Pro CF digital camera in conjunction with Image-Pro Plus Version 4.5.1.3 software (Media Cybernetics, Bethesda, MD, USA). The images were edited using Adobe Photoshop 5.5 software (Adobe Systems, McLean, VA, USA). The morphology of the fixed cells was observed, and LDs were enumerated at 100× in 50 consecutively scanned cells.

Analysis of LDs using FACS

The adherent cells were detached by trypsin-EDTA treatment (Invitrogen). Cells were washed in PBS, fixed with 4% paraformaldehyde, and incubated with 1 μM BP for 15 min at 37°C, and LD induction was measured at FL1 channel and was expressed as MFI. Bacterial association to cells was measured at FL2 or FL3 by PKH26- or PI-labeled bacteria, respectively. The index of bacterial association (percent) is expressed as percent of cells taking up PI- or PKH26-ML. Two-color flow cytometric acquisition and analysis were performed on a FACSCalibur flow cytometer (BD Biosciences, Heidelberg, Germany), and at least 10,000 cells were analyzed/sample. Quantitative data analysis was performed using BD CellQuest Pro software (BD Biosciences) and WinMDI analysis software.

Immunohistological analysis of ADRP expression

Lesional skin biopsies were obtained from a total of four LL patients diagnosed according to the Ridley-Jopling classification in attendance at the Leprosy Out-Patient Unit (Oswaldo Cruz Foundation). The Ethics Committee of the Oswaldo Cruz Foundation approved the procedures described in this study. Archived, snap-frozen in liquid N_2, tissue sections from leprosum lesions were subjected to immunohistochemical staining as described. Cryostat sections (5 μm-thick) were thawed on sylane-precoated slides and submitted to staining and immunostaining protocols. Standard staining was done with H&E for morphological analysis and Wade-Fite staining to identify the mycobacteria [42]. Immunostaining was performed to detect the ADRP protein and CD68 staining to highlight macrophage cells. For immunodetection of ADRP, biopsies were washed with PBS and blocked and permeabilized with blocking buffer [5% newborn calf serum (Invitrogen) and 0.01% Triton (Sigma Chemical Co.) in PBS] for 1 h at room temperature. Sections were incubated with mouse monoclonal anti-ADRP (AP125; Research Diagnostics Inc., Flanders, NJ, USA), diluted in blocking buffer at 1:25 for 1 h at room temperature. The streptavidin-biotin peroxidase immunostaining duet kit (StreptABComplex/HRP Duet, Dako, Hamburg, Germany) was used according to the manufacturer's protocol. A mouse IgG1 (BD Biosciences) was used as control. Sections were counterstained with hematoxylin. The slides were mounted in 20% glycerol and 1% n-propyl gallate in PBS (pH 7.8) containing 2 μM DAPI (Invitrogen). For immunofluorescence microscopy, biopsies were incubated with primary antibody against ADRP (1:25) or CD68 (1:100; Clone KP1, Dako), diluted in blocking buffer for 2 h at room temperature. Cells were washed extensively with PBS and then incubated with IgG goat anti-mouse secondary antibody conjugated to Alexa488 or Alexa568 (Molecular Probes; 1:250) for 1 h at room temperature. Cells were also labeled with the nuclear stain TO-PRO-3 (1:100; Molecular Probes) for 1 h. After washing with PBS, cells were lastly rinsed with water before mounting on slides. Negative controls were performed under each experimental condition by incubating tissue with secondary but not primary antibodies. Immunodetection was carried out using confocal microscopy. Fluorescence images were acquired with a LSM 510 Zeiss confocal microscope (Carl Zeiss Inc., Thornwood, NY, USA). Images were acquired, colored, and merged via LSM 510 Zeiss software.

Measurement of PGE_2

PGE_2 concentration was measured in cell-free supernatants via an EIA kit (Cayman Chemical Co., Ann Arbor, MI, USA), using a plate reader (Labsystems, Helsinki, Finland). The assays were conducted according to the manufacturer's protocol.

Lipid extraction and analysis

Skin biopsies from LL patients and healthy volunteers were taken with a 6-mm punch. After mechanic disruption of tissues, lipids were extracted with chloroform, methanol, and water (1:2:0.8 by vol) [43] and then partitioned with chloroform and methanol (2:1 by vol), according to the standard procedure of Folch et al. [44]. Neutral lipids were analyzed by one-dimensional HPTLC on Silica gel 60 plates (Merck, Darmstadt, Germany). Plates were first developed in hexane-ethyl ether-acetic acid (60:40:1 by vol) until the solvent front reached the middle of the plate and then in hexane-chloroform-acetic acid (80:20:1 by vol). HPTLC plates were stained by spraying with a charring solution consisting of 10% $CuSO_4$, 8% H_3PO_4, and heated to 180°C for 5–10 min [45]. The charred TLC plate was then subjected to densitometric analysis using a photodensitometer with automatic peak integration (Camag TLC Scanner II). The percentage of CHO and CHOE was calculated from the total amount of lipid (set as 100%) isolated in each skin biopsy.

Cytokine analysis

IL-4, IFN-γ, IL-6, IL-17, TNF-α, IL-12, IL-1β, IL-10, MCP, and keratinocyte-derived chemokine were analyzed simultaneously using luminex technology in supernatants from ML-infected macrophages. A mouse multiplex cytokine kit (Upstate Biotechnology, Lake Placid, NY, USA) was obtained, and the assay was performed according to the manufacturer's instructions using the Bio-Plex system (Bio-Rad, Hercules, CA, USA). Data analysis was performed with the Bio-Plex Manager software.

Statistical analysis

Data analysis was performed using the GraphPad InStat program (GraphPad Software, Inc., San Diego, CA, USA), and the statistical significance ($P<0.05$) was determined by the Student's *t*-test.

RESULTS

Detection of LDs in skin biopsies of LL patients

As described above, a highly characteristic feature seen in dermal lesions of LL patients is the accumulation of infected foam macrophages, also referred to as Virchow cells [21]. Given the fact that other mycobacterial species such as *M. bovis* BCG are good inducers of LD formation in macrophages [28], we hypothesized that Virchow cells are the result of ML-induced LD accumulation during the course of leprosy.

To investigate this hypothesis, we immune-stained tissue sections of LL lesions with specific antibodies that recognize ADRP, a LD marker, and CD68, a macrophage marker. The LL lesion was characterized by many parasitized foam cells containing large multibacillary vacuoles (**Fig. 1A**). The lesion exhibited strong staining for ADRP-labeled LDs (Fig. 1B). Moreover, immunofluorescence staining for CD68 and ADRP demonstrated that the ADRP-reactive cells were CD68+, confirming they were macrophages (Fig. 1C is isotype control; Fig. 1D is ADRP; Fig. 1E is CD68+; Fig. 1F is merged). These data suggest that the foamy aspect of ML-infected macrophages in LL lesions is derived from the accumulation of lipids stored in cellular organelles identified as LDs.

As LDs are known to be enriched in free CHO and CHOE [46–48], the relative content of these lipids was then examined by HPTLC comparing skin biopsies from LL versus healthy controls. This analysis revealed an increase of

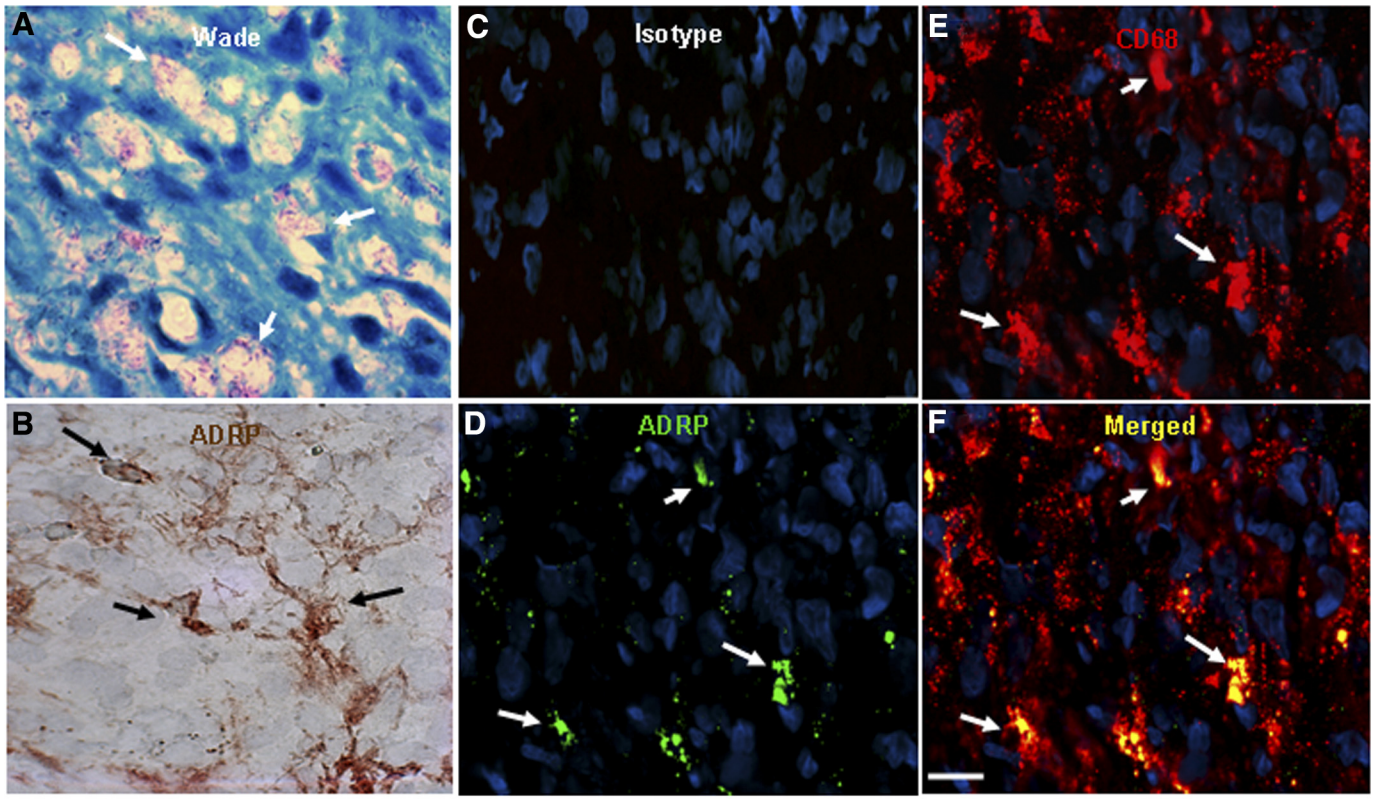

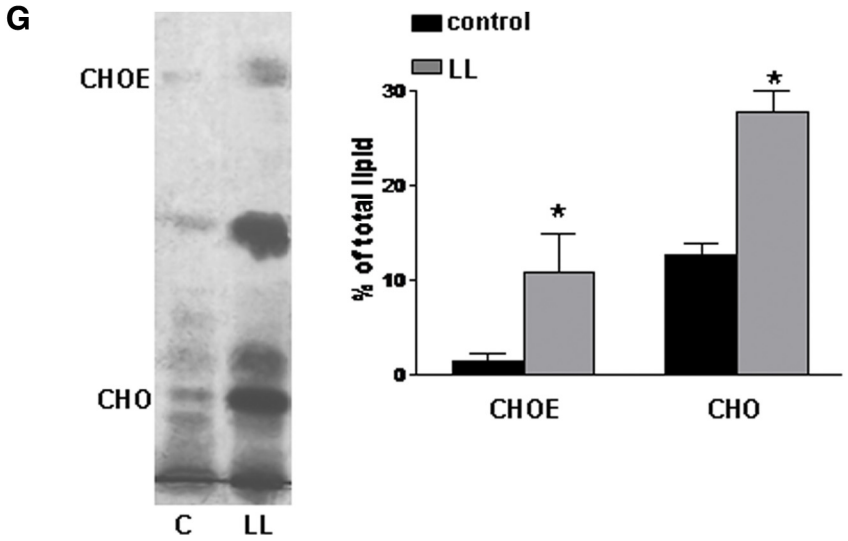

Figure 1. Expression of ADRP in skin biopsy specimens of LL lesions. Serial sections of skin biopsies from LL patients (n=4) were stained by Wade (A), showing foamy macrophages containing the characteristic ML bacilli (arrows), and by the immunoperoxidase method with a mAb specific for ADRP (B), showing positive staining (arrows). Imunofluorescence confocal images for the marker ADRP (green labeling indicated by the arrows, D) and CD68 (red labeling indicated by the arrows, E). The images were superimposed, and the colocalization is represented by the yellow signal (arrows, F). ADRP-positive cells were also positive for CD68. Nuclei (blue) were labeled with TO-PRO-3. No fluorescence was observed for the Alexa546-labeled mouse isotype control IgG (C). Original bar, 20 μm; original magnification, 63×. (G) HPTLC of neutral lipids extracted from skin biopsies of LL patients and healthy controls detected by charring. The content of each class of lipid was estimated by densitometry and plotted as a percentage. The vertical bars represent the SEM of CHO and CHOE levels of three LL patients and three controls performed in duplicates. Bands were identified using pure chemical standards. *, Statistically significant differences (P<0.05) when campared to control groups.

CHO and CHOE in LL as compared with healthy skin (Fig. 1G), suggesting that CHO homeostasis is modulated in response to ML infection, leading to its intracellular accumulation as LDs.

In vitro induction of LD formation by ML

To confirm the capacity of ML to induce the formation of LDs, murine peritoneal macrophages and human mononuclear phagocytes were stimulated in vitro with live and irradiated, killed bacteria. LD formation was determined by microscopic quantification and fluorescence changes measured by flow cytometry. For light microscopy analysis, cells were fixed appropriately, and LDs were enumerated after staining with osmium tetroxide (**Fig. 2A**). Alternatively, the cells were incubated with BP, a lipophilic fluorescent dye, and the LD formation was analyzed by fluorescence microscopy (Fig. 2, B and D) and flow cytometry (Fig. 2, C and E).

Murine and human ML-infected mononuclear phagocytes showed an increase of LD numbers and in the MFI of the BP probe in comparison with untreated cells (Fig. 2, C and E). Moreover, as shown in Figure 2D, the capacity to induce LD formation was independent of bacterial viability. Murine macrophages treated with live or dead ML resulted in similar bacterial associations (data not shown) and induction of LD formation (Fig. 2F). Therefore, as a result of difficulties in obtaining live bacteria, subsequent experiments used irradiated, killed mycobacteria. Cells were also stimulated with other mycobacterial species, corroborating the capacity of BCG (see Fig. 4A) but not *M. smegmatis* (data not shown) to induce LDs in macrophages. Finally, Figure 2G shows that ML-induced LD biogenesis was time-dependent. Murine macrophages were stimulated in vitro with bacteria for periods of time ranging from 24 h to 72 h, and LD formation reached maximum levels at 48 h after treatment (Fig. 2G).

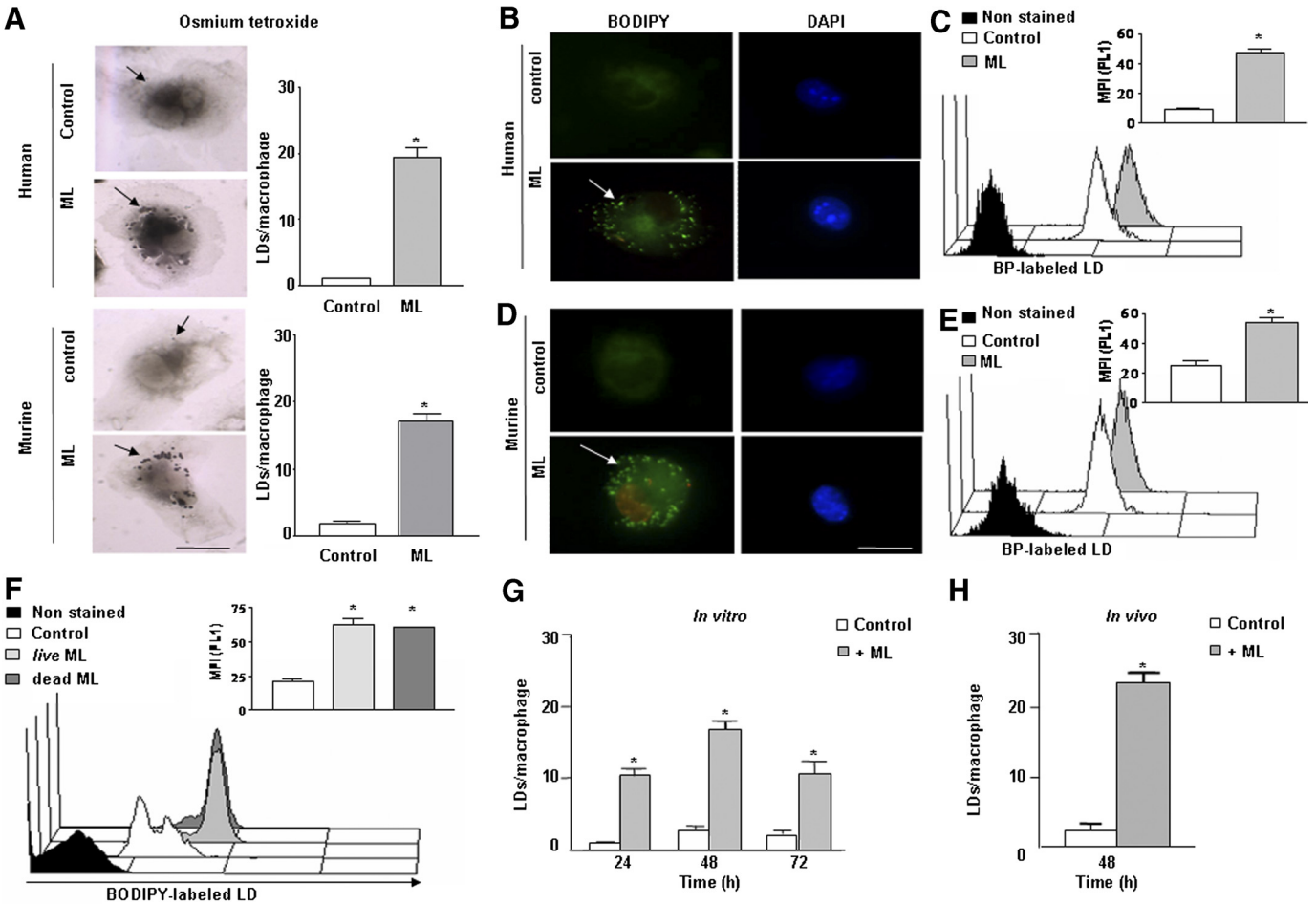

Figure 2. ML induces LD formation in human and murine mononuclear phagocytic cells. (A) LDs were visualized as black cytoplasmatic, punctuate inclusions (arrows) after osmium staining, and the quantification of these organelles was expressed in bar graphs as number of LD/macrophage. (B and D) BP-labeled LD at 48 h subsequent to ML treatment was visualized as green inclusions (arrows). Nuclei were labeled with DAPI. The LD level was monitored by flow cytometry using the BP staining method in human (C) and murine (E) cells. LD biogenesis was independent of bacterial viability (F). Inset graph shows MFI values of BP. Quantification of LD was determined by enumeration of these organelles after osmium staining in the time course of in vitro experiments (G) and in vivo assays (H). All experiments were performed using a MOI of 5, and LDs were determined after 48 h, except for the time-course experiments. *, Statistically significant differences ($P<0.05$) when compared with control groups. Original bars, 20 μm. Data are representative of four independent experiments and are expressed as the mean ± SD of triplicates.

Finally, the capacity of ML to induce LD formation in vivo was confirmed via an experimental model of mouse pleurisy induced upon bacterial i.pl. injection. Cells were recovered 24 h and 48 h after injection, and LDs were then stained with osmium tetroxide and quantified under a light microscope. Figure 2H shows that cells recovered 48 h after ML injection have increased formation of LDs markedly when compared with cells recovered from uninfected animals (from 2.5±0.5 LDs/macrophage in controls to 23.67±1.5 LDs/macrophage in ML-treated animals; P=0.0001). The same results were obtained when cells were analyzed at 24 h postinjection, regardless of whether the bacteria were alive or dead (data not shown). The in vivo and in vitro data obtained so far suggest that LD formation is a common response of macrophages during interaction with ML and that LD is induced notwithstanding mycobacterial viability.

ML-induced LD formation is observed in bacterium-associated cells and in cells with no bacterium

We next investigated whether the effect of ML on LD formation described herein was restricted to cells bearing bacteria. To this end, human peripheral monocytes were isolated and exposed to fluorescent-labeled ML. Cells untreated or exposed to PI-labeled ML were cultured for 48 h. Cells were then stained with BP, and ML-induced LDs were analyzed by flow cytometry and fluorescence microscopy. **Figure 3A** shows that in ML-treated cultures, the LDs were induced significantly in human macrophages bearing fluorescent-labeled bacterium (ML-positive cells, BP^+/PI^+) and in cells with no bacterium (ML-negative cells, BP^+/PI^-) in comparison with untreated cells. However, all bacterium-bearing cells were BP^+, and LD formation was significantly higher in these cells in comparison with those without bacterium (from a MFI value of 15.22±1.4 in ML-negative cells to 43.68±3.0 in ML-positive cells; P=0.0004). An identical result was obtained when murine macrophages were ML-stimulated in vitro (from a MFI value of 27.2±4.4 in ML-negative cells to 62.8±2.6 in ML-positive cells; P=0.002; Fig. 3B) and in vivo (from a MFI value of 132.7±23.1 in ML-negative cells to 633.3±7.0 in ML-positive cells; P=0.002; Fig. 3C). Moreover, immunofluorescence images obtained from murine macrophages treated with PI-labeled ML showed increased numbers of BP-staining LDs in bacterium-bearing cells and cells without bacterium (Fig. 3D).

Taken together, these results suggest that ML induces the secretion of soluble factors in bacterium-associated cells and that these soluble factors may act in a paracrine-signaling circuit to induce LD formation in uninfected cells.

TLR2, TLR6, and cytoskeleton are involved in ML induction of LD formation

The predominant receptor responsible for mycobacterium recognition on macrophages is TLR2 [49]. We have also shown previously that LD formation induced by BCG is mediated by TLR2 [28]. To understand how bacterial association modulates LD formation, the consequences resulting from the absence of TLR2 signaling in ML-stimulated LD formation were analyzed.

Peritoneal macrophages from WT and $TLR2^{-/-}$ mice were stimulated in vitro for 48 h with ML, and LD formation was estimated by flow cytometry analysis and quantified by microscopic analysis. As shown in **Figure 4A**, ML-induced LD formation was partially impaired in TLR2-knockout macrophages (Fig. 4A), although comparable levels of bacterial association were observed in mutant and WT macrophages (Fig. 4A). As expected, no effect of $TLR2^{-/-}$ on LD formation induced by LPS, a classical TLR4 ligand [50], was observed (Fig. 4A). In contrast, BCG, used as a positive control, behaved similarly to ML (Fig. 4A). These results show that although the induction of LD formation in response to ML appeared to be at least partially TLR2-dependent, it is dispensable for bacterial association, indicating that TLR2 does not mediate phagocytic recognition of ML in murine macrophages.

It has been demonstrated previously that TLR2 forms heterodimers with TLR1 or TLR6 in response to different ligands [12, 51–53]. In turn, we investigated whether the TLR2/TLR6 heterodimer is necessary for LD biogenesis during ML association by using $TLR6^{-/-}$ macrophages. LD formation was evaluated by FACS and microscopic analysis. As shown in Figure 4B, LD formation induced by ML was partially inhibited in the absence of TLR6. Moreover, as observed for TLR2, the absence of TLR6 did not affect bacterial association with murine macrophages (Fig. 4B). Thus, these results indicate that TLR6 plays a significant role in LD formation in response to ML, suggesting that the TLR2/6 heterodimer constitutes a ML receptor signal for LD biogenesis in macrophages.

To investigate whether bacterial phagocytosis is required to elicit LD formation, mononuclear cells were pretreated with the actin polymerization inhibitor Cyt B before the addition of ML. The inhibitory effect of Cyt B on phagocytosis was monitored by flow cytometry using bacteria prestained with PI. Figure 4C shows a 50% reduction in the number of cells with associated bacteria in the presence of the drug, coincident with the same reduction in number of LD (Fig. 4C, left) and BP fluorescence (MFI, Fig. 4C). This suggests that ML internalization is involved in triggering the signaling pathways that will culminate in LD formation, although other cytoskeleton-dependent mechanisms besides phagocytosis of the mycobacterium might also participate in the mechanisms involved in LD biogenesis.

TLR2, TLR6, and cytoskeleton are essential for the induction of LD formation by ML-infected cells in uninfected, neighboring cells

To better understand the mechanisms involved in LD induction by ML, we re-evaluated the effect of TLR2 and TLR6 depletions by looking separately at cells bearing or not bearing bacterium. This was performed by means of a two-color fluorescence FACS analysis using PI-labeled bacteria and LDs stained with BP. Interestingly, LD formation was abrogated completely in cells with no bacteria (PI^-; **Fig. 5, A** and **B**). However, the TLR2 or TLR6 effect on LD biogenesis in bacterium-bearing (PI^+) cells was less drastic, partially decreasing the LD formation observed in WT

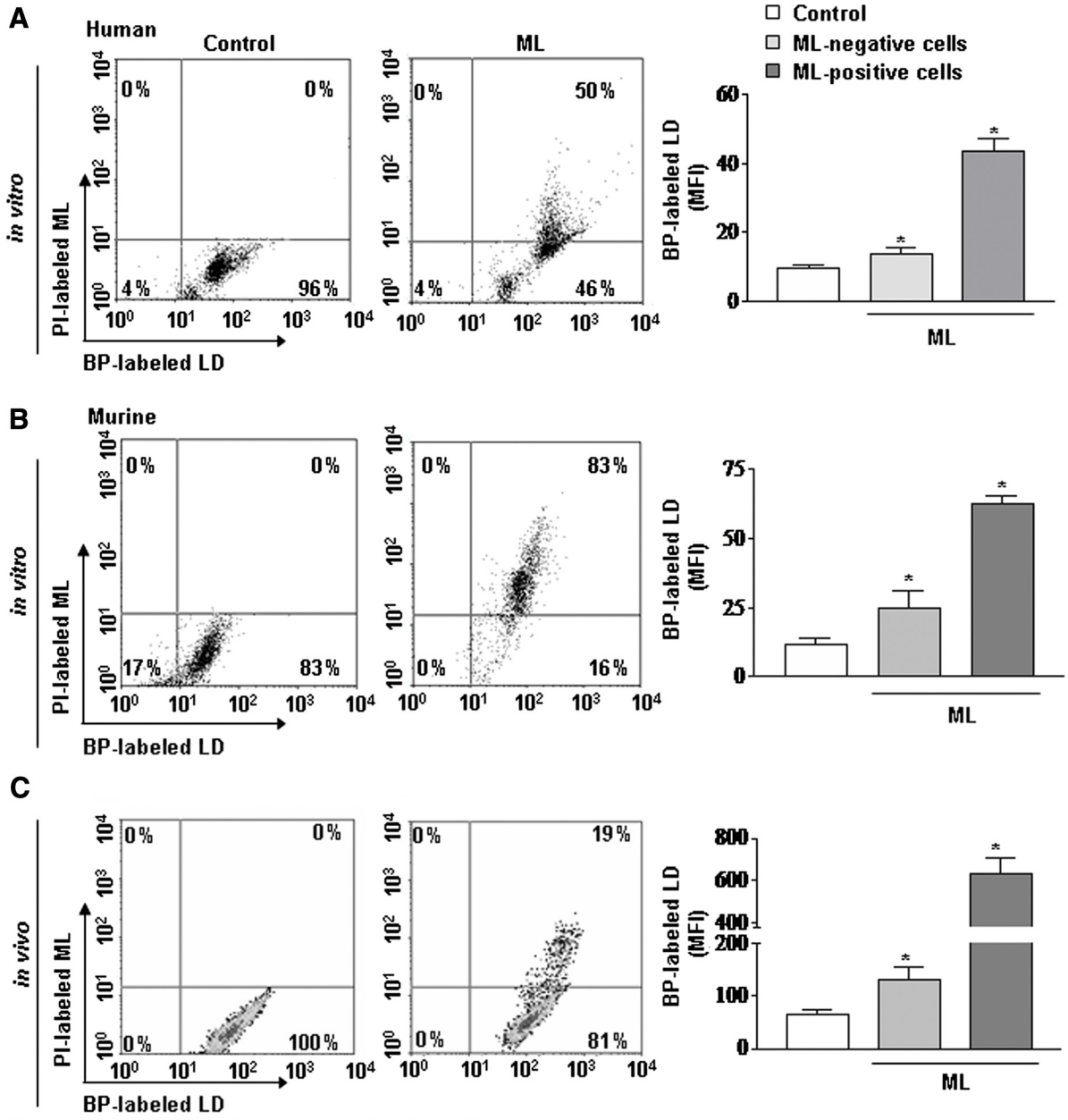

Figure 3. ML-induced LD formation is observed in bacterium-associated cells and in cells with no bacterium. Bacterial association and LDs were measured simultaneously by flow cytometry. The dot plot represents PI fluorescence (FL3) versus BP fluorescence (FL1) of human monocytes (A) and murine peritoneal macrophages (B) stimulated in vitro with PI-labeled ML or not (Control) for 48 h. Alternatively, PI-labeled ML (5×10^6 bacilli/cavity) was used to induce LD formation in a murine model of pleurisy (C). MFI values of BP are expressed in bar graphs. Separate analysis was performed in cells with no bacteria (PI-negative cells) and cells bearing bacteria (PI-positive cells). Results from five representative experiments are shown. *, Statistically significant differences ($P<0.05$) when compared with control cells. Fluorescence images of macrophage cultures showing LDs in cells associated or not with ML (D). Red arrow, PI-labeled ML; green arrows, BP-stained LDs. Original bar, 20 μm.

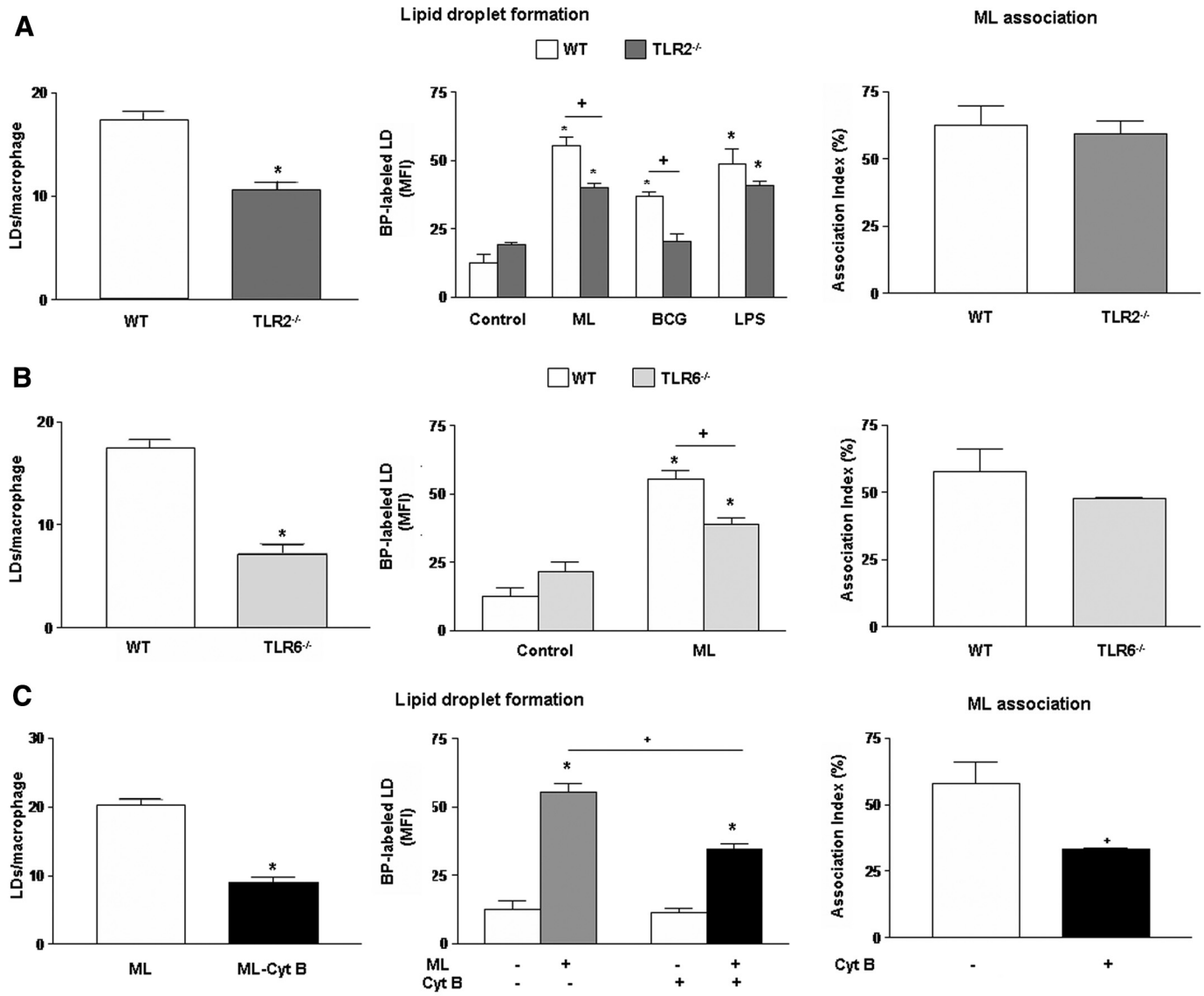

Figure 4. TLR2/TLR6 and cytoskeleton are involved in ML induction of LD formation. Peritoneal macrophages from WT, TLR2$^{-/-}$, or TLR6$^{-/-}$ B6 mice were treated with ML, and LD formation was determined by microscopic quantification (osmium staining) and flow cytometry as described in Figure 3. Reduced LD formation in response to ML was observed in TLR2 (A) and TLR6 (B) knockout macrophages, although the association index of ML with these cells was identical to that of WT macrophages. PI-labeled ML (PI-ML) was used to determine the percentage of cells bearing bacteria by flow cytometry. (A) Cells were also stimulated with BCG (MOI=5) or LPS (500 ng ml^{-1}) as positive and negative controls, respectively. (C) The addition of Cyt B reduced LD biogenesis and the bacterial association index significantly. Data are representative of five independent experiments. Data indicate mean ± SD of triplicates. *, Statistically significant differences ($P<0.05$) between ML-stimulated and control cells. +, Significant differences ($P<0.05$) between the different ML-treated cell groups.

cells. Identical results were obtained when the effect of Cyt B was analyzed (Fig. 5C), indicating that TLR2/TLR6 and the process of phagocytosis or other cytoskeleton-dependent mechanisms are required to complete induction of LD formation in bacterium-bearing cells. On the other hand, in infected cells, TLR2/TLR6 and phagocytosis are indispensable for the LD induction in uninfected, neighboring cells. Imunofluorescence images of the same cultures clearly show the exclusive presence of LDs in cells bearing ML in TLR2$^{-/-}$, TLR6$^{-/-}$, or Cyt B-treated macrophages (Fig. 5, A–C, right panel), in contrast to Cyt B-untreated WT cells, in which numerous LDs can be seen in infected and uninfected cells (Fig. 3D).

Media conditioned by ML-stimulated macrophages mimicked the LD induction activity of the bacteria

To test the hypothesis that ML induces macrophages to secrete soluble factors that regulate LD formation, the CM of ML-treated cells was tested for the capacity of CM to induce

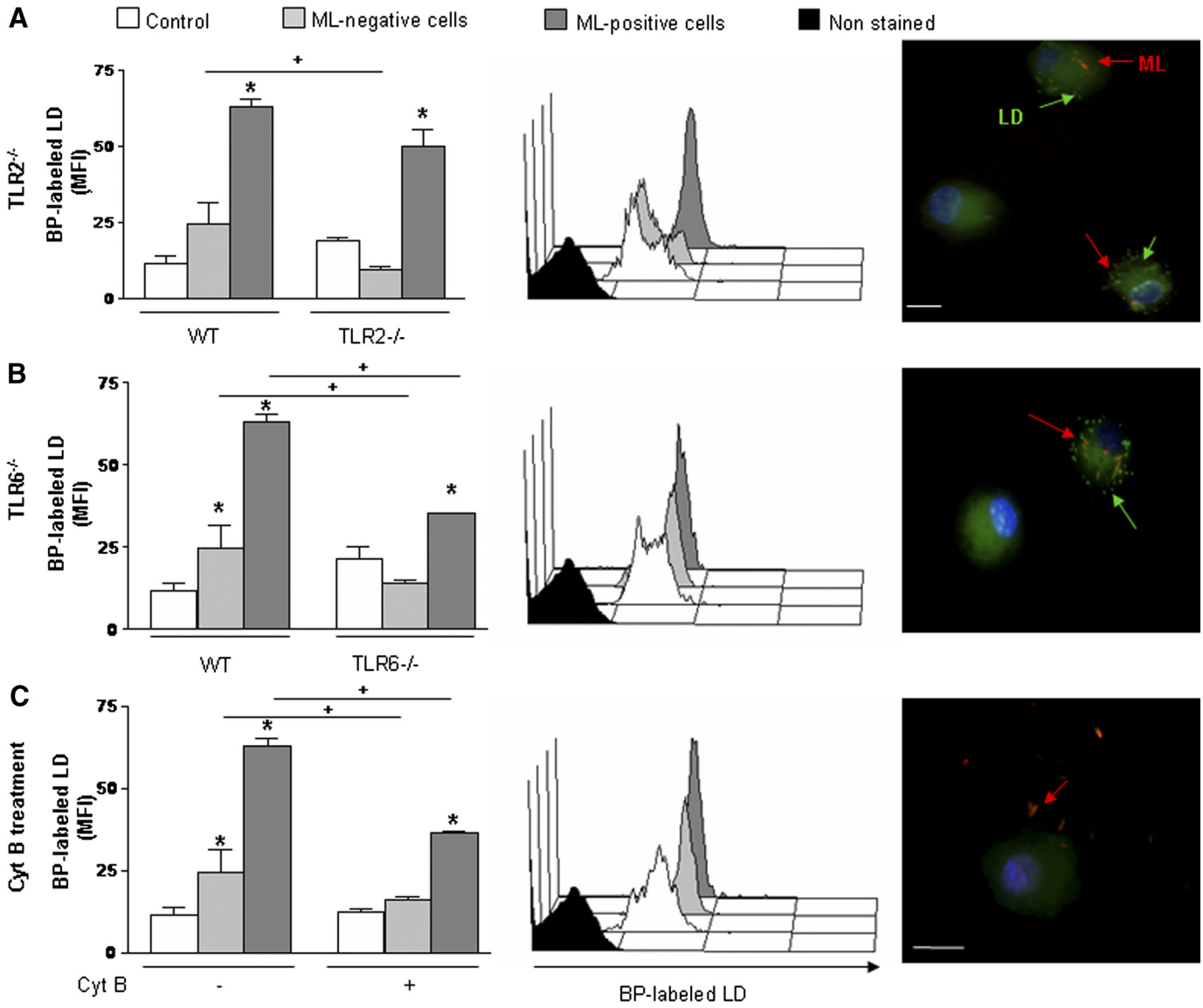

Figure 5. TLR2/TLR6 and cytoskeleton are essential for the induction of LD formation by ML-infected cells in neighboring, uninfected cells. Macrophages from WT, TLR2$^{-/-}$, and TLR6$^{-/-}$ B6 mice were stimulated with PI-labeled ML, and LD formation was monitored in cells bearing bacteria (PI^{+}) versus cells with no bacterium (PI^{-}; A and B). The same analysis was performed in WT macrophages pretreated or not with Cyt B (C). Histograms show LD fluorescence (FL1) in PI^{-} and PI^{+} ML-treated cells, in unstimulated macrophages, and unstained cells. (Right panels) Fluorescence images of BP-labeled LDs (green labeling, arrows) in macrophages after PI-labeled ML (red labeling, arrows) stimulation. Images correspond to TLR2$^{-/-}$ (A), TLR6$^{-/-}$ (B), or Cyt B-treated cells (C). Nucleated cells were marked with DAPI (blue). Original bars, 20 μm. Data are presented as the mean ± SD from three independent experiments. *, Statistically significant differences (P<0.05) between the macrophage groups treated with ML and control cells. +, Significant differences (P<0.05) between the WT and TLR macrophages and between macrophages pretreated or not with Cyt B.

LD formation. CMs were generated from peritoneal macrophages, treated or not with ML for 48 h, and then used to treat fresh cells for another 48 h. As shown in **Figure 6A**, incubation of macrophages with the CM from cells pretreated with ML resulted in significant LD induction relative to the CM from control cells (from a MFI value of 20.2±1.6 in control cells to 37.06±1.9 in cells treated with CM from ML-treated cells; P=0.002). This result confirms that soluble factors are secreted upon ML-macrophage interaction and that these factors are capable of inducing LD formation in uninfected cells.

Generation of the paracrine signal by ML-infected cells is dependent on cytoskeleton and TLR2

As cytoskeleton was shown previously to be essential in inducing LD formation in adjacent, uninfected cells, we next tested the capacity of the CM generated from ML-treated macrophages in the presence of Cyt B to induce LD forma-

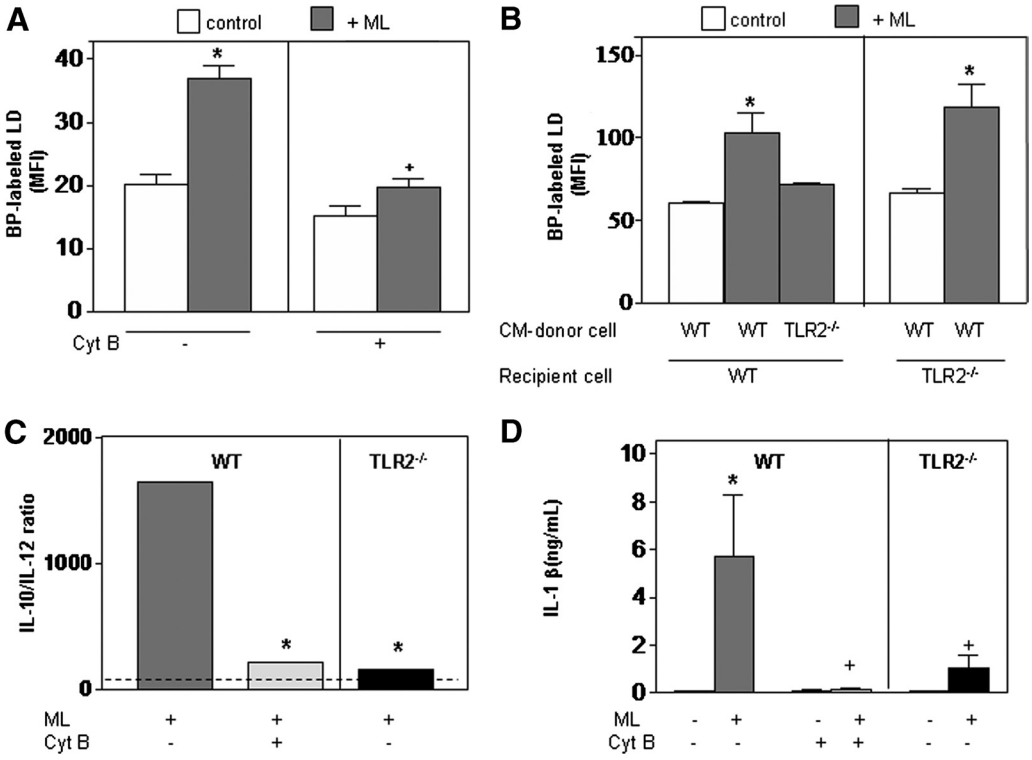

Figure 6. The generation of the paracrine signal in ML-infected cells is dependent on cytoskeleton and TLR2. (A) Murine macrophages were treated with CM from macrophages pretreated or not with ML, and LD formation was determined by flow cytometry. CM from ML-treated cells induced LD formation, in contrast to CM taken from control cells or cells pretreated with Cyt B prior to bacterial stimulation. (B) Effect of TLR on paracrine signaling induced by ML. WT or TLR2$^{-/-}$ macrophages were treated with CM from control WT cells, ML-treated WT cells (ML-WT), and ML-stimulated TLR2$^{-/-}$ cells (ML-TLR2$^{-/-}$). (C) Cytokine/chemokine levels were determined by multiplex assay in the CM following treatment with ML in macrophages pretreated with Cyt B or TLR2 depleted. IL-10/IL-12 ratios are expressed as percentage of the ratio observed in CM from control, ML-treated macrophages. (D) IL-1β production (ng mL^{-1}). Data are presented as the mean ± SE from three independent experiments. *, Statistically significant differences (P<0.05) between the macrophage groups treated with CM derived from ML-stimulated cells and cells treated with CM from control cells. +, Significant differences (P<0.05) between the macrophage groups treated with CM from ML-stimulated cells, pretreated or not with Cyt B.

tion. As expected, CM generated in the presence of the drug showed no effect on LD formation (Fig. 6A), suggesting that bacterial internalization is necessary to trigger cell-signaling events that would culminate in the release of LD-inducing molecules from ML-associated macrophages. As a whole, these results suggest that ML phagocytosis is essential to inducing the secretion of molecules that will act in a paracrine circuit to induce LD formation in adjacent cells.

The involvement of TLR2/TLR6 in the generation of this paracrine signaling was then investigated, as the absence of these receptors abrogated ML induction of LD formation completely in uninfected cells (Fig. 5, A and B). The TLR2/TLR6 heterodimer could be acting at the infected-cell level and participating in the signaling cascade necessary for the production of soluble factors, or the heretodimer may be acting as a pathogen-associated molecular pattern receptor on the membrane of uninfected cells in recognizing the bacterial molecules originating from cell-bearing bacteria. To discriminate between these two possibilities, we recovered CM from WT and TLR2$^{-/-}$ cells, pretreated or not with ML, and subsequently, tested the ability of CM to induce LDs in WT and TLR2$^{-/-}$ cells. When CM from WT ML-treated macrophages were used to stimulate TLR2$^{-/-}$ cells, a significant increase in LD formation was observed (from 60.3±0.6 LDs in control cells to 118.3±13.8 LDs in CM-treated cells; P=0.04), indicating that TLR2 is not required for macrophages to respond to LD-inducing molecules secreted by infected cells (Fig. 6B). However, CM obtained from ML-treated TLR2$^{-/-}$ cells failed to induce LD formation in cells expressing TLR2 (WT; from a MFI value of 66.8±2.2 in control cells to 71.4±1.3 in CM-treated cells; P=0.2), indicating that infected macrophages require TLR2 expression to generate the paracrine signal capable of inducing LD formation.

As reviewed extensively elsewhere, mycobacterial infection modulates the production by macrophages of a number of cytokines [54, 55]. In addition, it has been described previously that cytokines and chemokines may participate in the signaling that leads to LD formation [25, 47, 56, 57]. Thus, to investigate the potential involvement of cytokines/chemokines as LD-inducing molecules secreted by ML-infected macrophages, a multiplex cytokine analysis was performed comparing active (CM produced by ML-infected WT macrophages) with inactive (CM derived from ML-infected TLR2$^{-/-}$ and cells pretreated with Cyt B) LD-forming CM. The only cytokine that showed a significant decrease in CM Cyt B-treated and TLR2$^{-/-}$ ML-infected cells was derived from IL-1β (Fig. 6C). Interestingly, the IL-10/IL-12 ratio (taken as a reflection of an anti- vs. proinflammatory balance) followed a similar trend as IL-1β, with lower values in inactive CM, suggesting that this cytokine balance may favor LD formation in uninfected cells. In these assays, no correlating was observed with TNF-α and MCP-1 levels, corroborating previous results, in which these mediators were shown not to participate in LD induction promoted by BCG [28].

Correlation between LD formation and PGE_2 production in ML-treated mononuclear cells

We have demonstrated previously that LDs formed in response to BCG constitute sites for eicosanoid synthesis, leading to increased production of PGE_2 by infected macrophages [24, 28]. We then investigated whether regulation of LD numbers by ML also correlated with PG production.

Figure 7, A and **C**, shows that human and murine macrophages produced significantly increased levels of PGE_2 after 48 h of ML infection, coinciding with the time-point of the highest LD formation. Moreover, NS-398, a nonsteroidal, anti-inflammatory drug, shown previously to inhibit BCG-induced LD formation and PGE_2 production [28], was also able to abrogate ML-induced LD formation and PGE_2 production completely in murine macrophages (Fig. 7A). Lastly, treatment with Cyt B or the TLR2 knockout, conditions shown previously to reduce ML-induced LD formation, was also shown to inhibit PGE_2 production partially (Fig. 7, A and B). Thus, within the context of ML infection, these results indicate a correlation between LD formation and lipid mediator production.

DISCUSSION

Leprosy provides an excellent opportunity to investigate mechanisms of innate and adaptive immunity in humans. As LDs are emerging as key organelles involved in the innate immune response during bacterial infection [24, 28, 58], in the present study, we investigated the generation of these organelles during ML infection. The data herein presented show that LD formation is induced during ML infection, based on the following findings: the identification of LDs inside macrophages present in the dermal lesions of LL patients via immunodetection of ADRP; and the rapid accumulation of these organelles in ML-treated human monocytes and murine macrophages and subsequent to in vivo i.pl. infection.

Our results indicating the accumulation of LDs enriched in CHO and CHOE in LL lesions are consistent with previous reports demonstrating that several host genes involved in lipid metabolism, including ADRP and CD36, a selective lipid receptor, are up-regulated in LL lesions and that at least part of the lipids accumulated in macrophages are host-derived, oxidized phospholipids [23, 59, 60]. In further support of these data, another recent report has attested to the localization of ADRP in phagosomes containing ML in LL lesions and the capacity of ML to induce the expression of this protein in human phagocytes [61].

In vivo and in vitro assays showed that ML-induced LD formation was independent of bacterial viability, suggesting that bacteria may play a passive role in LD formation and that the host cell might be the active player in this process. This observation is consistent with our previous data showing that dead BCG (ref. [28] and K. A. Mattos, unpublished results) and mannose-capped lipoarabinomannan purified from BCG, a cell-wall constituent also present in ML, are able to induce LD in macrophages [28]. Another interesting observation was the capacity of ML to induce LD accumulation in bacterium-associated cells and in those cells with no bacterium. It was then possible to investigate the mechanisms of LD induction by ML

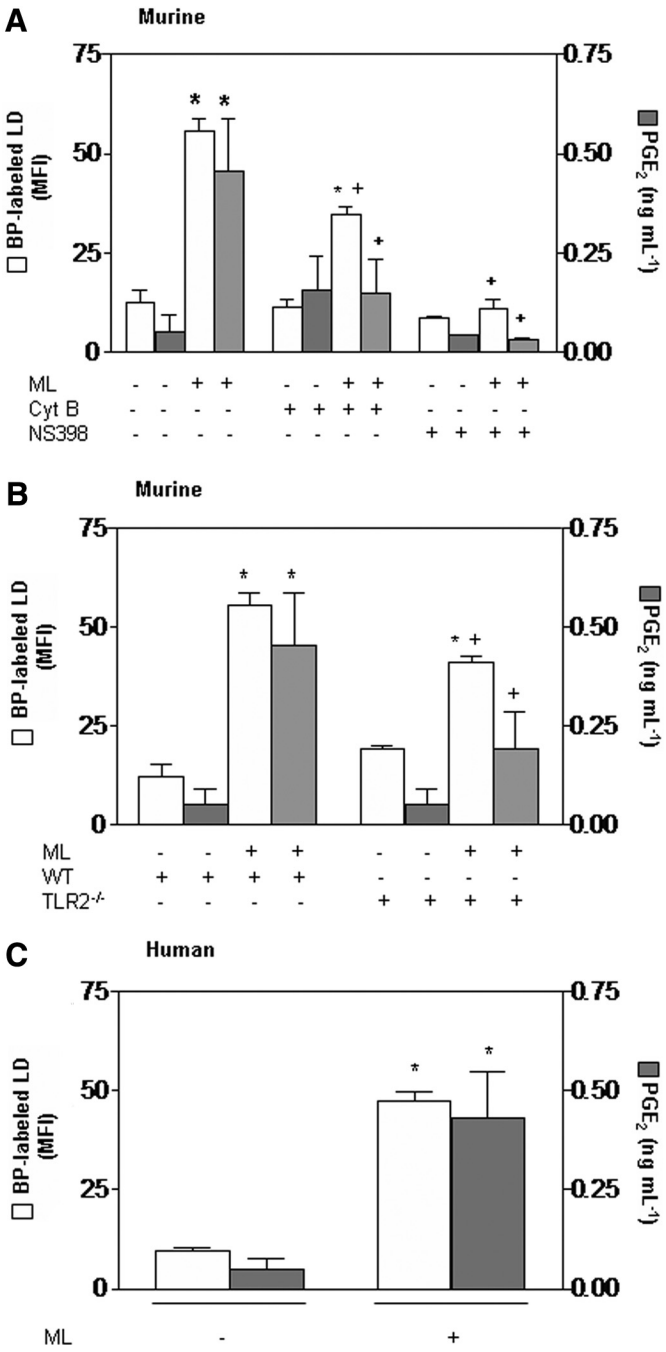

Figure 7. Correlation of PGE_2 production and LD formation in response to ML. The levels of LDs and PGE_2 were analyzed in murine peritoneal macrophages: (A) pretreated with Cyt B, NS-398 (1 μM), or an equal volume of vehicle or (B) WT peritoneal macrophages and $TLR2^{-/-}$ macrophages stimulated with ML or not. (C) LDs and PGE_2 production were analyzed in monocytes from human peripheral blood in response to ML. Induction of PGE_2 was measured by EIA in culture supernatants, and LD levels were determined by flow cytometry of BP-labeled cells. Data are representative of four experiments with SD. *, Statistically significant differences ($P<0.05$) between macrophage groups treated with ML and untreated, control cells. +, Significant differences ($P<0.05$) between different ML-treated cell groups.

in both cell populations. The TLR2 depletion did show a strong inhibitory effect on LD formation in cells with no bacteria, having less of an impact in infected cells. This preferential effect of the TLR2 absence on cells not bearing bacteria is explained by its effect on the generation of the paracine signal. This conclusion is supported by the inability of the CM from TLR2$^{-/-}$ cells, in contrast to the CM originating from WT cells, to induce LD formation in uninfected macrophages. Moreover, the generation of the paracrine signal was also abrogated by Cyt B, suggesting that TLR2 internalization is essential for this process to occur. This hypothesis is supported by a recent report showing that TLR2 is internalized and localized on the membrane of phagosomes that contain ML [62].

To define potential candidates involved in the paracrine signaling, we assessed the levels of some cytokines/chemokines in CM from ML-infected macrophages. Interestingly, a positive correlation of the IL-10/IL-12 ratio with the capacity of CM to induce LD formation in uninfected cells was found. This observation correlates with the characteristic pattern of IL-10 predominance in LL lesions [63]. Moreover, IL-10 has been implicated recently in foam cell formation in atherosclerosis disease, reinforcing the potential participation in vivo of the cytokine balance in the generation and maintenance of abundant LDs in LL lesions. Additionally, significantly higher levels of IL-1β were found in CM capable of inducing LDs, suggesting a potential contribution of this cytokine in promoting intracellular lipid storage, as has been pointed out recently [48]. A more detailed investigation of the soluble factors responsible for the paracrine LD-forming signaling produced by ML-infected macrophages is under course.

As a potential cofactor for LD induction in ML infection, the possible role of TLR6 was then studied, as it has been shown that the latter heterodimerizes with TLR2 [10, 64, 65]. The TLR6 deletion alone showed an even higher impact than the TLR2 deletion on ML-induced LD formation in infected macrophages (Fig. 5, A and B). These results are in agreement with the expression profile of TLRs in leprosy lesions reported recently. Krutzik et al. [66] showed that TLR2 was expressed more strongly in TT lesions as opposed to LL lesions. On the other hand, Bleharski et al. [67], although analyzing gene expression profiles in skin lesions of LL and TT leprosy patients, demonstrated that TLR6 was up-regulated significantly in LL lesions. It may, therefore, be speculated that these data are in correlation with the essential role of TLR6 in ML-induced LD formation, herein demonstrated along with the capacity of LL macrophages to accumulate LDs, in contrast to the reduced presence of these organelles in macrophages present in TT lesions [61].

Our data also indicate that ML-induced LD formation in infected macrophages depends on additional receptors associated with the innate immune response besides TLR2 and -6. Accordingly, TLR2-dependent signaling was shown to be essential, although not sufficient, to the LD biogenesis induced by BCG infection [28]. However, nonpathogenic *M. smegmatis*, which also triggers TLR2-dependent cytokine production, failed to induce LD formation, suggesting that cofactors may be involved in the mechanisms involved in LD formation in pathogenic mycobacteria [28, 68]. PGE_2 is a potent immune modulator that down-regulates Th1 responses and bactericidal activity toward intracellular organisms [69, 70], and LDs are intracellular sites for eicosanoid production. Our data suggest that ML-induced LDs also constitute intracellular sites for eicosanoid synthesis, which is sustained by the observation of a significant correlation between LD formation and PGE_2 generation by phagocytes treated with the bacteria. These data are in accordance with published reports, indicating the elevated production of PGE_2 by human monocytes from LL patients, and in the athymic mouse leprosy model [71–73]. Moreover, the expression of the inducible enzyme COX-2 was shown to be significantly higher in biopsies of LL than TT leprosy patients [19]. In reality, the high concentrations of PGE_2 produced by COX-2-positive macrophages in LL were able to inhibit Th1 cytokine production, most probably contributing to T cell anergy at this disease pole [19]. Thus, enhanced levels of macrophage-generated PGE_2 induced by ML could act as an endogenous-negative modulator of the immune response occurring in the microenvironment of the LL lesion.

In conclusion, it could be speculated that the lipid storage phenomenon observed in LL may play a critical role in leprosy pathogenesis by facilitating bacterial persistence in the host in at least two different ways. First, as described above, the Virchow cells, present abundantly in LL lesions, are probably catalytically active sites of PGE_2 synthesis, thereby favoring the inhibition of macrophage bactericidal activities and the down-regulation of the immune response. Second, it has been demonstrated recently that lipids constitute an important nutritional source for mycobacterial persistence in the host [74, 75]. Indeed, in a recent analysis of the ML proteome, we pointed out the presence of the fatty acid β-oxidation and glyoxylate cycle enzymes, reinforcing the idea that fatty acids, rather than carbohydrates, are more likely to be the dominant carbon substrate used by ML during infection [76].

AUTHORSHIP

K. A. M., H. D., P. T. B., and M. C. V. P. designed the study; K. A. M., H. D., L. S. R., and V. C. G. O. performed experiments; K. A. M., H. D., and L. S. R. collected and analyzed data; E. N. S. provided leprosy biopsies; H. D. and P. T. B. provided reagents and mice; K. A. M., P. T. B., and M. C. V. P. wrote the manuscript; G. M. P. performed flow cytometry analysis; G. C. A. performed lipid analysis; M. C. V. P., P. T. B., and E. N. S. gave technical support and conceptual advice. All authors discussed the results and implications and commented on the manuscript at all stages.

ACKNOWLEDGMENTS

This work was funded by CNPq/Brazil (individual grants to M. C. V. P. and P. T. B.) and PAPES-FIOCRUZ and FAPERJ (to P. T. B.). K. A. M. and H. D. were recipients of a fellowship from FAPERJ. L. S. R. and V. G. C. O. were recipients of a fellowship from CNPq. The authors are grateful to Dr. James Krahenbuhl for providing the ML, Pedro Paulo Manso for his assistance with the confocal images, and Judy Grevan for editing the text.

REFERENCES

1. World Health Organization WHO Report. (2008) *Leprosy Today*, http://www.who.int/lep/en/.
2. Hastings, R. C., Gillis, T. P., Krahenbuhl, J. L., Franzblau, S. G. (1988) Leprosy. *Clin. Microbiol. Rev.* **1,** 330–348.
3. Scollard, D. M., Adams, L. B., Gillis, T. P., Krahenbuhl, J. L., Truman, R. W., Williams, D. L. (2006) The continuing challenges of leprosy. *Clin. Microbiol. Rev.* **19,** 338–381.
4. Barker, L. P. (2006) *Mycobacterium leprae* interactions with the host cell: recent advances. *Indian J. Med. Res.* **123,** 748–759.
5. Modlin, R. L. (1994) Th1–Th2 paradigm: insights from leprosy. *J. Invest. Dermatol.* **102,** 828–832.
6. Parkash, O. (2009) Classification of leprosy into multibacillary and paucibacillary groups: analysis. *FEMS Immunol. Med. Microbiol.* **55,** 1–5.
7. Ismail, N., Olano, J. P., Feng, H. M., Walker, D. H. (2002) Current status of immune mechanisms of killing of intracellular microorganisms. *FEMS Microbiol. Lett.* **207,** 111–120.
8. Appelberg, R. (2006) Macrophage nutriprive antimicrobial mechanisms. *J. Leukoc. Biol.* **79,** 1117–1128.
9. Takeuchi, O., Kawai, T., Muhlradt, P. F., Morr, M., Radolf, J. D., Zychlinsky, A., Takeda, K., Akira, S. (2001) Discrimination of bacterial lipoproteins by Toll-like receptor 6. *Int. Immunol.* **13,** 933–940.
10. Takeuchi, O., Sato, S., Horiuchi, T., Hoshino, K., Takeda, K., Dong, Z., Modlin, R. L., Akira, S. (2002) Cutting edge: role of Toll-like receptor 1 in mediating immune response to microbial lipoproteins. *J. Immunol.* **169,** 10–14.
11. West, A. P., Koblansky, A. A., Ghosh, S. (2006) Recognition and signaling by Toll-like receptors. *Annu. Rev. Cell Dev. Biol.* **22,** 409–437.
12. Zähringer, U., Lindner, B., Inamura, S., Heine, H., Alexander, C. (2008) TLR2—promiscuous or specific? A critical re-evaluation of a receptor expressing apparent broad specificity. *Immunobiology* **213,** 205–224.
13. McCoy, C. E., O'Neill, L. A. J. (2008) The role of Toll-like receptors in macrophages. *Front. Biosci.* **13,** 62–70.
14. Pieters, J. (2001) Entry and survival of pathogenic mycobacteria in macrophages. *Microbes Infect.* **3,** 249–255.
15. Miyake, K. (2007) Innate immune sensing of pathogens and danger signals by cell surface Toll-like receptors. *Semin. Immunol.* **19,** 3–10.
16. De Chastellier, C. (2009) The many niches and strategies used by pathogenic mycobacteria for survival within host macrophages. *Immunobiology*, Epub ahead of print.
17. Via, L. E., Deretic, D., Ulmer, R. J., Hibler, N. S., Huber, L. A., Deretic, V. (1997) Arrest of mycobacterial phagosome maturation is caused by a block in vesicle fusion between stages controlled by rab5 and rab7. *J. Biol. Chem.* **272,** 13326–13331.
18. Koul, A., Herget, T., Klebl, B., Ullrich, A. (2004) Interplay between mycobacteria and host signaling pathways. *Nat. Rev. Microbiol.* **2,** 189–202.
19. Kiszewski, A. E. C., Becerril, E., Baquera, J., Ruiz-Maldonado, R., Hernandez Pando, R. (2003) Expression of cyclooxygenase type 2 in lepromatous and tuberculoid leprosy lesions. *Br. J. Dermatol.* **148,** 795–798.
20. Ridley, D. S. (1974) Histological classification and the immunological spectrum of leprosy. *Bull. World Health Organ.* **51,** 451–465.
21. Virchow, R. (1863) *Die krankhaften Geschwülste.* Berlin, Germany, August Hirschwald, 208.
22. Sakurai, I., Skinsnes, O. K. (1970) Lipids in leprosy 2. Histochemistry of lipids in human leprosy. *Int. J. Lepr. Other Mycobact. Dis.* **38,** 389–403.
23. Cruz, D., Watson, A. D., Miller, C. S., Montoya, D., Ochoa, M. T., Sieling, P. A., Gutierrez, M. A., Navab, M., Reddy, S. T., Witztum, J. L., Fogelman, A. M., Rea, T. H., Eisenberg, D., Berliner, J., Modlin, R. L. (2008) Host-derived oxidized phospholipids and HDL regulate innate immunity in human leprosy. *J. Clin. Invest.* **118,** 2917–2928.
24. D'Avila, H., Maya-Monteiro, C. M., Bozza, P. T. (2008) LBs in innate immune response to bacterial and parasite infections. *Int. Immunopharmacol.* **8,** 1308–1315.
25. Bozza, P. T., Magalhães, K. G., Weller, P. F. (2009) Leukocyte LBs—biogenesis and functions in inflammation. *Biochim. Biophys. Acta* **1791,** 540–551.
26. Bozza, P. T., Payne, J. L., Morham, S. G., Langenbach, R., Smithies, O., Weller, P. F. (1996) Leukocyte LB formation and eicosanoid generation: cyclooxygenase-independent inhibition by aspirin. *Proc. Natl. Acad. Sci. USA* **93,** 11091–11096.
27. Bozza, P. T., Bandeira-Melo, C. (2005) Mechanisms of leukocyte LB formation and function in inflammation. *Mem. Inst. Oswaldo Cruz* **100,** 113–120.
28. D'Avila, H., Melo, R. C. N., Parreira, G. G., Werneck-Barroso, E., Castro-Faria-Neto, H. C., Bozza, P. T. (2006) *Mycobacterium bovis* bacillus Calmette-Guérin induces TLR2-mediated formation of LBs: intracellular domains for eicosanoid synthesis in vivo. *J. Immunol.* **176,** 3087–3097.
29. Murphy, D. J. (2001) The biogenesis and functions of lipid bodies in animals, plants and microorganisms. *Prog. Lipid Res.* **40,** 325–438.
30. Bartz, R., Li, W. H., Venables, B., Zehmer, J. K., Roth, M. R., Welti, R., Anderson, R. G., Liu, P., Chapman, K. D. (2007) Lipidomics reveals that adiposomes store ether lipids and mediate phospholipid traffic. *J. Lipid Res.* **48,** 837–847.
31. Chang, B. H. J., Chan, L. (2007) Regulation of triglyceride metabolism. III. Emerging role of lipid droplet protein ADFP in health and disease. *Am. J. Physiol. Gastrointest. Liver Physiol.* **292,** G1465–G1468.
32. Liu, P., Bartz, R., Zehmer, J. K., Ying, Y. S., Zhu, M., Serrero, G., Anderson, R. G. (2007) Rab-regulated interaction of early endosomes with lipid droplets. *Biochim. Biophys. Acta* **1773,** 784–793.
33. Wan, H. C., Mello, R. C. N., Jin, Z., Dvorak, A. M., Weller, P. F. (2007) Roles and origins of leukocyte LBs: proteomic and ultrastructural studies. *FASEB J.* **21,** 167–178.
34. Yu, W., Bozza, P. T., Tzizik, D. M., Gray, J. P., Cassara, J., Dvorak, A. M., Weller, P. F. (1998) Co-compartmentalization of MAP kinases and cytosolic phospholipase A2 at cytoplasmic arachidonate-rich LBs. *Am. J. Pathol.* **152,** 759–769.
35. Yu, W., Cassara, J., Weller, P. F. (2000) Phosphatidylinositide 3-kinase localizes to cytoplasmic LBs in human polymorphonuclear leukocytes and other myeloid-derived cells. *Blood* **95,** 1078–1085.
36. Bozza, P. T., Melo, R. C., Bandeira-Melo, C. (2007) Leukocyte lipid bodies regulation and function: contribution to allergy and host defense. *Pharmacol. Ther.* **113,** 30–49.
37. Adams, L. B., Soileau, N. A., Battista, J. R., Krahenbuhl, J. L. (2000) Inhibition of metabolism and growth of *Mycobacterium leprae* by γ irradiation. *Int. J. Lepr. Other Mycobact. Dis.* **68,** 1–10.
38. Smits, E., Burvenich, C., Heyneman, R. (1997) Simultaneous flow cytometric measurement of phagocytotic and oxidative burst activity of polymorphonuclear leukocytes in whole bovine blood. *Vet. Immunol. Immunopathol.* **56,** 259–269.
39. Haworth, R., Gordon, S. (1998) Isolation and measuring the function of professional phagocytes: murine macrophages. In *Methods in Microbiology* (S. Kaufmann, D. Kabelitz, eds.), London, UK, Academic, 287–311.
40. Pagano, R. E., Sleight, R. G. (1985) Defining lipid transport pathways in animal cells. *Science* **229,** 1051–1057.
41. Bozza, P. T., Yu, W., Penrose, J. F., Morgan, E. S., Dvorak, A. M., Weller, P. F. (1997) Eosinophil LBs: specific, inducible intracellular sites for enhanced eicosanoid formation. *J. Exp. Med.* **186,** 909–920.
42. Wade, H. W. (1962) Zenker vs formalin fixation for the histopathology of leprosy tissues and other desirable features of technique. *Int. J. Lepr.* **30,** 477–488.
43. Bligh, E. G., Dyer, W. J. (1959) A rapid method for total lipid extraction and purification. *Can. J. Biochem. Physiol.* **37,** 911–917.
44. Folch, J., Lees, M., Stanley, G. H. S. (1957) A simple method for the isolation and purification of total lipides from animal tissues. *J. Biol. Chem.* **226,** 497–509.
45. Ruiz, J. I., Ochoa, B. (1997) Quantification in the subnanomolar range of phospholipids and neutral lipids by monodimensional thin-layer chromatography and image analysis. *J. Lipid Res.* **38,** 1482–1489.
46. Mahlberg, F. H., Glick, J. M., Jerome, W. G., Rothblat, G. H. (1990) Metabolism of cholesteryl ester lipid droplets in a J774 macrophage foam cell model. *Biochim. Biophys. Acta* **1045,** 291–298.
47. Van Meer, G. (2001) Caveolin, cholesterol, and lipid droplets? *J. Cell Biol.* **152,** F29–F34.
48. Persson, J., Nilsson, J., Lindholm, M. W. (2008) Interleukin-1β and tumor necrosis factor-α impede neutral lipid turnover in macrophage-derived foam cells. *BMC Immunol.* **25,** 70.
49. Heldwein, K. A., Fenton, M. J. (2002) The role of Toll-like receptors in immunity against mycobacterial infection. *Microbes Infect.* **4,** 937–944.
50. Poltorak, A., He, X., Smirnova, I., Liu, M-Y., Huffel, C. V., Du, X., Birdwell, D., Alejos, E., Silva, M., Galanos, C., Freudenberg, M., Ricciardi-Castagnoli, P., Layton, B., Beutler, B. (1998) Defective LPS signaling in C3H/HeJ and C57BL/10ScCr mice: mutations in Tlr4 gene. *Science* **282,** 2085–2088.
51. Underhill, D. M. (2003) Toll-like receptors: networking for success. *Eur. J. Immunol.* **33,** 1767–1775.
52. McInturff, J. E., Modlin, R. L., Kim, J. (2005) The role of Toll-like receptors in the pathogenesis and treatment of dermatological disease. *J. Invest. Dermatol.* **125,** 1–8.
53. Wetzler, L. M. (2003) The role of Toll-like receptor 2 in microbial disease and immunity. *Vaccine* **21** (Suppl. 2), S55–S60.
54. Moreno, C., Rees, A. J. (1993) Striking the right balance; the role of cytokines in mycobacterial disease. *Clin. Exp. Immunol.* **94,** 1–3.
55. Champsi, J. H., Bermudez, L. E., Young, L. S. (1994) The role of cytokines in mycobacterial infection. *Biotherapy* **7,** 187–193.
56. Halvorsen, B., Wæhre, T., Scholz, H., Clausen, O. P., von der Thüsen, J. H., Müller, F., Heimli, H., Tonstad, S., Hall, C., Frøland, S. S., Biessen, E. A., Damås, J. K., Aukrust, P. (2005) Interleukin-10 enhances the oxidized LDL-induced foam cell formation of macrophages by antiapoptotic mechanisms. *J. Lipid Res.* **46,** 211–219.
57. Pacheco, P., Vieira-de-Abreu, A., Gomes, R. N., Barbosa-Lima, G., Wermelinger, L. B., Maya-Monteiro, C. M., Silva, A. R., Bozza, M. T., Castro-Faria-Neto, H. C., Bandeira-Melo, C., Bozza, P. T. (2007) Monocyte chemoattractant protein-1/CC chemokine ligand 2 controls microtubule-driven biogenesis and leukotriene B_4-synthesizing function of macrophage lipid bodies elicited by innate immune response. *J. Immunol.* **179,** 8500–8508.
58. Cao, F., Castrillo, A., Tontonoz, P., Re, F., Byrne, G. I. (2007) *Chlamydia pneumoniae*-induced macrophage foam cell formation is mediated by Toll-like receptor 2. *Infect. Immun.* **75,** 753–759.

59. Kurup, G., Mahadevan, P. R. (1982) Cholesterol metobolism of macrophages in relation to the presence of *Mycobacterium leprae*. *J. Biosci.* **4,** 307–316.
60. Vithala, L., Talati, S., Mahadevan, P. R. (1983) An in vitro system to study drug sensitivity of *Mycobacterium leprae* using infected human tissue. *J. Biosci.* **5,** 235–241.
61. Tanigawa, K., Suzuki, K., Nakamura, K., Akama, T., Kawashima, A., Wu, H., Hayashi, M., Takahashi, S., Ikuyama, S., Ito, T., Ishii, N. (2008) Expression of adipose differentiation-related protein (ADRP) and perilipin in macrophages infected with *Mycobacterium leprae*. *FEMS Microbiol. Lett.* **289,** 72–79.
62. Suzuki, K., Takeshita, F., Nakata, N., Ishii, N., Makino, M. (2006) Localization of CORO1A in the macrophages containing *Mycobacterium leprae*. *Acta Histochem. Cytochem.* **39,** 107–112.
63. Yamamura, M., Uyemura, K., Deans, R. J., Weinberg, K., Rea, T. H., Bloom, B. R., Modlin, R. L. (1991) Defining protective responses to pathogens: cytokine profiles in leprosy lesions. *Science* **254,** 277–279.
64. Ozinsky, A., Underhill, D. M., Fontenot, J. D., Hajjar, A. M., Smith, K. D., Wilson, C. B., Schroeder, L., Aderem, A. (2000) The repertoire for pattern recognition of pathogens by the innate immune system is defined by cooperation between Toll-like receptors. *Proc. Natl. Acad. Sci. USA* **97,** 13766–13771.
65. Takeda, K., Akira, S. (2001) Roles of Toll-like receptors in innate immune responses. *Genes Cells* **6,** 733–742.
66. Krutzik, S. R., Ochoa, M. T., Sieling, P. A., Uematsu, S., Ng, Y. W., Legaspi, A., Liu, P. T., Cole, S. T., Godowski, P. J., Maeda, Y., Sarno, E. N., Norgard, M. V., Brennan, P. J., Akira, S., Rea, T. H., Modlin, R. L. (2003) Activation and regulation of Toll-like receptors 2 and 1 in human leprosy. *Nat. Med.* **9,** 525–532.
67. Bleharski, J. R., Li, H., Meinken, C., Graeber, T. G., Ochoa, M. T., Yamamura, M., Burdick, A., Sarno, E. N., Wagner, M., Röllinghoff, M., Rea, T. H., Colonna, M., Stenger, S., Bloom, B. R., Eisenberg, D., Modlin, R. L. (2003) Use of genetic profiling in leprosy to discriminate clinical forms of the disease. *Science* **301,** 1527–1530.
68. Almeida, P. E., Silva, A. R., Maya-Monteiro, C. M., Törõcsik, D., D'Avila, H., Dezsõ, B., Magalhães, K. G., Castro-Faria-Neto, H. C., Nagy, L., Bozza, P. T. (2009) *Mycobacterium bovis* bacillus Calmette-Guérin infection induces TLR2-dependent peroxisome proliferator-activated receptor γ expression and activation: functions in inflammation, lipid metabolism, and pathogenesis. *J. Immunol.* **183,** 1337–1345.
69. Van der Pouw Kraan, T. C., Boeije, L. C., Smeenk, R. J., Wijdenes, J., Aarden, L. A. (1995) Prostaglandin-E_2 is a potent inhibitor of human interleukin 12 production. *J. Exp. Med.* **181,** 775–779.
70. Harbrecht, B. G., Kim, Y. M., Wirant, E. A., Simmons, R. L., Billiar, T. R. (1997) Timing of prostaglandin exposure is critical for the inhibition of LPS- or IFN-γ-induced macrophage NO synthesis by PGE_2. *J. Leukoc. Biol.* **61,** 712–720.
71. Misra, N., Selvakumar, M., Singh, S., Bharadwaj, M., Ramesh, V., Misra, R. S., Nath, I. (1995) Monocyte derived IL 10 and PGE_2 are associated with the absence of Th 1 cells and in vitro T cell suppression in lepromatous leprosy. *Immunol. Lett.* **48,** 123–128.
72. Montreewasuwat, N., Curtis, J., Turk, J. L. (1987) Interleukin 1 and prostaglandin production by cells of the mononuclear phagocyte system isolated from mycobacterial granulomas. *Cell. Immunol.* **104,** 12–23.
73. Adams, L. B., Gillis, T. P., Hwang, D. H., Krahenbuhl, J. L. (1997) Effects of essential fatty acid deficiency on prostaglandin E2 production and cell-mediated immunity in a mouse model of leprosy. *Infect. Immun.* **65,** 1152–1157.
74. Ehrt, S., Schnappinger, D. (2007) *Mycobacterium tuberculosis* virulence: lipids inside and out. *Nat. Med.* **13,** 284–285.
75. Pandey, A. K., Sassetti, C. M. (2008) Mycobacterial persistence requires the utilization of host cholesterol. *Proc. Natl. Acad. Sci. USA* **105,** 4376–4380.
76. Marques, M. A., Neves-Ferreira, A. G., da Silveira, E. K., Valente, R. H., Chapeaurouge, A., Perales, J., da Silva, B. R., Dobos, K. M., Spencer, J. S., Brennan, P. J., Pessolani, M. C. (2008) Deciphering the proteomic profile of *Mycobacterium leprae* cell envelope. *Proteomics* **8,** 2477–2491.

KEY WORDS:
macrophage · prostaglandin E_2 · foamy cell · lepromatous leprosy · mycobacteria

Cellular Microbiology (2010) doi:10.1111/j.1462-5822.2010.01533.x

Modulation of lipid droplets by *Mycobacterium leprae* in Schwann cells: a putative mechanism for host lipid acquisition and bacterial survival in phagosomes

Katherine A. Mattos,[1] Flavio A. Lara,[1] Viviane G. C. Oliveira,[1] Luciana S. Rodrigues,[1] Heloisa D'Avila,[2] Rossana C. N. Melo,[2] Pedro P. A. Manso,[3] Euzenir N. Sarno,[4] Patricia T. Bozza[5†] and Maria Cristina V. Pessolani[1*†]

[1]*Laboratório de Microbiologia Celular, Instituto Oswaldo Cruz, Fundação Oswaldo Cruz, Rio de Janeiro 21045-900, RJ, Brazil.*

[2]*Laboratório de Biologia Celular, Departamento de Biologia, Universidade Federal de Juiz de Fora, Juiz de Fora 36036-330, MG, Brazil.*

[3]*Laboratório de Patologia, Instituto Oswaldo Cruz, Fundação Oswaldo Cruz, Rio de Janeiro 21045-900, RJ, Brazil.*

[4]*Laboratório de Hanseníase, Instituto Oswaldo Cruz, Fundação Oswaldo Cruz, Rio de Janeiro 21045-900, RJ, Brazil.*

[5]*Laboratório de Imunofarmacologia, Instituto Oswaldo Cruz, Fundação Oswaldo Cruz, Rio de Janeiro 21045-900, RJ, Brazil.*

Summary

The predilection of *Mycobacterium leprae* (ML) for Schwann cells (SCs) leads to peripheral neuropathy, a major concern in leprosy. Highly infected SCs in lepromatous leprosy nerves show a foamy, lipid-laden appearance; but the origin and nature of these lipids, as well as their role in leprosy, have remained unclear. The data presented show that ML has a pronounced effect on host-cell lipid homeostasis through regulation of lipid droplet (lipid bodies, LD) biogenesis and intracellular distribution. Electron microscopy and immunohistochemical analysis of lepromatous leprosy nerves for adipose differentiation-related protein expression, a classical LD marker, revealed accumulating LDs in close association to ML in infected SCs. The capacity of ML to induce LD formation was confirmed in *in vitro* studies with human SCs. Moreover, via confocal and live-cell analysis, it was found that LDs are promptly recruited to bacterial phagosomes and that this process depends on cytoskeletal reorganization and PI3K signalling. ML-induced LD biogenesis and recruitment were found to be independent of TLR2 bacterial sensing. Notably, LD recruitment impairment by cytoskeleton drugs decreased intracellular bacterial survival. Altogether, our data revealed SC lipid accumulation in ML-containing phagosomes, which may represent a fundamental aspect of bacterial pathogenesis in the nerve.

Received 22 July, 2010; revised 23 September, 2010; accepted 24 September, 2010. For correspondence. *E-mail cpessola@ioc.fiocruz.br; Tel. (+55) 21 2598 4467; Fax (+55) 21 22709997.
†These senior authors contributed equally to this work.

Introduction

Leprosy remains an important cause of morbidity in developing countries with the detection of approximately 250 000 new cases per annum (WHO, 2010). Also known as Hansen's disease, leprosy manifests as a spectrum of clinical forms in correlation with the nature and magnitude of the innate and adaptive immune response generated during *Mycobacterium leprae* (ML) infection.

At one extreme, individuals with tuberculoid leprosy have few lesions, presenting a contained, self-limited infection in which scarce bacilli are detected. At the other end, lepromatous leprosy (LL) is a progressive and disseminated disease characterized by extensive bacterial multiplication within host cells (Scollard *et al*., 2006). Preferentially found inside Schwann cells (SCs) and macrophages (Virchow, 1863; Job, 1970; Scollard *et al*., 2006), ML, the obligate intracellular causative agent of leprosy, displays a strong tropism for peripheral nerves. ML nerve-fibre colonization results in loss of sensation, an early symptom of leprosy, which, untreated, is capable of evolving into progressive nerve damage and neuropathy. Multidrug therapy treats the infection but is unable to either arrest or prevent the nerve damage responsible for disfigurement and disabilities. In-depth investigation of ML–nerve interaction aiming to develop new strategies for prevention and treatment of leprosy-related nerve impairments is therefore of great importance.

An important aspect deserving of attention as it is known to play an important role in host–pathogen interactions is lipid homeostasis (Wenk, 2006; van der Meer-Janssen

et al., 2010). This also seems to occur in leprosy, characterized by collections of heavily infected macrophages with a typically 'foamy' appearance (also referred to as Virchow or Lepra cells) in LL dermal lesions (Virchow, 1863; Scollard *et al*., 2006). Close examination of these cells reveals that ML resides and replicates within enlarged, lipid-filled phagosomes (Chatterjee *et al*., 1959), suggesting an important lipid metabolism alteration during infection. Although it was initially believed that these lipids were ML-derived (such as phthiocerol dimycocerosate/dimycocerosate and phenolic glycolipid-1) (Sakurai and Skinsnes, 1970; Kaplan *et al*., 1983; Brennan, 1984), a recent report has indicated the accumulation of host-derived oxidized phospholipids in these cells (Cruz *et al*., 2008).

It has been shown as well that Virchow cells are highly positive for adipose differentiation-related protein (ADRP), a classical lipid droplet (LD) marker, indicating that their foamy appearance is at least in part derived from the accumulation of LDs (Tanigawa *et al*., 2008; Mattos *et al*., 2010) in infected cells. Moreover, ADRP has been found to be induced by ML infection and to localize to ML-containing phagosomes in macrophage cells, indicative of a close association between LDs and the pathogen-containing vacuole (Tanigawa *et al*., 2008).

Also termed lipid bodies or adiposomes, LDs are dynamic lipid storage organelles found in all cell types. One suggested major LD function is the distribution of neutral lipids and phospholipids to various membrane-bound organelles within the cell (Zehmer *et al*., 2009). Moreover, contemporary evidence points to LDs as inflammatory organelles involved in the synthesis and secretion of inflammatory mediators (Bozza *et al*., 2009; Bozza and Viola, 2010).

In LL nerve biopsies, highly infected SCs also demonstrate a foamy, lipid-laden aspect, similar to that of the Virchow cells found in dermal lesions (Job, 1970). The present study investigated the origin of these lipid deposits in ML-infected SCs and the mechanism involved in their accumulation in bacterial-containing vesicles. Our findings point to a central role for LDs as being responsible for originating foamy degeneration of ML-infected SCs in LL nerves, suggesting that LD recruitment represents a mechanism by which host-cell lipids are delivered to ML in the phagosome.

Results

LDs localize to ML in foamy SCs in nerve biopsies of LL patients

In LL nerves, highly infected SCs display a foamy appearance, a sign of lipid accumulation by these cells (Fig. 1A). To investigate whether the foamy aspect of SCs results from LD accumulation, cross sections of the nerve biopsies of four LL patients were immune stained with antibodies that specifically recognize ADRP, a LD marker, and S100, a SC marker. ML was identified by an antibody capable of recognizing whole bacterium or lipoarabinomannan (LAM), a component of the mycobacterial envelope. Figure S1A shows intense ML-immune reactive SCs, indicative of the presence of bacteria in these cells. The nerve specimens also exhibited positive staining for ADRP-labelled LDs, and immunofluorescence staining for both S100 and ADRP demonstrated that the ADRP-reactive cells were SCs (Figs 1B and S1B).

Alternatively, tissue sections were double immunostained for ADRP and ML (Figs 1C–G and S1C). Worthy of note was the close association between LDs and ML in infected SCs (Fig. 1C). Three-dimensional (3D) reconstruction images showed well-circumscribed, isolated bacilli and differentiated bacterial *globis* surrounded by ADRP (Figs 1D and S1C). In fact, most bacteria were found in association with LDs (Fig. S1C). Finally, to highlight the intimate contact between LDs and ML, their colocalization is shown in detail by 2D images with orthogonal analysis (Fig. 1E–G).

The ultrastructural features of infected SCs were studied by transmission electron microscopy (TEM). These cells showed a large number of cytoplasmic membrane-bound phagosomes with varying sizes containing bacteria (Fig. 2A and B). Phagosomes with a high number of bacteria were observed in cell sections (Fig. 2B). TEM revealed the presence of typical LDs in close association to bacterium-containing phagosomes (Fig. 2A, arrowheads). TEM quantitative analyses were performed on 72 randomly taken electron micrographs, resulting in, per SC section, 3.4 ± 0.6 (mean $\pm$ SEM) phagosomes, 65% of which showed bacteria enmeshed in a LD content.

ML induces LD formation in SCs

It has been recently shown that ML induces LD biogenesis in macrophages (Mattos *et al*., 2010). To determine if ML evokes a similar effect on SCs, human SCs were infected *in vitro* and LD biogenesis was analysed after 48 h. First, cells were incubated with BODIPY 493/503, a lipophilic fluorescent dye, and LD formation was observed by fluorescence microscopy. ML-infected cultures displayed more intense fluorescence staining in comparison with the controls (Fig. 3A), suggesting increased LD production. LD formation was determined by enumerating these organelles after staining with osmium tetroxide (Fig. 3B). The number of LDs in ML-infected cells was approximately twofold as compared with non-infected cells. The total area of the cell cytoplasm occupied by LDs was then

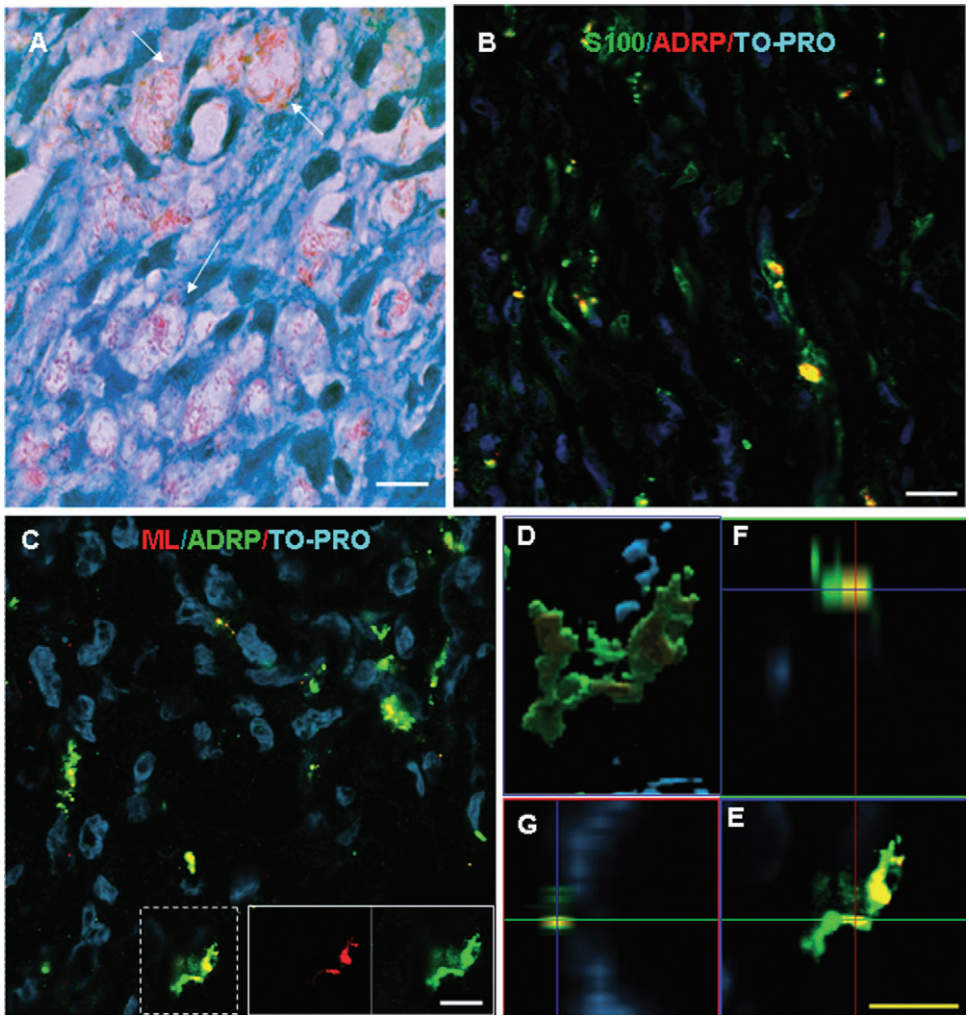

Fig. 1. LDs colocalize with ML in foamy SCs in nerve biopsies of LL patients. Serial sections of nerve biopsies from LL patients ($n = 4$) were analysed.
A. Wade staining showing foamy SCs with multiple acid-fast bacilli (arrows).
B. Double-immunofluorescent labelling of a LL lesion for anti-S100 and anti-ADRP (Pearson's coefficient: 0.81).
C. LD–ML association within SCs.
D. High magnification of the boxed areas visualized by 3D reconstruction (Pearson's coefficient: 0.70).
E–G. By orthogonal sections (Pearson's coefficient: 0.73).
Nuclei were stained with TO-PRO-3. No fluorescence was observed for the isotype control IgG (data not shown). Bars: white = 10 μm; yellow = 5 μm. Ax, Axon; S100 is a SC marker; ADRP (Adipose Differentiation Related Protein) is a LD marker; LAM (lipoarabinomannan) was used as a ML marker.

measured as these organelles tend to occur in clusters in infected SCs and their enumeration may underestimate LD formation. Figure 3C represents the measurement of this area per cell following LD staining with the fluorescent oil red O (ORO) dye. A significantly larger LD area was observed in ML-infected SCs as compared with the controls, reinforcing the occurrence of lipid accumulation upon ML infection. Figure S2A shows cells stained with ORO for LDs. Figure S2B shows the mean size (diameter) of LDs per cell, indicating that, besides the number, their size increases in infected cells.

Alternatively, LD formation was analysed by flow cytometry (Fig. 3D and E) after cell incubation with BODIPY 493/503. ML infection induced an increase in mean fluorescence intensity of the BODIPY probe in comparison with that of the control (Fig. 3D and E). In cells treated with latex beads, however, induction of LD formation was not seen, indicating that a phagocytic stimulus *per se* was unable to induce these organelles (Fig. 3A, D and E). Analysis was then extended to compare the ML-induced LD formation with *Mycobacterium bovis* BCG, an attenuated mycobacterium strain. As shown in Fig. 2D and E, BCG failed to induce LD formation in SCs. Besides, increased ADRP expression levels were observed in ML-treated cells when examined by Western blot (Fig. 3F). In summary, these results

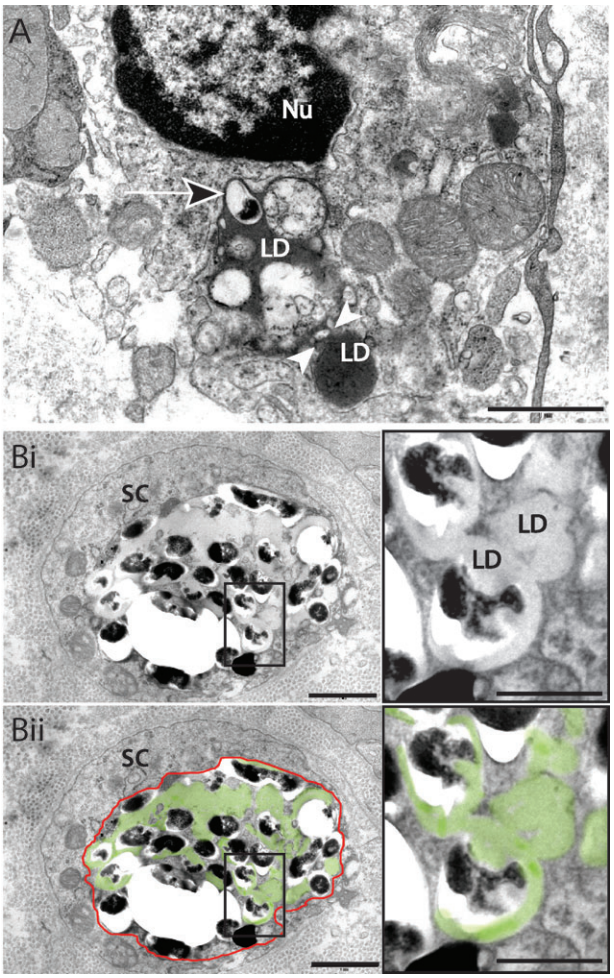

Fig. 2. Ultrastructure of ML-infected SCs.
A. A typical LD is seen in close apposition (arrowheads) to a phagosome-containing bacterium (arrow). Note that accumulating LDs are also observed within the phagosome.
Bi. A large phagosome (outlined in red in Bii) shows a large number of bacteria enmeshed in a LD content (highlighted in green in Bii). Nu, nucleus. Bars, 1 μm (A and B), 500 nm (high magnification of the boxed areas).

demonstrate the capacity of ML to induce LD formation in SCs, and that this effect involves bacterial-driven events.

Because LDs are known to be enriched in triacylglycerol (TGA), phospholipids (PL), free cholesterol (CHO), and cholesterol ester (CHOE) (Mahlberg *et al*., 1990; van Meer, 2001; Persson *et al*., 2008), the relative content of these lipids was then examined by HPTLC comparing SC cultures infected or not with ML. This analysis revealed an increase in these lipids, mainly CHO and CHOE in infected SCs as compared with non-infected cells (Fig. 3G), suggesting that lipid homeostasis is deeply affected in responding to ML infection, leading to its intracellular accumulation as LDs.

Intracellular ML is enveloped by LDs in SCs

The investigation of a possible association between LD and ML subsequent to *in vitro* infection of SCs proceeded. To that end, primary human SCs were treated with PKH26-labelled ML for 48 h followed by BODIPY staining. Interestingly, the green fluorescent pattern surrounding ML adopted the bacterial shape (Fig. 4A, inset 3), in contrast to the classical spherical shape (green arrow) assumed by LDs when free in the cytoplasm (Fig. 4A). Strikingly, different stages of LD association to ML were observed, as indicated by the insets (1 to 3) in Fig. 4A. In the stage shown in 1, some droplets can be seen in the vicinity of the bacterium; and one of them is in intimate contact with ML. LD–ML association subsequent steps in the LD–ML association are highlighted in insets 2 and 3, in which, respectively, the organisms are partially involved and then completely enveloped by LDs. To verify whether the neutral-lipid-rich structures enveloping ML constituted classical LDs, cells were immune stained with anti-ADRP; and the localization of ML to ADRP was monitored in 3D reconstructions and in 2D images by orthogonal analysis (Figs 4B, S3D and E). These images showed isolated, well-circumscribed bacilli enveloped by LDs. Although most bacteria were, associated to LDs, bacteria in association (yellow arrows) or not (red arrow) with LDs were observed (Fig. 4B inset). Cells were also treated with inert fluorescent latex beads (Fig. 4C). In contrast to ML, however, internalized latex beads only poorly colocalized to LDs, indicating that the ability to affect intracellular LD distribution is a bacterial-driven process (Fig. 4D, the percentage of LDs in close association with ML or latex beads were $78.05 \pm 0.59\%$ and $5.12 \pm 1.09\%$, respectively). The same LD–ML association pattern was also found in ST88-14 SCs (Fig. S3F–I). Interestingly, 3D reconstruction (Fig. S3G and I) showed physical 'bridges' between the LDs (Fig. S3I, white arrow) and between LDs and bacteria (Fig. S3I, yellow arrows), as indicated. These results suggest that the interaction between LDs and ML in *in vitro* SCs is similar to what has been observed in LL nerve lesions (Figs 1 and 2).

The next step involved monitoring the intracellular localization of ML by selectively staining host-cell plasma membranes with FM1-43X and subsequently infecting SCs with PKH26-labelled ML for 48 h. It was found that most organisms were in membrane-bound, FM1-43X-labelled compartments, signifying a phagosomal location (Fig. 5A and B). Consequently, the association of LDs to ML-containing phagosomes by colocalization of the FM-labelled membrane, PKH26-labelled ML and P96-labelled LD was analysed (Fig. 5C). This association was revealed by the appearance of the P96 stain as a clear,

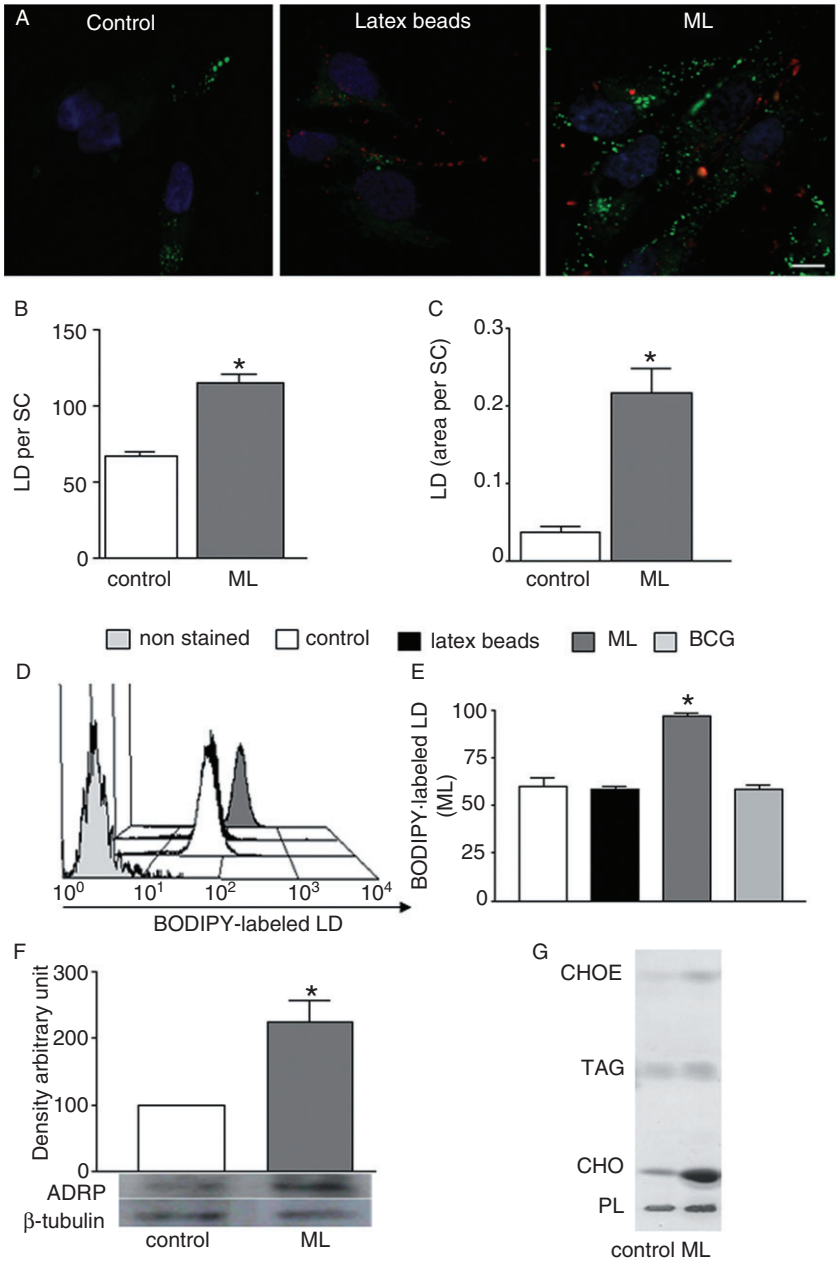

Fig. 3. ML induces LD formation in human SCs. Primary human SCs were stimulated for 48 h before evaluation of LD formation.
A. LDs (green) were visualized after BODIPY staining at 48 h subsequent to treatment or not with ML (red) or fluorescent latex beads (red).
B. Quantification of LDs was determined by enumeration of these organelles after osmium tetroxide staining.
C. Measurement of this area per cell, following LD staining with the fluorescent ORO dye.
D. A representative histogram plot of LD levels determined by flow cytometry using the BODIPY staining method. Cells were untreated (control) or treated with ML, BCG and fluorescent latex beads.
E. Bar graph shows BODIPY MFI values; and nuclei were labelled in blue with DAPI.
F. ADRP expression was determined by Western blot analysis.
G. HPTLC of neutral lipids extracted from SC cultures infected or not with ML detected by charring. Bands were identified using pure chemical standards: CHO, cholesterol; CHOE, cholesterol ester; TGA, triacylglycerol; and PL, phospholipid.
Statistically significant ($P < 0.05$) differences between the stimulated and control groups are indicated by asterisks. Data are representative of four independent experiments and are expressed as the mean ± SD of triplicates. Bar: 10 = μm. ADRP (Adipose Differentiation Related Protein), ORO and BODIPY are LDs markers; MFI, mean fluorescence intensity.

fluorescent ring surrounding and filling out the phagosomes, evidencing lipid transfers from LDs to phagosomes. FM1-43X, while specifically labelling the phagosome membranes, was unable to reach the ER membrane, as shown by the lack of colocalization with P96-labelled LDs (green arrow). Moreover, P96-labelled ML was not observed in the absence of the phagosomal membrane (data not shown). Interestingly, LDs were shown as cytoplasmic punctuate inclusions close to ML-containing phagosomes (blue arrow), one of them apparently docking on the surface of this organelle (Fig. 5C merge ML/FM/P96, white arrow).

ML recruits LDs during internalization into SCs

To study the dynamics of the LD–ML association in living cells, a time-lapse sequence of SCs infected with PKH26-labelled ML was investigated via confocal microscopy and time-lapse recordings. A first set of experiments was carried out after 2 h of ML infection (Fig. 6A). Dynamic movement of cytosolic LDs stained with BODIPY was projected in a time-lapse sequence at 30 s intervals for 40 min. The 3D data showed three marked events: (i) LDs clearly adhered to or possibly fused with each other, (ii) LDs moved in direction of the bacterium (Fig. 6A) and

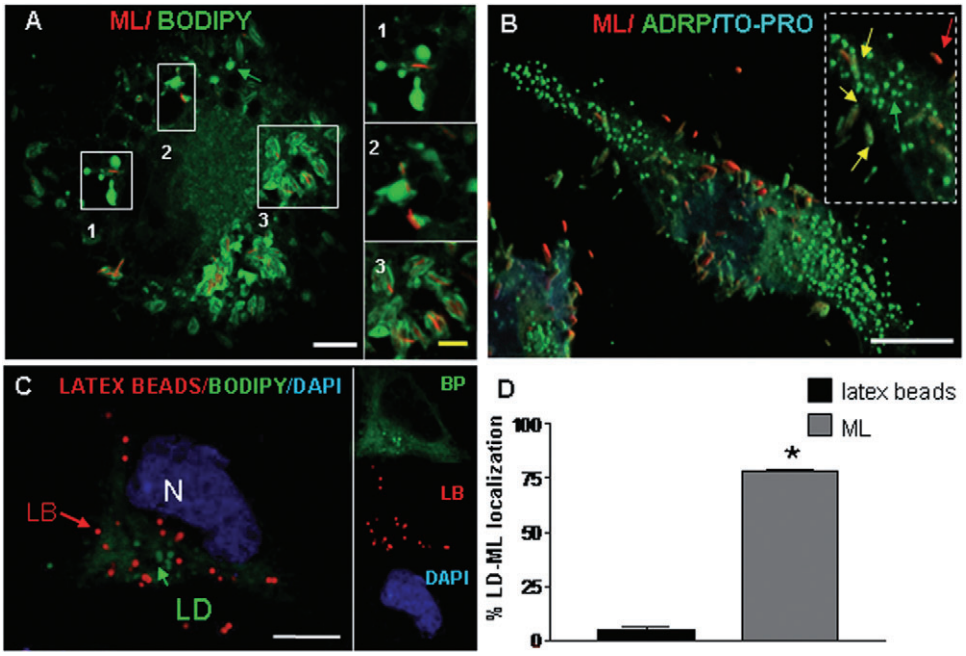

Fig. 4. Intracellular ML is enveloped by LDs in *in vitro* infected SCs. (A and B) Primary human SCs were infected with PKH26-labelled ML (red) for 48 h.
A. LDs were visualized using BODIPY label (BP) (green). A close-up of different steps in LD–ML association (labelled 1-to-3). The images show some LDs in the vicinity of the ML and one of them in intimate contact with the bacterium (1) (Pearson's coefficient: 0.08). ML partially enveloped by LDs (2) (Pearson's coefficient: 0.12) and bacteria completely enveloped by LDs (3) (Pearson's coefficient: 0.64).
B. Imunofluorescence confocal images for ADRP (green labelling) and PKH26-ML. Note staining for ADRP is seen around the ML surface in 3D reconstruction (inset, yellow arrows; Pearson's coefficient: 0.62). The green and red arrows indicate LDs and ML respectively.
C. Association of LD (green) with fluorescent latex beads (red).
D. Bar graph shows percentage of LDs in close association with latex beads (black bar) and with ML (gray bar) at 48 h time-points ($n = 6$). Statistically significant ($P < 0.001$) differences between treated and untreated cells are indicated by asterisks. Bars: white = 10 μm; yellow = 5 μm. ADRP (Adipose Differentiation Related Protein) and BODIPY are LDs markers.

(iii) There was a notably prompt redistribution of LDs in the ML-infected cells, culminating in the circumferential localization of the LDs around the bacterial-containing vacuole (Fig. 6A, $t = 2$ h 30 min and Fig. S4). In all cases, only cells with internalized ML were used for analysis.

To examine whether LD recruitment occurred at the earliest time points in bacterial–SC interaction, cells were incubated with ML followed by a time-lapse analysis 15 min after initiating the infection in culture. ML adherence to the cell surface was detected by differential interferential contrast, and the cytosolic area surrounding the bacterium was then monitored via time-lapse confocal microscopy. Images with live SCs via 4D reconstruction over time and space showed the formation of typical homocomplexes between LDs and heterocomplexes, between LDs and bacteria (Fig. 6B). This reconstruction shows that the LDs of the visualized region were re-directed by the bacterial presence to the site of phagocytosis. As observed above regarding internalized bacterium, a continuous LD movement towards the bacillus was evident. The kinetics of LD recruitment to ML over time was determined by measuring the spatial distance variation (μm) between the bacterial and LD centres (Fig. 6C and D). The bars show that, in most cases, these distances were reduced to almost zero, pointing to an intimate LD–ML association. These results clearly show that ML phagocytosis triggers a pathogen-driven recruitment process of cytoplasmic LDs to bacterial-containing phagosomes.

ML-driven LD formation and recruitment occur independently of TLR2 signalling

TLR2 has been shown to play an important role in mycobacterial sensing by host cells (Quesniaux *et al.*, 2004). Based on our previous data indicating that TLR2 signalling participates in mycobacteria-induced LD biogenesis in macrophages (D'Avila *et al.*, 2006; Almeida *et al.*, 2009; Mattos *et al.*, 2010), the role played by TLR2 in ML-induced LD biogenesis and recruitment in SCs was tackled. Comparable induction levels of these organelles were observed in WT and TLR2-KO SCs (Fig. 7A) after mycobacterial infection, showing that TLR2 signalling is not essential for ML-induced LD formation in SCs. As an experimental control, the bacterial association index was determined and similar levels of ML infection were

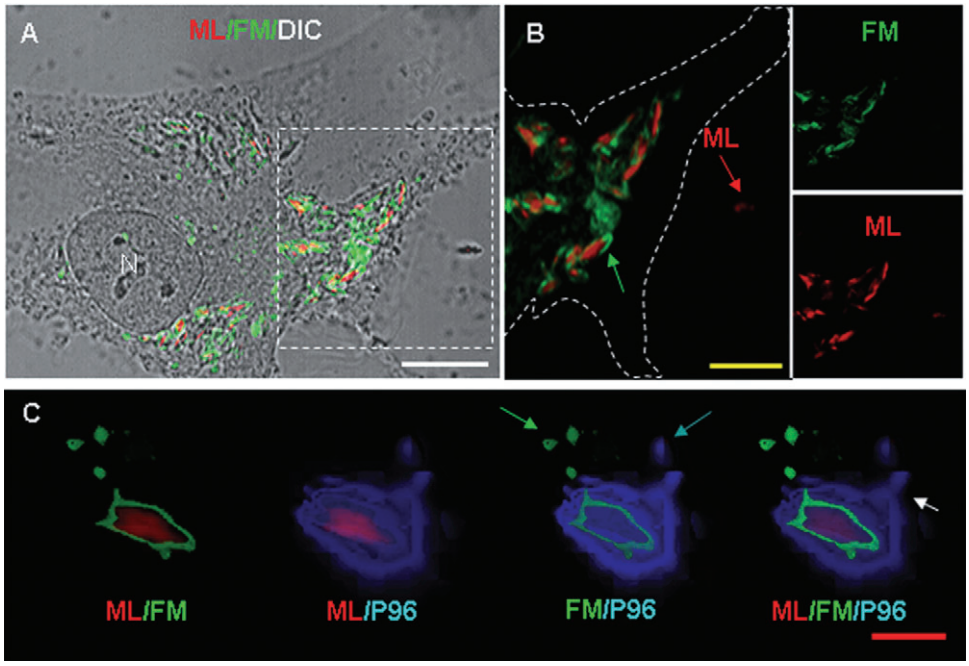

Fig. 5. LDs are recruited to ML-containing phagosomes in infected SCs.
A. Cells labelLed with FM1-43X (green) were infected with PKH26-labelLed ML (red) for 48 h and observed by confocal microscopy. Differential interference contrast (DIC) and fluorescence merge show that all the bacteria within SCs were labelled to FM1-43X.
B. Enlarged view shows one not-internalized ML (arrow) without FM1-43X labelling. Dashed line indicates the cell surface.
C. Close-up of ML-bearing phagosome localizing to LDs (Pearson's coefficient: 0.78). Note three LDs (blue dots) arriving at the ML-containing phagosome (blue arrow). LDs (derived from ER membranes) do not stain with FM1-43X. FM1-43X-labelled vesicles (green arrow) are distinct (merge FM/P96). The white arrow in the merge (ML/FM/P96) suggests the fusion 'bridges' between these organelles.
Bars: white = 10 μm; yellow = 5 μm, red = 2 μm. FM1-43X was used to stain the plasma membrane; P96 was used to stain the LD.

observed in both WT and SCs isolated from TLR2-KO mice (Fig. 7B). To verify whether ML-induced LD recruitment depends on TLR2 signalling, TLR2-KO SCs were infected for 48 h. The LD–ML association was subsequently determined and quantified by confocal microscopy using BODIPY labelling (Fig. 7C and D). A similar percentage of LD–ML localization was observed when comparing SCs from WT (82.72 ± 4.27) and TLR2-KO mice (81.22 ± 3.14) (Fig. 7C). As a whole, these data show that ML induces LD biogenesis and recruitment in SCs by way of TLR2-independent signalling.

ML-driven LD recruitment relies on cytoskeletal rearrangement and PI3K signalling

It has been shown that LD intracellular traffic is mediated by microtubules (Pol *et al*., 2000; Boström *et al*., 2005; Pacheco *et al*., 2007; Boulant *et al*., 2008). As such, it was decided to examine the involvement of the cellular cytoskeleton in the LD recruitment process observed in ML-infected cells. In cells stained with anti-tubulin, microtubules enveloping both LDs and ML were found (Fig. 8A and B), suggesting that LDs migrate to ML-containing phagosomes by a microtubule-dependent way, culminating in intimate LD–ML interaction (Fig. 8A, white arrow). For comparison, microtubules organization in non-infected cells is shown in Fig. S5. To investigate the role of microtubules in LD movement during the ML recruitment process, cells were treated with taxol, a microtubule-stabilizing drug, and cytochalasin D (cytD), an actin-disrupting drug (Grigoriev *et al*., 1999). Cells were exposed to bacteria for 6 h before adding the drug and chased 4 h later to determine the effect of the cytoskeleton on LD–ML complex formation. The quantification of LD–ML localization is seen in Fig. 8C. Examination ensued of the effect of LY294002, a specific pharmacological inhibitor of PI3K and a major pathway involved in cytoskeletal rearrangement (Lasunskaia *et al*., 2006) on LD distribution in infected cells. As shown in Fig. 8C, the LD–ML association was inhibited in LY294002-treated cells, suggesting the involvement of PI3K signalling in the early cytoskeletal rearrangements required for LD mobility. The decrease in LD–ML association was not a secondary effect resulting from drug's impairment of LD formation as similar LD levels were observed in both untreated and drug-treated cells at this early time point (Fig. 8C inset). These results indicate that movements around the cell in the microtubule network are able to correctly position the LDs in the vicinity of ML-bearing phagosome organelles in a PI3K-dependent signalling pathway.

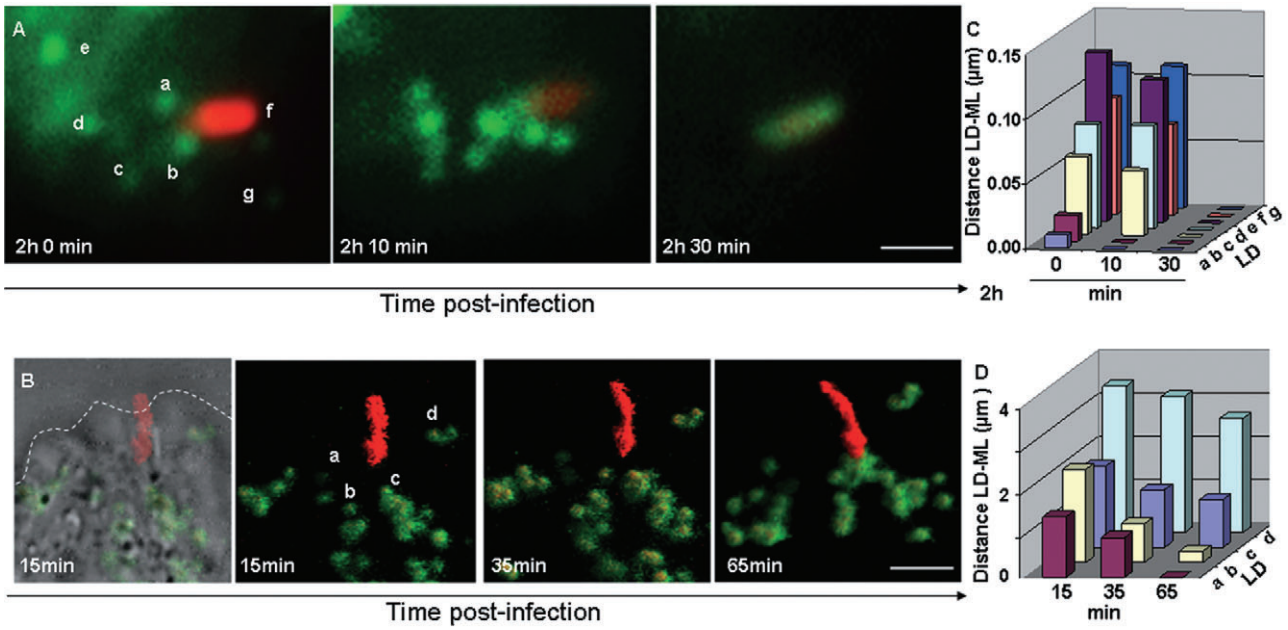

Fig. 6. Kinetic recruitment of LDs by ML in SCs. The LDs in ML-infected SCs were stained with BODIPY; and the time-lapse sequence of the recruitment processes was investigated using confocal and conventional fluorescence microscopes.
A. Representative time-lapse series examining late-time course of LD recruitment during ML infection. Neutral lipids in the cytoplasm (LDs) were stained with BODIPY after 2 h of bacterial infection and time-lapse photography of the cells at 30 s intervals for 40 min followed. ML (red) was completely enveloped by LDs (green) after 30 min post-infection ($t = 2$ h 30 min, Pearson's coefficient: 0.80).
B. Representative time-lapse experiments examining LD recruitment at early time points during ML association (15 min). 3D images were acquired by confocal microscopy through the time-series of Z-stack reconstruction at intervals of 10 min for 60 min. The series shows times at 15, 35 and 65 min post-infection (zero time for image acquisition corresponds to 15 min of infection). Bacterial presence at the site of phagocytosis was detected by differential interference contrast.
C and D. Kinetics of recruitment was estimated by manual tracing of the distance between the bacterial centre and the centre of LD via AxionVision software. Pearson's coefficient in the region of LD (a) and ML is 0.56. Bar graph shows the distance values (µm) between LD and ML during association. Dashed line indicates cell surface.
Bars: 2 µm. BODIPY was used to stain LDs.

Inhibition of LD recruitment decreases ML survival inside SCs

Accumulating evidence has suggested that LD biogenesis and traffic may favour intracellular bacterial survival and/or replication (D'Ávilla *et al.*, 2008; van der Meer-Janssen *et al.*, 2010). Because LDs are organelles rich in neutral lipids, we investigated whether LD recruitment to bacterial phagosomes favours mycobacterial survival. Cells were infected for 6 h with ML and then treated with cytD or taxol to inhibit LD traffic. After incubation for 72 h, mycobacterial viability was assessed by flow cytometry via the LIVE/DEAD Baclight Bacterial viability Kit. As shown in Fig. 8D, treatment with cytD and taxol significantly increased the percentage of dead ML as compared with the results of the vehicle treatment (37.84 ± 2.175, 33.84 ± 2.17 and 6.66 ± 0.7, respectively).

Discussion

The present report investigated the biology of ML inside SCs, one of its favourite niches in the human host. The *in vivo* and *in vitro* data presented herein show that ML infection has a pronounced effect on SC lipid homeostasis via regulation of LD biogenesis and traffic, which favours ML intracellular survival. This conclusion is supported by the following findings in our report: (i) LD accumulation in infected SCs in LL nerve biopsies, (ii) induction of LD biogenesis in *in vitro* ML-infected SCs, (iii) intimate association between both *in vivo* and *in vitro* ML and SC LDs, (iv) prompt recruitment of LDs to ML-containing phagosomes upon bacterial infection and (v) decreased bacterial survival in the event of LD biogenesis and traffic impairment. Collectively, our data indicate that the lipid-laden, bacterial-bearing vacuoles observed in the heavily infected SCs in LL nerve biopsies might be formed by the continuous formation and recruitment of LDs, giving rise to their foamy appearance. In all likelihood, a similar process might also be responsible for the formation of the Virchow cells in the dermal lesions of LL patients, as the capacity of ML to induce LDs and maintain a close association with these organelles in infected macrophages has also been recently demonstrated (Tanigawa *et al.*, 2008; Mattos *et al.*, 2010).

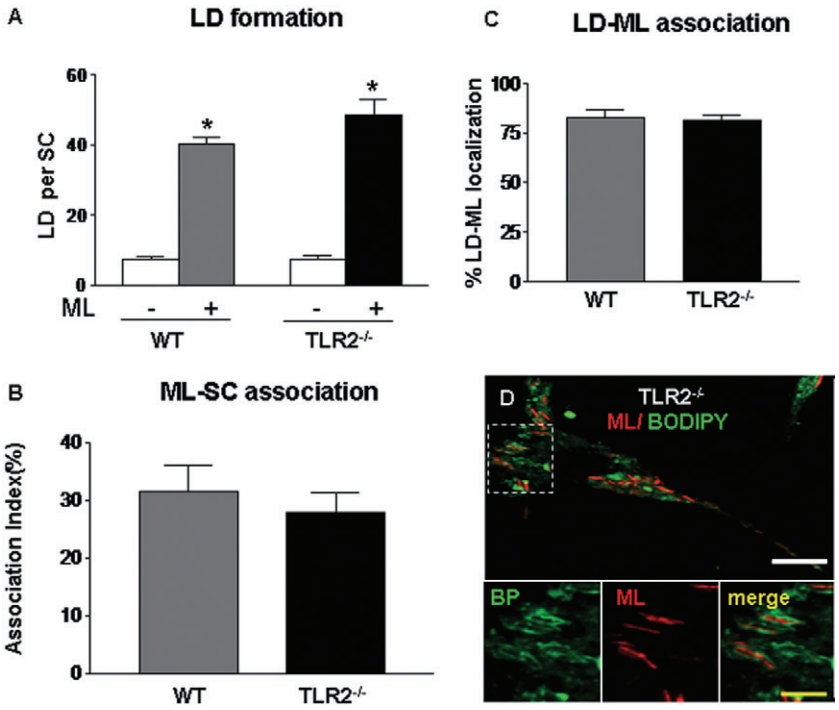

Fig. 7. TLR2 signalling is not involved in *M. leprae* uptake, induction of LD biogenesis, or LD–ML complex formation in SCs. SCs were isolated from WT and TLR2-KO mice and infected with ML during 48 h.
A. LD modulation was monitored by mean fluorescence intensity values of BODIPY dye using flow cytometry analysis.
B. PKH26-labelled ML was used to determine the bacterial association index by flow cytometry.
C. Localization of LDs to ML was quantified using confocal microscopy. The difference between WT and TLR2-KO cells was not statistically significant ($n = 6$).
D. Representative image of LD–ML complex formation in TLR2-KO SCs. Bar: white = 10 μm; yellow = 2 μm. BODIPY was used to stain LDs.

The data, however, likewise indicate that the mechanisms ML uses to regulate LDs in SCs are distinct from those observed in macrophages. We have recently shown that both ML and *M. bovis* BCG induce LD biogenesis in macrophages in a TLR2-dependent way (D'Avila *et al*., 2006; Almeida *et al*., 2009; Mattos *et al*., 2010). In sharp contrast to macrophages, although SCs express TLR2 (Oliveira *et al*., 2003), signalling through this receptor does not seem to be essential to LD biogenesis. In this connection, we have recently shown that both ML and *M. bovis* BCG induce LD biogenesis in macrophages in a TLR2-dependent way (D'Avila *et al*., 2006; Almeida *et al*., 2009; Mattos *et al*., 2010). Moreover, only ML but not BCG was able to induce LD biogenesis in SCs, reinforcing the idea that unique and yet unknown features of LD regulation occur during ML–SC interaction. Further investigation is required to define the cell receptors, mycobacterial ligands and signalling events involved in ML-induced LD accumulation in SCs.

Our data are supportive of the current view that LDs are involved in host–parasite interactions, as has been demonstrated in the context of such diverse pathogens as viruses, bacteria, protozoa and worms (Wenk, 2006; D'Ávila *et al*., 2008; van der Meer-Janssen *et al*., 2010). LDs have been shown to play a fundamental role in the formation of dengue (Samsa *et al*., 2009) and hepatitis C viral particles (Barba *et al*., 1997). Of note, a close association and/or the presence of host-cell LDs in pathogen-containing vesicles has been detected in cells infected with *Mycobacterium tuberculosis* (Cáceres *et al*., 2009; Russell *et al*., 2009), *M. bovis* BCG (D'Avila *et al*., 2006; Almeida *et al*., 2009) and *Trypanosoma cruzi* (Melo *et al*., 2003). Additionally, the pathogen-driven LD recruitment reported here has previously been described in epithelial cells infected with *Chlamydia*, a bacterium that shares with ML the inability to grow outside the host (Cocchiaro *et al*., 2008).

It is known that pathogens require host-cell lipids to insure successful host colonization and infection progression (Wenk, 2006; van der Meer-Janssen *et al*., 2010). Mycobacterium is not an exception (Marri *et al*., 2006). For ML, early metabolic studies (Wheeler, 1989; 2003) and recent proteomic analyses (Marques *et al*., 2008) indicate that fatty acid beta-oxidation is an active pathway in *in vivo*-grown bacteria, implying that lipids, rather than carbohydrates, are the dominant carbon substrate mobilized during infection. As such, the most reliable method to measure ML viability to date is based on the assumed capacity of ML to oxidize fatty acids (Franzblau, 1988). The role of lipids in ML metabolism is further supported by an active glyoxylate cycle (Marques *et al*., 2008), referred to as the dominant, anaplerotic pathway during fatty acid growth.

Despite the central role enacted by lipids in mycobacteria, little is known about the mechanisms involved in *in vivo* lipid acquisition. Based on our results, we propose that LD recruitment and biogenesis may constitute an effective ML intracellular strategy to acquire host-SC lipids and promote bacterial survival. Two lipases and one phospholipase that the ML genome codes for could possibly

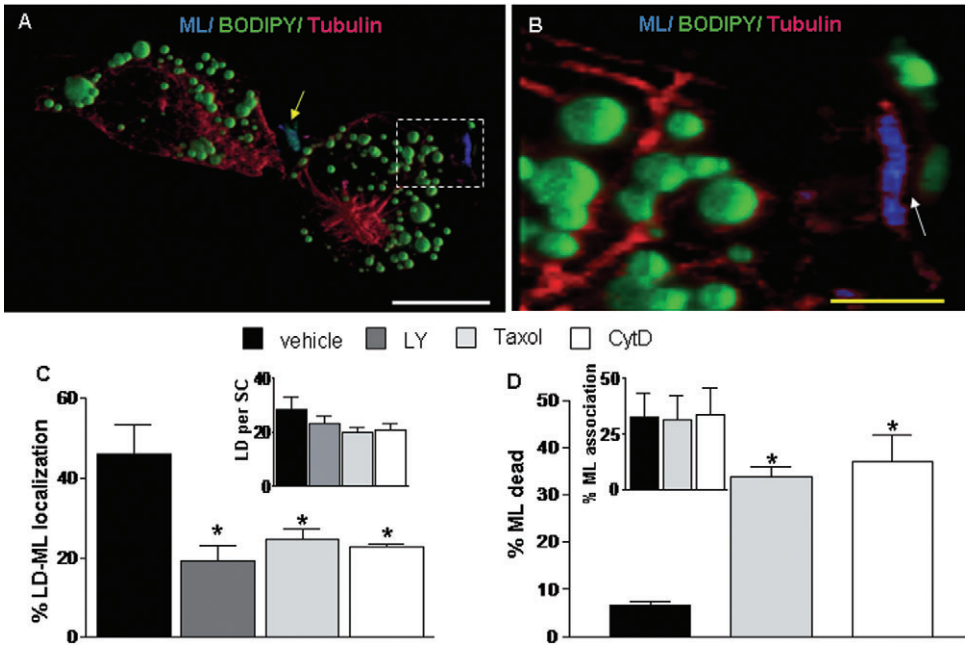

Fig. 8. LD recruitment induced by *M. leprae* relies on cytoskeletal rearrangement and favours intracellular bacterial survival. ML-induced LD recruitment depends on microtubular dynamics in SCs. Cells were exposed to bacteria for 6 h before drug addition and chased 4 h later to determine the effect of the cytoskeleton on LD–ML complex formation. Mycobacterium was labelled with anti-ML and visualized in blue; LD was stained by BODIPY (green) and the microtubular network was stained with α-tubulin antibody (α-tub, red).
A. General view by 3D reconstruction of ML-infected SCs. The LD–ML complex is indicated (yellow arrow). No fluorescence was observed for the isotype control IgG.
B. Enlarged view showing close association between the cytoskeleton and both LD and ML (white arrow).
C. LD–ML complex was observed by confocal microscopy and quantified. Bar graph shows percentage of LD–ML association ($n = 6$) in the presence of DMSO vehicle (control), LY (10 μM), Taxol (1 μM) and CytD (1 μM). Inset shows LD quantification.
D. Percentage of live and dead bacteria was evaluated using a LIVE/DEAD BacLight Bacterial Viability Kit in combination with flow cytometry after 72 h of drug treatment. Inset shows bacterial association ($n = 4$). Statistically significant ($P < 0.05$) differences between control and drug-treated groups are indicated by asterisks.
Bars: white = 10 μm; yellow = 5 μm. BODIPY was used to stain LDs.

favour ML assimilation of the fatty acids originating from the neutral lipids and phospholipids found in LDs (Cole *et al*., 2001). In addition, enzymes from the host cell may, in fact, be complementing these bacterial genes, as recently suggested by a study describing the overexpression of lipases and phospholipases in LL lesions (Cruz *et al*., 2008).

Notably, however, two recent reports have implicated LD formation and the intimate association of bacterium-containing phagosomes with the bacterial capacity to persist in a long-term dormant state within the human host (Bentrup and Russell, 2001; Peyron *et al*., 2008). These data suggest an interesting additional role for host lipids as efficient, hydrophobic, safe shelters. This barrier would ultimately curb access to some essential nutrients limiting bacterial growth. It is not impossible that LD recruitment constitutes a prime example of 'organelle mimicry' whereby ML successfully escapes host recognition by cloaking itself in these fat-rich structures.

Finally, the accumulation of host-derived lipids in infected SCs may also contribute to a permissive environment for ML proliferation within LL nerves by dampening the immunoinflammatory response to the pathogen at the infection site. It has recently been shown that host-derived, oxidized phospholipids that have accumulated within foamy macrophages of LL lesions inhibit the innate immunity response (Cruz *et al*., 2008). Furthermore, our laboratory has recently demonstrated that the LDs formed in response to ML constitute sites for eicosanoid synthesis, ultimately leading to the increased production of PGE_2 by infected macrophages (Mattos *et al*., 2010). In reality, the high PGE_2 concentration produced by COX-2-positive macrophages in LL were able to inhibit Th1 cytokine production, and, in that way, most probably contribute to T-cell anergy at this disease pole (Betz and Fox, 1991). As has been proposed for Virchow cells in the context of dermal lesions (Tanigawa *et al*., 2008; Mattos *et al*., 2010), it is reasonable to speculate that the lipid storage phenomenon observed in ML-infected SCs is an important contributor to the immunoinflammatory function of these cells in LL nerve lesions. Accordingly, SCs are capable of secreting a vast array of cytokines and inflammatory mediators (namely, IL-1, IL-6, IL-8, TNF-α, prostaglandins, TGF-β and NO) and actively participate in the

immunoinflammatory responses in neuritic processes (Lisak *et al*., 1997; Rutkowski *et al*., 1999; Teles *et al*., 2007; Cámara-Lemarroy *et al*., 2010). It is therefore deemed necessary to investigate the capacity of ML-infected SCs to secrete prostaglandins and cytokines along with the manner in which this secretion may be intimately related to LD formation.

In conclusion, the *in vivo* and *in vitro* data presented here show that ML triggers a pronounced alteration on host-cell lipid homeostasis through regulation of LD biogenesis and recruitment of these organelles to bacterial phagosomes. Accumulating evidence from different cell system give support to our observation of homotypic fusion of LDs to create larger ones as well as the capacity of LDs to fuse with endosomal compartments in ML-infected SCs (Boström *et al*., 2007; Robenek and Severs, 2009). The modulation of LDs contributes to the foamy phenotype of infected SCs and favours intracellular bacterial survival, likely representing a fundamental aspect of ML pathogenesis. Needless to say, this underling regulatory mechanism may hold the key to the development of novel strategies aiming to prevent or, at a minimum, limit peripheral nerve injury in leprosy.

Experimental procedures

Antibodies

The following antibodies were used: guinea pig, and mouse monoclonal against Adipose Differentiation Related Protein (ADRP, Research Diagnostics), monoclonal anti-β-tubulin (BD Transduction Laboratories), monoclonal anti-α-tubulin (Santa Cruz Biotechnology), rabbit anti-S100 (DakoCytomation), CS-35 anti-LAM monoclonal, rabbit anti-whole ML (kindly provided by Dr Patrick J. Brennan, Colorado State University, Fort Collins, CO, USA; NIH/NIAID contract 1AI25469), fluorescent labelled (Alexa Fluor 488, 555, and 633) goat anti-rabbit and anti-mouse (Molecular Probes, Eugene, OR, USA), donkey anti-guinea pig fluorescent-dye-Cy2 conjugated, and, finally, control IgG (Jackson ImmunoResearch Laboratories).

Patients and clinical specimens

Lepromatous leprosy patients were classified according to Ridley and Jopling criteria (Ridley and Jopling, 1966). Punch skin biopsy specimens (6 mm diameter) were obtained at diagnosis. The specimens were snap-frozen in liquid nitrogen and stored at −70°C until sectioned. The procedures described in this work were approved by the Ethic Committee of the Oswaldo Cruz Foundation. Written informed consent was voluntarily obtained from each patient.

Human SCs

Human primary SCs were isolated from peripheral nerve tissues (a generous gift from Dr Patrick Wood, University of Miami, Miami, FL USA). The purity of these cultures was > 95% by labelling with anti-S100 antibody. These cells were seeded on plates previously treated with mouse laminin-1 (4 μg ml^{-1}) (Invitrogen) in PBS and grown for 24 h at 33°C with 5% CO_2 in DMEM high glucose (Invitrogen) supplemented with 2% of FBS (Hyclone), 2 nM heregulin (Calbiochem) and 0.4 μM forskolin (Calbiochem). The human schwannoma cell line ST88-14 was kindly provided by Dr Jonathan Fletcher (Harvard University, Boston, MA, USA). Cells were grown in RPMI-1640 (Invitrogen) supplemented with 2% FBS and 20 mM L-glutamate.

Isolation and purification of mouse primary SCs

Mouse SCs from wild-type (WT) C57BL/6 (B6) and Toll-like receptor 2 (TLR2) knockout (TLR2-KO) mice with a homogeneous B6 background (donated by Dr S. Akira, Osaka University, Osaka, Japan) were prepared from the nerve explants of adult animals, as described (Singh *et al*., 1996). SC purity was assessed by immunostaining with S100 antibody (Pelc *et al*., 1986), which revealed *c.* 95% S100-positive cells. All procedures involving animals were conducted according to the requirements of the Animal Welfare Committee of the Oswaldo Cruz Foundation.

ML

Mycobacterium leprae prepared from the footpads of athymic *nu/nu* mice was kindly provided by Dr James Krahenbuhl (National Hansen's Disease Program, Laboratory Research Branch, Louisiana State University, Baton Rouge, LA, USA) through American Leprosy Missions, the Order of St Lazarus and the National Institute of Allergy and Infectious Diseases (NIAID/NIH) (Bethesda, MD, USA), Contract No. 155262. Before interactive assays, bacteria were pre-labelled via the PKH26 Red Fluorescence cell linker Kit (Sigma) according to the manufacturer's instructions. Alternatively, ML was detected by immunolabelling using antibody anti-ML.

ML–*SC interaction assays*

Schwann cell were cultured at a density of 1×10^5 cells per well on 12-well plates for flow cytometric assays. For microscopy experiments, cells were plated at 7×10^4 cells per well on 24-well plates containing glass coverslips. For live-cell microscopy, cells were seeded at 5×10^4 cells in 35 mm poly-D-lysine coated glass-bottom dishes (generously donated by MatTek, Ashland, MA, USA). For Western blot analysis, SCs were seeded onto 6-well tissue culture plates at a density of 1×10^6 cells per well. SCs were incubated with ML at a multiplicity of infection (MOI) of 50:1. Alternatively, SCs were stimulated with fluorescent latex beads (50:1, Polysciences) or *M. bovis* BCG (MOI of 50:1). In inhibition assays, SCs were infected with ML for 6 h, washed to remove free mycobacteria and treated with LY294002 (10 μM, BIOMOL Research Laboratories) for phosphatidylinositol 3-kinase (PI3K) inhibition or treated with taxol (1 μM, Sigma) and cytochalasin D (1 μM, Sigma), for cytoskeletal alteration for 30 min. Cells were then washed and incubated for an additional 4 h in medium with 2% serum. As a control, the same volume of DMSO vehicle was added to the cell culture. The percentages of the LD–ML association and LD formation were determined by counting 20 random fields for each sample. After 48 h of incuba-

tion, cell viability was over 90%, as revealed by the trypan blue (Sigma) exclusion assay. Bacterial association to cells was measured at FL2 by PKH26-labelled bacteria using flow cytometry analysis, as described (Mattos *et al*., 2010). Index of bacterial association (%) is expressed as % of cells taking up PKH26-labelled ML. All assays were performed at 33°C to maximize bacterial viability (Hagge *et al*., 2002).

Immunohistological analysis

Immunohistochemical procedures to detect LD organelles and ML in SCs from LL nerves were performed, as described (Mattos *et al*., 2010). Briefly, tissue sections were thawed on sylane precoated slides and submitted to staining and immunostaining protocols. Standard staining was done with haematoxylin and eosin for morphological analysis and Wade-Fite staining to identify the mycobacteria (Wade, 1962). Immunostaining was performed by incubation with primary antibodies to ADRP, S100, and ML (anti-whole bacteria or anti-LAM). Two-colour immunofluorescence staining was carried out by the serial incubation of sections with combinatorial antibodies against: (i) S100 (1:100) and ADRP (1:25), (ii) S100 (1:100) and ML (1:25), and (iii) ML (1:25) and ADRP (1:25).

LD evaluation

Cells adhering to coverslips were fixed in 4% PFA in Ca^{2+}/Mg^{2+}-free HBSS pH 7.4 for 10 min. LDs were enumerated in 200 consecutively scanned cells after osmium tetroxide staining (Mattos *et al*., 2010). For fluorescent LD-labelling, cells were incubated with BODIPY493/503 dye (4,4-difluoro-1,3,5,7,8-pentamethyl-4-bora-3a,4a-diaza-s-indacene, Molecular Probes) or P96 (1-pyrenedodecanoic acid, Molecular Probes) (D'Ávila *et al*., 2008; Mattos *et al*., 2010). For LD immunodetection, cells were permeabilized and blocked in blocking buffer [5% new-born calf serum (Invitrogen) and 0.01% Triton (Sigma) in PBS] for 1 h at room temperature and then incubated with anti-ADRP primary antibodies followed by Alexa Fluor-conjugated anti-mouse or anti-rabbit IgG secondary antibodies. To visualize the interaction between the microtubular network with ML and LDs, cells were incubated with anti-α-tubulin (1:100) conjugated with Alexa 555 Nuclei and bacterial DNA were stained with TO-PRO-3 (Molecular Probes). Alternatively, nuclei were stained with 2 μM DAPI (Molecular Probes) at room temperature for 5 min. Cells were mounted with the VectashieldHard set mounting medium (Vector Laboratories) and observed under a confocal microscope. Alternatively, the area occupied by LDs per cell was estimated following LD staining with fluorescent ORO. The images (taken with a 60 objective lens and at least 10 fields per slide) were transformed into black and white pictures and analysed via ImageJ software (Image-J 1.35 d). The spots were determined by automatic spot detection; and the total area and average size of fluorescent LDs was obtained for each field and divided by the number of cells in the respective field. In addition, LD induction was measured by flow cytometric analysis, as previously described (Mattos *et al*., 2010).

Fluorescence microscopy

Contrast images were acquired using differential interferential contrast. Confocal images were acquired using a LSM 510 Zeiss confocal microscope (Zeiss) and processed by LSM 510 Zeiss software. To obtain a 3D model of the LD–ML complex, 30 confocal planes of 0.3 μm thickness were integrated.

In the time-lapses of living cells, 4D (Z-stacks over time) experiments were performed via the LSM 510 confocal microscope, acquiring 3D image reconstructions from stacks of 1.05 μm thickness every 10 min for 60 min. Alternatively, in 3D time-lapse experiments, images were collected every 30 s during 40 min with a Zeiss Axio Observer microscope and processed using ImageJ software (National Institutes of Health, Bethesda, MD, USA; http://rsb.info.nih.gov/ij/). At each time point, stacks of two fluorescent channels (488 nm for BODIPY-labelled LD and 633 nm for PKH26-labelled ML) were taken sequentially. Images were recorded with a planapochromatic 63 ×/1.4 oil-immersion objective. Quantitative colocalization analysis was performed by Pearson's correlation coefficient (P) employing LSM 510 Zeiss software.

Phagosome labelling

Cells were pre-labelled by incubation with 1 μg ml^{-1} FM1-43X (Molecular Probes) for 15 min at 4°C in order to specifically label the cytoplasmic membranes. Cells were washed to remove the excess of dye and then challenged with PKH26-labelled ML for 48 h at 37°C. Before LD labelling, cells were washed to remove extracellular bacteria. Slides were processed and analysed immediately via fluorescence microscopy, as described above.

Processing for electron microscopy

Lepromatous leprosy nerve biopsies were processed for TEM, as described (Kaplan *et al*., 1983). Briefly, biopsies were fixed in 2.5% glutaraldehyde in a 0.1 M cacodylate buffer containing 0.1 M sucrose (pH 7.4). The tissue was postfixed for 6 h at 4°C with 2% osmium tetroxide. Sections were stained with 0.25% uranyl acetate, dehydrated in a graded series of ethanol, and embedded in epon blocks. Ultra-thin sections were stained with uranyl acetate and lead citrate and then observed under a Hitachi-HU-12 transmission electron microscope (Hitachi).

Western blot analysis

Cell lysates were prepared in reducing and denaturing conditions and subjected to electrophoresis in 15% acrylamide SDS-PAGE gels. Western blot was performed, as described previously (Gao *et al*., 2000), and developed with anti-ADRP antibody. β-tubulin was used as the loading control. For densitometry analysis, the images of the developed films were analysed via Image Master 2D platinum Ver. 6.0 software (GE Healthcare).

ML viability determined by flow cytometry

A live/dead staining protocol based on the LIVE/DEAD Baclight Bacterial viability Kit (Invitrogen) was applied to study the viable versus nonviable ML obtained from SCs treated with cytD, taxol or vehicle. In brief, SCs (2×10^6 cells $well^{-1}$) were infected with ML (MOI 50:1) for 6 h, then treated with cytD (1 μM), taxol

(1 μM) or vehicle for 30 min at 33°C, followed by three PBS washes to remove any non-internalized bacteria. SCs were then incubated for 72 h after infection in RPMI cell culture medium. Afterwards, cells were lysed with 0.1% saponin and bacterial-containing suspensions were labelled with the LIVE/DEAD kit and the percentages of live/dead bacteria were determined by flow cytometry according to the manufacturer's instructions. As control, bacterial suspensions were exposed to the same drugs using the conditions described above and this parameter was used to exclude the direct drugs effect on bacterial metabolism. Flow cytometry measurements were performed on a FACSCalibur (BD Bioscience) and analysed via CellQuest software (BD Bioscience).

Cellular toxicity

The MTT assay was used to measure cellular toxicity in response to drug treatments. Cell lines were inoculated into 96-well plates (10 000 cells well^{-1}) and allowed to attach for 24 h. MTT [3-(4,5-dimethylthiazol-2-yl)-2,5-diphenyltetrazolium bromide] (Sigma) formazan was quantified following 72 h after drug treatments in accordance with previously published procedures (Mosmann, 1983).

Lipid extraction and analysis

ST8814 SCs were infected or not with viable ML for 48 h. Cultures were detached by trypsin-EDTA treatment and washed twice with PBS. The cell number was determined and adjusted to 3×10^6 cells ml^{-1} before mechanic disruption of cells. The lipids were extracted with chloroform, methanol and water (1:2:0.8 by vol) (Bligh and Dyer, 1959) and then partitioned with chloroform and methanol (2:1 by vol), according to the standard procedure of Folch *et al*. (Folch *et al*., 1957). Neutral lipids were analysed by one-dimensional HPTLC on Silica gel 60 plates (Merck). Plates were first developed in hexane-ethyl ether-acetic acid (60:40:1 by vol) until the solvent front reached the middle of the plate and then in hexane-chloroform-acetic acid (80:20:1 by vol). HPTLC plates were stained by spraying with a charring solution consisting of 10% $CuSO_4$ and 8% H_3PO_4 and then heated to 180°C for 5–10 min.

Statistical analysis

Results are representative of at least 3–8 independent experiments. Data points in graphics are average ± SE. Statistical analysis was performed using two-tailed Student's *t*-test assuming unequal variances via GraphPad Prism software (GraphPad). Statistical significance was assumed at $P < 0.05$.

Acknowledgements

This work was funded by CNPq, PAPES-FIOCRUZ and FAPERJ (Brazil). They would also like to thank Drs O. J. M. Nascimento and M.G. de Freitas from the Antonio Pedro Hospital (Rio de Janeiro, RJ, Brazil) for their important technical assistance, Dr M. Marcelo Pelajo from LABPAT/IOC/Fiocruz (Brazil) for his thorough scientific review of the manuscript, Marcia Triunfol of Publicase for her constructive criticism and Judy Grevan for editing the final version of the manuscript.

References

Almeida, P.E., Silva, A.R., Maya-Monteiro, C.M., Töröcsik, D., D'Avila, H., Dezsö, B., *et al*. (2009) *Mycobacterium bovis* bacillus Calmette-Guérin infection induces TLR2-dependent peroxisome proliferator-activated receptor gamma expression and activation: functions in inflammation, lipid metabolism, and pathogenesis. *J Immunol* **183:** 1337–1345.

Barba, G., Harper, F., Harada, T., Kohara, M., Goulinet, S., Matsuura, Y., *et al*. (1997) Hepatitis C virus core protein shows a cytoplasmic localization and associates to cellular lipid storage droplets. *Proc Natl Acad Sci USA* **94:** 1200–1205.

Bentrup, K.H., and Russell, D.G. (2001) Mycobacterial persistence: adaptation to a changing environment. *Trends Microbiol* **9:** 597–605.

Betz, M., and Fox, B.S. (1991) Prostaglandin E2 inhibits production of Th1 lymphokines but not of Th2 lymphokines. *J Immunol* **146:** 108–113.

Bligh, E.G., and Dyer, W.J. (1959) A rapid method for total lipid extraction and purification. *Can J Biochem Physiol* **37:** 911–917.

Boström, P., Rutberg, M., Ericsson, J., Holmdahl, P., Andersson, L., Frohman, M.A., *et al*. (2005) Cytosolic lipid droplets increase in size by microtubule-dependent complex formation. *Arterioscler Thromb Vasc Biol* **25:** 1945–1951.

Boström, P., Andersson, L., Rutberg, M., Perman, J., Lidberg, U., Johansson, B.R., *et al*. (2007) SNARE proteins mediate fusion between cytosolic lipid droplets and are implicated in insulin sensitivity. *Nat Cell Biol* **9:** 1286–1293.

Boulant, S., Douglas, M.W., Moody, L., Budkowska, A., Targett-Adams, P., and McLauchlan, J. (2008) Hepatitis C virus core protein induces lipid droplet redistribution in a microtubule- and dynein-dependent manner. *Traffic* **9:** 1268–1282.

Bozza, P.T., and Viola, J.P. (2010) Lipid droplets in inflammation and cancer. *Prostaglandins Leukot Essent Fatty Acids* **82:** 243–250.

Bozza, P.T., Magalhães, K.G., and Weller, P.F. (2009) Leukocyte lipid bodies – biogenesis and functions in inflammation. *Biochim Biophys Acta* **1791:** 540–551.

Brennan, P. (1984) *Mycobacterium leprae* – the outer lipoidal surface. *J Biosci* **6:** 685–689.

Cáceres, N., Tapia, G., Ojanguren, I., Altare, F., Gil, O., Pinto, S., *et al*. (2009) Evolution of foamy macrophages in the pulmonary granulomas of experimental tuberculosis models. *Tuberculosis* **89:** 175–182.

Cámara-Lemarroy, C.R., Guzmán-de la Garza, F.J., and Fernández-Garza, N.E. (2010) Molecular inflammatory mediators in peripheral nerve degeneration and regeneration. *Neuroimmunomodulation* **17:** 314–324.

Chatterjee, K.R., Das Gupta, N.N., and De, M.L. (1959) Electron microscopic observations on the morphology of *Mycobacterium leprae*. *Exp Cell Res* **18:** 521–527.

Cocchiaro, J.L., Kumar, Y., Fischer, E.R., Hackstadt, T., and Valdivia, R.H. (2008) Cytoplasmic lipid droplets are trans-

located into the lumen of the *Chlamydia trachomatis* parasitophorous vacuole. *Proc Natl Acad Sci USA* **105:** 9379–9384.

Cole, S.T., Eiglmeier, K., Parkhill, J., James, K.D., Thomson, N.R., Wheeler, P.R., *et al*. (2001) Massive gene decay in the leprosy bacillus. *Nature* **409:** 1007–1011.

Cruz, D., Watson, A.D., Miller, C.S., Montoya, D., Ochoa, M.T., Sieling, P.A., *et al*. (2008) Host-derived oxidized phospholipids and HDL regulate innate immunity in human leprosy. *J Clin Invest* **118:** 2917–2928.

D'Ávila, H., Melo, R.C.N., Parreira, G.G., Werneck-Barroso, E., Castro-Faria-Neto, H.C., and Bozza, P.T. (2006) *Mycobacterium bovis* bacillus calmette-guérin induces TLR2-mediated formation of lipid bodies: intracellular domains for eicosanoid synthesis *in vivo*. *J Immunol* **176:** 3087–3097.

D'Ávila, H., Maya-Monteiro, C.M., and Bozza, P.T. (2008) Lipid bodies in innate immune response to bacterial and parasite infections. *Int J Immunopharmacol* **8:** 1308–1315.

Folch, J., Lees, M., and Stanley, G.H.S. (1957) A simple method for the isolation and purification of total lipides from animal tissues. *J Biol Chem* **226:** 497–509.

Franzblau, S.G. (1988) Oxidation of palmitic acid by *Mycobacterium leprae* in an axenic medium. *J Clin Microbiol* **26:** 18–21.

Gao, J., Ye, H., and Serrero, G. (2000) Stimulation of adipose differentiation related protein (ADRP) expression in adipocyte precursors by long-chain fatty acids. *J Cell Physiol* **182:** 297–302.

Grigoriev, I.S., Chernobelskaya, A.A., and Vorobjev, I.A. (1999) Nocodazole, vinblastine and taxol at low concentrations affect fibroblast locomotion and saltatory movements of organelles. *Membr Cell Biol* **13:** 23–48.

Hagge, D.A., Oby Robinson, S., Scollard, D., McCormick, G., and Williams, D.L. (2002) A new model for studying the effects of *Mycobacterium leprae* on Schwann cell and neuron interactions. *J Infect Dis* **186:** 1283–1296.

Job, C.K. (1970) *Mycobacterium leprae* in nerve lesions in lepromatous leprosy: an electron microscopic study. *Arch Pathol* **89:** 195–207.

Kaplan, G., Van Voorhis, W.C., Sarno, E.N., Nogueira, N., and Cohn, Z.A. (1983) The cutaneous infiltrates of leprosy. A transmission electron microscopy study. *J Exp Med* **158:** 1145–1159.

Lasunskaia, E.B., Campos, M.N.N., de Andrade, M.R.M., DaMatta, R.A., Kipnis, T.L., Einicker-Lamas, M., and Da Silva, W.D. (2006) Mycobacteria directly induce cytoskeletal rearrangements for macrophage spreading and polarization through TLR2- dependent PI3K signaling. *J Leukoc Biol* **80:** 1480–1490.

Lisak, R.P., Skundric, D., Bealmear, B., and Ragheb, S. (1997) The role of cytokines in Schwann cell damage, protection, and repair. *J Infect Dis* **176:** 173–179.

Mahlberg, F.H., Glick, J.M., Jerome, W.G., and Rothblat, G.H. (1990) Metabolism of cholesteryl ester lipid droplets in a J774 macrophage foam cell model. *Biochim Biophys Acta* **1045:** 291–298.

Marques, M.A., Neves-Ferreira, A.G., da Silveira, E.K., Valente, R.H., Chapeaurouge, A., Perales, J., *et al*. (2008) Deciphering the proteomic profile of *Mycobacterium leprae* cell envelope. *Proteomics* **8:** 2477–2491.

Marri, P.R., Bannantine, J.P., and Golding, G.B. (2006) Comparative genomics of metabolic pathways in *Mycobacterium* species: gene duplication, gene decay and lateral gene transfer. *FEMS Microbiol Rev* **30:** 6906–6925.

Mattos, K.A., D'Avila, H., Rodrigues, L.S., Oliveira, V.G.C., Sarno, E.N., Atella, G.C., *et al*. (2010) Lipid droplet formation in Leprosy: Toll-like Receptor-regulated organelles involved in eicosanoid formation and *Mycobacterium leprae* pathogenesis. *J Leukoc Biol* **87:** 371–384.

van der Meer-Janssen, Y.P., van Galen, J., Batenburg, J.J., and Helms, J.B. (2010) Lipids in host-pathogen interactions: pathogens exploit the complexity of the host cell lipidome. *Prog Lipid Res* **1:** 1–26.

Melo, R.C.N., D'Avila, H., Fabrino, D.L., Almeida, P.E., and Bozza, P.T. (2003) Macrophage lipid body induction by Chagas disease *in vivo*: putative intracellular domains for eicosanoid formation during infection. *Tissue Cell* **35:** 59–67.

Mosmann, T. (1983) Rapid colorimetrie assay for cellular growth and survival: application to proliferation and cytotoxicity assays. *J Immunol Methods* **55:** 55–63.

Oliveira, R.B., Ochoa, M.T., Sieling, P.A., Rea, T.H., Rambukkana, A., Sarno, E.N., and Modlin, R.L. (2003) Expression of toll-like receptor 2 on human schwann cells: a mechanism of nerve damage in leprosy. *Infect Immun* **71:** 1427–1433.

Pacheco, P., Vieira-de-Abreu, A., Gomes, R.N., Barbosa-Lima, G., Wermelinger, L.B., Maya-Monteiro, C.M., *et al*. (2007) Monocyte chemoattractant protein-1/CC chemokine ligand 2 controls microtubule-driven biogenesis and leukotriene B4-synthesizing function of macrophage lipid bodies elicited by innate immune response. *J Immunol* **179:** 8500–8508.

Pelc, S., Gompel, C., and Simonet, M.L. (1986) S-100 protein expression in satellite and schwann cells in neuroblastoma. An immunohistochemical and ultrastructural study. *Virchows Arch B Cell Pathol Incl Mol Pathol* **51:** 487–495.

Persson, J., Nilsson, J., and Lindholm, M.W. (2008) Interleukin-1β and tumor necrosis factor-α impede neutral lipid turnover in macrophage-derived foam cells. *BMC Immunol* **25:** 70.

Peyron, P., Vaubourgeix, J., Poquet, Y., Levillain, F., Botanch, C., Bardou, F., *et al*. (2008) Foamy macrophages from tuberculous patients' granulomas constitute a nutrient-rich reservoir for *M. tuberculosis* persistence. *PLoS Pathog* **4:** 1000204.

Pol, A., Lu, A., Pons, M., Peiró, S., and Enrich, C. (2000) Epidermal growth factor-mediated caveolin recruitment to early endosomes and MAPK activation. Role of cholesterol and actin cytoskeleton. *J Biol Chem* **275:** 30566–30572.

Quesniaux, V., Fremond, C., Jacobs, M., Parida, S., Nicolle, D., Yeremeev, V., *et al*. (2004) Toll-like receptor pathways in the immune responses to mycobacteria. *Microbes Infect* **6:** 946–959.

Ridley, D.S., and Jopling, W.H. (1966) Classification of leprosy according to immunity: a five-group system. *Int J Lepr* **34:** 255–273.

Robenek, H., and Severs, N.J. (2009) Lipid droplet growth by fusion: insights from freeze-fracture imaging. *J Cell Mol Med* **13:** 4657–4661.

Russell, D.G., Cardona, P.J., Kim, M.J., Allain, S., and Altare,

F. (2009) Foamy macrophages and the progression of the human tuberculosis granuloma. *Nat Immunol* **10:** 943–948.
Rutkowski, J.L., Tuite, G.F., Lincoln, P.M., Boyer, P.J., Tennekoon, G.I., and Kunkel, S.L. (1999) Signals for proinflammatory cytokine secretion by human Schwann cells. *J Neuroimmunol* **101:** 47–60.
Sakurai, I.S., and Skinsnes, O.K. (1970) Lipids in leprosy 2. Histochemistry of lipids in human leprosy. *Int J Lepr Other Mycobact Dis* **38:** 389–403.
Samsa, M.M., Mondotte, J.A., Iglesias, N.G., Assunção-Miranda, I., Barbosa-Lima, G., Da Poian, A.T., *et al.* (2009) Dengue virus capsid protein usurps lipid droplets for viral particle formation. *PLoS Pathog* **5:** e1000632.
Scollard, D.M., Adams, L.B., Gillis, T.P., Krahenbuhl, J.L., Truman, R.W., and Williams, D.L. (2006) The continuing challenges of leprosy. *Clin Microbiol Rev* **19:** 338–381.
Singh, A.K., Shirasawa, N., Kyoshima, K., Kobayashi, S., and Shimizu, Y. (1996) Schwann cell culture from the adult animal sciatic nerve: technique and review. *J Clin Neurosci* **3:** 69–74.
Tanigawa, K., Suzuki, K., Nakamura, K., Akama, T., Kawashima, A., Wu, H., *et al.* (2008) Expression of adipose differentiation-related protein (ADRP) and perilipin in macrophages infected with *Mycobacterium leprae*. *FEMS Microbiol Lett* **289:** 72–79.
Teles, R.M., Antunes, S.L., Jardim, M.R., Oliveira, A.L., Nery, J.A., Sales, A.M., *et al.* (2007) Expression of metalloproteinases (MMP-2, MMP-9, and TACE) and TNF-alpha in the nerves of leprosy patients. *J Peripher Nerv Syst* **12:** 195–204.
Van Meer, G. (2001) Caveolin, cholesterol, and lipid droplets? *J Cell Biol* **152:** F29–F34.
Virchow, R. (1863) *Die krankhaften Geschwülste*. Berlin: Hirschwald. 3: 325–327.
Wade, H.W. (1962) Zenker vs formalin fixation for the histopathology of leprosy tissues and other desirable features of technique. *Int J Lepr* **30:** 477–488.
Wenk, M.R. (2006) Lipidomics of host-pathogen interactions. *FEBS Lett* **580:** 5541–5551.
Wheeler, P.R. (1989) Biosynthetic pathways in *Mycobacterium leprae*. *Acta Leprol* **7:** 21–24.
Wheeler, P.R. (2003) Leprosy – clues about the biochemistry of *Mycobacterium leprae* and its host-dependency from the genome. *World J Microbiol Biotechnol* **19:** 1–16.
WHO (2010) *WHO Leprosy Today, WHO Report 2010*. [WWW document]. URL http://www.who.int/lep/en/
Zehmer, J.K., Huang, Y., Peng, G., Pu, J., Anderson, R.G.W., and Liu, P. (2009) A role for lipid droplets in inter-membrane lipid traffic. *Proteomics* **9:** 914–921.

Supporting information

Additional Supporting Information may be found in the online version of this article:

Fig. S1. Lipid droplets colocalize with *M. leprae* in foamy Schwann cells in nerve biopsies of LL patients. (A) Double-immunofluorescent labelling of a LL lesion for anti-S100 and anti-ML, evidencing the massive bacterial presence associated with SC; (B) LL lesion stained with anti-S100 and anti-ADRP (Pearson's coefficient: 0.81); (C) LD–ML association within SCs visualized by 3D reconstruction (yellow arrows) (Pearson's coefficient: 0.70). Nuclei were stained with TO-PRO-3. No fluorescence was observed for the isotype control IgG (data not shown). Bars: white = 10 μm; yellow = 5 μm. S100 is a Schwann cell (SC) marker; ADRP (Adipose Differentiation Related Protein) is a lipid droplet (LD) marker; LAM (lipoarabinomannan) was used as a *Mycobacterium leprae* (ML) marker.

Fig. S2. *M. leprae* infection induces increase in lipid droplet's size and number. Human SCs were stimulated for 48 h before evaluation of LD formation. LDs were stained with oil red O (ORO) (A). LD diameters were determined from microscopy images using ImageJ software. The distribution of lipid droplet size within individual cells was used to determine mean LD diameter on a per cell basis (B). The statistically significant ($P < 0.05$) difference between control and ML-treated cells is indicated by asterisks. Bars: 10 μm.

Fig. S3. Intracellular *M. leprae* is enveloped by lipid droplets in *in vitro* infected Schwann cells. (A–E) Primary and (F–I) lineage (ST88-14) human SCs were infected with PKH26-labelled ML (red) for 48 h. (A–C) LDs were visualized using BODIPY label (BP) (green). Note the LD–ML colocalization by 3D reconstruction (B) and in 2D images with orthogonal analysis (C). (D and E) Imunofluorescence confocal images for ADRP (green labelling) and PKH26-ML. An enlarged 3D view of LD–ML interaction, also shown in 2D images with orthogonal analysis (Pearson's coefficient: 0.43). Note staining for ADRP is seen surrounding the ML surface in 3D reconstruction (D). The green and red arrows indicate LDs and ML respectively. In (F), general view of LD–ML localization in ST88-14 cells. (G) Close ML–LD association seen by 3D reconstruction. (I) Close-up showing fusion 'bridges' among LDs (white arrow) and the LD–ML complex (inset, yellow arrows, Pearson's coefficient: 0.83). (H) 2D image of the fattened z-stack. Bars: white = 10 μm; red = 2 μm. ADRP (Adipose Differentiation Related Protein) and BODIPY are lipid droplet (LD) markers; LAM (lipoarabinomannan) was used as a *Mycobacterium leprae* (ML) marker.

Fig. S4. Corresponding to Fig. 3A. SCs were infected with PKH26-labelled ML (red) and LDs were stained by BODIPY (green) and investigated via time-lapse recording. Droplets move towards the bacterium and adhere to it, merging into a single structure. The film is 6.29 s long, representing 30 min consisting of 44 frames, in which each second represents 4.76 min.

Fig. S5. Cytoskeleton distribution in uninfected SCs. The visualization of the association between LDs and cytoskeleton in uninfected cells. LDs were stained with BODIPY (green) and the microtubular network was stained with α-tubulin antibody (α-tub, red). Bars: white = 5 μm; yellow = 2 μm.

Please note: Wiley-Blackwell are not responsible for the content or functionality of any supporting materials supplied by the authors. Any queries (other than missing material) should be directed to the corresponding author for the article.

Metabolic consequences of stored neutral lipid in leprosy: linking the lipid metabolism and immune system by lipid droplets organelles regulation through new Toll like receptor 6 signaling pathway in Schwann cells.

[1]Mattos, K.A, [1]Oliveira, V.G.C; [1]Rodrigues, L.S, [2]D'Avila, H., [3]Olmo, R.P, [3]Sarno, E. N., [2*]Bozza, P.T. and [1*]Pessolani, M.C.V.

[1]Laboratory of Cellular Microbiology, [2]Laboratory of Immunopharmacology and Laboratory of Hanseniase, Instituto Oswaldo Cruz, FIOCRUZ, RJ, 21045-900 Brazil.

*Address correspondence to:
Maria Cristina Vidal Pessolani
e-mail: cpessola@ioc.fiocruz.br
Tel. (+55) 21 2598 4467; FAX: (+55) 21 2270 9997
Oswaldo Cruz Institute
Oswaldo Cruz Foundation – FIOCRUZ
Av. Brasil, 4365 – Manguinhos
Rio de Janeiro, RJ 21045 900
Brazil

ABSTRACT

The predilection of Schwann cells (SCs) by *Mycobacterium leprae* (ML) represents a unique feature in leprosy. The frequent association of large numbers of ML with foamy degeneration emphasizes the importance of lipids in the biology of ML infection and suggests possible strategies to combat nerve damage. The origin and nature of these lipids, as well as their function and contribution to leprosy disease remain unclear. In this study, we analyzed the mechanism of lipid droplet (LD) organelle biogenesis by ML in SCs. Firstly; the capacity of ML to induce LD formation was confirmed by *in vitro* studies with human and murine SCs using microscopy and FACS analysis. Our observations indicated that ML-LD induction occurs in a time and dose-dependent manner and requires the uptake of live bacteria. LD biogenesis was also inhibited by microtubules and actin-disrupting drugs confirming its dependence on cytoskeleton. In addition, only ML, but not *M. smegmatis* or BCG was able to induce LD in SCs. Finally, a role for TLR2 and 6 in pathogen recognition and signaling to form LD was investigated. TLR6 but not TLR2 depletion affected LD biogenesis. Interestingly, a concomitant reduction of live ML within $TLR6^{-/-}$ cells was observed, confirming the requirement of bacterial internalization to modulate the lipid metabolism in SCs. LDs as inflammatory organelles were determined by correlation between LD formation, eicosanoid synthesis and cytokine production in response to bacterial infection. We observed that ML infection induced significant increase in LD number and PGE_2 synthesis as well as the increase of IL-10 and inhibition of IL-12 production by SCs. Interestingly, NS-398 (COX inhibitors) and C75 (fatty acid synthase inhibitor) down-regulated LD formation and PGE_2 synthesis, induce an inverse correlation between IL-10 and IL-12 production and decrease the intracellular ML viability. Immunohistochemistry analysis of nerves from lepromatous leprosy patients showed SCs highly positive for both ML and adipophilin (ADRP), a marker of LD and co-localization with COX-2, suggesting that their foamy aspect is at least in part derived from LD accumulation induced during infection and these organelles are intracellular sites for PGE_2 synthesis. Altogether, our data describe the ML-induced LD function as intracellular signaling platforms in inflammatory mediator production and that this process is dependent on bacterial viability and regulation by a new TLR6-dependent signaling pathway. These findings open the possibility of interfering with ML ability to modulate host lipid metabolism, which may contribute to bacterial survival and subsequently leprosy pathogenesis.